

4-2015

Optimizing Reservoir Operations to Adapt to 21st Century Expectations of Climate and Social Change in the Willamette River Basin, Oregon

Julia A. Jones

Follow this and additional works at: https://digitalrepository.unm.edu/uc_rio_chama

Recommended Citation

Jones, Julia A.. "Optimizing Reservoir Operations to Adapt to 21st Century Expectations of Climate and Social Change in the Willamette River Basin, Oregon." (2015). https://digitalrepository.unm.edu/uc_rio_chama/5

This Article is brought to you for free and open access by the The Utton Transboundary Resources Center at UNM Digital Repository. It has been accepted for inclusion in Law of the Rio Chama by an authorized administrator of UNM Digital Repository. For more information, please contact amywinter@unm.edu, lsloane@salud.unm.edu, sarahrk@unm.edu.

AN ABSTRACT OF THE DISSERTATION OF

Kathleen M. Moore for the degree of Doctor of Philosophy in Geography presented on April 30, 2015.

Title: Optimizing Reservoir Operations to Adapt to 21st Century Expectations of Climate and Social Change in the Willamette River Basin, Oregon

Abstract approved:

Julia A. Jones

Reservoir systems in the western US are managed to serve two main competing purposes: to reduce flooding during the winter and spring, and to provide water supply for multiple uses during the summer. Because the storage capacity of a reservoir cannot be used for both flood damage reduction and water storage at the same time, these two uses are traded off as the reservoir fills during the transition from the wet to the dry season. Climate change, population growth, and development in the western US may exacerbate dry season water scarcity and increase winter flood risk, creating a need to critically evaluate the status quo for reservoir operations.

Focusing on a system of thirteen reservoirs (the Willamette Project) in the Willamette River Basin, Oregon, we estimated the values of reservoir management for reducing expected damages in the floodplain and for storing water for recreation in and around the reservoirs. We then used these values in a dynamic program to estimate the optimal fill path over the winter-spring transition period for both historical conditions and future scenarios of climate and social change.

The value of stored water for summertime reservoir recreation was estimated based on the response of recreational use day counts to variation in water levels at nine of the reservoirs over the period 2001 to 2011. Visitor days were found to decline by as much as 2% per foot of drop in water level below full pool. The implied value of water to recreational users varied from \$0.10 to \$78 per acre-foot per month, depending on the reservoir. This range of values is comparable to prior estimates of the value of reservoir recreation in other parts of the western US, and is also similar to the value of water to irrigated agriculture in the Willamette River Basin, estimated in other studies. Because water cannot be used for recreation and irrigation at the same time, these results suggest that management of the Willamette reservoirs may benefit society by releasing stored water in summer for downstream needs from some reservoirs, while maintaining full pool for recreation in others, as prescribed currently.

The expected value of flood damage reduction was estimated based on the probability of floods, flood inundation depth, and reservoir capacity, for three scenarios of future development in the Willamette River Basin, which were simulated by the Willamette Water 2100 land transition model over the period from present to 2100 using mid-range projections of future climate (MIROC5) and assumptions about future population growth. Estimates of expected flood damage reduction varied as a function of flood risk over the course of the winter and spring, as well as the rate of population growth and associated development in the floodplain. At a weekly time scale the expected benefits of flood damage reduction ranged from a high in mid-January of \$304 million to \$1,284 million (depending on the rate of population growth), to near zero at the end of May.

Finally, these analyses were combined in a dynamic programming approach to evaluate the optimal rate of fill for the Willamette Project reservoirs, at a weekly time step over the period

from January to the end of May. This was done by treating the system of thirteen reservoirs as a single reservoir. The dynamic program found the fill path that minimized the sum of flood damages and foregone recreation benefits, subject to the constraint of available water inflows to the reservoir system. The estimated optimal fill path depended on the rate of decline of expected flood damages from mid-January to May. Anticipated future increases in winter flood risk and reduced spring streamflow, associated with climate change, shifted the optimal fill path to begin earlier and to fill more slowly, compared to the optimal fill path under historical conditions. The model confirms the intuitive result that the greater the value of stored water the earlier the optimal date to begin filling. Conversely, the greater the expected value of flood damage reduction the later the initiation of fill.

Despite uncertainties in the estimated values of expected flood damage reduction and stored water for recreation, as well as the limitations of the dynamic program in modelling the coordinated management of multiple reservoirs, the approach and findings of this analysis contribute to our understanding of how reservoir management may need to adapt to future changes in water supply and demand.

©Copyright by Kathleen M. Moore
April 30, 2015
All Rights Reserved

OPTIMIZING RESERVOIR OPERATIONS TO ADAPT TO 21ST CENTURY
EXPECTATIONS OF CLIMATE AND SOCIAL CHANGE IN THE WILLAMETTE RIVER
BASIN, OREGON

by

Kathleen M. Moore

A DISSERTATION

submitted to

Oregon State University

in partial fulfillment of
the requirements for the
degree of

Doctor of Philosophy

Presented April 30, 2015
Commencement June 2015

Doctor of Philosophy dissertation of Kathleen M. Moore presented April 30, 2015.

APPROVED:

Major Professor, representing Geography

Dean of the College of Earth, Ocean, and Atmospheric Sciences

Dean of the Graduate School

I understand that my dissertation will become part of the permanent collection of Oregon State University libraries. My signature below authorizes release of my dissertation to any reader upon request.

Kathleen M. Moore, Author

ACKNOWLEDGEMENTS

I owe many thanks to Julia Jones and Bill Jaeger who advised me in this research, and provided mentorship and encouragement in my academic pursuits. I would also like to express my thanks to my committee members Anne Nolin, Steve Hostetler, Fred Swanson, and Andreas Schmittner for taking an interest in my research and for providing constructive review.

I am very grateful to Jeff McDonnell for his sage mentorship and for connecting me to Andrew Plantinga and Bill Jaeger.

I would like to thank the College of Earth, Ocean, and Atmospheric Sciences for providing me with an academic home, and for supporting me throughout my graduate studies. I would also like to thank Roy Haggerty for supporting my research as part of the Willamette Water 2100 project, and I would like to acknowledge the funding of this project by the National Science Foundation.

Finally, I am most grateful for the unwavering support of my family and friends.

CONTRIBUTION OF AUTHORS

Julia Jones and William Jaeger provided guidance in the development of each chapter.

TABLE OF CONTENTS

	<u>Page</u>
Chapter 1: Introduction	1
1.1 Motivation.....	1
1.2 References.....	3
Chapter 2: The Value of Reservoir Operations for Flood Damage Reduction under Future Scenarios of Climate, Population, and Development in the Willamette River Basin, Oregon	5
2.1 Abstract.....	5
2.2 Introduction.....	6
2.3 Study Site	7
2.4 Methods	12
2.4.1 Flood inundation mapping.....	12
2.4.2 Flood damages	17
2.4.3 Flood frequency analysis.....	25
2.4.4 The value of flood damage reduction	30
2.5 Results.....	32
2.5.1 Flood inundation mapping.....	32
2.5.2 Land cover scenarios.....	53
2.5.3 Flood damages	62
2.5.4 The value of reservoir management for flood damage reduction.....	71
2.6 Discussion	77
2.6.1 Accuracy of flood inundation mapping.....	77
2.6.2 Accuracy of flood damage estimation.....	79
2.6.3 Seasonal pattern of flood damages	81
2.7 Summary and Conclusions	82
2.8 Acknowledgements	83
2.9 References.....	84
Chapter 3: The Value of Stored Water for Summertime Reservoir Recreation in the Willamette River Basin, Oregon.....	87
3.1 Abstract.....	87

TABLE OF CONTENTS (Continued)

	<u>Page</u>
3.2 Introduction.....	88
3.3 Study Site.....	91
3.4 Theory and Methods.....	95
3.4.1 Theoretical model.....	95
3.4.2 Estimating response in recreational visitor days to reservoir water level.....	96
3.4.3 Estimating total visitor days for all reservoirs.....	103
3.4.4 Estimating benefits per visit for reservoir recreation.....	107
3.5 Results.....	107
3.6 Discussion.....	113
3.6.1 Methodological uncertainty in estimating the value of stored water.....	114
3.6.2 Sources of uncertainty in data and model structure.....	115
3.6.3 Differences among reservoirs in the value of stored water.....	116
3.6.4 Implications for reservoir management.....	117
3.7 Conclusions.....	118
3.8 Acknowledgements.....	119
3.9 References.....	119
Chapter 4: Optimizing Reservoir Operations to Adapt to 21st Century Expectations of Climate and Social Change in the Willamette River Basin, Oregon.....	122
4.1 Abstract.....	122
4.2 Introduction.....	123
4.3 Study Site.....	128
4.4 Methods.....	132
4.4.1 Theoretical framework.....	132
4.4.2 Bellman’s Principle of Optimality and Dynamic Programming.....	133
4.4.3 Reference case model.....	136
4.4.4 Alternative model specifications.....	142
4.5 Results.....	148
4.5.1 Reference case model.....	148
4.5.2 Sensitivity to downstream flow requirements.....	153

TABLE OF CONTENTS (Continued)

	<u>Page</u>
4.5.3 Comparison to the existing fill path.....	157
4.5.4 Sensitivity to changes in use values.....	159
4.5.5 Sensitivity to changes in hydrology.....	164
4.6 Discussion.....	171
4.7 Conclusions.....	175
4.8 Acknowledgments.....	177
4.9 References.....	177
Chapter 5: Conclusions.....	180

LIST OF FIGURES

<u>Figure</u>	<u>Page</u>
Figure 2.1 The extent of the Columbia River Basin within the United States, and the location of the Willamette River sub-basin.	10
Figure 2.2. The Willamette River Basin, Oregon. The Willamette Project reservoirs are located in the southern portion on the basin, predominately on tributaries draining the Western Cascades. The mainstem of the Willamette River is indicated with a thicker line.	11
Figure 2.3. Classification of flood damages. The highlighted box indicates the type of damages evaluated in this study. Source: U.S. Army Engineer Institute for Water Resources (2013).....	21
Figure 2.4. The estimated relationship between structural values and land values (Pearson $r=0.65$) based on detailed historical data for 10 counties in the Willamette Basin described in <i>Jaeger et al.</i> , [2014].	22
Figure 2.5. Depth-damage curve for structural value losses. The average (solid line) of the depth-damage curves provided by the USACE was used in estimating structural damage as a percent of structural value. The dotted lines show the range of damages given by the USACE curves. The water depth is given relative to the first (ground) flood of a structure.....	23
Figure 2.6. Depth-damage curve for content value losses. The average (solid line) of the depth-damage curves provided by the USACE was used in estimating content damage as a percent of structural value. The dotted lines show the range of damages given by the USACE curves. The water depth is given relative to the first (ground) flood of a structure.....	24
Figure 2.7. Estimated log-Pearson Type III skewness coefficients.	26
Figure 2.8. Comparison of probability and cumulative density functions derived from the full historical record and the post dam construction period for the week starting Jan 1st.	27
Figure 2.9. Probability density functions by week Jan 1st-May 20th derived from the full historical record.....	28
Figure 2.10. Cumulative density functions by week Jan 1st-May 20th derived from the full historical record.....	29
Figure 2.11. Inundation within the Willamette River’s mainstem floodplain at Corvallis estimated at the bankfull stage flood category. Orthoimagery as of 2012 from the National Map Viewer.	35

LIST OF FIGURES (Continued)

<u>Figure</u>	<u>Page</u>
Figure 2.12. Inundation within the Willamette River’s mainstem floodplain at Salem estimated at the bankfull stage flood category. Orthoimagery as of 2012 from the National Map Viewer.....	36
Figure 2.13. Inundation within the Willamette River’s mainstem floodplain at Portland estimated at the bankfull stage flood category. Orthoimagery as of 2012 from the National Map Viewer.....	37
Figure 2.14. Inundation within the Willamette River’s mainstem floodplain at Corvallis estimated at the flood stage category. Orthoimagery as of 2012 from the National Map Viewer.....	38
Figure 2.15. Inundation within the Willamette River’s mainstem floodplain at Salem estimated at the flood stage category. Orthoimagery as of 2012 from the National Map Viewer.	39
Figure 2.16. Inundation within the Willamette River’s mainstem floodplain at Portland estimated at the flood stage category. Orthoimagery as of 2012 from the National Map Viewer. ...	40
Figure 2.17. Inundation within the Willamette River’s mainstem floodplain at Corvallis estimated at the moderate flood category. Orthoimagery as of 2012 from the National Map Viewer.....	41
Figure 2.18. Inundation within the Willamette River’s mainstem floodplain at Salem estimated at the moderate flood category. Orthoimagery as of 2012 from the National Map Viewer. .	42
Figure 2.19. Inundation within the Willamette River’s mainstem floodplain at Portland estimated at the moderate flood category. Orthoimagery as of 2012 from the National Map Viewer.	43
Figure 2.20. Inundation within the Willamette River’s mainstem floodplain at Corvallis estimated at the major flood category. Orthoimagery as of 2012 from the National Map Viewer.....	44
Figure 2.21. Inundation within the Willamette River’s mainstem floodplain at Salem estimated at the major flood category. Orthoimagery as of 2012 from the National Map Viewer.	45
Figure 2.22. Inundation within the Willamette River’s mainstem floodplain at Portland estimated at the major flood category. Orthoimagery as of 2012 from the National Map Viewer. ...	46
Figure 2.23. Inundation within the Willamette River’s mainstem floodplain at Corvallis estimated at the historical high flood category. Orthoimagery as of 2012 from the National Map Viewer.	47

LIST OF FIGURES (Continued)

<u>Figure</u>	<u>Page</u>
Figure 2.24. Inundation within the Willamette River’s mainstem floodplain at Salem estimated at the historical high flood category. Orthoimagery as of 2012 from the National Map Viewer.....	48
Figure 2.25. Inundation within the Willamette River’s mainstem floodplain at Portland estimated at the historical high flood category. Orthoimagery as of 2012 from the National Map Viewer.....	49
Figure 2.26. Comparison of inundation within the Willamette River’s mainstem floodplain at Corvallis estimated at the major flood category with the extent of the 1996 flood estimated by Hulse et al. (2002). Orthoimagery as of 2012 from the National Map Viewer.....	50
Figure 2.27. Comparison of inundation within the Willamette River’s mainstem floodplain at Eugene estimated at the major flood category with the extent of the 1996 flood estimated by Hulse et al. (2002). Orthoimagery as of 2012 from the National Map Viewer.	51
Figure 2.28. Comparison of inundation within the Willamette River’s mainstem floodplain at Portland estimated at the major flood category with the extent of the 1996 flood estimated by Hulse et al. (2002). Orthoimagery as of 2012 from the National Map Viewer.	52
Figure 2.29. The location and value of structural development in the Willamette’s mainstem floodplain at Corvallis under the high population growth scenario in 2030. Orthoimagery as of 2012 from the National Map Viewer. The arrows indicate errors of commission where sections of land are shown as developed, but are unlikely to contain structures given the location within the inundation zone, as well as errors of omission where the land cover model failed to capture areas of development.....	56
Figure 2.30. The location and value of structural development in the Willamette’s mainstem floodplain at Corvallis under the high population growth scenario in 2100. Orthoimagery as of 2012 from the National Map Viewer.	57
Figure 2.31. The location and value of structural development in the Willamette’s mainstem floodplain at Salem under the high population growth scenario in 2030. Orthoimagery as of 2012 from the National Map Viewer. The arrows indicate some of the errors of commission where sections of land are shown as developed, but are unlikely to contain structures given the location within the inundation zone.	58
Figure 2.32. The location and value of structural development in the Willamette’s mainstem floodplain at Salem under the high population growth scenario in 2100. Orthoimagery as of 2012 from the National Map Viewer. The arrows indicate some of the errors of commission where sections of land are shown as developed, but are unlikely to contain structures given the location within the inundation zone.	59

LIST OF FIGURES (Continued)

<u>Figure</u>	<u>Page</u>
Figure 2.33. The location and value of structural development in the Willamette’s mainstem floodplain at Portland under the high population growth scenario in 2030. Orthoimagery as of 2012 from the National Map Viewer. The arrows indicate some of the errors of commission where sections of land are shown as developed, but are unlikely to contain structures given the location within the inundation zone.	60
Figure 2.34. . The location and value of structural development in the Willamette’s mainstem floodplain at Portland under the high population growth scenario in 2100. Orthoimagery as of 2012 from the National Map Viewer.	61
Figure 2.35. Flood damages in the Willamette’s mainstem floodplain at Corvallis under the high population growth scenario in 2030. Orthoimagery as of 2012 from the National Map Viewer.....	65
Figure 2.36. Flood damages in the Willamette’s mainstem floodplain at Corvallis under the high population growth scenario in 2100. Orthoimagery as of 2012 from the National Map Viewer.....	66
Figure 2.37. Flood damages in the Willamette’s mainstem floodplain at Salem under the high population growth scenario in 2030. Orthoimagery as of 2012 from the National Map Viewer.....	67
Figure 2.38. Flood damages in the Willamette’s mainstem floodplain at Salem under the high population growth scenario in 2100. Orthoimagery as of 2012 from the National Map Viewer.....	68
Figure 2.39. Flood damages in the Willamette’s mainstem floodplain at Portland under the high population growth scenario in 2030. Orthoimagery as of 2012 from the National Map Viewer.....	69
Figure 2.40. Flood damages in the Willamette’s mainstem floodplain at Portland under the high population growth scenario in 2100. Orthoimagery as of 2012 from the National Map Viewer.....	70
Figure 2.41. The expected value of flood damages that could be averted using reservoir capacity in the WRB by week from January 1 st – May 20 th estimated under the Reference Case scenario in 2030.....	75
Figure 2.42. The modeled function for the expected loss of flood damage buffering due to reservoir fill in the WRB by week from January 1 st – May 20 th estimated under the Reference Case scenario in 2030.....	76

LIST OF FIGURES (Continued)

<u>Figure</u>	<u>Page</u>
Figure 2.43. Flood category stages at the Corvallis, Salem, and Portland gauging stations as defined by NOAA (colored bars labeled "observed") compared to the flood category stages predicted by the inundation model at these locations. The maximum observed stage height reached during the 1996 flood as well as the historical high crest is also shown for each gauge.	79
Figure 3.1. Locations of the Willamette Project reservoirs and nearby population centers.....	90
Figure 3.2. The change in volume of stored water as the water level falls below full pool at each of the Willamette Project storage reservoirs.	94
Figure 3.3. The decline in the water surface area at each of the Willamette Project storage reservoirs as the water level falls below full pool.	95
Figure 3.4. Summary statistics of summertime (June-August) water level variation by reservoir during the study period from 2001-2011. The horizontal line within each box gives the median, the box extents give the 25 th and 75 th percentiles, the box whiskers give the most extreme values within 1.5 times the interquartile range, and the dots give the values of observations that fall beyond this range.	102
Figure 3.5. The Willamette Project storage reservoirs symbolized according to the estimated relative value (\$/acre-foot) of stored water to recreation (Table 3.8).	112
Figure 4.1. The location of the Willamette River Basin in the Pacific Northwest.	126
Figure 4.2. An operations rule curve gives the tradeoff between the flood damage reduction and the stored water benefits of a reservoir.	127
Figure 4.3. The Willamette River Basin, Oregon. The Willamette Project reservoirs are located in the southern portion on the basin, predominately on tributaries draining the Western Cascades.....	130
Figure 4.4. The target storage level across the Willamette Project reservoirs as specified by the current rule curves.	131
Figure 4.5. Expected reservoir inflow for the reference case model specification was estimated by fitting an OLS regression equation for the 5 th order polynomial to the historical streamflow record. The grey box indicates the period modelled for reservoir refill.	140
Figure 4.6. The expected reservoir inflows and the lower 99th percentile inflows based on the historical record. The grey box indicates the period modelled for reservoir refill.....	141

LIST OF FIGURES (Continued)

<u>Figure</u>	<u>Page</u>
Figure 4.7. Reservoir inflows available for storage under the reference case specification and under Alternative 1 specification where available inflows were reduced to account for downstream flow requirements. The grey box indicates the period modelled for reservoir refill.	145
Figure 4.8. Reservoir inflows available for storage under the reference case specification, the Alternative 6 specification in which future reservoir inflows were assumed to resemble historical streamflow in the rain-dominated zone of the Cascade Range, and the Alternative 7 specification in which future reservoir inflows were assumed to resemble historical streamflow in southern Oregon representing both a future loss of snowpack, as well as increases in evapotranspiration relative to historical conditions. The grey box indicates the period modelled for reservoir refill.	146
Figure 4.9. The product of the time dependent terms of flood loss function (the “flood loss multiplier”) under the reference case model specification, and under the Alternative 9 specification, which simulates increased flood costs in the winter and decreased flood costs in the spring.	147
Figure 4.10. The optimal reservoir fill path derived under the reference case model specification.	149
Figure 4.11. The optimal policy for additions of water to reservoir storage under the reference case model specification.	150
Figure 4.12. The optimal reservoir fill path under the reference case specification compared to the optimal reservoir fill path given an increase in the value of stored water at full pool to \$15/acre-foot/3 month summer period – the increase required to achieve full pool storage by May 21 st , all else the same.	151
Figure 4.13. The optimal policy for additions of water to reservoir storage under the reference case specification compared to the optimal policy for additions of water to reservoir storage given an increase in the value of stored water at full pool to \$15/acre-foot/3 month summer period – the increase required to achieve full pool storage by May 21 st , all else the same.	152
Figure 4.14. The optimal reservoir fill path under the reference case specification compared to the optimal reservoir fill path given modified discretionary inflows as specified in Alternative 1 to account for downstream flow requirements.....	154
Figure 4.15. The optimal policy for additions of water to reservoir storage under the reference case specification compared to the optimal policy for additions of water to reservoir storage given modified discretionary inflows as specified in Alternative 1 to account for downstream flow requirements.	155

LIST OF FIGURES (Continued)

<u>Figure</u>	<u>Page</u>
Figure 4.16. The optimal reservoir fill path compared for expected inflows under the reference case specification and modified discretionary inflows for downstream flow requirements, given the increase in the value of stored water at full pool required to achieve full pool storage by May 21 st , all else the same.	156
Figure 4.17. The optimal policy for additions of water to reservoir storage compared for expected inflows under the reference case specification and modified discretionary inflows for downstream flow requirements, given the increase in the value of stored water at full pool required to achieve full pool storage by May 21 st , all else the same.	157
Figure 4.18. Comparison of the current USACE target fill path for the Willamette Project reservoirs to the estimated optimal reservoir fill paths under 1) the reference case specification, 2) reduced discretionary inflows to account for downstream flow requirements, and 3) reduced discretionary inflows to account for downstream flow requirements as well as the increase in the value of stored water at full pool required to achieve full pool storage by May 21 st , all else the same.	159
Figure 4.19. The optimal reservoir fill path compared for the reference case model specification, the Alternative 2 specification in which the price of stored water at full pool was increased to \$17/acre-foot – the estimated value of water to irrigated agriculture in the WRB, and the Alternative 3 specification in which the price of stored water at full pool was increased further to \$34/acre-foot.	161
Figure 4.20. The optimal policy for additions of water to reservoir storage compared for the reference case model specification, the Alternative 2 specification in which the price of stored water at full pool was increased to \$17/acre-foot – the estimated value of water to irrigated agriculture in the WRB, and the Alternative 3 specification in which the price of stored water at full pool was increased further to \$34/acre-foot.	162
Figure 4.21. The optimal reservoir fill path compared for the reference case model specification, the Alternative 4 specification in which flood losses were increased by 33% relative to the reference case as estimated for the year 2030, and the Alternative 5 specification in which flood losses were increased by 136% relative to the reference case as estimated for the year 2070.	163
Figure 4.22. The optimal policy for additions of water to reservoir storage compared for the reference case model specification, the Alternative 4 specification in which flood losses were increased by 33% relative to the reference case as estimated for the year 2030, and the Alternative 5 specification in which flood losses were increased by 136% relative to the reference case as estimated for the year 2070.	164

LIST OF FIGURES (Continued)

<u>Figure</u>	<u>Page</u>
Figure 4.23. The optimal reservoir fill path compared for the reference case model specification, the Alternative 6 specification in which future reservoir inflows were assumed to resemble historical streamflow in the rain-dominated zone of the Cascade Range, the Alternative 7 specification in which future reservoir inflows were assumed to resemble historical streamflow in southern Oregon representing both a future loss of snowpack, as well as increases in evapotranspiration relative to historical conditions, the Alternative 8 specification in which the stochastic shock was doubled to simulate increased variability in streamflow, and the Alternative 9 specification the coefficients in the time dependent terms of flood loss function were altered to simulate increased flood costs in the winter and decreased flood costs in the spring.	167
Figure 4.24. The optimal policy for additions of water to reservoir storage compared for the reference case model specification, the Alternative 6 specification in which future reservoir inflows were assumed to resemble historical streamflow in the rain-dominated zone of the Cascade Range, the Alternative 7 specification in which future reservoir inflows were assumed to resemble historical streamflow in southern Oregon representing both a future loss of snowpack, as well as increases in evapotranspiration relative to historical conditions, the Alternative 8 specification in which the stochastic shock was doubled to simulate increased variability in streamflow, and the Alternative 9 specification the coefficients in the time dependent terms of flood loss function were altered to simulate increased flood costs in the winter and decreased flood costs in the spring.	168
Figure 4.25. The optimal reservoir fill path compared for the reference case model specification, the Alternative 6 specification in which future reservoir inflows were assumed to resemble historical streamflow in the rain-dominated zone of the Cascade Range, and the Alternative 7 specification in which future reservoir inflows were assumed to resemble historical streamflow in southern Oregon representing both a future loss of snowpack, as well as increases in evapotranspiration relative to historical conditions, given the increase in the value of stored water at full pool required to achieve full pool storage by May 21st, all else the same.	169
Figure 4.26. The optimal policy for additions of water to reservoir storage compared for the reference case model specification, the Alternative 6 specification in which future reservoir inflows were assumed to resemble historical streamflow in the rain-dominated zone of the Cascade Range, and the Alternative 7 specification in which future reservoir inflows were assumed to resemble historical streamflow in southern Oregon representing both a future loss of snowpack, as well as increases in evapotranspiration relative to historical conditions, given the increase in the value of stored water at full pool required to achieve full pool storage by May 21st, all else the same.	170

LIST OF FIGURES (Continued)

<u>Figure</u>	<u>Page</u>
Figure 4.27. The current USACE fill path for the Willamette Project reservoirs compared to the derived optimal reservoir fill paths for the Alternative 1 specification, which best represents current expectations for hydrology and downstream flow requirements, with the value of stored water at full pool increased to \$64/acre-foot, for all else the same, and the Alternative 7 specification in which future reservoir inflows available for storage were assumed to resemble historical streamflow in southern Oregon representing both a future loss of snowpack, as well as increases in evapotranspiration relative to historical conditions, with the value of stored water at full pool increased to \$181/acre-foot, all else the same.	174

LIST OF TABLES

<u>Table</u>	<u>Page</u>
Table 2.1. DEM datasets used to map the topographic surface of the Willamette River floodplain.	15
Table 2.2. Flood category stages for stream gauges along the mainstem of the Willamette River. For each gauge the given flood stage heights mark the minimum increase in river surface elevation relative to the gauge datum, necessary to reach each flood category. Source: NOAA.	16
Table 2.3. River stage and associated floodplain inundation for each flood category relative to bankfull stage. The river stage for each flood category was defined as the average difference between bankfull stage and the lower bound of that category across the stream gauges (Table 2.2).	17
Table 2.4. The total area of land in developed use within the WRB mainstem floodplain, under the WW2100 scenarios for the Reference Case model, the High Population Growth model, and the Relaxed UGB model in 2030, 2070, and 2100. WW2100 model outputs downloaded August 19, 2014.	55
Table 2.5. The total value of structures within the WRB mainstem floodplain, under the WW2100 scenarios for the Reference Case model, the High Population Growth model, and the Relaxed UGB model in 2030, 2070, and 2100. WW2100 model outputs downloaded August 19, 2014.	55
Table 2.6. Total flood damages within the WRB mainstem floodplain, estimated for the intersection of each flood category with the WW2100 land cover scenarios for the Reference Case model, the High Population Growth model, and the Relaxed UGB model in 2030, 2070, and 2100. WW2100 model outputs downloaded August 19, 2014. For each scenario the total damage estimates were adjusted down by the damages estimated at bankfull stage, which were assumed to be estimation error.	64
Table 2.7. Marginal costs associated with each flood stage category calculated as the instantaneous change in total flood damages with respect to the associated increase in the volume of floodplain inundation within the WRB mainstem floodplain, for the Reference Case, the High Population Growth, and the Relaxed UGB scenarios of the WW2100 land cover change model for 2030, 2070, and 2100.	73
Table 2.8. The maximum expected value of flood damage reduction using reservoir capacity in the WRB for each week from January 1 st – May 20 th given land cover in the Reference Case model in 2030, and 2070, and the High Population Growth model in 2100.	74
Table 3.1. Characteristics of the Willamette Project storage reservoirs. Source: USACE.	93
Table 3.2. The range in visitor days at recreation sites at the Willamette Project reservoirs for the months of June-August, averaged over the period 2001-2011.	101

LIST OF TABLES (Continued)

<u>Table</u>	<u>Page</u>
Table 3.3. Control variables included in the vector X' in the empirical model estimating the effect of reservoir water level on recreational visitor days. Data Sources: U.S. Historical Climatology Network (station 351862), Population Research Center at Portland State University and Google maps.	103
Table 3.4. Comparison of three estimates of recreational visitor days at Willamette Project reservoirs. Column 2 shows the total number of visitor days per month (Jun-Aug) observed by the USACE vehicle monitors used in this study. Column 3 provides the number of “Activity Days” by boat owners during 2007 based on a survey by the Oregon State Marine Board. Column 4 provides the expected number of visitor days at each reservoir per month (Jun-Aug) calculated in this study using eq. 3.4.	106
Table 3.5 The average willingness-to-pay (2014 dollars) per visitor day (\$/visitor/day) from the meta-analysis by Loomis (2005) for recreational activities that are expected to occur at reservoir sites.	107
Table 3.6. Results of the empirical model estimation for the five model structures, each of which omitted outliers according to different rules.	110
Table 3.7. The magnitude of the visitation response to declining reservoir water levels and the associated marginal value of stored water to recreation at Fern Ridge, Fall Creek, and Foster reservoirs.	111
Table 3.8. The marginal value of stored water to recreation at the Willamette Project reservoirs based on 1) the expected number of visit days per month for Jun-Aug at each reservoir (Table 3.4), the average response across the reservoirs of a reduction of 0.3% in the number of visitor days for every foot the water levels drops below full pool, and 3) an estimated willingness-to-pay per visit of \$55 based on the <i>Loomis</i> (2005) meta-analysis (Table 3.5).	111
Table 4.1. Names and storage capacities of Willamette Project reservoirs. Source: USACE (2012).	131
Table 4.2. Model specifications. The first row provides the specification for the reference case. The rows following provide the changes for each alternative specification relative to the reference case model.	144

Optimizing Reservoir Operations to Adapt to 21st Century Expectations of Climate and Social Change in the Willamette River Basin, Oregon

Chapter 1: Introduction

1.1 Motivation

A central characteristic of many large river basins in the western US is the lack of spatial and temporal concurrence between the supply of and demand for water. Water sources typically are concentrated in forested mountain regions distant from municipal and agricultural water users, while precipitation is super-abundant in winter and deficient in summer. To cope with these disparities, systems of reservoirs were constructed throughout the western US, predominantly in the 1950s through 1970s [*Graf, 1999*]. The basins can be seen as coupled natural-human systems in which people and ecosystems have adapted to, and rely upon, environmental conditions as modified by the management of the reservoir system [*Poff et al., 1997; Graf, 2001*].

Flood damage reduction is achieved by maintaining unfilled storage capacity in reservoirs, which is used to temporarily store and release floodwaters during the winter flood season, reducing downstream flooding. Because the storage capacity of a reservoir cannot be used for both flood damage reduction and water storage at the same time, these two competing uses are traded off during the transition from the wet to the dry season, as the most important or dominant use of the reservoir shifts from reducing flood peaks to storing water. This tradeoff is expressed in the reservoir fill path given by a rule curve for reservoir operations that specifies the target level to which the reservoir is filled throughout the year [*USACE, 2011*]. Ideally a rule curve accurately captures the societal values placed on the competing uses of the reservoir, taking account of the levels and variability of expected streamflows. While reservoir rule curves

are usually established with limited data at the time the reservoir is built, climate change, population growth, and shifting social goals may alter the suitability of a rule curve over time [Chou and Wu, 2013; Vonk *et al.*, 2014; Yu *et al.*, 2014]. Because climate change and population growth may increase winter flood risk and exacerbate water scarcity in the western US [Barnett *et al.*, 2008; Elsner *et al.*, 2010; Salathé *et al.*, 2014], current reservoir operations deserve careful reexamination.

The objective of this work is to estimate the optimal rule curve for the system of reservoirs operated by the United States Army Corp of Engineers (USACE) in the Willamette River Basin (WRB), Oregon under current and future scenarios of climate change and population growth. In chapter 2 we estimate the expected value of reservoir operations for flood damage reduction using historical flood frequency information combined with spatially explicit estimates of the value of current and future structural development in the Willamette River floodplain simulated by the Willamette Water 2100 (WW2100) land transition model over the period from the present to 2100 using mid-range projections of future climate (MIROC5) and assumptions about future population growth.

In chapter 3 we estimate the value of stored water for summertime reservoir recreation in order to assess the cost of not being able to fill the reservoirs. To do this we rely on the response of recreational use day counts to variation in water levels at nine of the Willamette Project reservoirs over the period 2001 to 2011. We then compare the estimated value of stored water for recreation to the value of water for irrigated agriculture in the WRB, estimated in other studies, since this may be a competing use for stored water.

In chapter 4 we use a dynamic programming approach to social welfare maximization, and estimate the optimal fill path for the Willamette Project reservoirs over the transition from

the wet to the dry season based on expectations for streamflow and the values of flood damage reduction and stored water estimated in chapters 2 and 3. The findings of this analysis may contribute to better policy decisions regarding how reservoir management can adapt to the future changes in water supply and demand.

1.2 References

- Barnett, T. P. et al. (2008), Human-Induced Changes in the Hydrology of the Western United States, *Science*, 319(5866), 1080–1083, doi:10.1126/science.1152538.
- Chou, F. N.-F., and C.-W. Wu (2013), Expected shortage based pre-release strategy for reservoir flood control, *Journal of Hydrology*, 497, 1–14, doi:10.1016/j.jhydrol.2013.05.039.
- Elsner, M. M., L. Cuo, N. Voisin, J. S. Deems, A. F. Hamlet, J. A. Vano, K. E. B. Mickelson, S.-Y. Lee, and D. P. Lettenmaier (2010), Implications of 21st century climate change for the hydrology of Washington State, *Climatic Change*, 102(1-2), 225–260, doi:10.1007/s10584-010-9855-0.
- Graf, W. L. (1999), Dam nation: A geographic census of American dams and their large-scale hydrologic impacts, *Water Resources Research*, 35(4), 1305–1311, doi:10.1029/1999WR900016.
- Graf, W. L. (2001), Damage control: restoring the physical integrity of America’s rivers, *Annals of the Association of American Geographers*, 91(1), 1–27.
- Poff, N. L., J. D. Allan, M. B. Bain, J. R. Karr, K. L. Prestegard, B. D. Richter, R. E. Sparks, and J. C. Stromberg (1997), The Natural Flow Regime, *BioScience*, 47(11), 769–784, doi:10.2307/1313099.
- Salathé, E. P., A. F. Hamlet, C. F. Mass, S.-Y. Lee, M. Stumbaugh, and R. Steed (2014), Estimates of Twenty-First-Century Flood Risk in the Pacific Northwest Based on Regional Climate Model Simulations, *Journal of Hydrometeorology*, 15(5), 1881–1899, doi:10.1175/JHM-D-13-0137.1.
- USACE (2011), Willamette Valley - Operating the reservoirs, introducing the rule curve, Available from: http://www.nwp.usace.army.mil/Portals/24/docs/pubs/WV_water_mgmt_FS_2011a.pdf (Accessed 26 February 2015)
- Vonk, E., Y. P. Xu, M. J. Booij, X. Zhang, and D. C. M. Augustijn (2014), Adapting Multireservoir Operation to Shifting Patterns of Water Supply and Demand, *Water Resources Management*, 28(3), 625–643, doi:10.1007/s11269-013-0499-5.

Yu, P.-S., T.-C. Yang, C.-M. Kuo, J.-C. Chou, and H.-W. Tseng (2014), Climate change impacts on reservoir inflows and subsequent hydroelectric power generation for cascaded hydropower plants, *Hydrological Sciences Journal*, 59(6), 1196–1212, doi:10.1080/02626667.2014.912035.

Chapter 2: The Value of Reservoir Operations for Flood Damage Reduction under Future Scenarios of Climate, Population, and Development in the Willamette River Basin, Oregon

2.1 Abstract

Flood damage reduction, which requires reservoirs to maintain unfilled storage capacity, is the priority use of many reservoirs in the Pacific Northwest. However, both climate change and increased population are expected to exacerbate dry season water scarcity, implying a need to critically evaluate the status quo for reservoir operations. The recent availability of high resolution topographic information (LiDAR) and spatially explicit estimates of structural development in the Willamette River floodplain provide the opportunity to quantify expected flood damages under future scenarios of climate, population, and development. We estimated the value of flood damage reduction based on land use, the probability of floods, the depth of flood inundation, and reservoir capacity, for three scenarios of future land cover change in the Willamette River Basin simulated by the Willamette Water 2100 (WW2100) model using mid-range projections of future climate (MIROC5) and assumptions about future population growth. The estimated value of flood damage reduction at the weekly time scale ranged from a high in mid-January of \$304 million to \$1,284 million (depending on the rate of population growth), to near zero at the end of May. Estimated flood damages varied greatly, depending on changing weekly flood risk over the course of the winter and spring, as well as the assumed rate of population growth and associated assumptions in the WW2100 model about land use in the floodplain. The approach developed in this study provides a means of estimating flood damage reduction that may contribute better decisions regarding the tradeoff between flood damage reduction and other reservoir management objectives.

2.2 Introduction

Systems of reservoirs were constructed throughout the western US, predominantly in the 1950s through 1970s, to provide various benefits to water users [Graf, 1999]. Many of these reservoir systems were constructed primarily for the purpose of flood damage reduction. However, they also serve additional uses including recreation and the provision of downstream flow requirements during the dry summer season. Reservoir management reduces flood damages by maintaining unfilled storage capacity in reservoirs, which is used to temporarily store and release floodwaters during the winter flood season, reducing downstream flooding. Because the storage capacity of a reservoir cannot be used for both flood damage reduction and water storage at the same time, these two competing uses are traded off during the transition from the wet to the dry season, when the dominant use of the reservoir shifts from reducing flood peaks to storing water. This tradeoff is expressed in a rule curve for reservoir operations that specifies the target level to which the reservoir is filled throughout the year [USACE, 2011].

Climate change is expected to increase winter flood risk and reduce spring streamflow in the Pacific Northwest [Stewart *et al.*, 2005; Chang and Jung, 2010; Elsner *et al.*, 2010; Salathé *et al.*, 2014], coinciding with the transition period when reservoirs are filling according to a rule curve. Population growth and development in the floodplain also will affect future flood risk. As population increases, more land is expected to be converted to developed use [Jaeger *et al.*, 2014]. Resulting expansion of urban growth boundaries [Department of Land Conservation and Development, 2010] may increase the potential for flood damages, if new development occurs in the floodplain. The expected effects of climate change, population growth, and development imply a need to critically evaluate reservoir operations [Jaeger *et al.*, 2014] and the expected value of flood damage reduction.

The objective of this chapter is to quantify expected flood damages under various future scenarios of climate, population, and development in Willamette River Basin, Oregon. Using fine-scale topographic information (LiDAR), combined with historical flood frequency information, and spatially explicit estimates of current and future value of structural development in the Willamette River floodplain, we investigated the following research questions:

- 1) What is the magnitude and seasonal pattern of expected flood damages?
- 2) What is the spatial distribution of expected flooding and flood damages?
- 3) What is the value and seasonal pattern of flood damage reduction given current reservoir capacity?
- 4) How does the value and spatial distribution of expected flood damages change under alternate scenarios of climate and land cover?

2.3 Study Site

The Willamette River Basin (WRB) is the predominant sub-basin of the Columbia River located west of the Cascade Range (Figure 2.1). The Columbia River delivers the largest volume of streamflow from North America to the Pacific Ocean. While the WRB represents only 4% of the drainage area in the Columbia River Basin, it contributes approximately 15% of the total annual runoff [*Chang and Jung, 2010*]. The WRB contains the majority of Oregon's population. The state's three largest cities – Portland, Eugene, and Salem – are situated along the mainstem of the Willamette River, and they are experiencing more rapid population growth than the state or the nation [*Population Research Center, 2012*].

The study region consists of the mainstem of the Willamette River, which flows north through the Willamette Valley from the confluence of the Coast Fork and Middle Fork, just south of Eugene, to the mouth at the Columbia River at Portland (Figure 2.2). The WRB

encompasses an area of approximately 29,000 km², including parts of the Oregon Coast Range to the west and the Cascade Mountains to the east. Elevation in the basin ranges from close to sea level to over 3000 m. The climate is classified as Mediterranean with cool, dry summers and mild, wet winters. Annual precipitation ranges from 1000 mm in the Willamette Valley to 4000 mm at the crest of the Cascades, and approximately 80% of annual precipitation falls between October and May [*Chang and Jung*, 2010]. The topographic effects of the Coast Range and the Cascades result in a slight rain shadow in the western part of the basin and steep orographically controlled precipitation gradients in the Cascades. Up to half of the annual precipitation falls as snow in the high elevations of the Cascades [*Serreze et al.*, 1999] while a negligible proportion of snow occurs in the Coast Range and the Willamette Valley. Annual streamflow hydrographs are dominated by snowmelt in the High Cascades, by mixed rain and snow in the western Cascades, and by rain in the Coast Range. Streamflows in the Willamette River show the same seasonal pattern as precipitation: at the mainstem Salem gauge (USGS station number 14166000) more than half the annual flow occurs between November and February and approximately 87% of flow for the water year (Oct-Sep) occurs by the end of May.

The United States Army Corp of Engineers (USACE) operates a system of 13 reservoirs, including 11 storage reservoirs, known as the Willamette Project in the WRB. These dams were originally authorized by the 1938 Flood Control Act for the purposes of flood damage reduction and navigation [*USACE*, 2011; *USACE and OWRD*, 2011]. While flood damage reduction remains the priority use of the Willamette Project, the dams are now also managed to support additional authorizations including water quality, instream flows, irrigation, municipal water supply, hydropower, and recreation [*USACE*, 2009]. The reservoirs are located mainly in the southern portion on the basin, predominately on tributaries draining the Western Cascades

(Figure 2.2). The combined full pool storage capacity of the reservoirs have a just over 1.7 million acre-feet (2097 million cubic meters). During the winter flood season from December to February, the volume of water in the WRB reservoirs is kept at a minimum to provide storage capacity to buffer storm events. Starting February 1st the USACE begins adding water to storage with the goal of having the reservoirs full by May 20th, before the Memorial Day holiday. The reservoirs are kept as full as possible for recreation through the summer, with prioritized releases for downstream uses and flow requirements [USFWS, 2008; USACE, 2012]. The operation of the Willamette Project reservoirs has therefore altered the natural flow regime of the river [Poff *et al.*, 1997], lowering peak flows during the winter for flood damage reduction and increasing summer low flows [Hulse *et al.*, 2002].

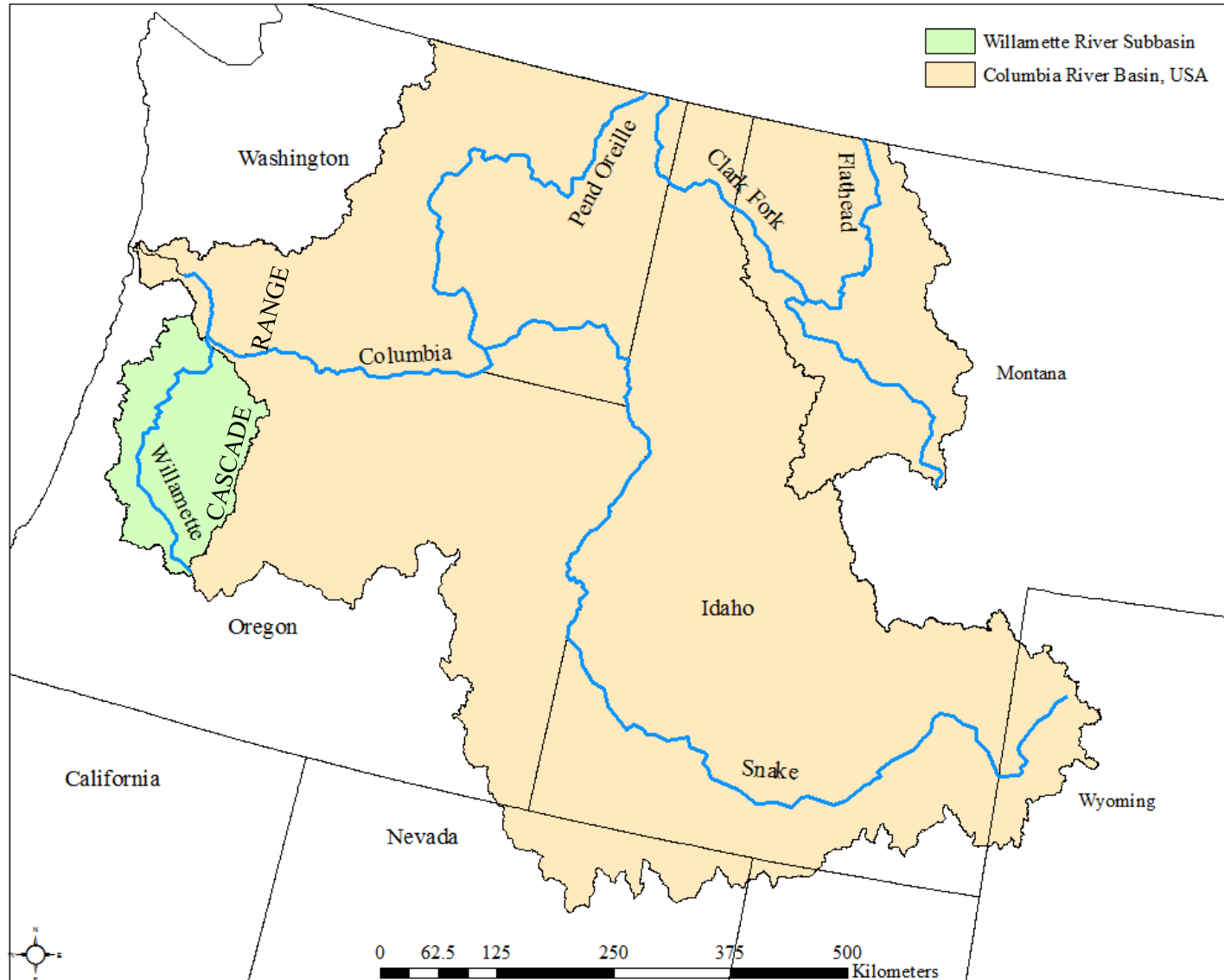


Figure 2.1 The extent of the Columbia River Basin within the United States, and the location of the Willamette River sub-basin.

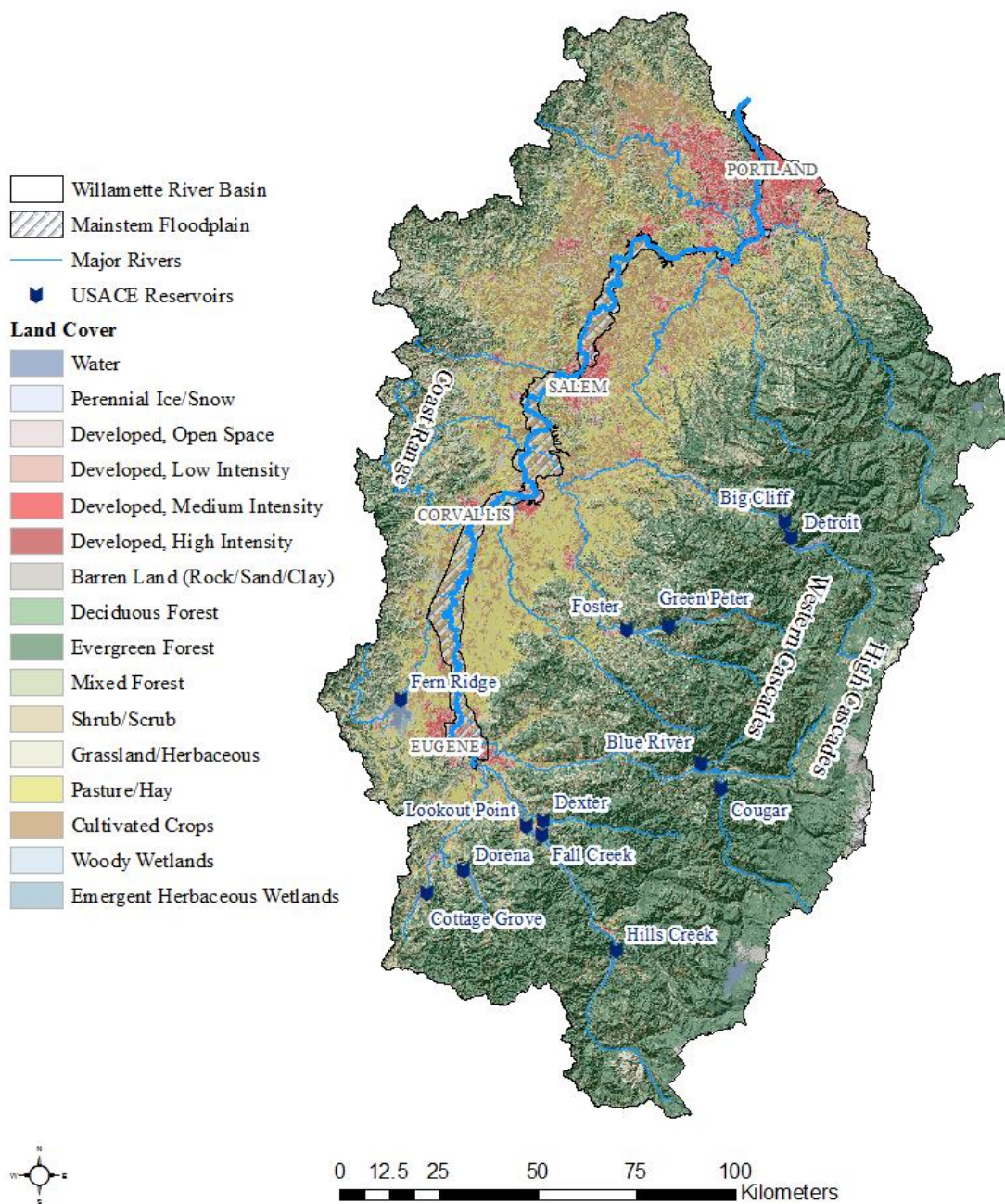


Figure 2.2. The Willamette River Basin, Oregon. The Willamette Project reservoirs are located in the southern portion on the basin, predominately on tributaries draining the Western Cascades. The mainstem of the Willamette River is indicated with a thicker line.

2.4 Methods

Conceptually, the value of flood damage reduction depends on the value and spatial arrangement of land use, the depth of inundation, the probability of floods, and the reservoir capacity. We developed a procedure for estimating the value of flood damage reduction that included the following steps: 1) estimate the depth and extent of flood inundation associated with flood stage, 2) evaluate flood damages associated with flood stage given expectations of future land cover, 3) assess flood frequency and timing, and 4) evaluate expected flood losses and the related value of reservoir management for flood damage reduction given the modeled flood inundation, assessed flood frequency distributions and the predicted land use.

2.4.1 Flood inundation mapping

A ‘bathtub’ analysis approach was used to estimate the depth and extent of inundation within the floodplain associated with flood stage [*River Design Group, 2012*]. In this approach the stage height of water in each reach of the river was associated with the lateral extent of the floodplain that is at right angles to it. The difference between the water elevation in the river reach and the associated topographic land surface represented the depth of flooding. In concept the floodplain is filled like a bathtub as the stage height in the river increases with flood severity. The effective floodplain was delineated according to the SLICES data layer developed by the Pacific Northwest Ecosystem Research Consortium [*Hulse et al., 2002*]. This data layer divides the floodplain into cross-sectional slices each of which corresponds to a 100 m section of the river. The outer edges of the floodplain slices were determined by the combined extents of historical flooding in 1861, 1890, 1943, 1964, and, 1996 adjusted to exclude areas that are known to be outside of the contemporary floodplain [*Hulse et al., 2002*].

Spatial analyses were conducted using ArcGIS, unless otherwise noted. The topographic surface within the floodplain was mapped using a digital elevation model (DEM) based on high-resolution light detection and ranging (LIDAR) data where available, supplemented with coarser-resolution data (≤ 10 m) as needed (Table 2.1). The River Design Group (<http://www.riverdesigngroup.com/>) provided the data originally acquired from the Oregon Department of Geology and Minerals Industries (DOGAMI) and the Puget Sound LiDAR Consortium (PSLC). Data from the USGS were obtained via the National Map Viewer (<http://viewer.nationalmap.gov/viewer/>). The DEMs were projected to a common coordinate system: Oregon Statewide Lambert Conformal Conic, NAD83 (HARN)/NAVD88 (Geoid03), with units of international feet. The PSLC and USGS data were also resampled to a resolution of 3 ft. The DEMs were then mosaicked together and clipped to the extent of the floodplain.

Hydrography data, including the stream network, the delineation of river reaches, and location of streamgauges were obtained from the National Hydrography Dataset (NHD). The Willamette River polyline was extracted from the stream network and clipped to the extent of the mainstem. To assign the appropriate elevation given by the DEM to each river reach polyline and its associated floodplain slice, the following modeling steps were taken:

1. The DEM was converted from a raster to polygon format. This allowed it to be interacted with the Willamette River polyline.
2. The DEM polygon layer from step 1 was intersected with the Willamette River polyline to assign the appropriate elevation from the DEM layer to each reach of the river.
3. The layer resulting from step 2 was spatially joined to the SLICES floodplain layer. This allowed the elevation of each stream reach to be associated with its floodplain slice.

4. In cases where a floodplain slice did not intersect the Willamette River polyline, it was manually assigned the elevation in the stream reach given by the closest floodplain slice that did intersect the Willamette River polyline.
5. The layer resulting from steps 3 and 4 was converted from a polygon to a raster format. The resolution of this raster was set to 3 feet to match the resolution of the DEM. The value of each grid cell in this raster is the elevation given by the DEM of the Willamette River in the reach associated with the location of the grid cell. On average the elevation along the Willamette River given by the DEM was found to be an estimated 7 feet below bankfull at the gauging stations.
6. Raster calculator was used to determine the difference in elevation between the layer obtained in step 5 and the DEM for every grid cell. This difference represents the change in associated river reach stage (height of water in the river reach) necessary for inundation to occur at the location of each grid cell in the floodplain.

Five flood stages covering the range of historical flooding were characterized based on the National Ocean and Atmospheric Administration's (NOAA) designation of flood category at each streamgauge (Table 2.2). The inundation depth in each grid cell of the DEM was given by the difference between the flood category river height in the corresponding section of the river and the DEM elevation. The associated volume of floodwater in the floodplain beyond bankfull capacity was estimated by summing the increased volume across all grid cells using the bankfull inundation surface as a baseline (Table 2.3).

Table 2.1. DEM datasets used to map the topographic surface of the Willamette River floodplain.

<u>Dataset Source</u>	<u>Area (acres)</u>	<u>Percent of Floodplain</u>	<u>Resolution</u>
DOGAMI	198,464	94.84	3 feet
PSLC	2,615	1.25	6 feet
USGS	6,971	3.33	1/9 arc-second
USGS	1,221	0.58	1/3 arc-second

Table 2.2. Flood category stages for stream gauges along the mainstem of the Willamette River. For each gauge the given flood stage heights mark the minimum increase in river surface elevation relative to the gauge datum, necessary to reach each flood category. Source: NOAA.

<u>Stream gauge (ID)</u>	<u>Location (Decimal Degrees)</u>	<u>Datum (NAVD29)</u>	<u>Flood Category Initiating Stage (feet)</u>				
			<u>Bankfull</u>	<u>Flood</u>	<u>Moderate Flood</u>	<u>Major Flood</u>	<u>Historical High</u>
Eugene (EUGO3)	44.05, -123.08	390.00	20.20	23.00		29.00	
Harrisburg (14166000)	44.27, -123.17	288.39	10.80	14.00		17.00	23.00
Corvallis (14171600)	44.57, -123.26	181.95	26.00	30.00	33.00	36.00	42.00
Albany (14174000)	44.64, -123.17	167.18	21.60	25.00	30.00	32.00	39.00
Salem (14191000)	44.94, -123.04	106.14	21.20	28.00		32.00	47.00
Oregon City, Above Falls (14207740)	45.35, -122.62	0.00	62.00	64.00		67.00	70.00
Oregon City, Below Falls (14207770)	45.36, -122.61	0.00	25.00	27.00	35.00	40.00	51.00
Portland (14211720)	45.52, -122.67	1.55	18.00	18.00	24.00	28.00	33.00

Table 2.3. River stage and associated floodplain inundation for each flood category relative to bankfull stage. The river stage for each flood category was defined as the average difference between bankfull stage and the lower bound of that category across the stream gauges (Table 2.2).

<u>Flood Category</u>	<u>River Stage</u> (Feet above bankfull)	<u>Inundated Floodplain</u> Area (acres)	<u>Inundation Volume</u> (KAF over bankfull)
Flood	3	19,824	294
Moderate Flood	5	33,361	523
Major Flood	9	59,766	1064
Historical High	17	88,179	2360

2.4.2 Flood damages

Flood damages accrue in a variety of ways (Figure 2.3), but this study evaluated tangible, direct, physical damages to developed parcels of land only. Tangible damages such as property damage can be directly measured, whereas intangible damages, such as emotional hardship cannot be readily measured. Tangible damages are further classified into direct and indirect damages. Direct damages result from physical contact with flood waters, and include physical and non-physical effects. For example, a factory may incur direct, physical damages in the form of structural damage from inundation, but direct, non-physical damages could also accrue through lost income if production is impacted. Indirect damages resemble non-physical damages except that they capture contingent effects in places that did not experience direct damages. Continuing with the factory example, suppliers of production inputs located outside of the flooded area may also experience income losses if demand for their goods is reduced as a result of decreased factory production.

This study attempted to assess only physical damages to structural and content property (together these are generally referred to as “improvements”) on land in developed use. Structural

damages refer to costs imposed on real property, i.e. items of permanence that are not moved, whereas content damages apply to movable personal property. Flood damages to structural and content property may depend on multiple variables including water depth, duration of inundation, velocity of flood waters, presence of debris, and sediment load. Of these variables, increasing water depth (inundation) is the one factor that is always expected to increase flood damages [U.S. Army Engineer Institute for Water Resources, 2013]. Therefore, in this study we define total damages as a function of the following variables:

$$\text{Damages} = f(\text{Inundation}, \text{Improvement Value}) \quad (2.1)$$

Improvement values were estimated to vary with market prices for lands that are, or could be developed based on three scenarios of the Willamette Water 2100 model (hereafter WW2100) [Jaeger *et al.*, 2014] for the years 2030, 2070, and 2100. In the WW2100 model, the WRB landscape consists of a set of delineated land units, which ranged in size from 2-20 hectares. A market price is estimated for each land unit in the WW2100 model for one of three uses: agriculture, forest, and developed according to methods described in Jaeger *et al.*, [2014]. We use the following WW2100 model scenarios (downloaded from <http://envision.bioe.orst.edu/StudyAreas/WW2100/Outputs/> on August 19, 2014):

1. The **reference case scenario** uses mid-range expectations for climate change and population growth, and assumes that institutional structures such as land-use planning policies are expected to continue operating in their present form. The climate expectations were based on projections made by the MIROC5 global climate model, which estimated that summer temperatures (July-September) in the Willamette Valley

will increase an average of 0.57 °C per decade between 2010 and 2100 and that there will be little change in precipitation [Jaeger *et al.*, 2014]. The population growth rate in the WRB was estimated at 1.4% per year between 2010 and 2100 based on projections from the Oregon Office of Economic Analysis [Jaeger *et al.*, 2014]. The urban growth boundary (UGB) land use policy in Oregon [Department of Land Conservation and Development, 2010] limits the conversion of agricultural and forest land to developed use. This scenario includes an assumption that the UGB expands only when 80% of the land within the boundary has been converted to the developed category.

2. The **high population growth scenario** increased the predicted rate of population growth to 2.7% per year between 2010 and 2100. In model output, higher population growth rates increased land values and led to additional shifts of land parcels from agriculture or forest to developed use categories, relative to the reference case.
3. The **relaxed Urban Growth Boundary (UGB) expansion scenario** reduces the threshold at which UGB expansion occurs from 80% under the reference case model to 70%. The reduced UGB threshold led to additional shifts of land parcels from agriculture or forest to developed use categories, relative to the reference case.

Land values from the WW2100 model were used to estimate structural values with the empirical relationship in equation 2.2 (Pearson $r=0.65$), which was estimated using detailed historical data for 10 counties in the Willamette Basin (Figure 2.4) described in *Jaeger et al.*, [2014]:

$$\frac{\text{Structural Value}}{\text{Land Value}} = 1.61 \quad (2.2)$$

Inundated flood areas (Section 2.4.1, Table 2.3) were intersected with structural values using a model built with ModelBuilder (ArcGIS, version 10.1). Spatial data were resampled to a grid resolution of 45 feet (14 meters). This spatial resolution corresponds to the smallest tax lot in the historical data used to define structural value, and balances the resolution of the estimated flood inundation and the resolution of land parcel delineation against computing efficiency. For each grid cell, the depth of inundation was determined from the inundation model, the value of structures was determined from the associated land parcel, and the damages for that grid cell were determined as a percent of the value for both the structure and contents depending on the depth of inundation as recommended by the USACE [*U.S. Army Engineer Institute for Water Resources*, 2013].

For each land parcel and flood category, the flood damage was defined as a proportion of structural and content values, based on simplified version of "depth-damage" relationships developed from flood loss records across the United States [*USACE*, 2000, 2003]. Because the land data from WW2100 does not specify the type of structures on land parcels, we averaged the six USACE damage curves (specified for various dwellings with and without basements) for both structural (Figure 2.5) and content damages (Figure 2.6). We simplified these relationships

by fitting cubic functions, adjusting the depth of inundation relative to the ground surface (Eq. 2.3 and 2.4, $R^2 > .99$), and further modifying each curve to set negative damages to zero when the water tables was more than 4 feet below the surface (Figure 2.5 and Figure 2.6). Damages from inundation levels greater than maximum depth given by the USACE curves (16 feet/5 meters) were set equal to the maximum: 80% for structural damage and just over 40% for content damage (Figure 2.5 and Figure 2.6). Total flood damages were assessed for the entire Willamette floodplain for five flood categories and three scenarios, in each of the three periods ($n=5 \times 3 \times 3=45$).

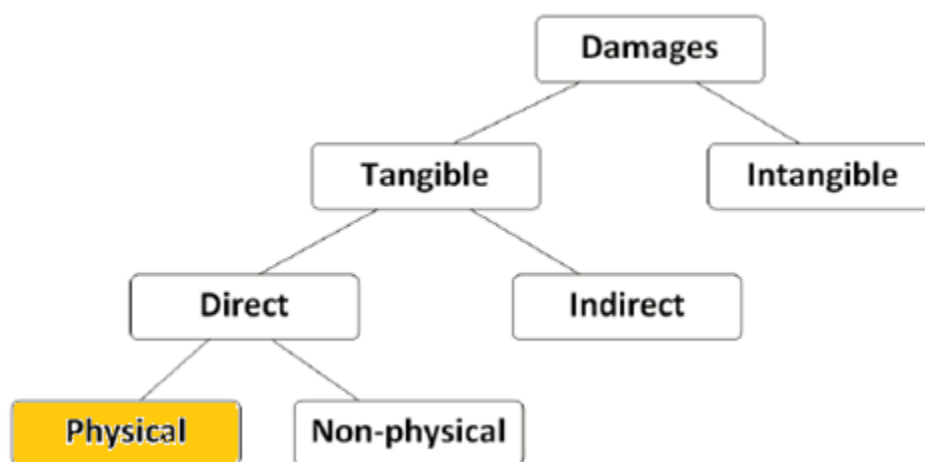


Figure 2.3. Classification of flood damages. The highlighted box indicates the type of damages evaluated in this study. Source: U.S. Army Engineer Institute for Water Resources (2013).

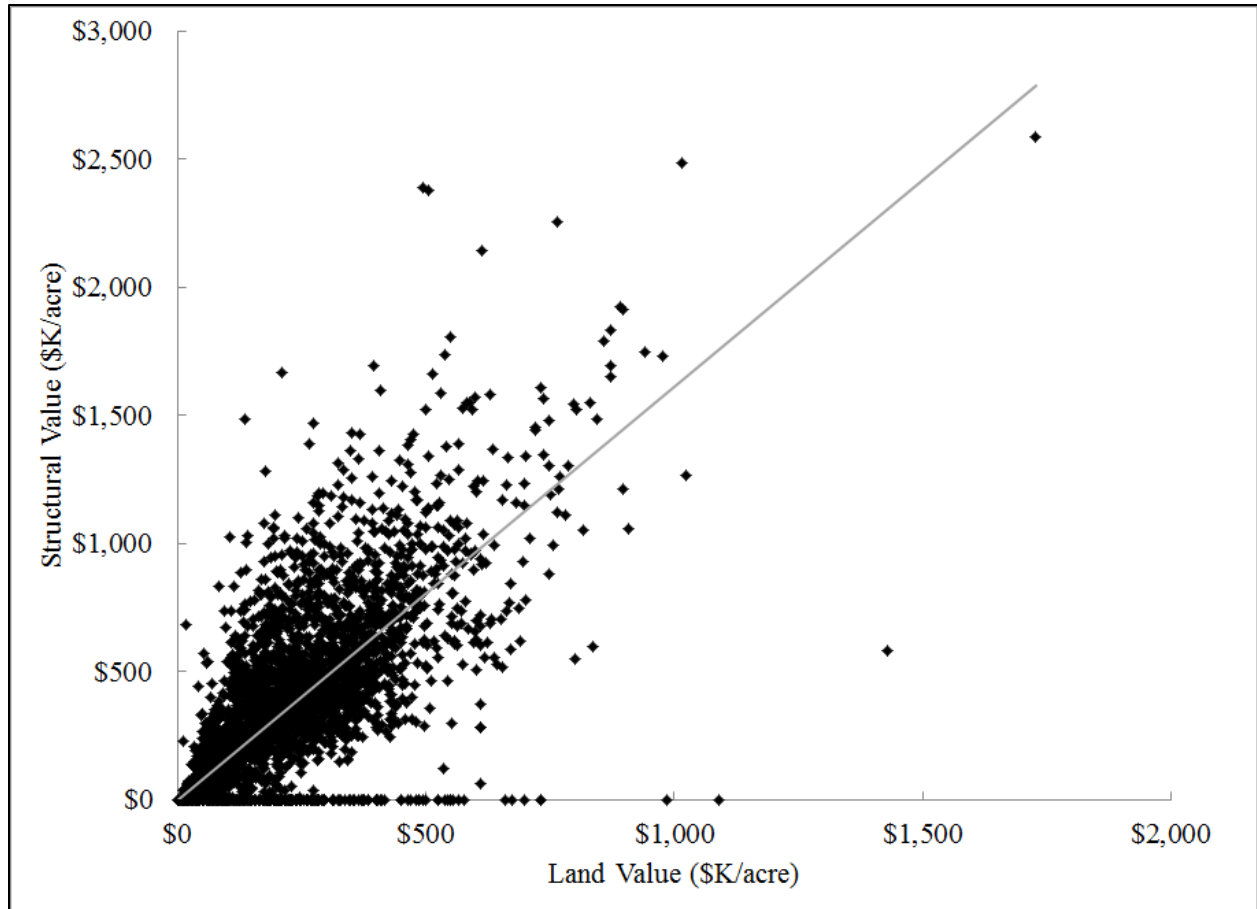


Figure 2.4. The estimated relationship between structural values and land values (Pearson $r=0.65$) based on detailed historical data for 10 counties in the Willamette Basin described in *Jaeger et al.*, [2014].

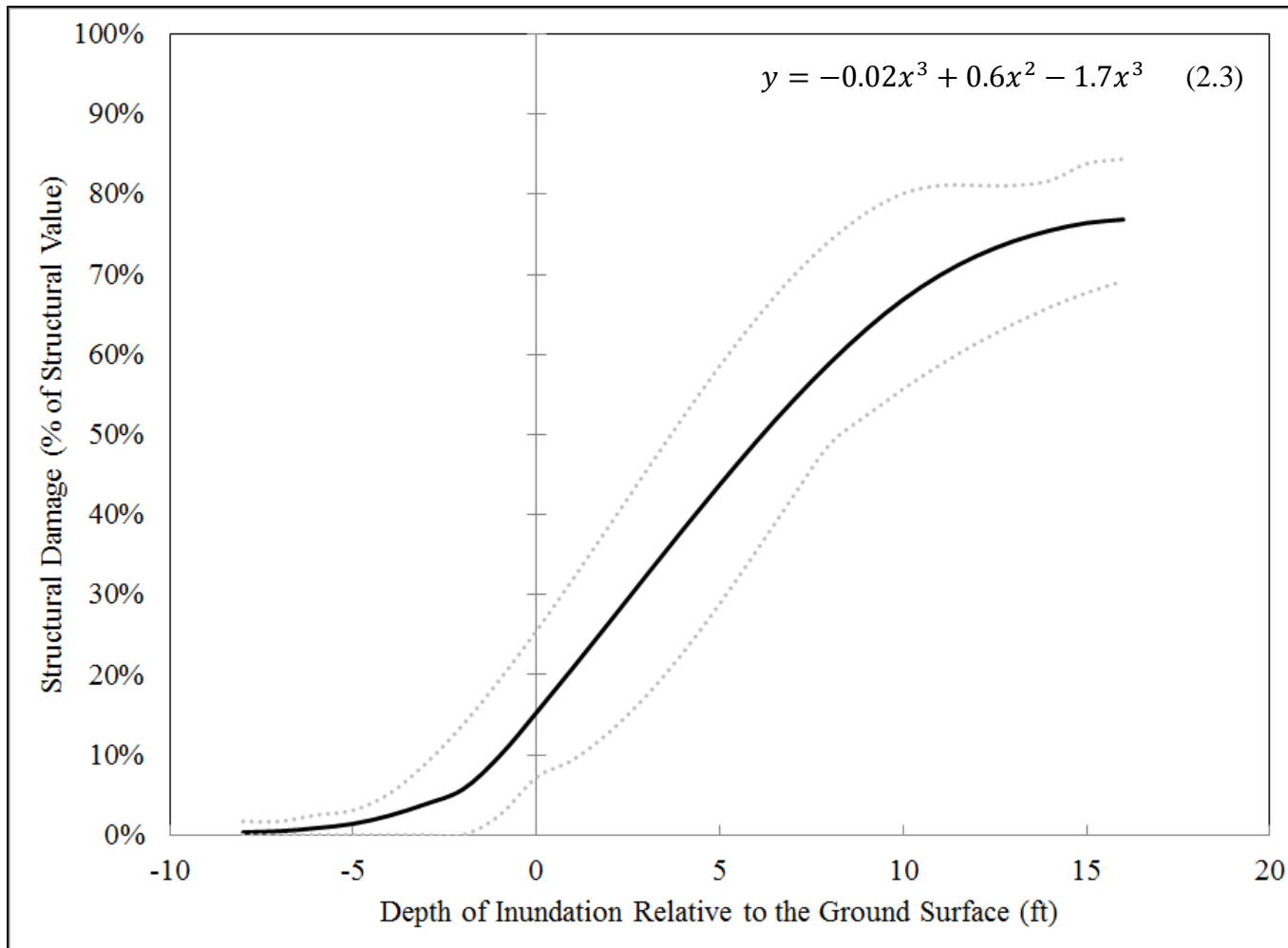


Figure 2.5. Depth-damage curve for structural value losses. The average (solid line) of the depth-damage curves provided by the USACE was used in estimating structural damage as a percent of structural value. The dotted lines show the range of damages given by the USACE curves. The water depth is given relative to the first (ground) flood of a structure.

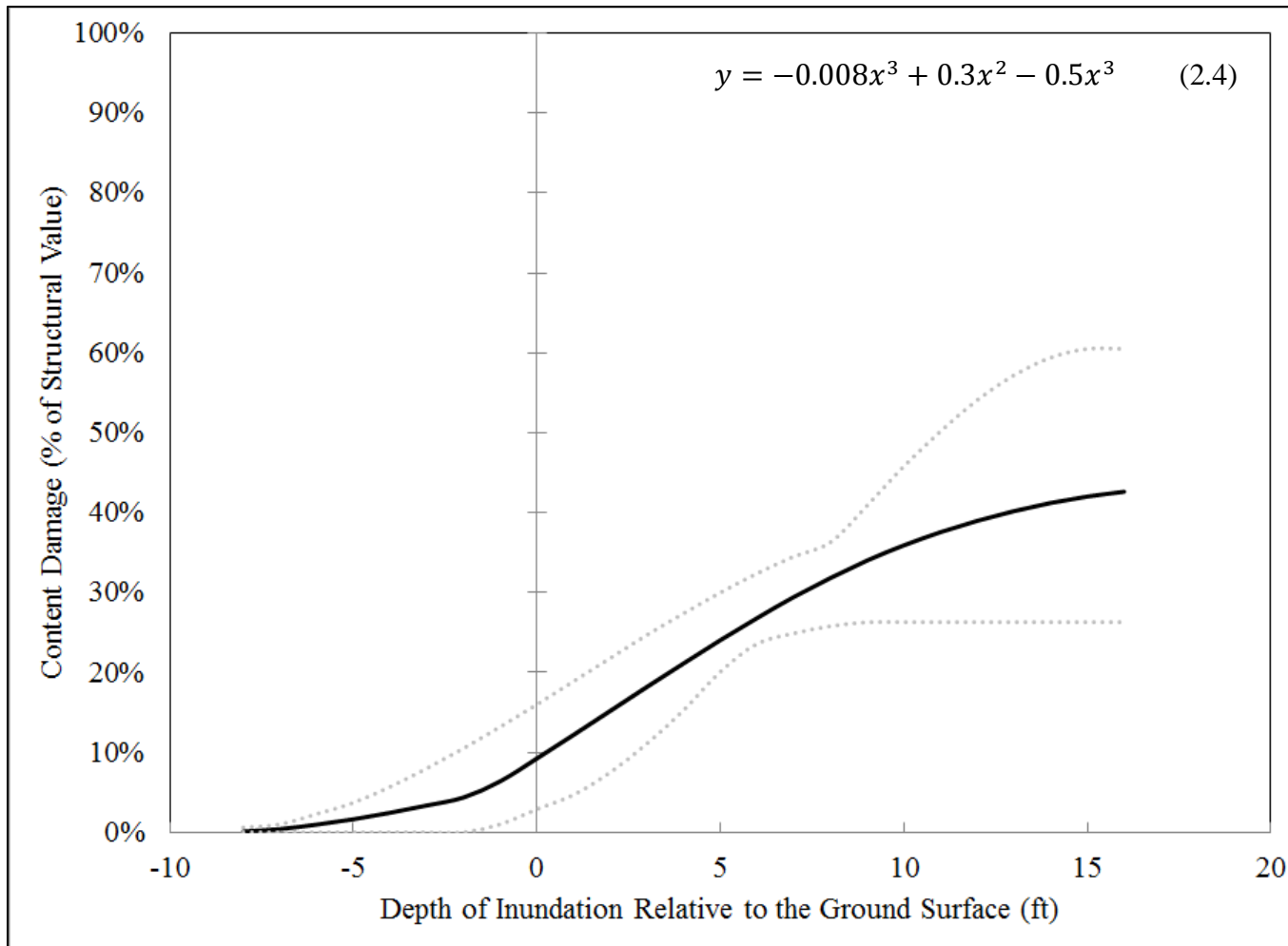


Figure 2.6. Depth-damage curve for content value losses. The average (solid line) of the depth-damage curves provided by the USACE was used in estimating content damage as a percent of structural value. The dotted lines show the range of damages given by the USACE curves. The water depth is given relative to the first (ground) flood of a structure.

2.4.3 Flood frequency analysis

Since we aim to understand how expected flood damages change over the course of a season for the purposes of reservoir management, we estimated flood probabilities by week for the 20-week period from Jan 1st – May 20th, the timeframe over which water managers are balancing the benefits of flood protection against future benefits from stored water. Log-Pearson Type III distributions were used to estimate flood frequency, as recommended by the U.S. Water Advisory Committee on Water Data [*U.S. Interagency Advisory Committee on Water Data*, 1982]. The distributions were estimated using daily streamflow data from the gauge at Salem (USGS gauge 14191000) because this gauge 1) is downstream of all Willamette Project reservoirs, 2) has a rating curve to relate discharge to stage height, and 3) is unaffected by tides. Two periods of record: the full historical record (98 observations over the period 1910-2013) and the period following the completion of all the Willamette Project reservoirs (45 observations over the period 1969-2013), were used to fit the distributions. The skewness coefficients, which were determined from the data records, tended to trend upward over the course of the season (Figure 2.7). For the weeks in January and early February, when annual peak flows often occur, the skew estimates derived from the full historical record were consistent with published estimates for annual peak flows in the region [*U.S. Interagency Advisory Committee on Water Data*, 1982; *Richard M. Cooper*, 2005]. The divergence between the skew estimates prior to February for the two data periods likely reflects the reduction in flood peaks resulting from reservoir management. Relative to the full period of record, post-dam flood frequency distributions are shifted towards the left with a disproportionate reduction in flood stages (Figure 2.8). Flood stage probabilities also decline faster than probabilities of lower flows over time from winter to early summer (Figure 2.9; Figure 2.10).

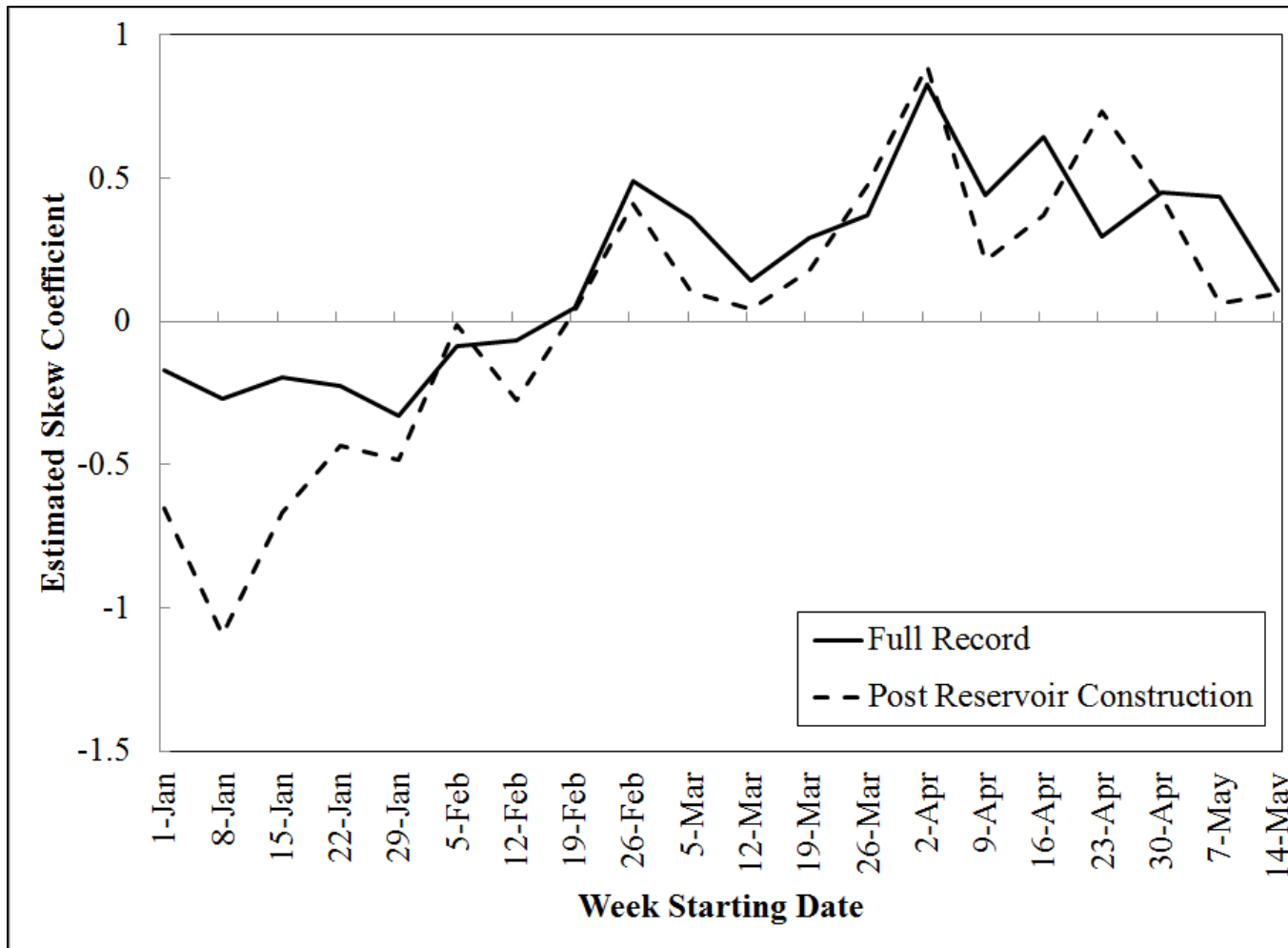


Figure 2.7. Estimated log-Pearson Type III skewness coefficients.

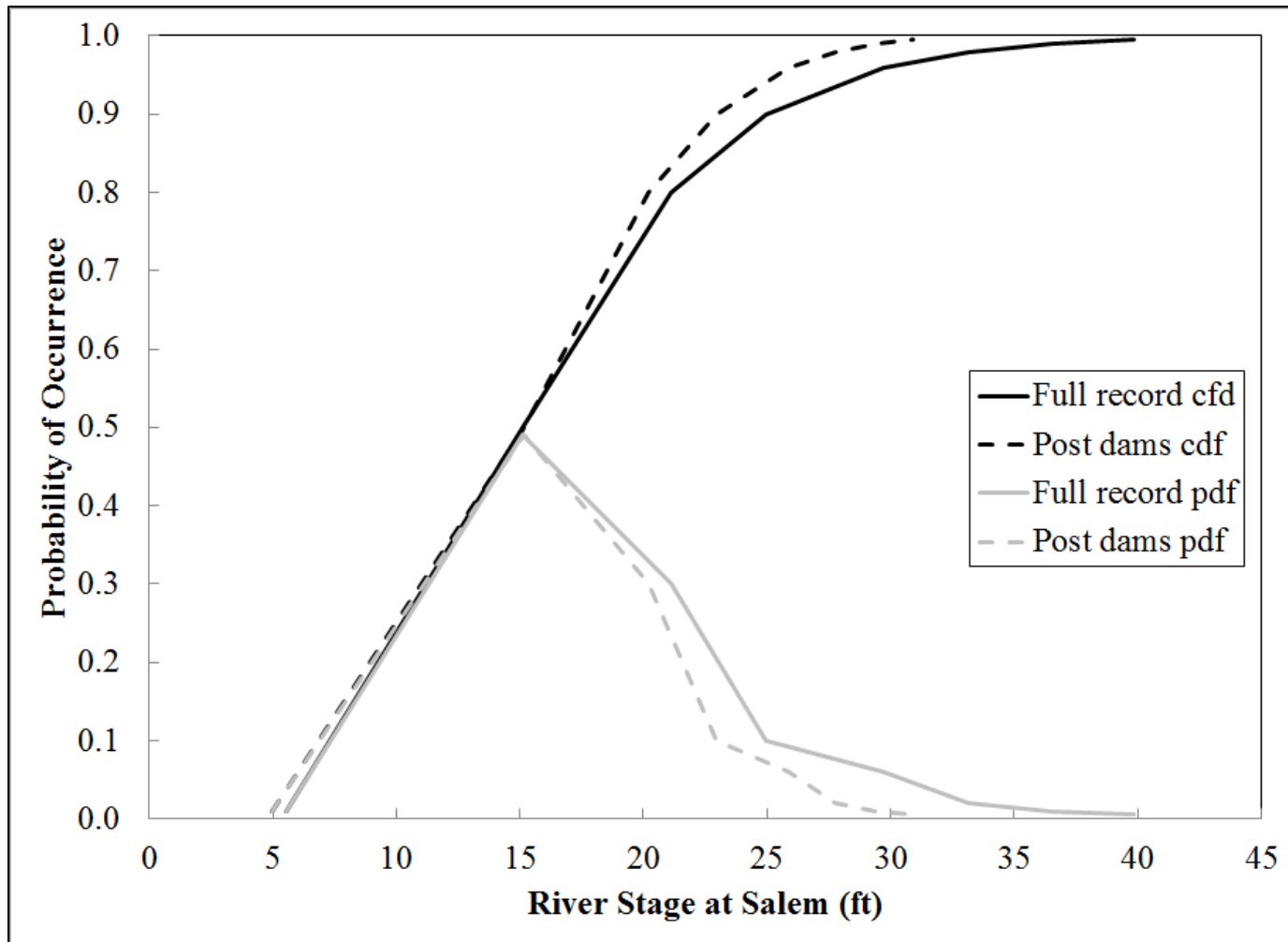


Figure 2.8. Comparison of probability and cumulative density functions derived from the full historical record and the post dam construction period for the week starting Jan 1st.

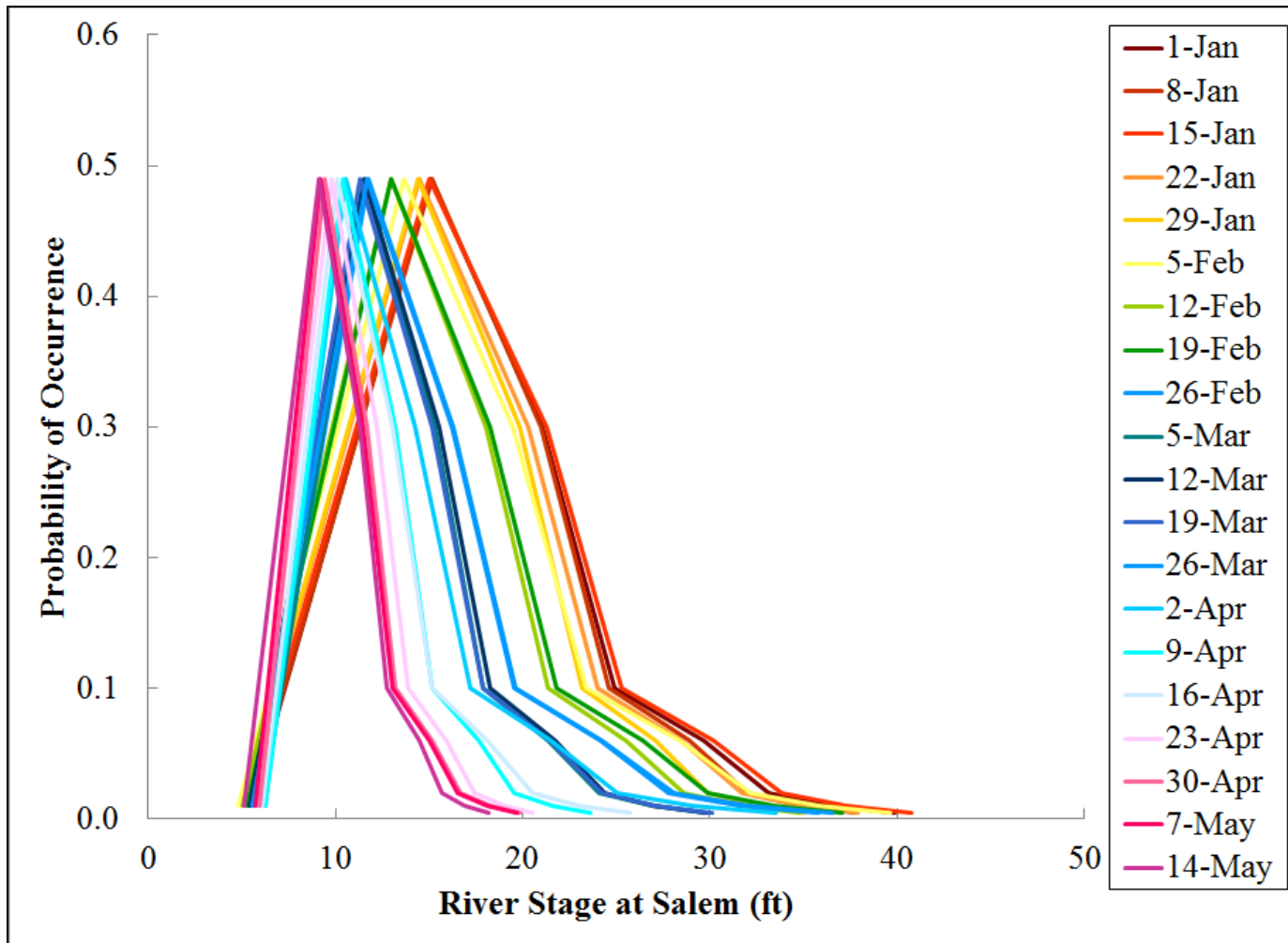


Figure 2.9. Probability density functions by week Jan 1st-May 20th derived from the full historical record.

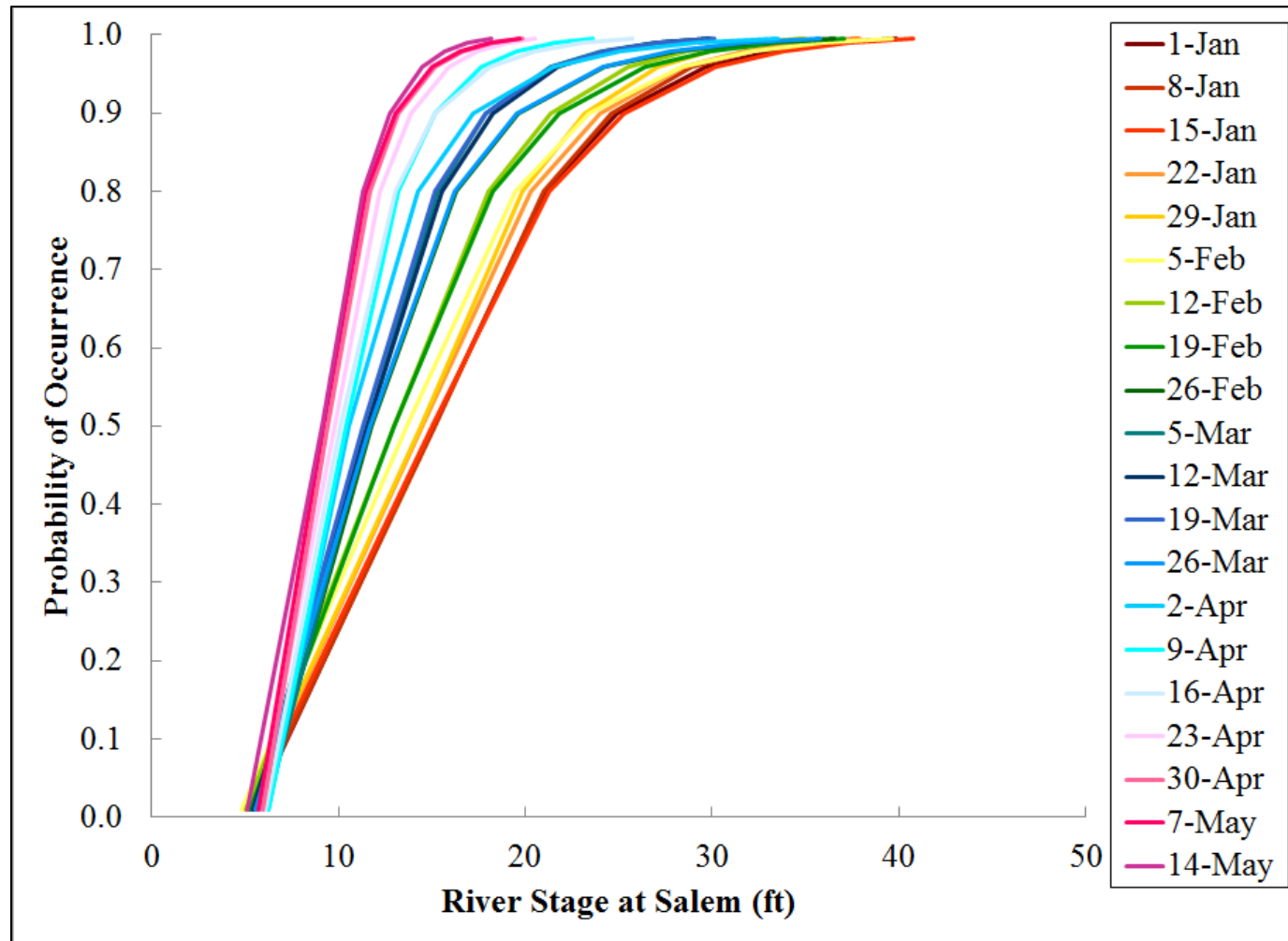


Figure 2.10. Cumulative density functions by week Jan 1st-May 20th derived from the full historical record.

2.4.4 The value of flood damage reduction

The expected value of flood damage reduction for each week (for the period Jan 1st – May 20th) was calculated by combining estimated total damages for each flood category (Table 2.3) and weekly flood frequency distributions (Figure 2.9). Because reservoir operations reduce downstream inundation by storing flood waters, the value of flood damage reduction operations was defined as the flood costs that could be averted by using available reservoir capacity to reduce inundation. This value, the marginal cost (MC_i) of increasing flood stage (i), was calculated as the change in estimated total damages (TD) with respect to the associated increase in floodplain inundation volume (V):

$$MC_i = \frac{\partial TD}{\partial V} \quad (2.5)$$

The expected marginal cost, $E(MC_t)$ of flooding in each week (t), was calculated as the sum of marginal costs for each flood category stage weighted by its likelihood of occurrence (P_{it}), as given by the flood frequency distribution for that week:

$$E(MC_t) = \int_{i=1}^{i=i(max)} MC_i \times P_{it} \quad (2.6)$$

The expected value of flood damage reduction using reservoir operations in each week, $E(AD_t)$, was then estimated as:

$$E(AD_t) = \int_{i=1}^{i=i(max)} P_{it} \cdot \int_{V_i-C_k}^{V_i} MC_i \cdot dv \quad (2.7)$$

Where V_i is the volume of floodplain inundation associated with flood stage (i) and C_k is the reservoir capacity available for storing flood waters.

We want to estimate flood damage reduction for purposes of evaluating the tradeoffs between storage and flood prevention (addressed in chapter 4). To do this a parametric relationship was estimated as described in Eq. 2.8 where the dependent variable (L) was defined as in the expected loss in flood damage buffering associated with increasing the reservoir fill level (s) each week (t):

$$L_t = \alpha * (s)^2 * (1 - \beta)^t * (1 - \gamma)^{t^2} * (1 - \rho)^{t^3} \quad (2.8)$$

Where: $t = 0, 1, \dots, 19$

The functional form ensures that losses 1) are less than or equal to zero, 2) increase monotonically as the reservoir fills, and 3) can change over time at a flexible rate. For each scenario the value of α was estimated using an OLS regression equation for loss in flood damage buffering with increasing reservoir fill for the week when the highest expected flood damages were estimated to occur. A value of α was also determined as a historical estimate for 2000 by extrapolating the reference scenario values of alpha from 2030 and 2070. The values of β , γ , and

ρ were estimated using the excel solver functionality to minimize the model sum of squared errors.

2.5 Results

2.5.1 Flood inundation mapping

The mapped inundation areas for bankfull stage at Corvallis and Salem show that ponds and side channels of the river were filled (Figure 2.11, Figure 2.12). The water table was also within 8 feet of the surface under some areas currently in agricultural and open space use (mapped orthoimagery from the National Map Viewer dated 2012), with above ground ponding occurring in parts. At Portland, inundation was confined to the river channel at bankfull stage, and in the surrounding floodplain the water table generally remained more than 8 feet below the surface (Figure 2.13). Relative to bankfull stage, inundation mapping of the flood stage category showed expanded areas of ponding on agricultural and open space areas at Corvallis and Salem. At Portland the water table was predicted to rise within 8 feet of the surface in a few small areas of urban development (Figure 2.14, Figure 2.15, Figure 2.16).

Inundation maps of the moderate flood stage category show the water table within 8 feet of the surface in small areas of structural development at Corvallis and Salem (Figure 2.17, Figure 2.18, and Figure 2.19). At the major flood stage category, inundation maps show the water table within 8 feet of the surface in large areas of the floodplain, and some areas of ponding, including in areas of structural development, at Corvallis, Salem, and Portland (Figure 2.20, Figure 2.21, and Figure 2.22). At Corvallis and Salem inundation maps at the major flood category show widespread inundation of secondary river channels, low-lying agricultural areas and open spaces. At the historical high flood category inundation maps show the water table within 8 feet of the ground surface across most of the floodplain, excepting some high elevation

areas, at Corvallis, Salem, and Portland (Figure 2.23, Figure 2.24, and Figure 2.25). Historical high flood category inundation maps show extensive inundation of agricultural and open space at Corvallis and Salem, as well as inundation of areas with structural development near the Mary's River and along the I-34 highway east of Corvallis, in west Salem, and in a large portion of downtown Portland.

According to the maps compiled by Hulse et al., [2002], the 1996 flood inundated agricultural fields, open spaces and a few developed areas at Corvallis (Figure 2.26), Salem (Figure 2.27) and Portland (Figure 2.28). The 1996 flood crested half a foot above moderate flood stage at Corvallis, a little over three feet above major flood stage at Salem, and half a foot above major flood stage at Portland. The inundation map for the major flood category shows less surface inundation than the 1996 flood maps in agricultural fields and open space around Corvallis and Salem, but in many of these areas the inundation maps show the water table to be within 8 feet of the surface. At Corvallis the 1996 flood also inundated some areas of development near the Mary's River tributary and along the I-34 highway where the inundation maps show a water table within 8 feet of the surface. The inundation maps, which are restricted to the Willamette mainstem floodplain boundary, also do not show flooding along the Mary's River tributary evident in the 1996 flood maps. At Salem the 1996 flood maps show surface flooding in developed areas in north east Salem, which do not appear in inundation maps for a major flood. Conversely, the inundation maps for a major flood in west Salem show the water table within 8 feet of the surface, but these areas are not shown as flooded in the 1996 flood maps. At Portland the 1996 flood map shows surface flooding to be largely confined to the river channel, with a few small areas of surface water near the banks of the river. The inundation map for a major flood at Portland shows the water table within 8 feet of the surface or just above the

surface in these areas, but it also shows that the water table was within 8 feet of the surface over a much larger area of the floodplain with structures than was shown as flooded in the 1996 flood maps (Figure 2.28).

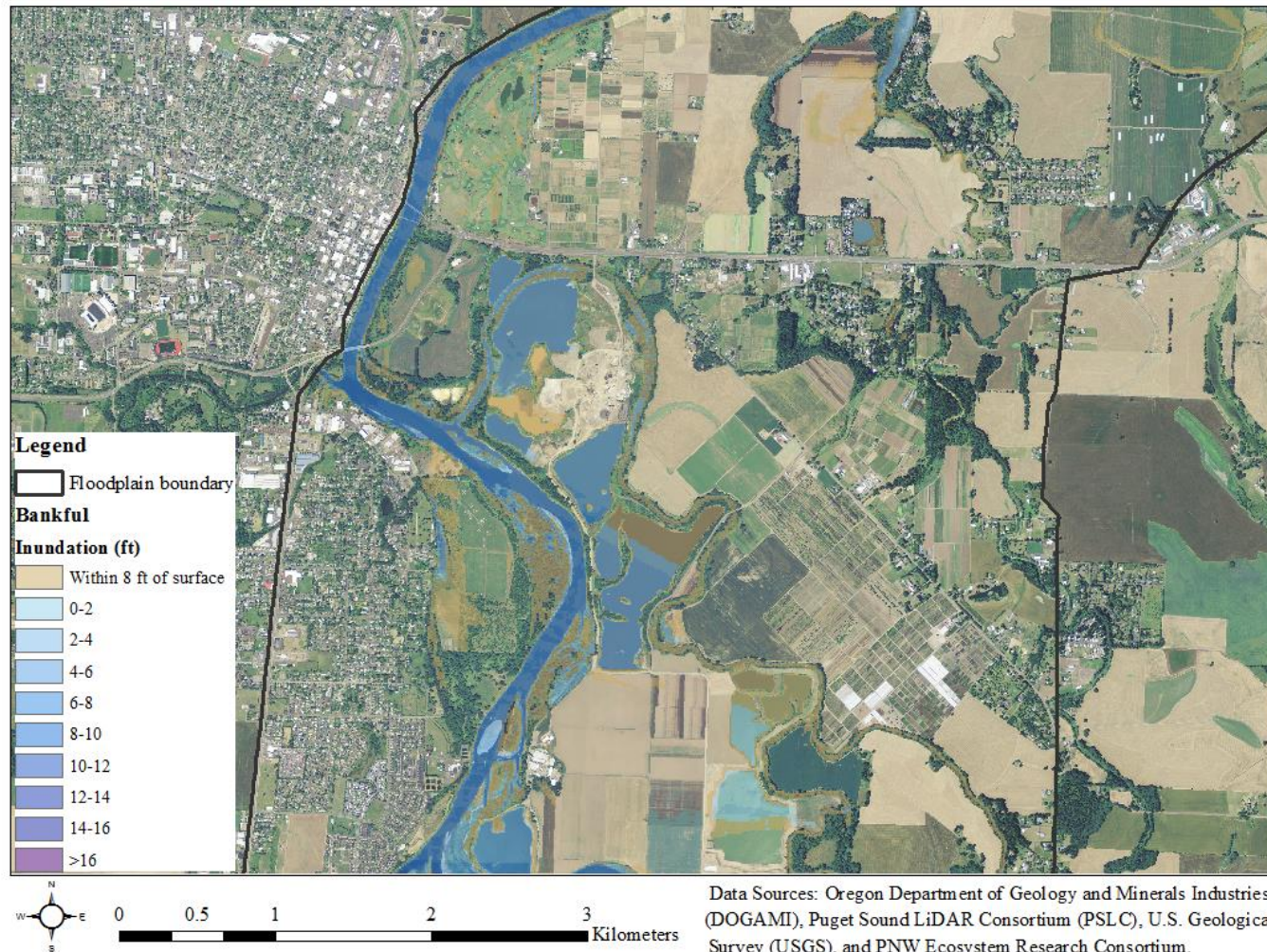


Figure 2.11. Inundation within the Willamette River's mainstem floodplain at Corvallis estimated at the bankfull stage flood category. Orthoimagery as of 2012 from the National Map Viewer.

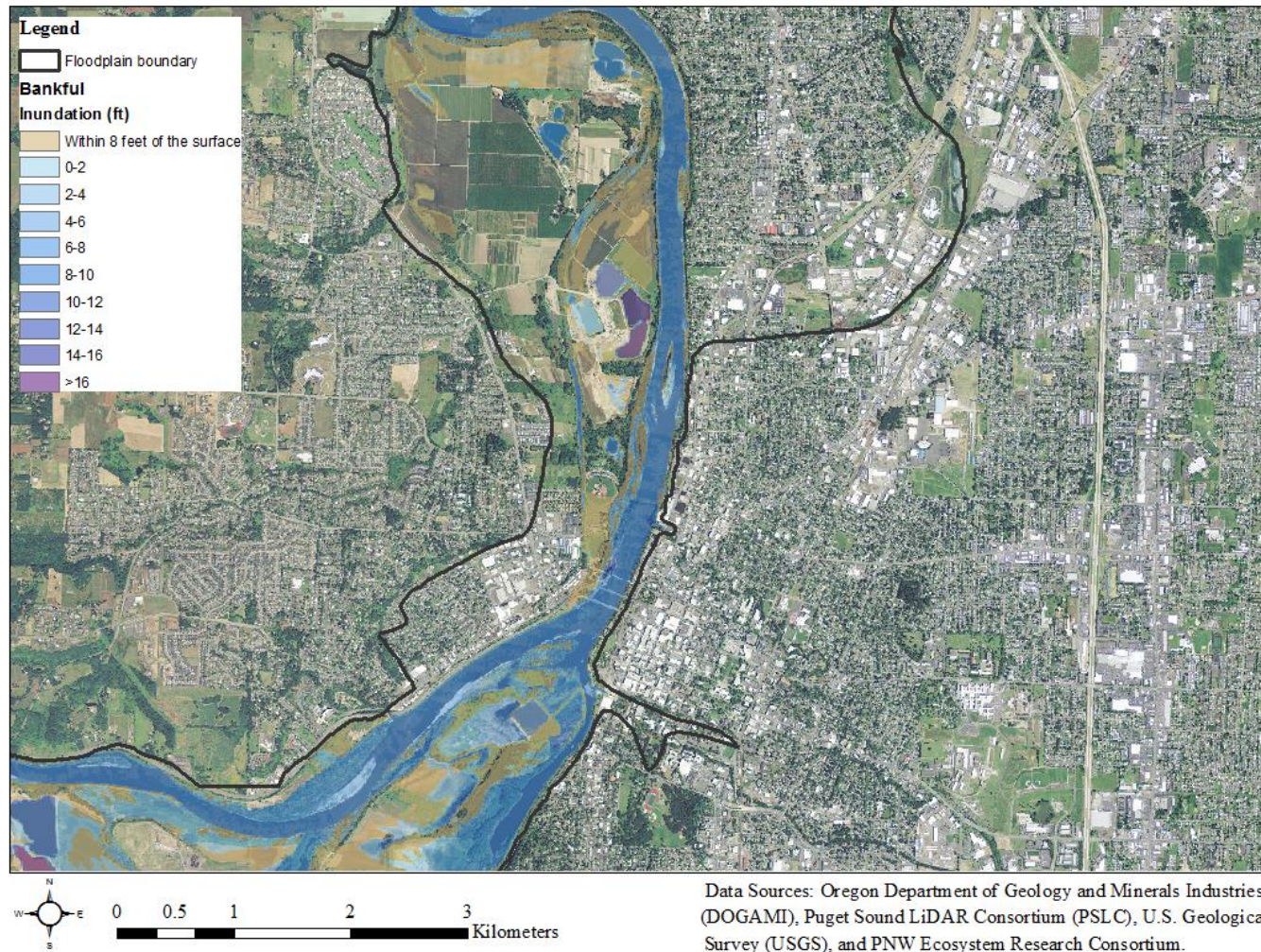


Figure 2.12. Inundation within the Willamette River's mainstem floodplain at Salem estimated at the bankfull stage flood category. Orthoimagery as of 2012 from the National Map Viewer.

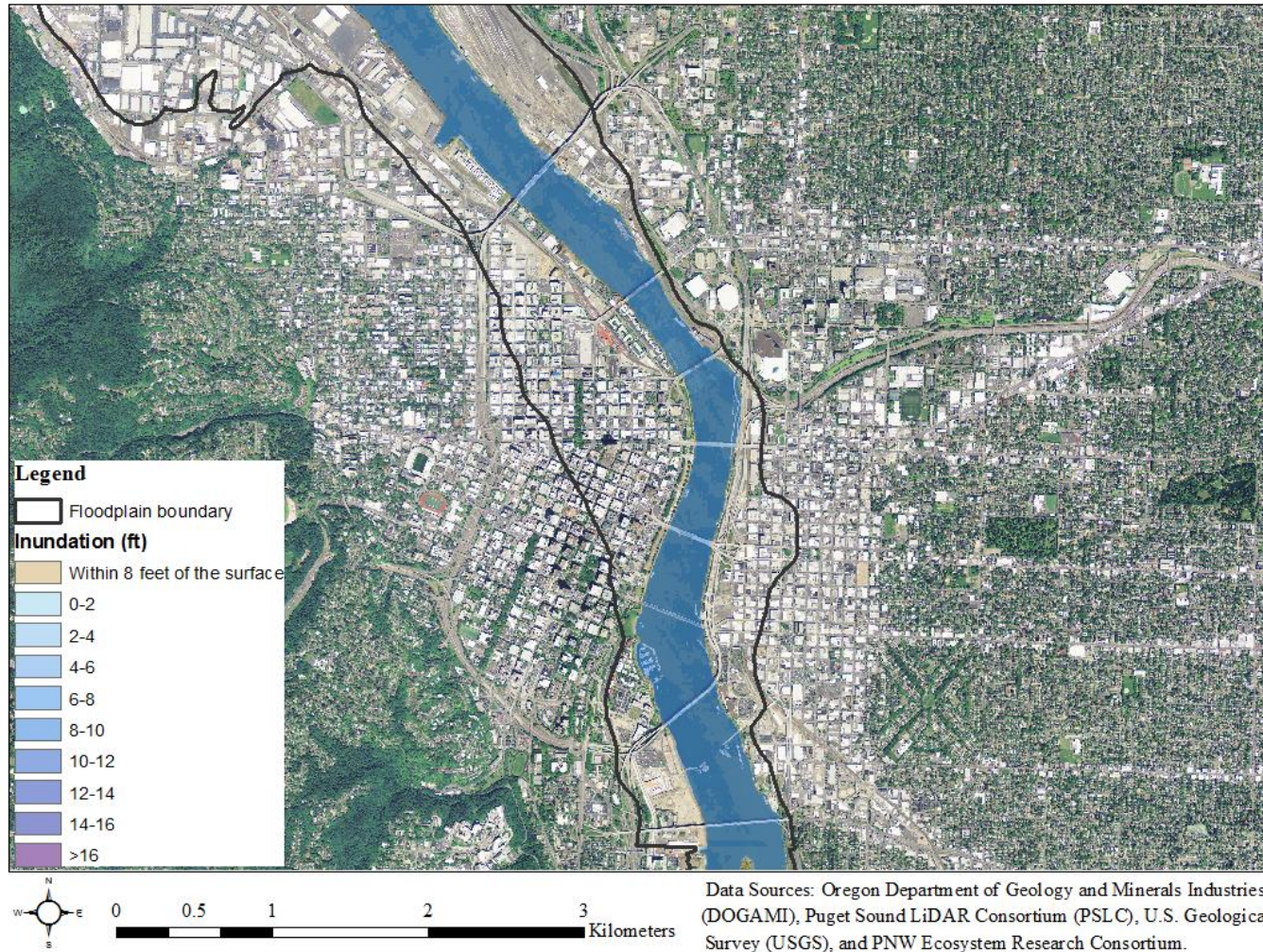


Figure 2.13. Inundation within the Willamette River's mainstem floodplain at Portland estimated at the bankfull stage flood category. Orthoimagery as of 2012 from the National Map Viewer.

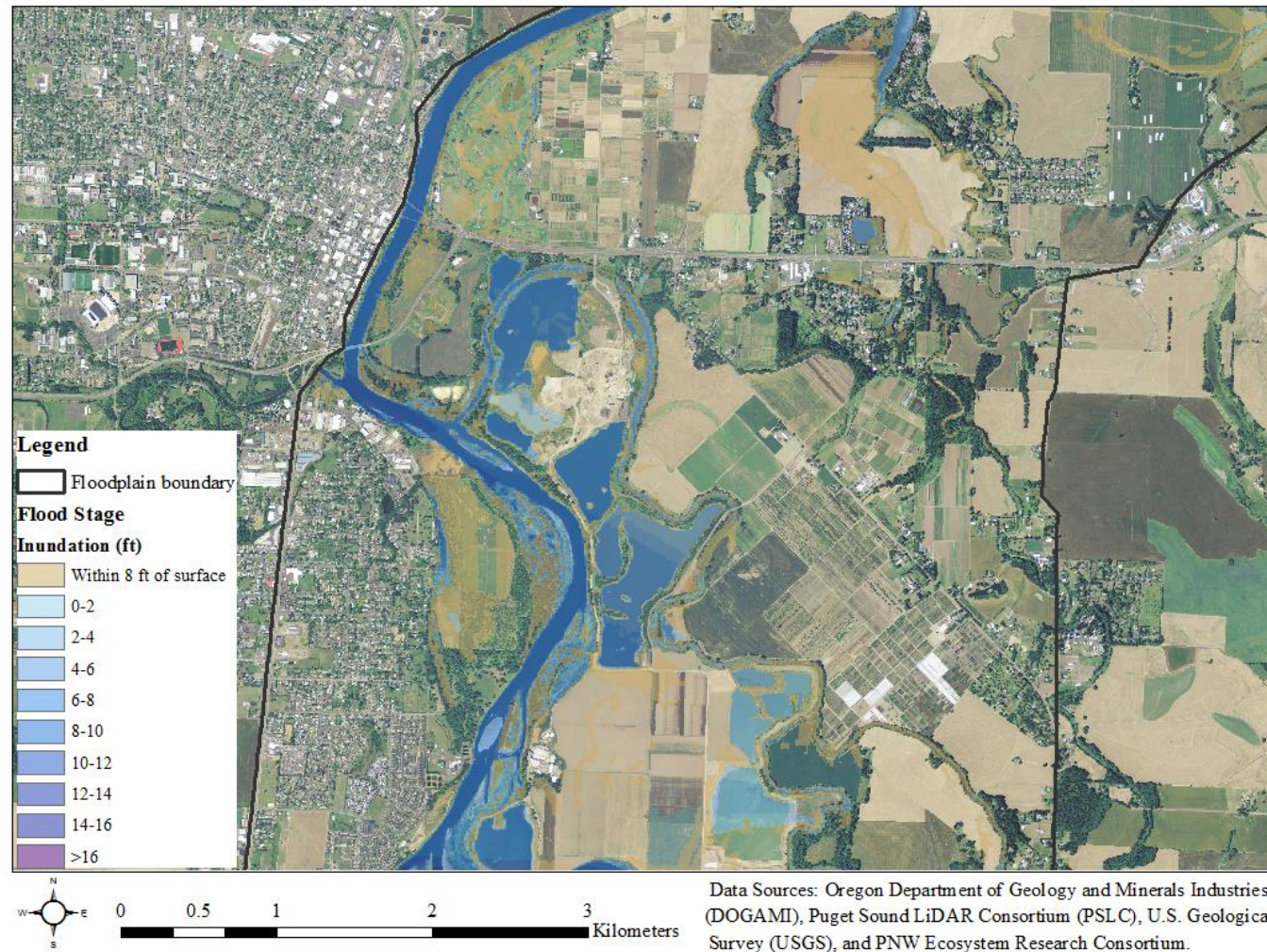


Figure 2.14. Inundation within the Willamette River's mainstem floodplain at Corvallis estimated at the flood stage category. Orthoimagery as of 2012 from the National Map Viewer.

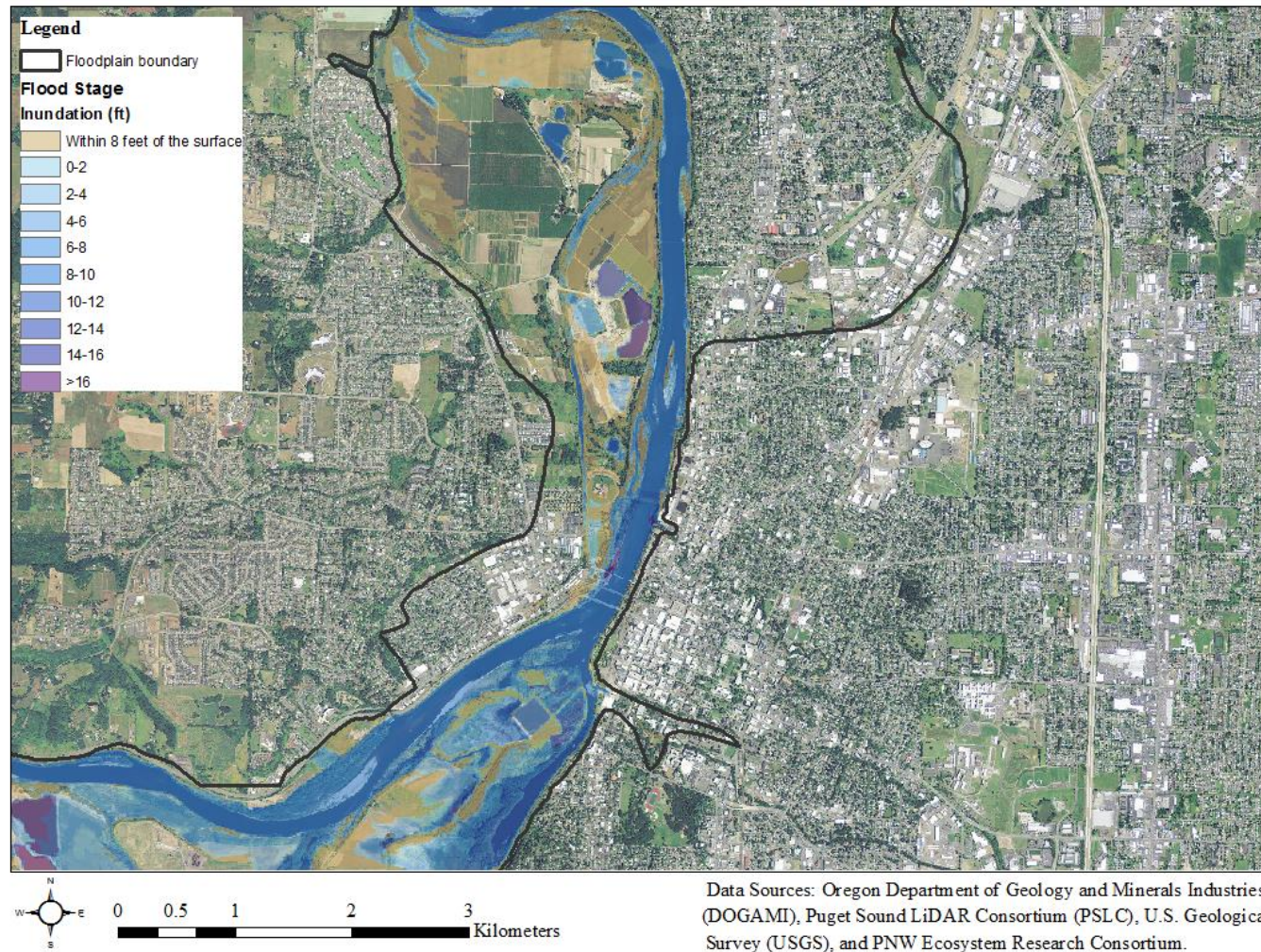


Figure 2.15. Inundation within the Willamette River's mainstem floodplain at Salem estimated at the flood stage category. Orthoimagery as of 2012 from the National Map Viewer.

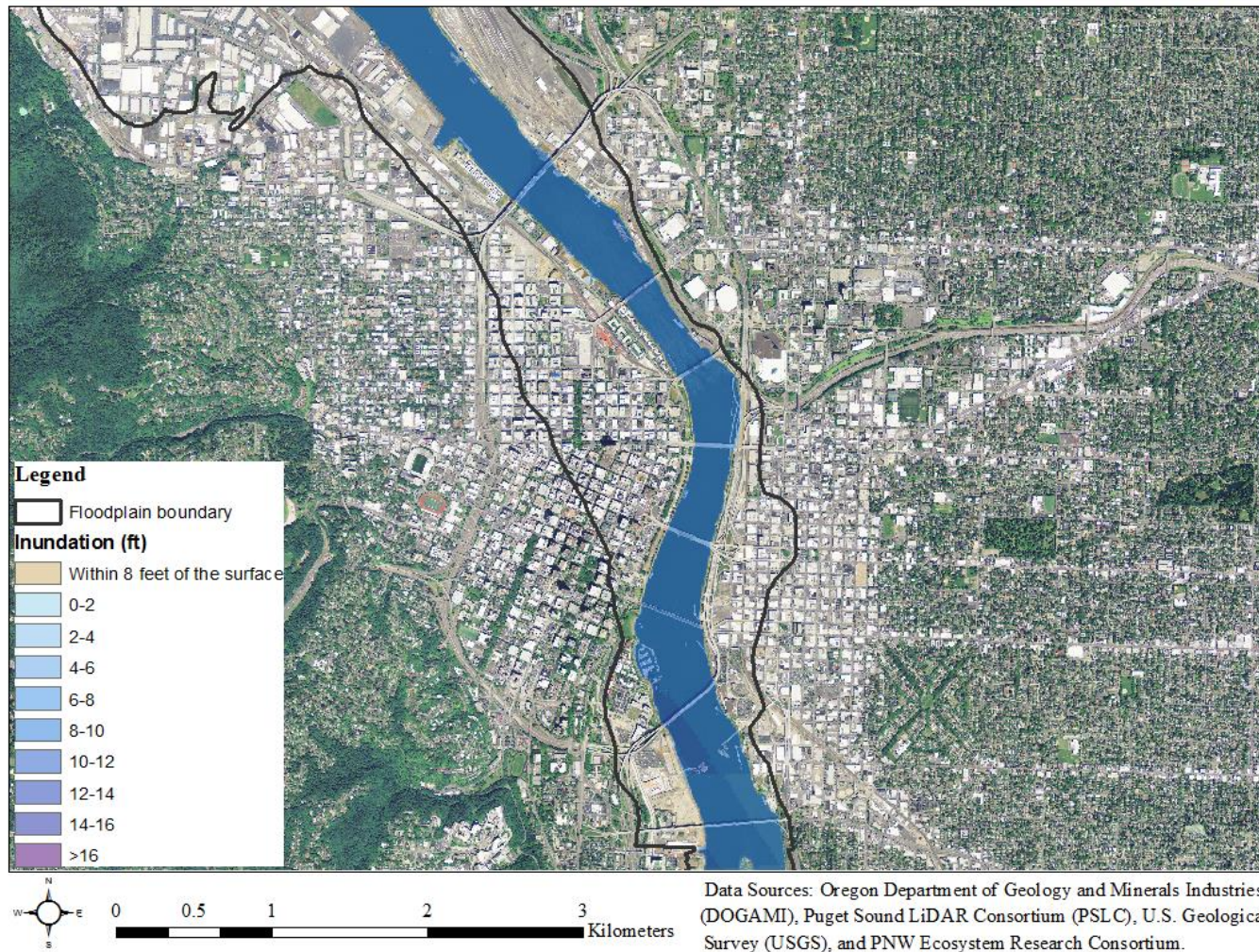


Figure 2.16. Inundation within the Willamette River's mainstem floodplain at Portland estimated at the flood stage category. Orthoimagery as of 2012 from the National Map Viewer.

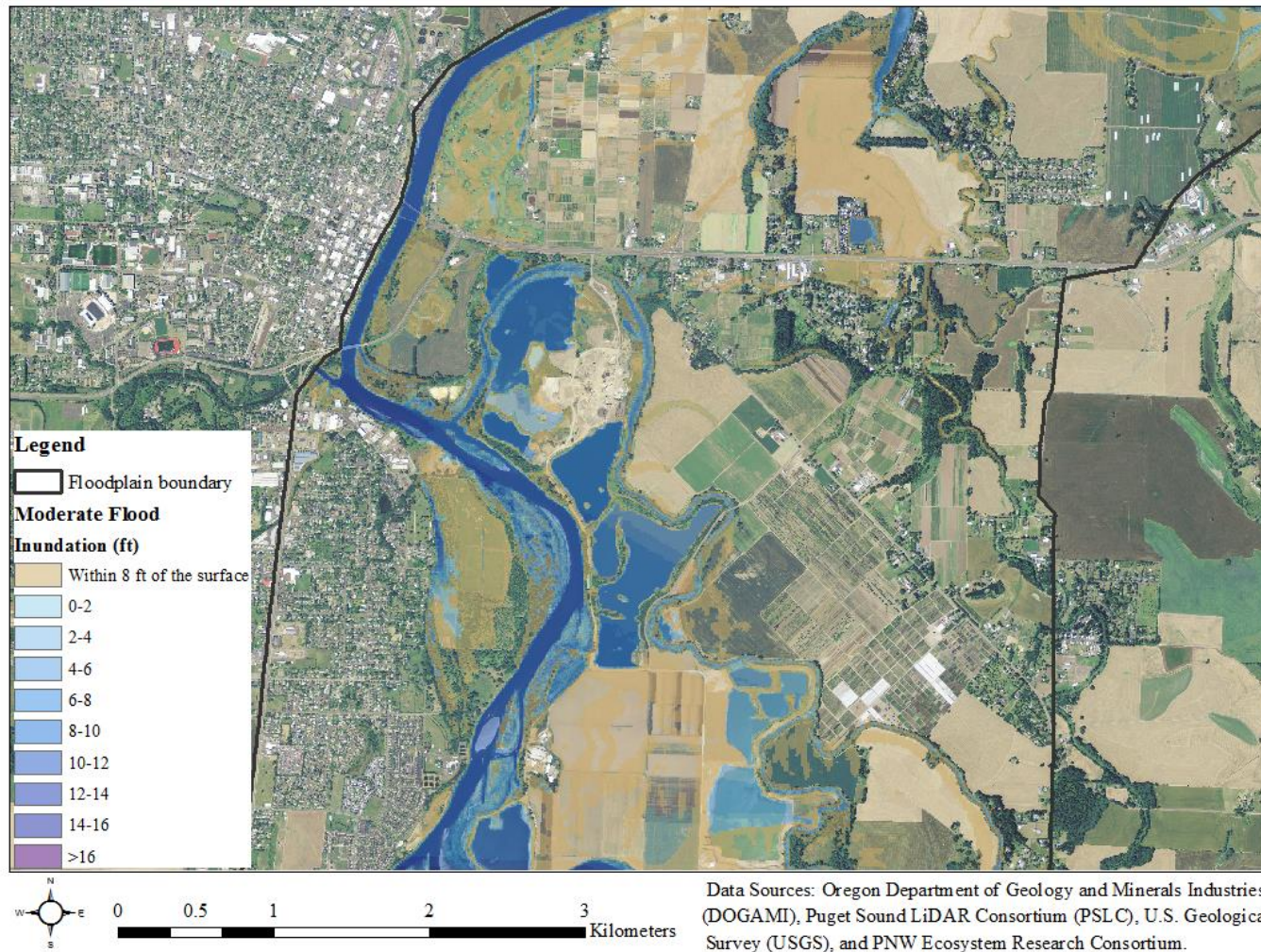


Figure 2.17. Inundation within the Willamette River's mainstem floodplain at Corvallis estimated at the moderate flood category. Orthoimagery as of 2012 from the National Map Viewer.

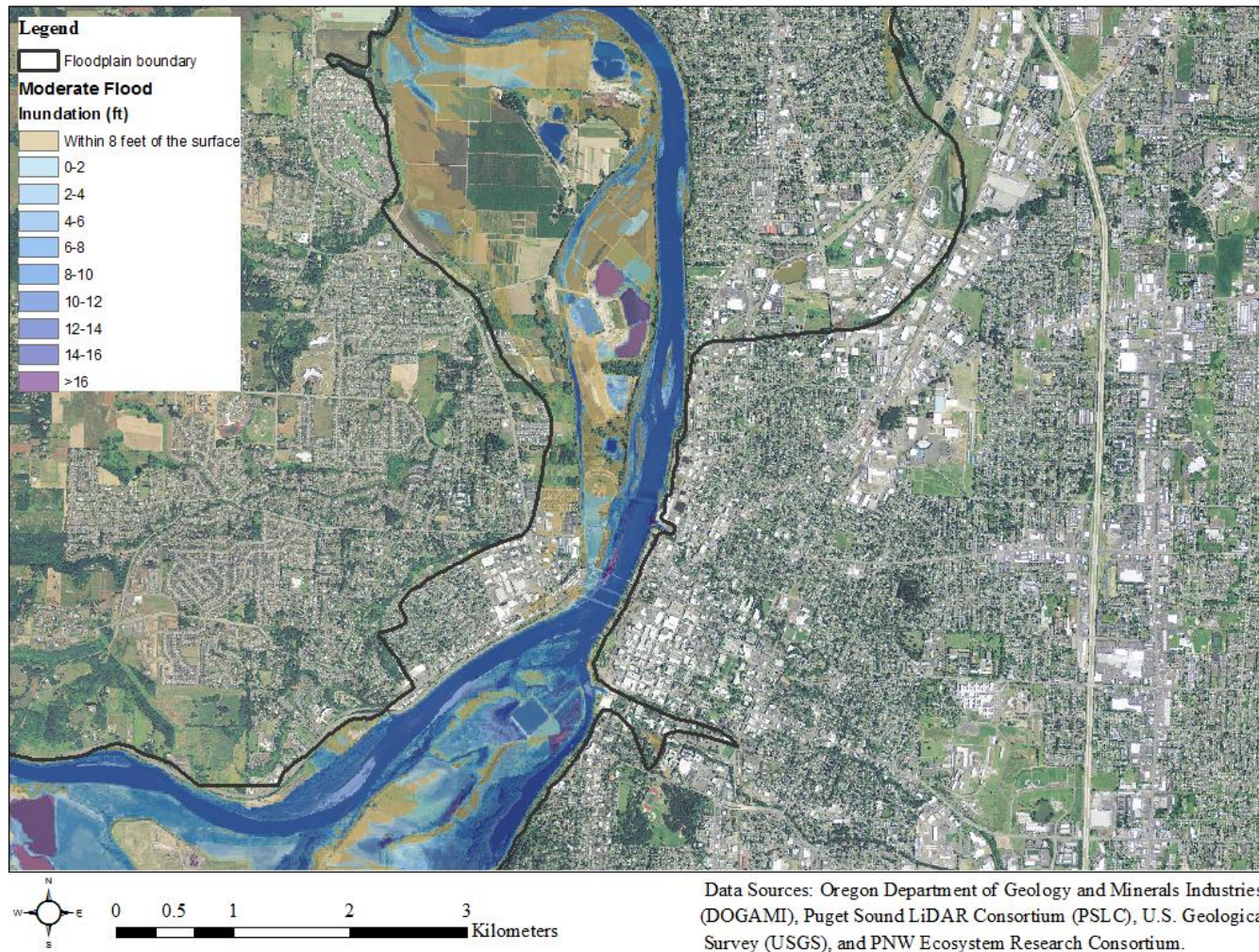


Figure 2.18. Inundation within the Willamette River's mainstem floodplain at Salem estimated at the moderate flood category. Orthoimagery as of 2012 from the National Map Viewer.

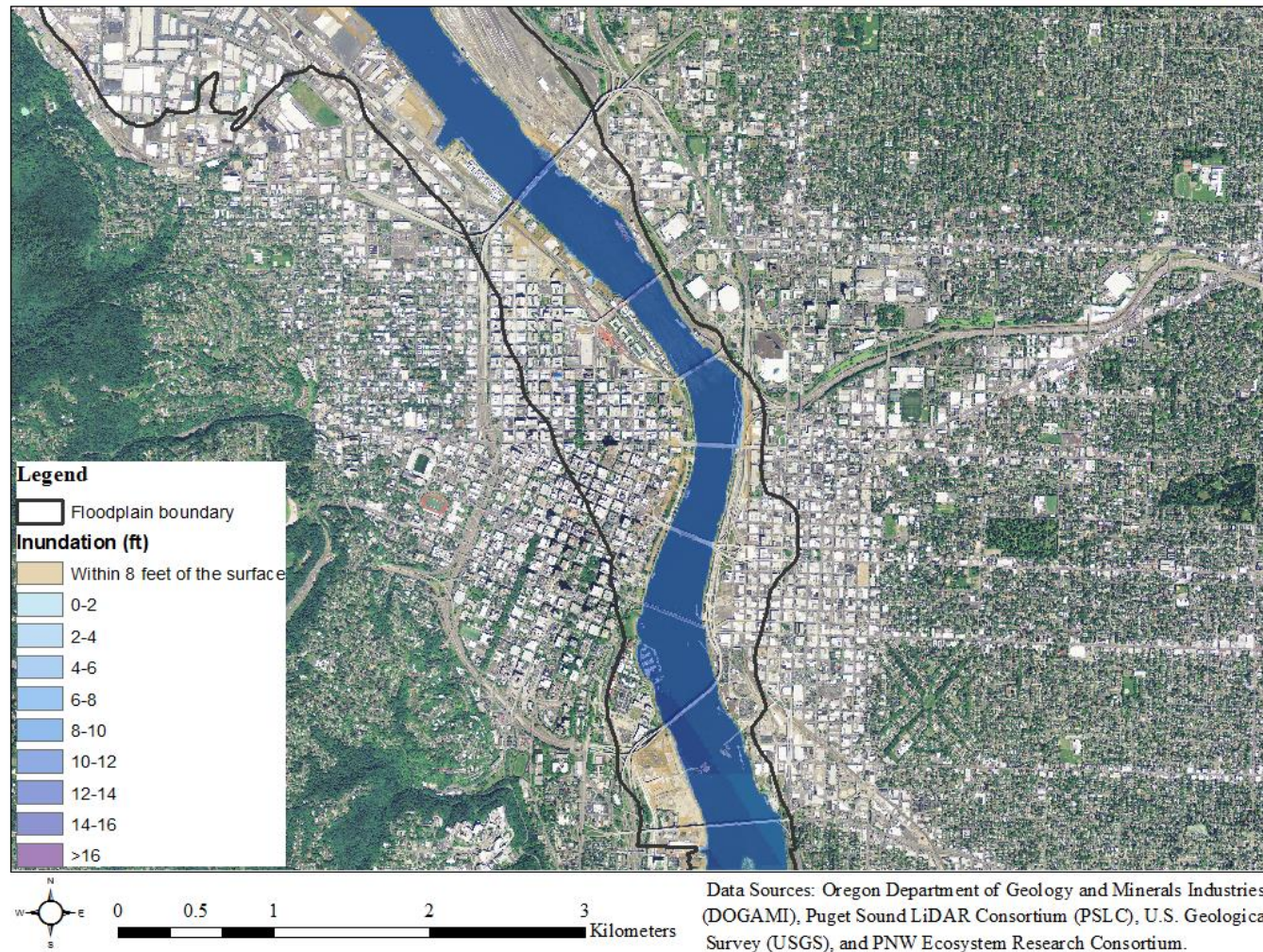


Figure 2.19. Inundation within the Willamette River's mainstem floodplain at Portland estimated at the moderate flood category. Orthoimagery as of 2012 from the National Map Viewer.

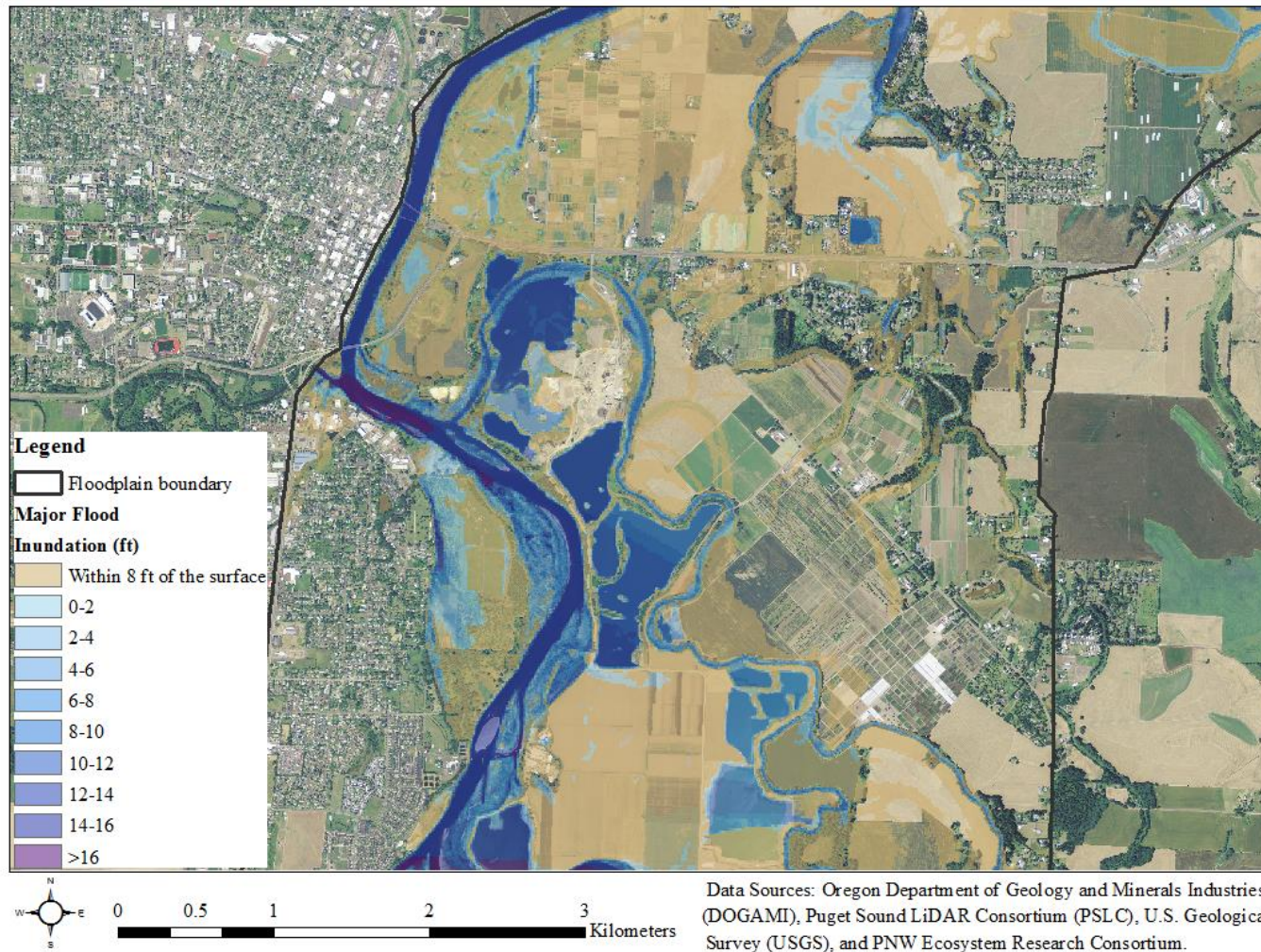


Figure 2.20. Inundation within the Willamette River's mainstem floodplain at Corvallis estimated at the major flood category. Orthoimagery as of 2012 from the National Map Viewer.

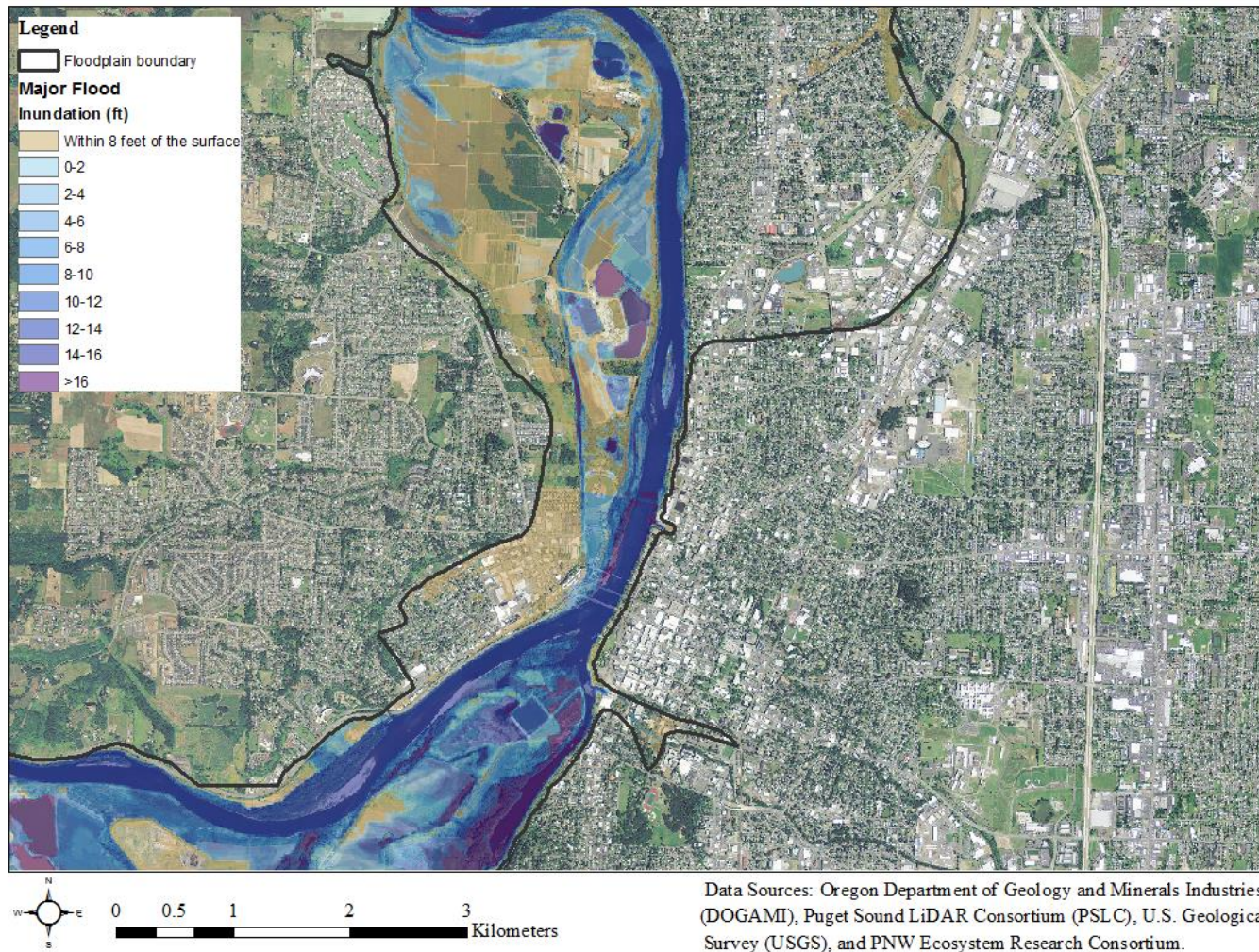


Figure 2.21. Inundation within the Willamette River's mainstem floodplain at Salem estimated at the major flood category. Orthoimagery as of 2012 from the National Map Viewer.

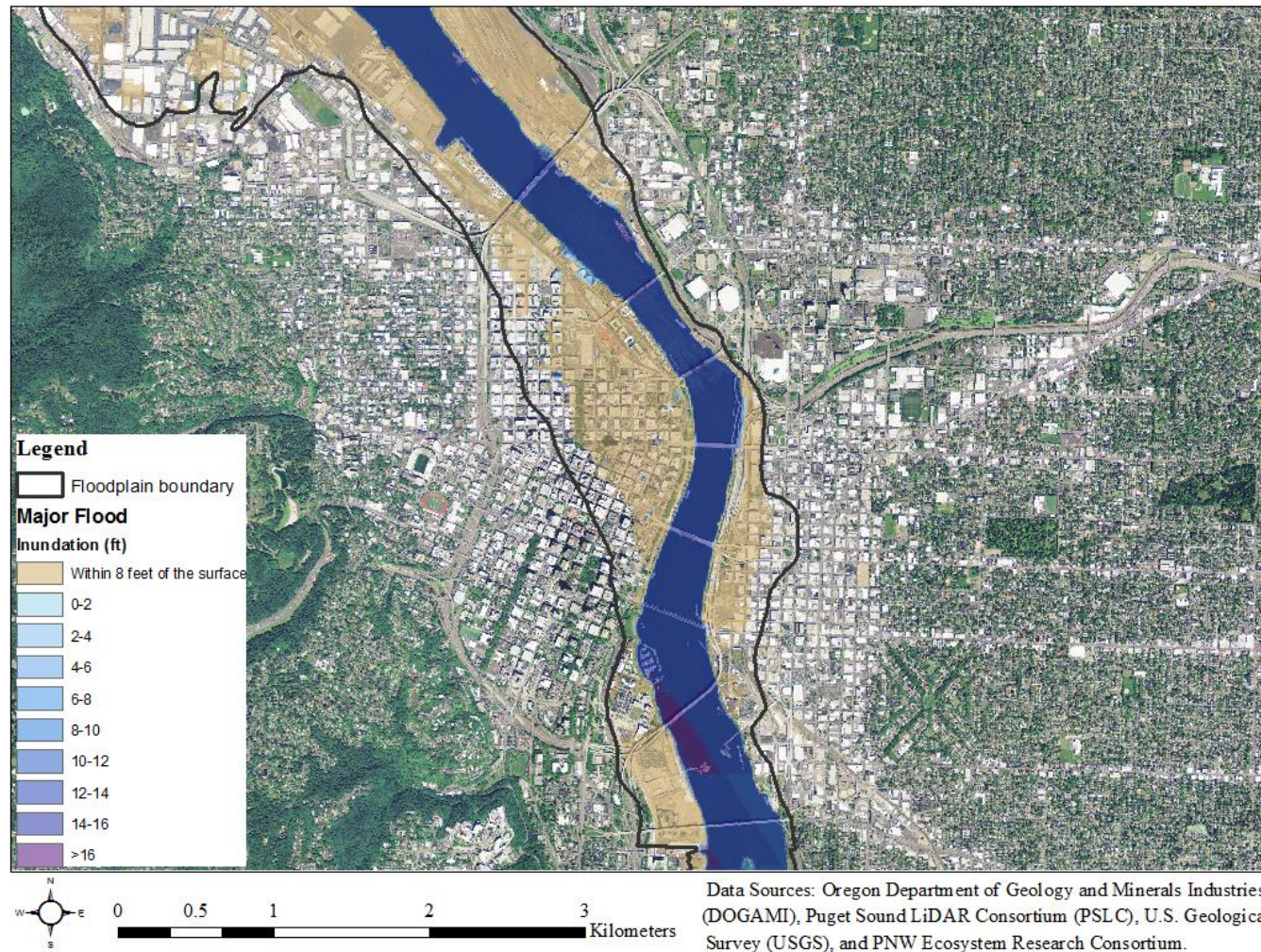


Figure 2.22. Inundation within the Willamette River's mainstem floodplain at Portland estimated at the major flood category. Orthoimagery as of 2012 from the National Map Viewer.

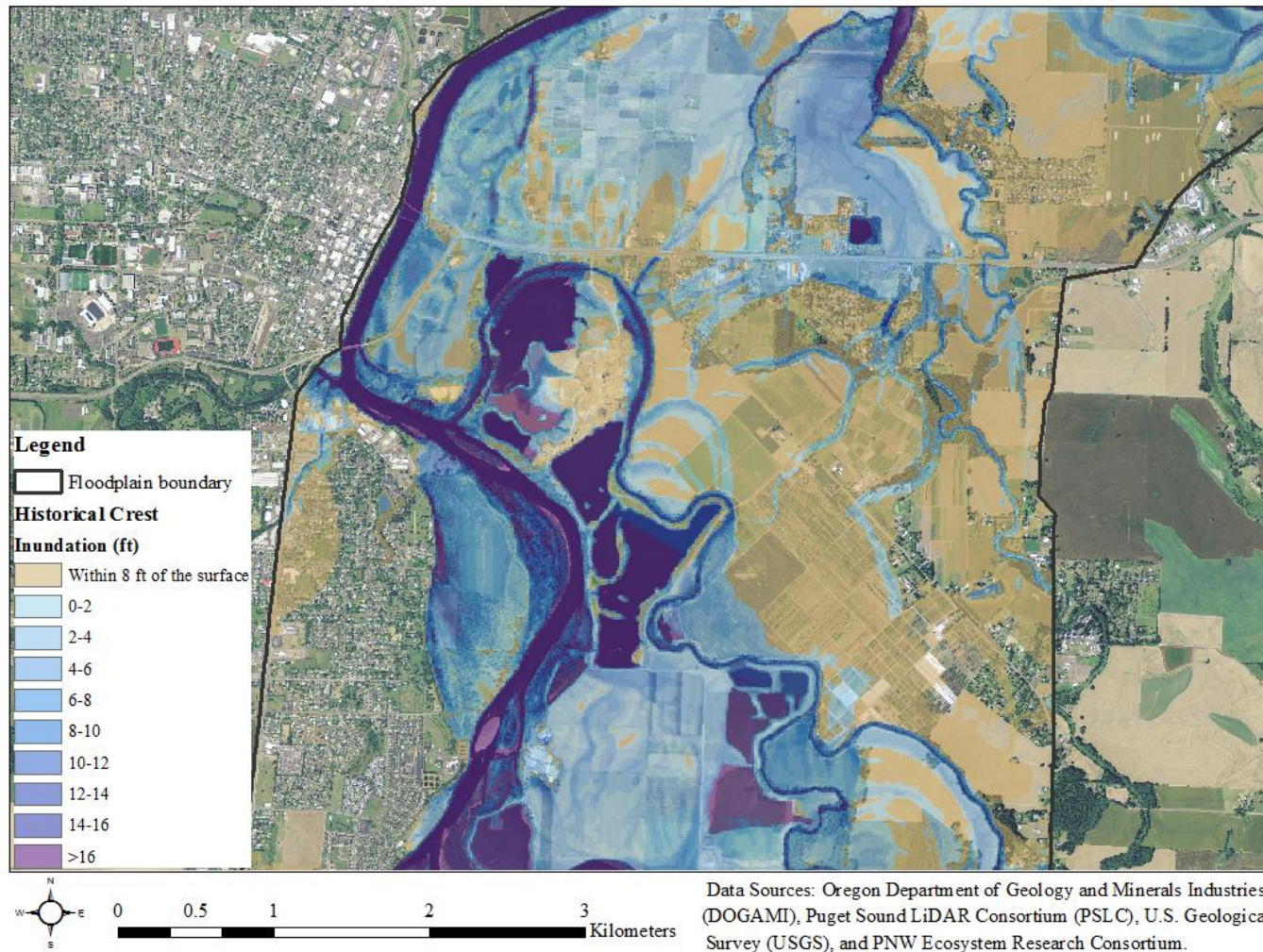


Figure 2.23. Inundation within the Willamette River's mainstem floodplain at Corvallis estimated at the historical high flood category. Orthoimagery as of 2012 from the National Map Viewer.

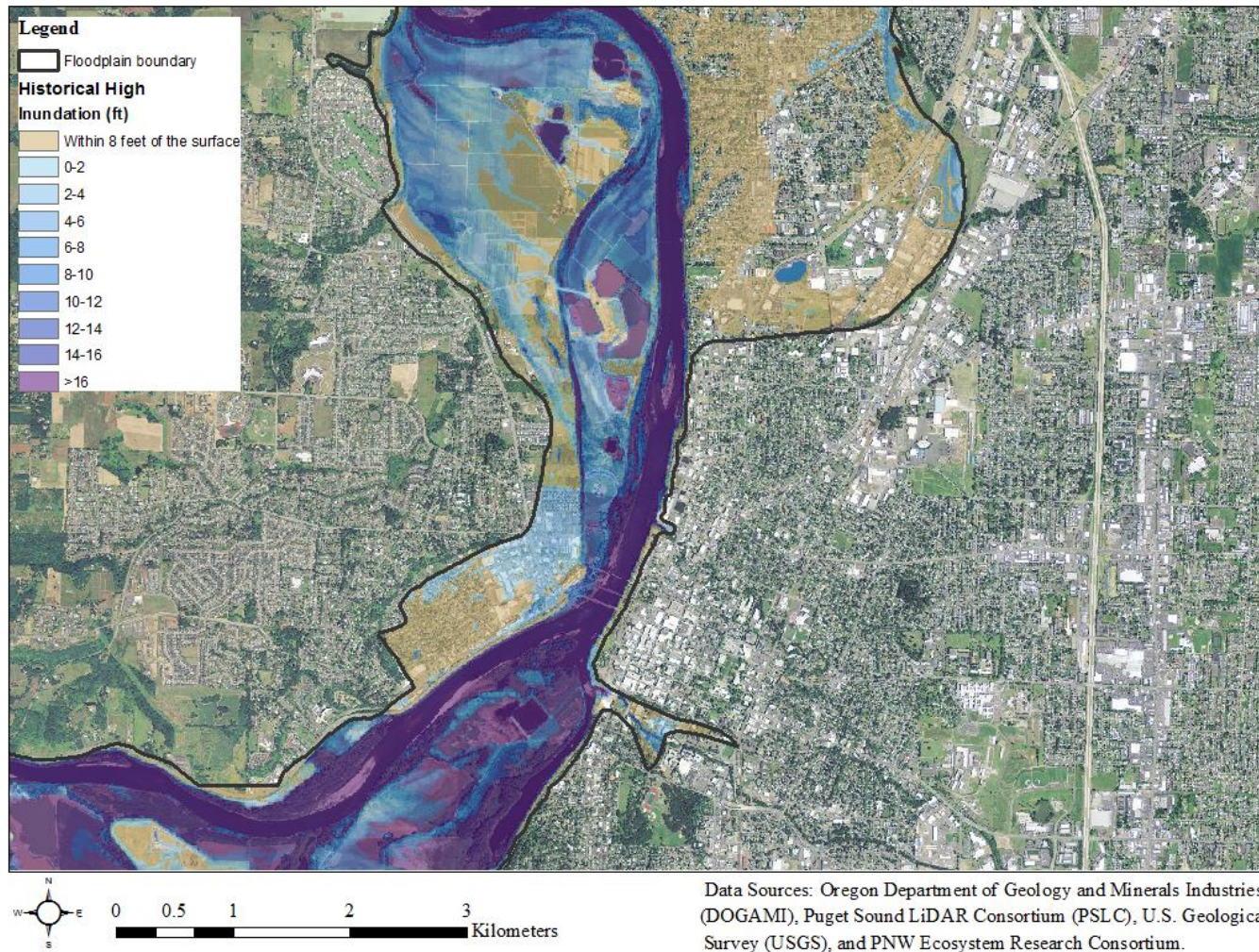


Figure 2.24. Inundation within the Willamette River's mainstem floodplain at Salem estimated at the historical high flood category. Orthoimagery as of 2012 from the National Map Viewer.

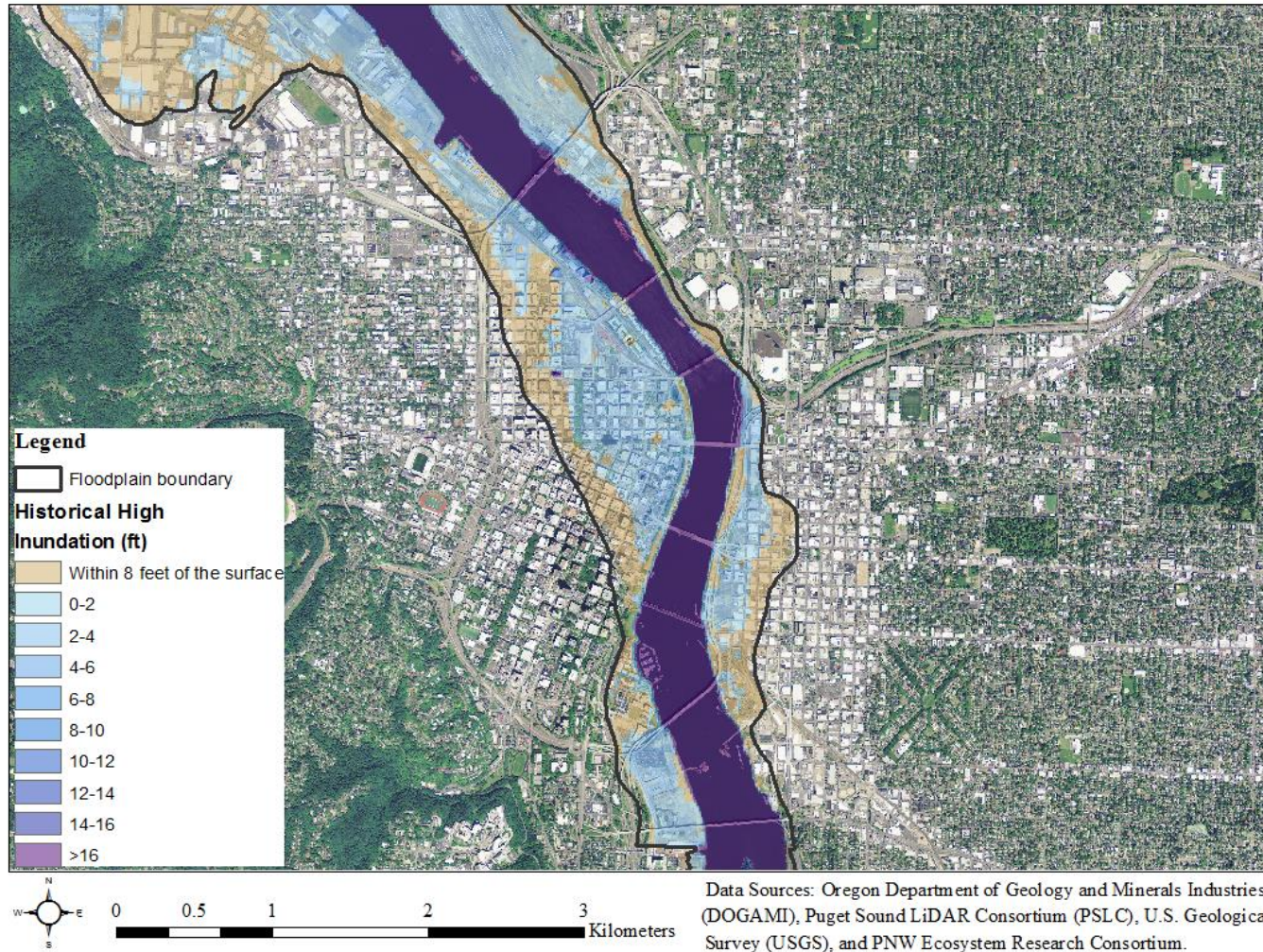


Figure 2.25. Inundation within the Willamette River's mainstem floodplain at Portland estimated at the historical high flood category. Orthoimagery as of 2012 from the National Map Viewer.

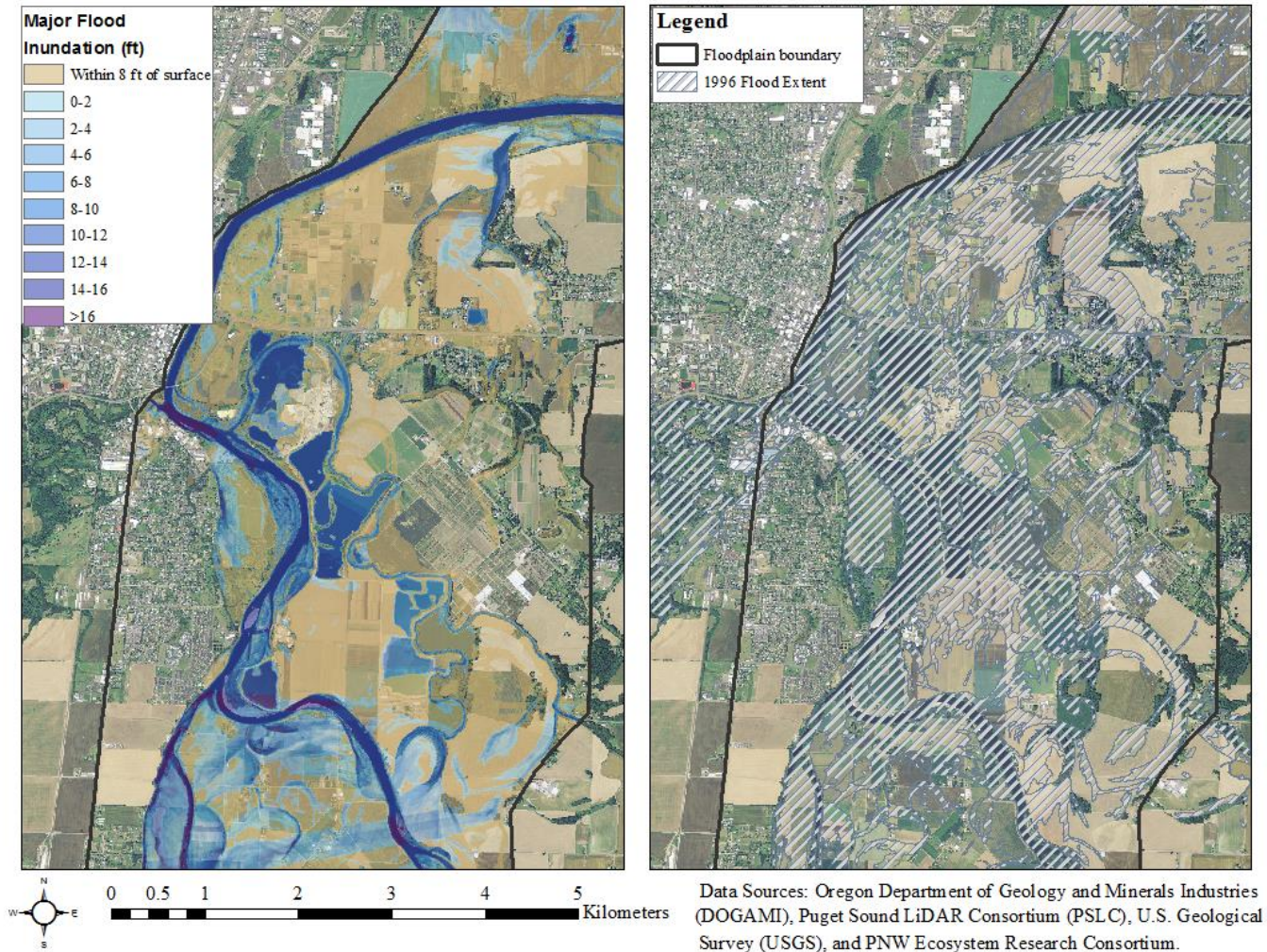


Figure 2.26. Comparison of inundation within the Willamette River's mainstem floodplain at Corvallis estimated at the major flood category with the extent of the 1996 flood estimated by Hulse et al. (2002). Orthoimagery as of 2012 from the National Map Viewer.

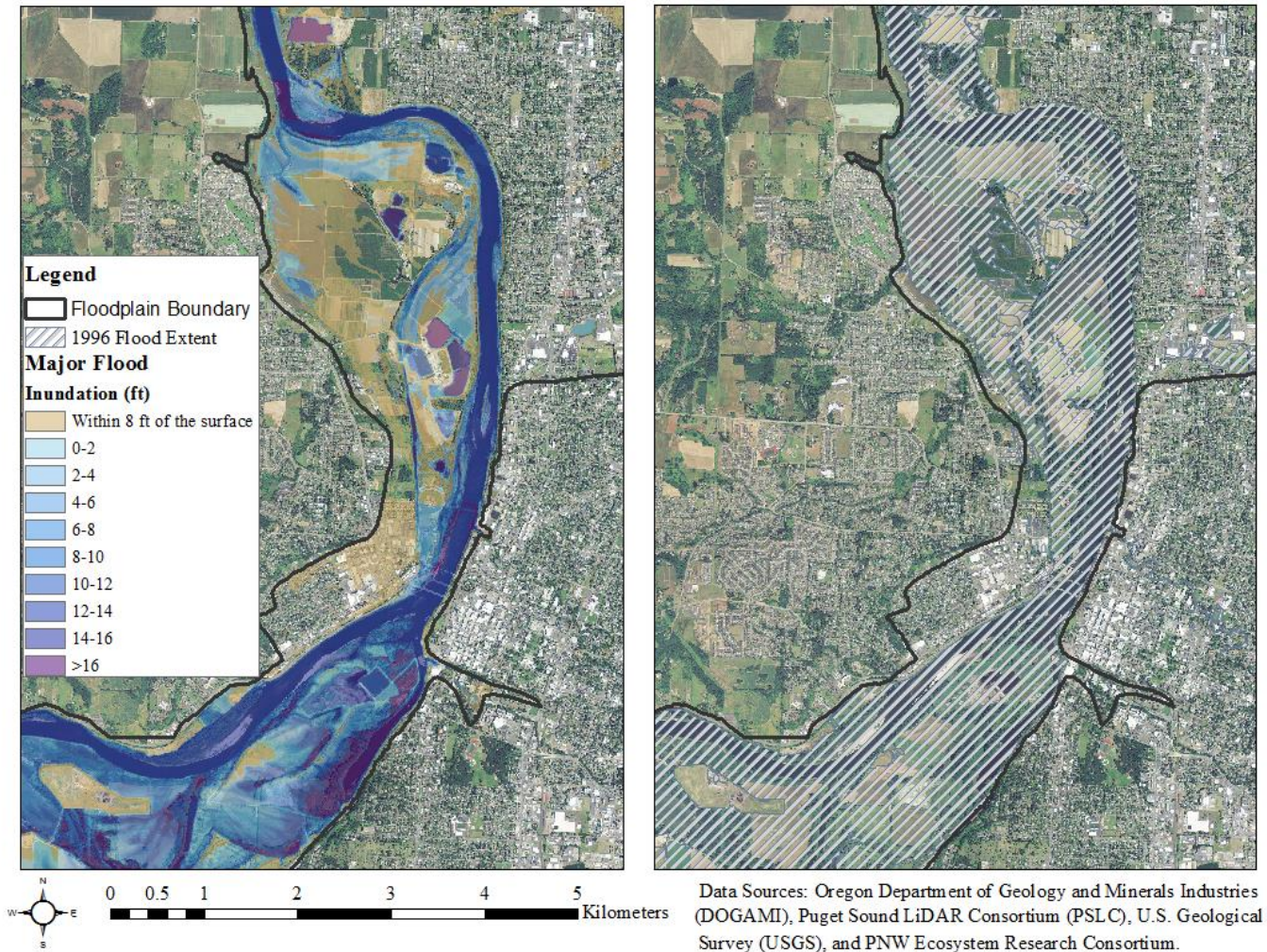


Figure 2.27. Comparison of inundation within the Willamette River's mainstem floodplain at Eugene estimated at the major flood category with the extent of the 1996 flood estimated by Hulse et al. (2002). Orthoimagery as of 2012 from the National Map Viewer.

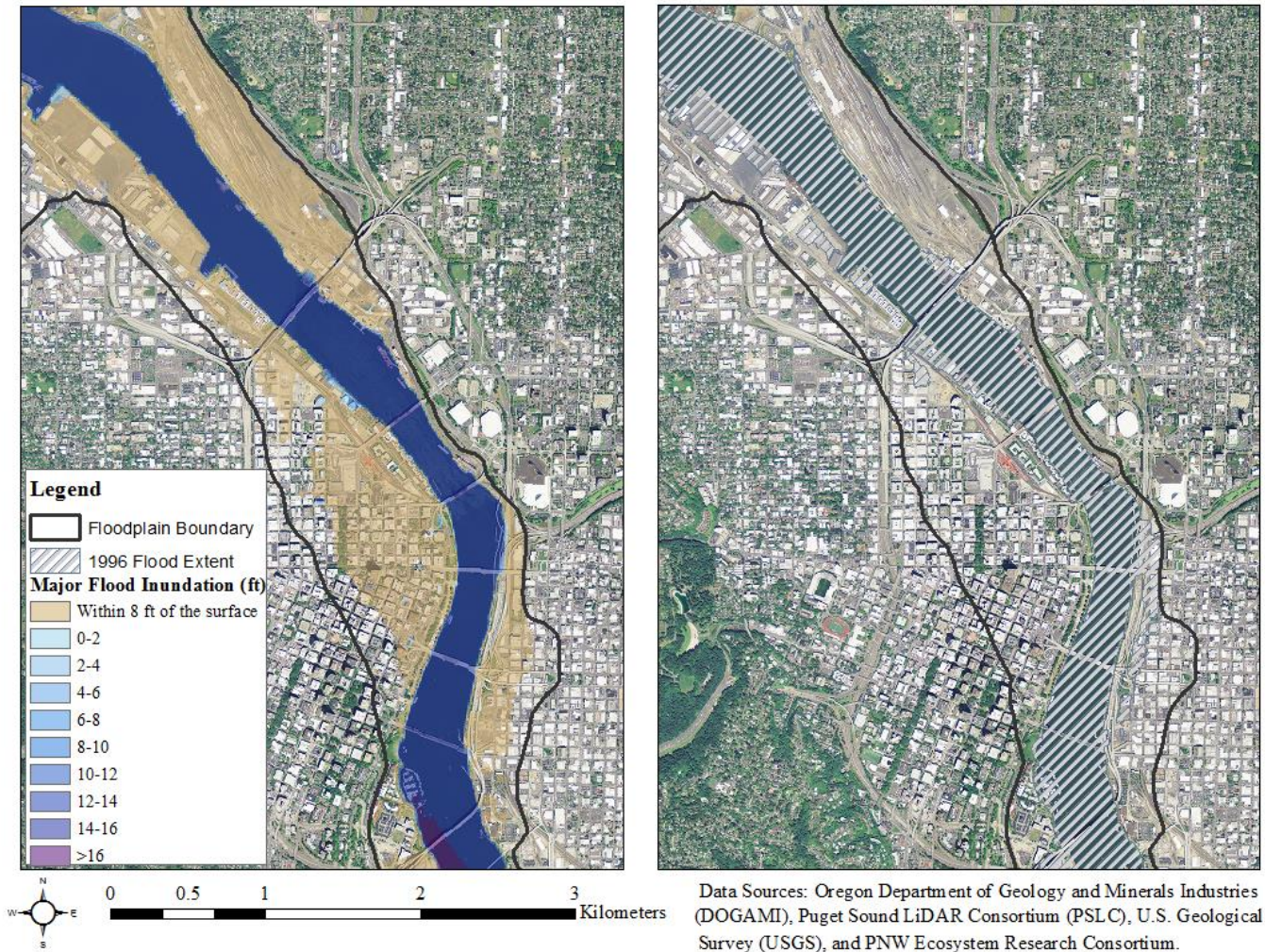


Figure 2.28. Comparison of inundation within the Willamette River's mainstem floodplain at Portland estimated at the major flood category with the extent of the 1996 flood estimated by Hulse et al. (2002). Orthoimagery as of 2012 from the National Map Viewer.

2.5.2 Land cover scenarios

In each of the WW2100 scenarios, development within the floodplain increased over time (Table 2.4). The total area in developed use in 2030 ranged from 30,647 to 30,688 acres (approximately 15% of the floodplain area) in all three scenarios. The WW2100 model predicted 4% more developed area in the floodplain in 2070 and 13% more in 2100 in the high population growth scenario relative to the reference scenario. In contrast, developed area was predicted to be similar in the reference case and relaxed UGB scenarios. The total value of structures on developed land parcels in the entire mainstem Willamette floodplain ranged from \$20.3 billion for the relaxed UGB scenario in 2030 to \$66.2 billion for the high population growth scenario in 2100 (Table 2.5). The structural value of development for the high population growth scenario was estimated at \$16 billion more than the reference case scenario in 2070, rising to \$20 billion more in 2100. The reference case and relaxed UGB scenarios differed little in the estimated total structural value.

Within the floodplain at Corvallis, the land parcels designated as developed from the WW2100 model output had structural values ranging from less than \$25,000 to \$50,000 per 1/20th of an acre (or up to \$250,000 per quarter acre) under the high population scenario in 2030 (Figure 2.29). Most of this developed area was located on the west side of the Willamette River, primarily in southeast Corvallis. The area predicted to be developed by the WW2100 model included housing visible in the underlying orthophoto (obtained in 2012), but it omitted an area of current development further south. The predicted area of development also included some areas that are currently in agriculture and open space use, notably parts of the river bank and channel north of the Mary's River tributary and extending along the downtown area of Corvallis. The WW2100 model also predicted development east of the Willamette River, along the right

bank and along major roads, in areas which currently are open space. The pockets of development included many but not all the locations of current development as well as some areas currently in agricultural use. By 2100 the value of structural improvements per 1/20th acre under high population model scenario at Corvallis increased to range from \$25,000-\$100,000 (Figure 2.30). Most of the area of development on the west side of the Willamette River increased in value to range between \$50,000-\$75,000 with the area near the Mary's River tributary and north along the downtown increasing further to \$75,000-\$100,000. The extent of this development also increased to include most of the currently developed area towards the south and additional area towards the river currently in open space use. The area of predicted development on the east side of the Willamette River did not change but increased in value to range from \$25,000-\$50,000 per 1/20th acre.

At Salem structural development within the floodplain in 2030 for the high population scenario of the WW2100 model ranged in value from \$25,000-\$50,000 per 1/20th acre (Figure 2.31). The areas with predicted structural value matched current development visible in the underlying orthophoto from 2012. The model also classified some additional areas as developed that are currently in agriculture and open space use. This included areas along the border of the floodplain but also parts of the river bank and channel as was the case in Corvallis. By 2100 the value of structural improvements per 1/20th acre under high population model scenario at Salem increased to range from \$75,000 to greater than \$100,000 (Figure 2.32) and development was predicted in a large area previously in agricultural use on the west side of the river and north of downtown Salem, as well as areas that were previously primarily in open space use along the east of the main river channel south of downtown Salem. Some of this predicted development

also extended onto the river banks, channel, and areas that are mapped as inundated at bankful stage (Figure 2.12).

At Portland structural development within the floodplain under the high population scenario ranged in value from \$75,000-\$100,000 per 1/20th acre in 2030 (Figure 2.33), increasing to greater than \$100,000 in 2100 (Figure 2.34). Apart from the river channel, essentially the entire floodplain is predicted as developed as currently also shown by the orthophoto. However, similar to Corvallis and Salem, the area of predicted development included some small sections of the river channel close to the banks.

Table 2.4. The total area of land in developed use within the WRB mainstem floodplain, under the WW2100 scenarios for the Reference Case model, the High Population Growth model, and the Relaxed UGB model in 2030, 2070, and 2100. WW2100 model outputs downloaded August 19, 2014.

<u>Year</u>	<u>Developed Area (acres)</u>		
	<u>Reference Case</u>	<u>High Population Growth</u>	<u>Relaxed UGB</u>
2030	30,647	30,669	30,688
2070	31,859	33,145	32,144
2100	34,353	38,833	34,885

Table 2.5. The total value of structures within the WRB mainstem floodplain, under the WW2100 scenarios for the Reference Case model, the High Population Growth model, and the Relaxed UGB model in 2030, 2070, and 2100. WW2100 model outputs downloaded August 19, 2014.

<u>Year</u>	<u>Total Structural Value (\$ Billions)</u>		
	<u>Reference Case</u>	<u>High Population Growth</u>	<u>Relaxed UGB</u>
2030	20.7	25.3	20.3
2070	35.4	51.4	35.4
2100	46.1	66.2	45.1

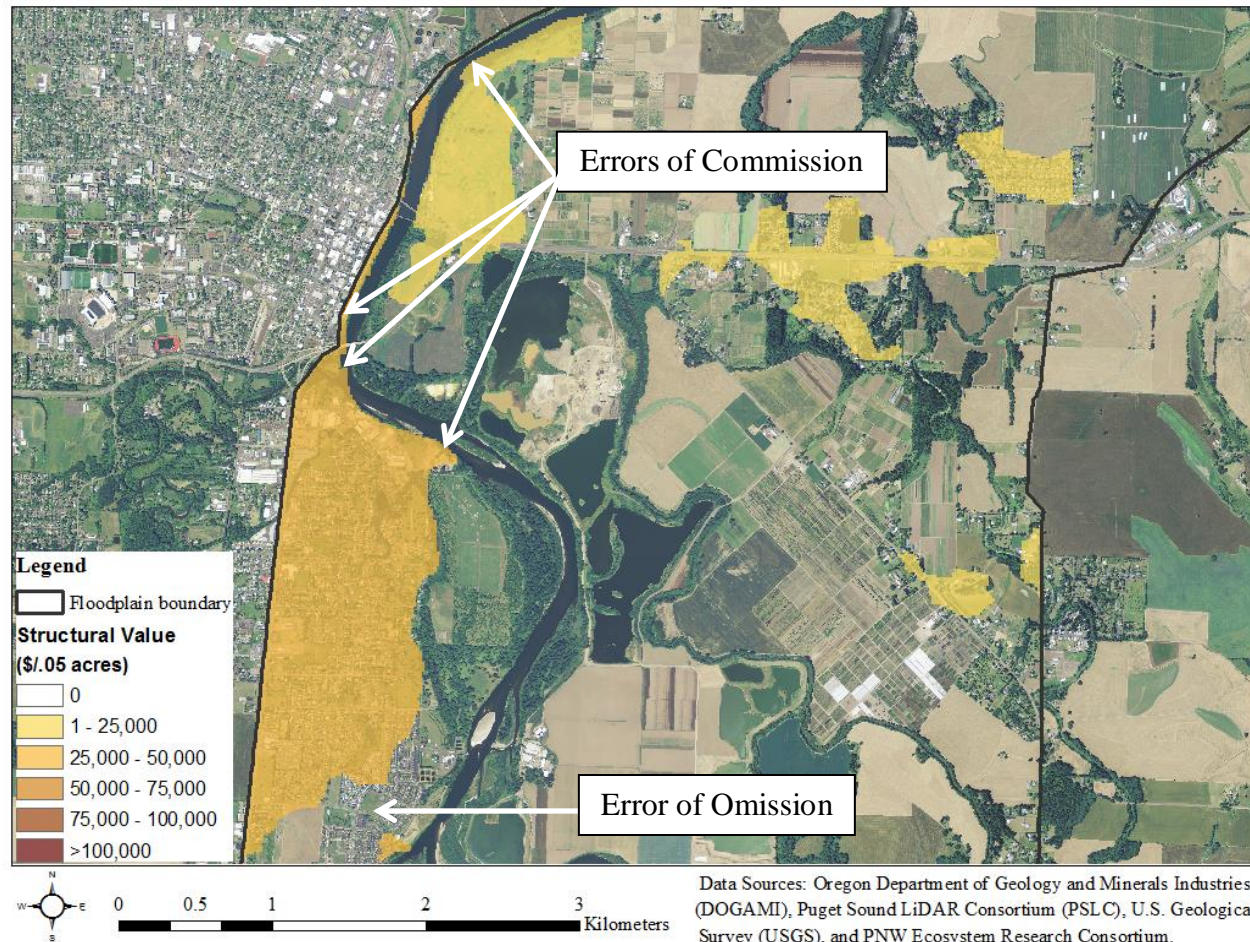


Figure 2.29. The location and value of structural development in the Willamette's mainstem floodplain at Corvallis under the high population growth scenario in 2030. Orthoimagery as of 2012 from the National Map Viewer. The arrows indicate errors of commission where sections of land are shown as developed, but are unlikely to contain structures given the location within the inundation zone, as well as errors of omission where the land cover model failed to capture areas of development.

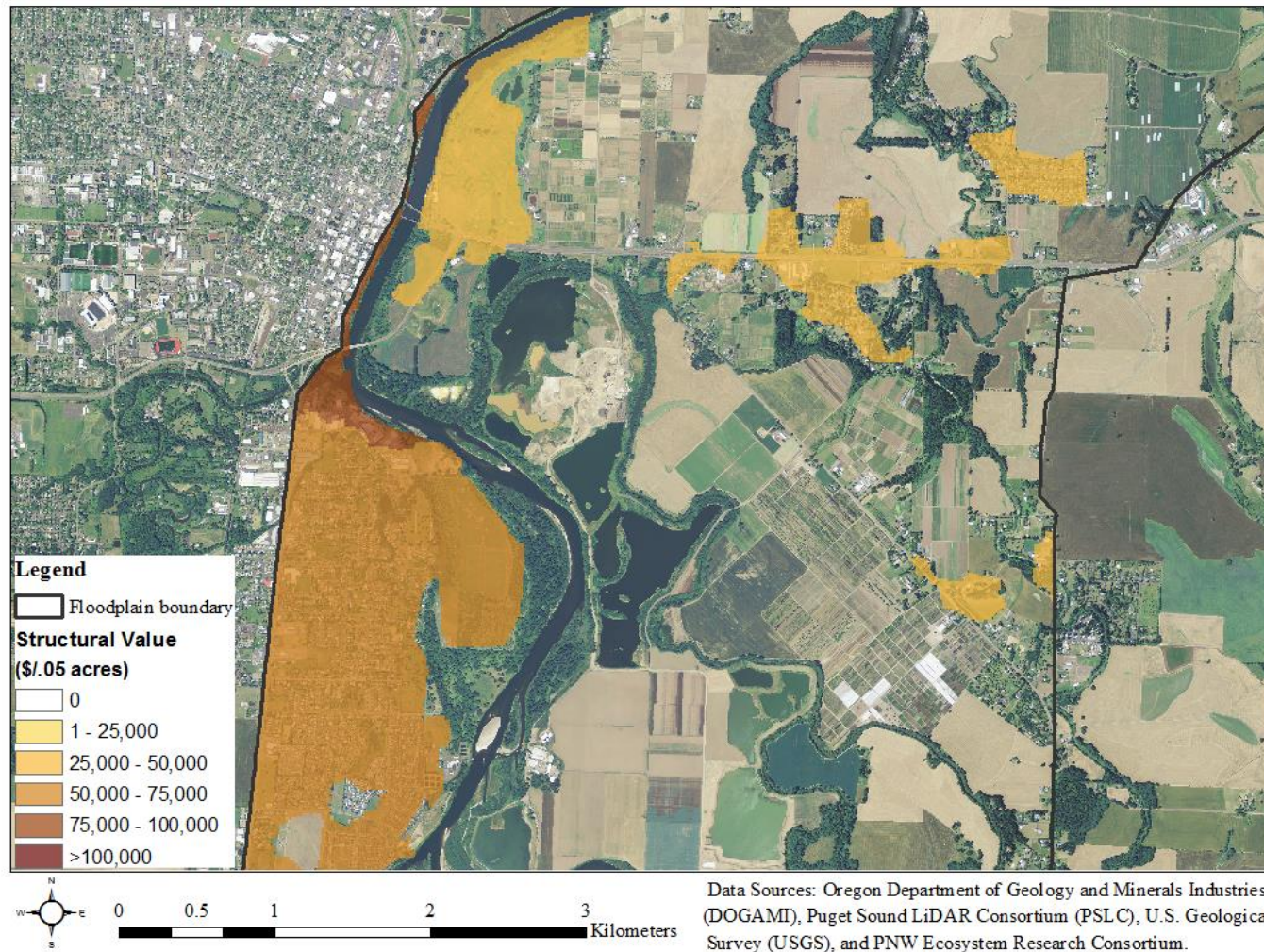


Figure 2.30. The location and value of structural development in the Willamette's mainstem floodplain at Corvallis under the high population growth scenario in 2100. Orthoimagery as of 2012 from the National Map Viewer.

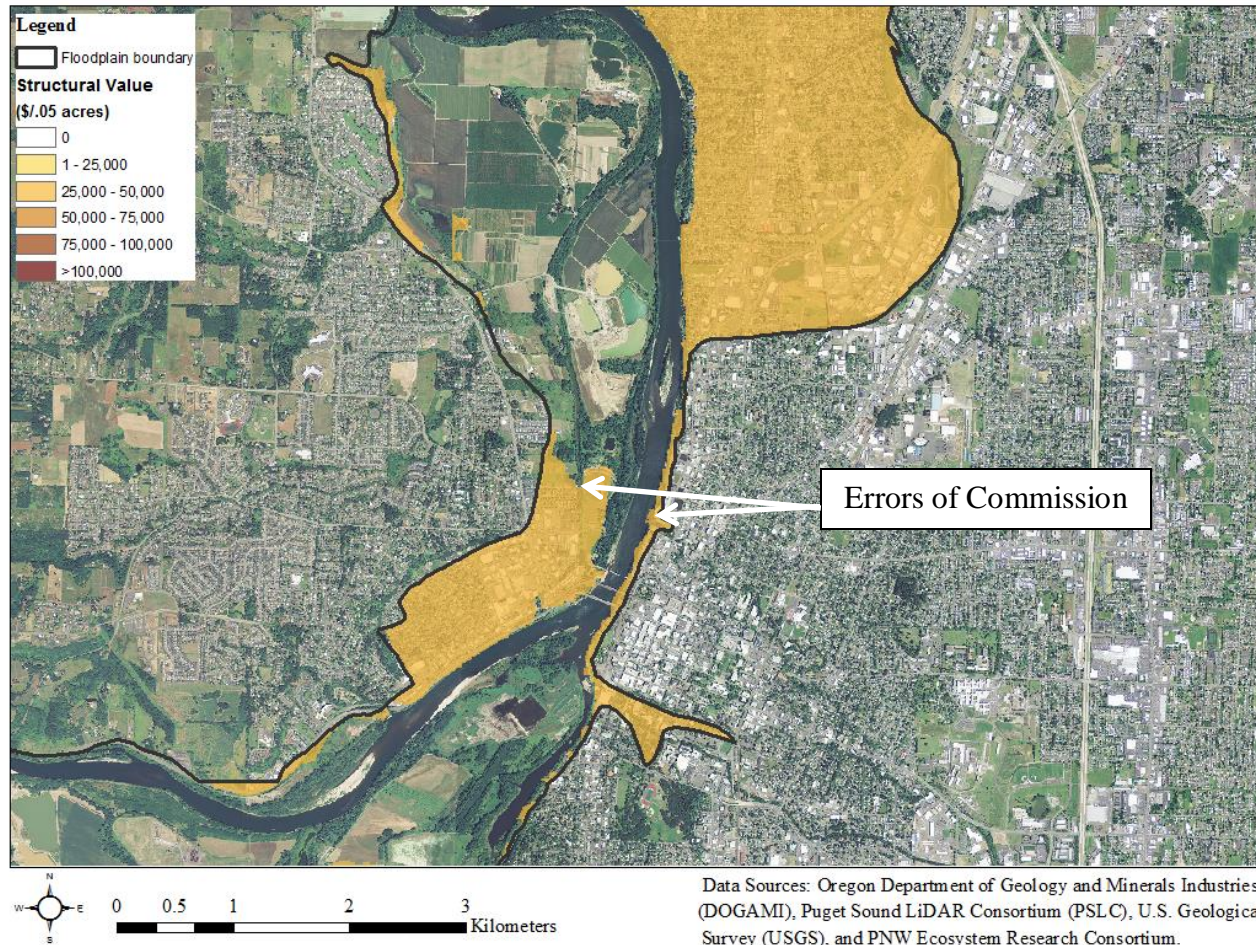


Figure 2.31. The location and value of structural development in the Willamette's mainstem floodplain at Salem under the high population growth scenario in 2030. Orthoimagery as of 2012 from the National Map Viewer. The arrows indicate some of the errors of commission where sections of land are shown as developed, but are unlikely to contain structures given the location within the inundation zone.

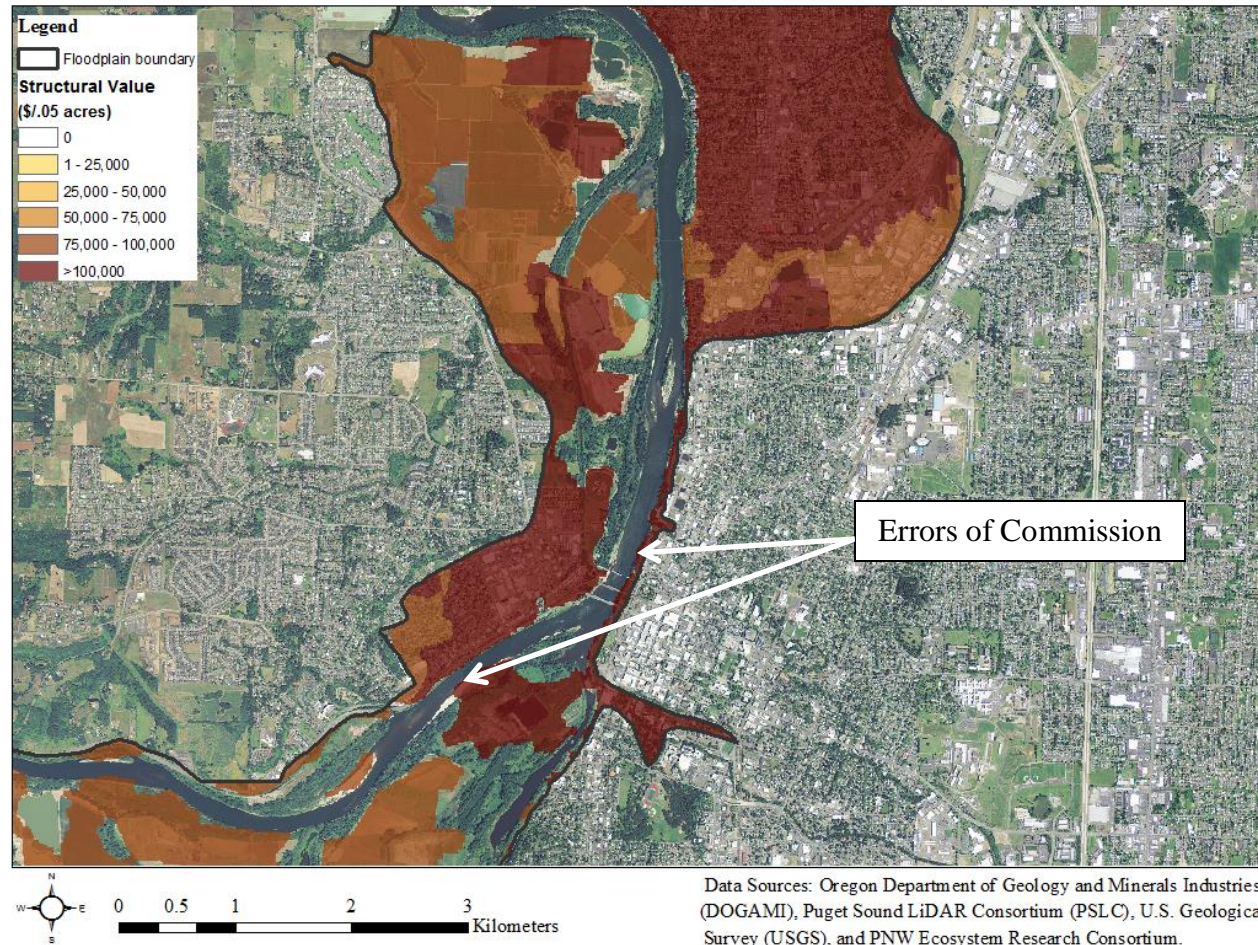


Figure 2.32. The location and value of structural development in the Willamette's mainstem floodplain at Salem under the high population growth scenario in 2100. Orthoimagery as of 2012 from the National Map Viewer. The arrows indicate some of the errors of commission where sections of land are shown as developed, but are unlikely to contain structures given the location within the inundation zone.

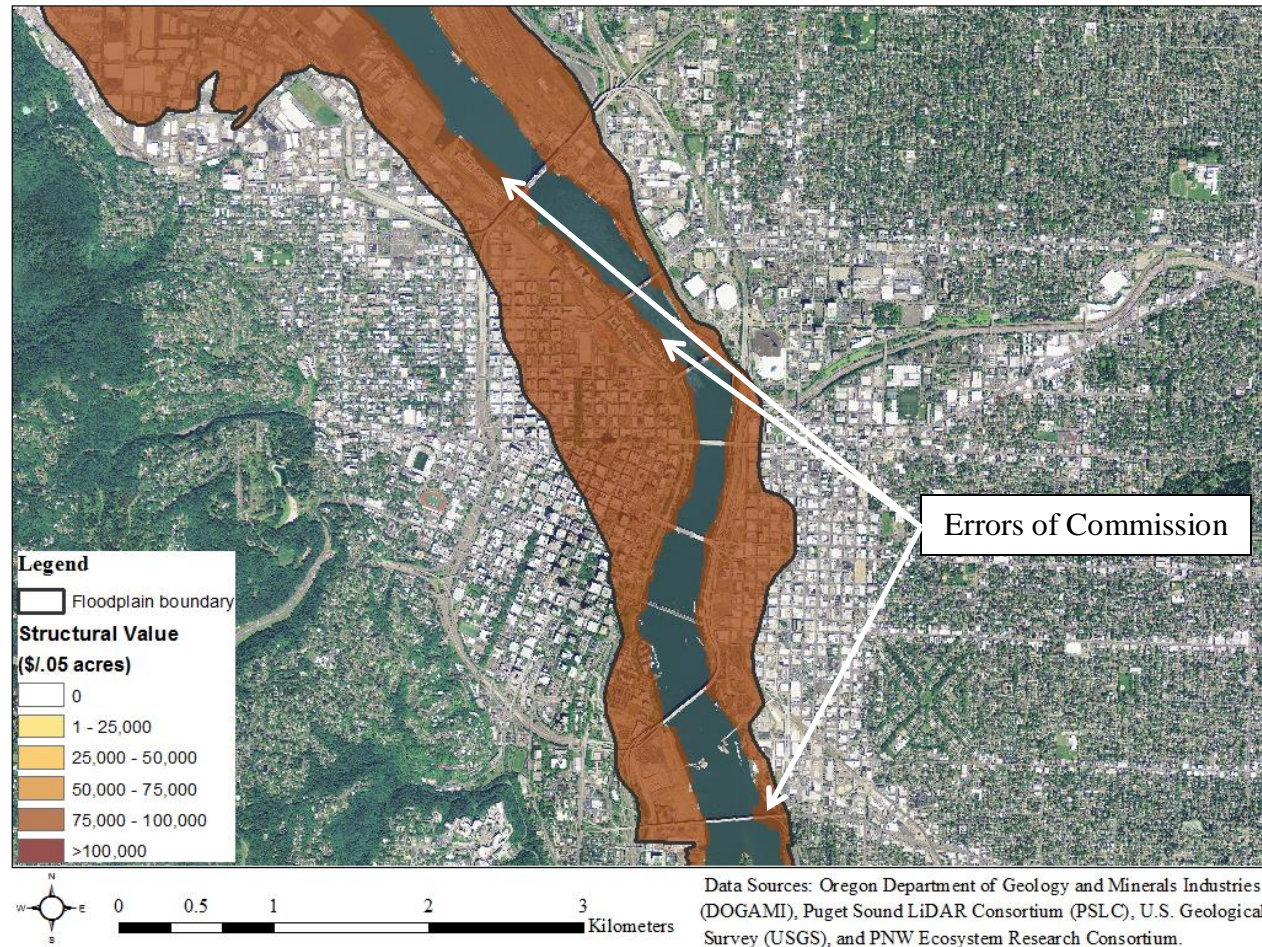


Figure 2.33. The location and value of structural development in the Willamette’s mainstem floodplain at Portland under the high population growth scenario in 2030. Orthoimagery as of 2012 from the National Map Viewer. The arrows indicate some of the errors of commission where sections of land are shown as developed, but are unlikely to contain structures given the location within the inundation zone.

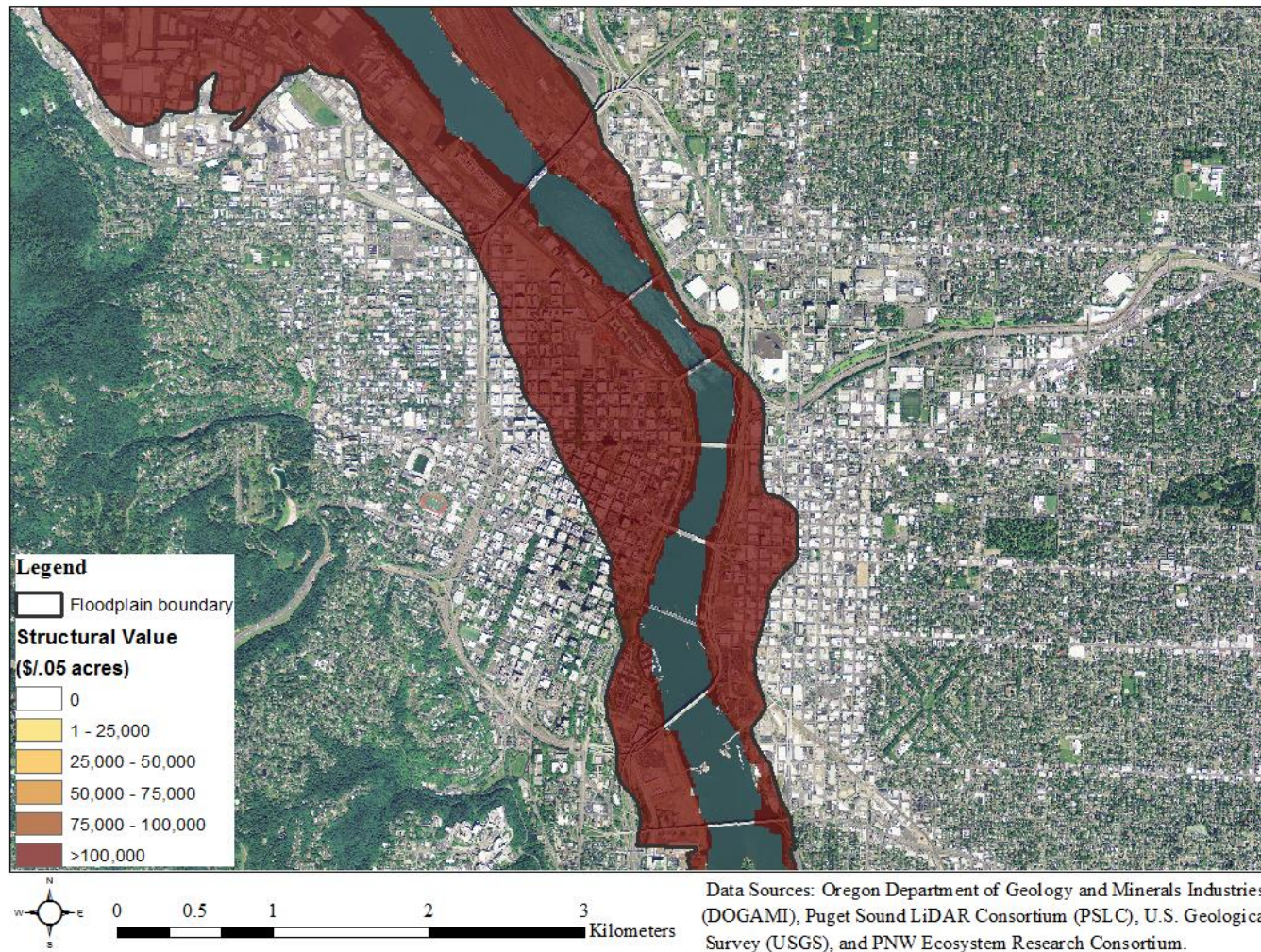


Figure 2.34. . The location and value of structural development in the Willamette’s mainstem floodplain at Portland under the high population growth scenario in 2100. Orthoimagery as of 2012 from the National Map Viewer.

2.5.3 Flood damages

Estimated total flood damages within the floodplain ranged from approximately \$500 million to \$22 billion depending on the flood stage and scenario, after adjusting for damages estimated at bankfull stage (Table 2.6). The flood damages estimated at bankfull stage ranged from \$900 million under the reference case scenario in 2030 to \$4 billion under the high population growth scenario in 2100. Since flood damages should be close to zero at bankfull stage, these values were considered to represent an estimation error due to inaccuracies in the modelling of structural development within the floodplain and the mapping of flood inundation.

Under the reference case scenario in 2030, estimated flood damages reached \$2 billion and \$6 billion for the major and historical high crest floods respectively. These values were estimated to increase to \$4 billion and \$11 billion in 2070, and \$5 billion and \$14 billion in 2100. This represents losses ranging from 10-11% of the estimated structural value in the floodplain for a major flood and 30-31% for a historical high crest flood. Under the high population growth scenario, flood damages in 2070 are estimated to increase by \$2 billion and \$6 billion relative to the reference case scenario for the major and historical high crest floods respectively. In 2100 this difference increases to \$3 billion and \$8 billion respectively. These losses represent 11-13% of the estimated structural value in the floodplain for a major flood and 32-33% for a historical high crest flood. The reference case and the relaxed UGB scenarios have similar estimated total flood damages, differing by approximately \$0.2 billion or less.

The mapped flood damages at Corvallis for the major flood category under the high population scenario in 2030 showed losses of up to \$50,000 per 1/20th acre (Figure 2.35). The highest valued losses occurred near the Mary's River tributary; along a channel on the edge of the currently developed area west of the Willamette River; and in small spots along the west side

of the river in the downtown. Damages also occurred on the east side of the Willamette River, both in the area predicted to be developed along the river channel as well as some of the lower lying pockets of development primarily along the I-34 highway. In 2100, with similar flooding, expected flood losses for the major flood category increased up to \$100,000 per 1/20th acre at Corvallis by 2100 under the high population growth scenario (Figure 2.36) because of increases in the amount and value of land in developed use. Estimated flood damages in 2100 were highest along the riverfront in Corvallis, which is currently undeveloped.

In Salem, flood damages for the major flood category under the high population scenario in 2030 at Salem were as high as \$75,000 per 1/20th acre (Figure 2.37). Damages primarily occurred in the northern half of the developed area west of the river, but also in smaller areas along the eastern boundary of the floodplain and along the river banks. By 2100 under the high population growth scenario, expected flood losses at Salem for the major flood category were predicted exceed \$100,000 per 1/20th acre in some areas (Figure 2.38). The extent of predicted flood damages in 2100 included an area east of the main river channel and south of downtown Salem, which had previously been primarily in open space use, as well as an area previously in agricultural use on the west side of the river and north of downtown Salem.

At Portland flood damages for the major flood category under the high population scenario exceeded \$100,000 per 1/20th acre along the river banks in both 2030 and 2100 (Figure 2.39 and Figure 2.40), including areas that appear to be within the current river channel, but were classified as developed according to the WW2100 model. Beyond the areas adjacent to the river banks, damages declined to \$25,000 per 1/20th acre or less in both 2030 and 2100. Although the spatial extent of flood damages was similar in 2030 and 2100 in Portland, the estimated flood

losses along the west river bank in the south of the mapped area were \$75,000-\$100,000 per 1/20th acre in 2030, but exceeded \$100,000 per 1/20th acre in 2100.

Table 2.6. Total flood damages within the WRB mainstem floodplain, estimated for the intersection of each flood category with the WW2100 land cover scenarios for the Reference Case model, the High Population Growth model, and the Relaxed UGB model in 2030, 2070, and 2100. WW2100 model outputs downloaded August 19, 2014. For each scenario the total damage estimates were adjusted down by the damages estimated at bankfull stage, which were assumed to be estimation error.

Scenario	Year	Total Damages (\$ Millions)			
		Flood	Moderate Flood	Major Flood	Historical High
Reference Case	2030	486	901	1,976	6,238
	2070	876	1,618	3,507	10,564
	2100	1,265	2,332	4,999	14,088
High Population Growth	2030	573	1,061	2,331	7,545
	2070	1,470	2,697	5,736	16,215
	2100	2,145	3,951	8,395	22,074
Relaxed UGB	2030	474	883	1,947	6,120
	2070	878	1,633	3,586	10,780
	2100	1,244	2,311	5,022	14,106

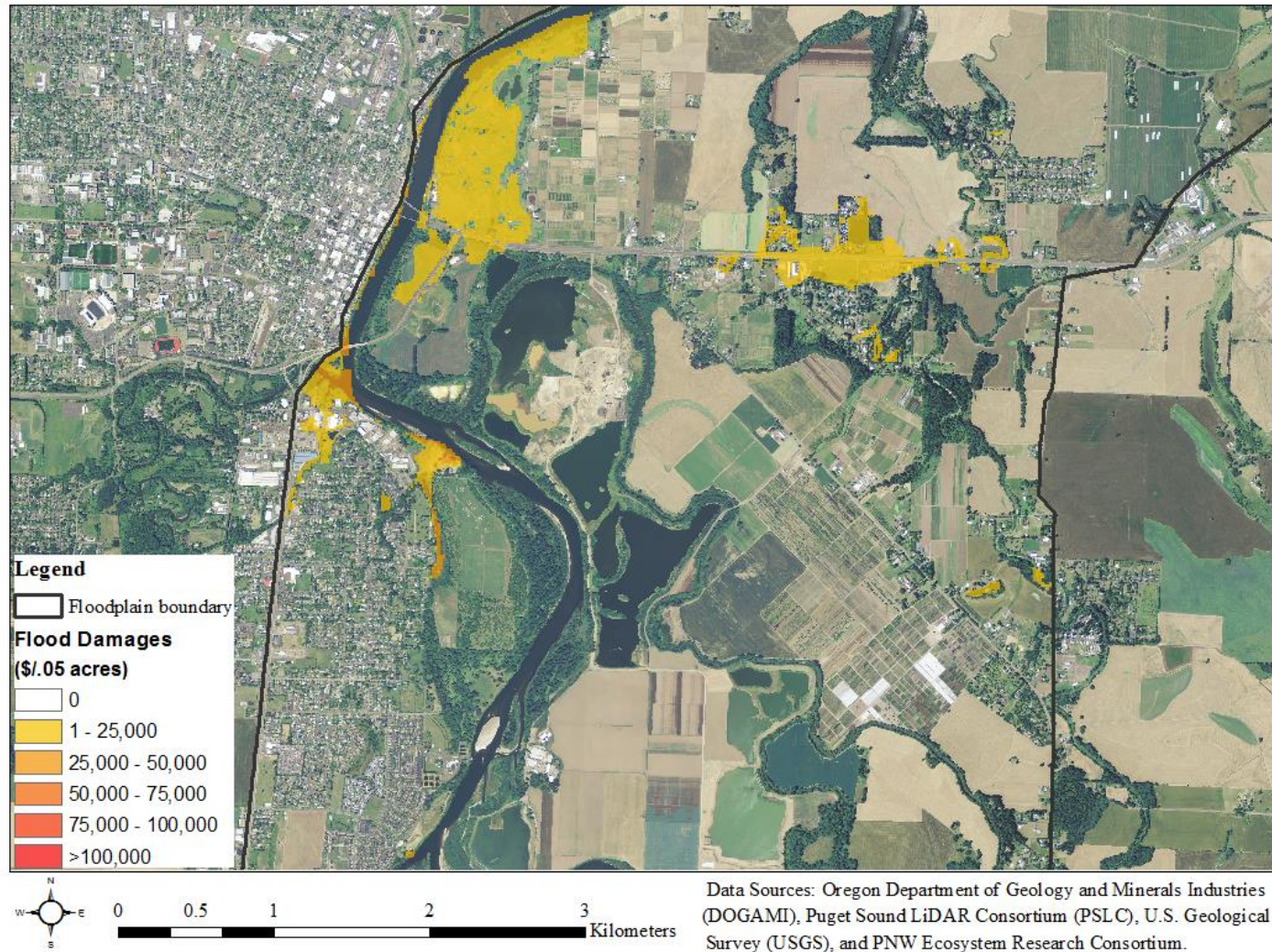


Figure 2.35. Flood damages in the Willamette's mainstem floodplain at Corvallis under the high population growth scenario in 2030. Orthoimagery as of 2012 from the National Map Viewer.

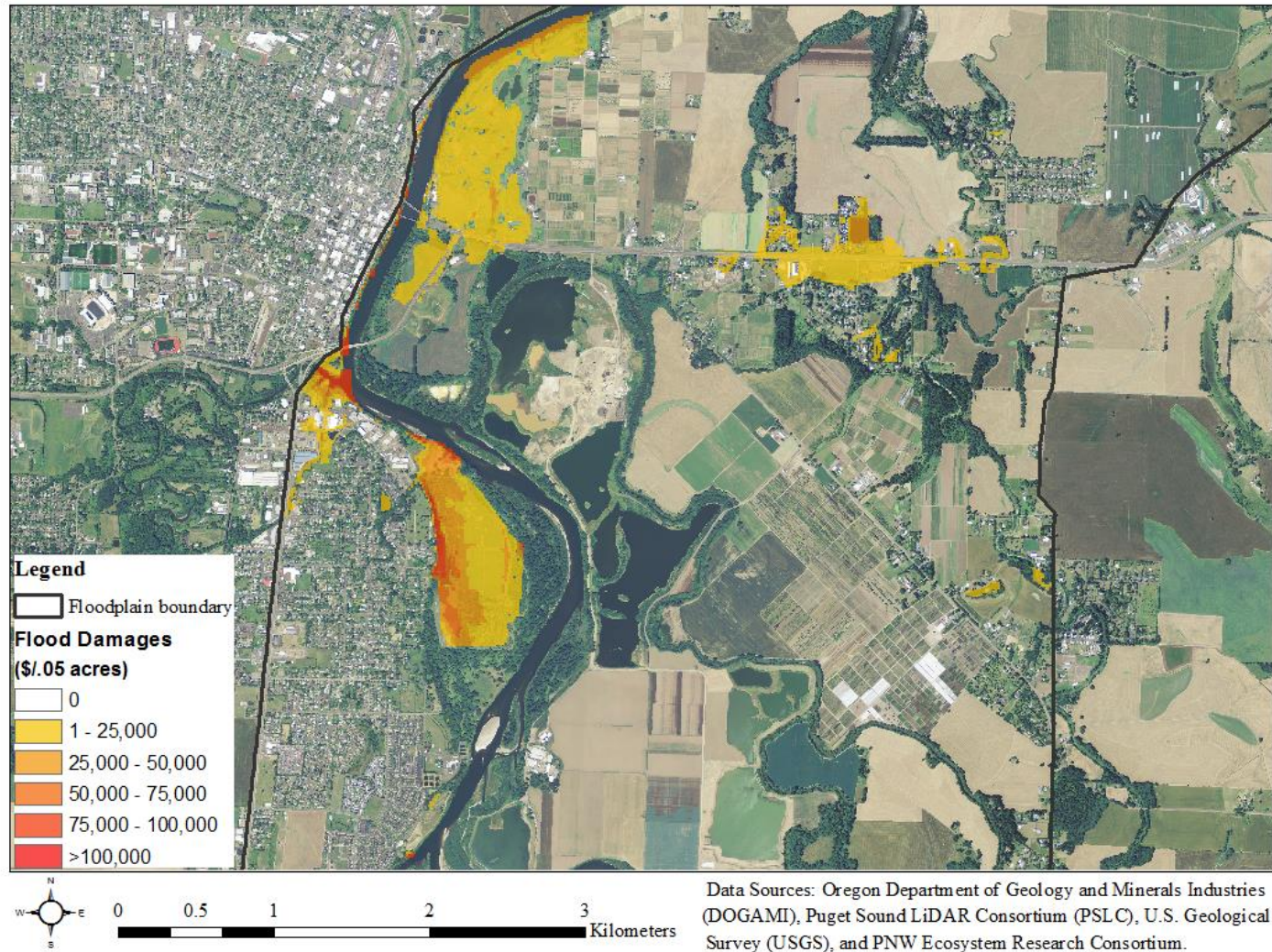


Figure 2.36. Flood damages in the Willamette's mainstem floodplain at Corvallis under the high population growth scenario in 2100. Orthoimagery as of 2012 from the National Map Viewer.

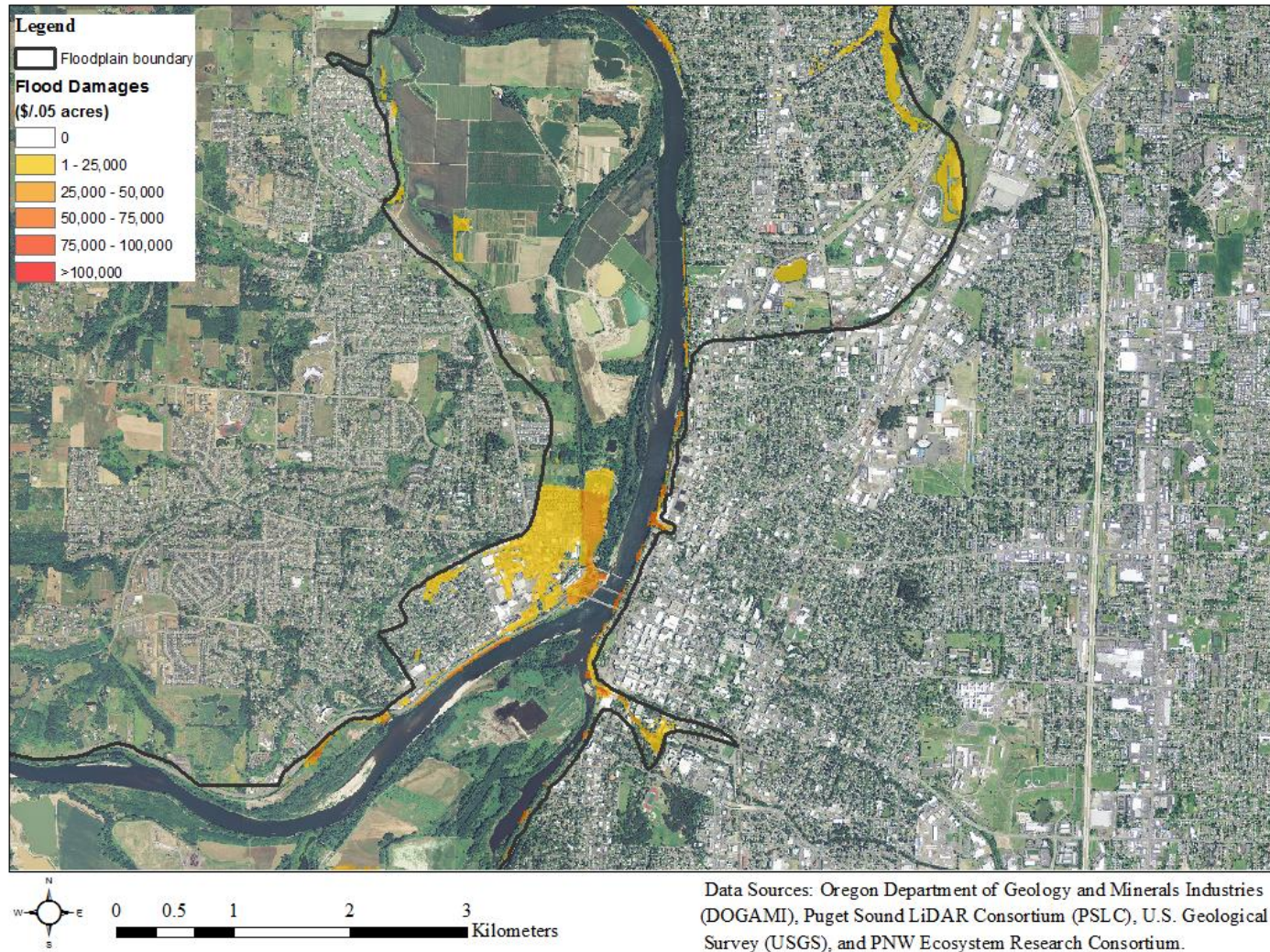


Figure 2.37. Flood damages in the Willamette's mainstem floodplain at Salem under the high population growth scenario in 2030. Orthoimagery as of 2012 from the National Map Viewer.

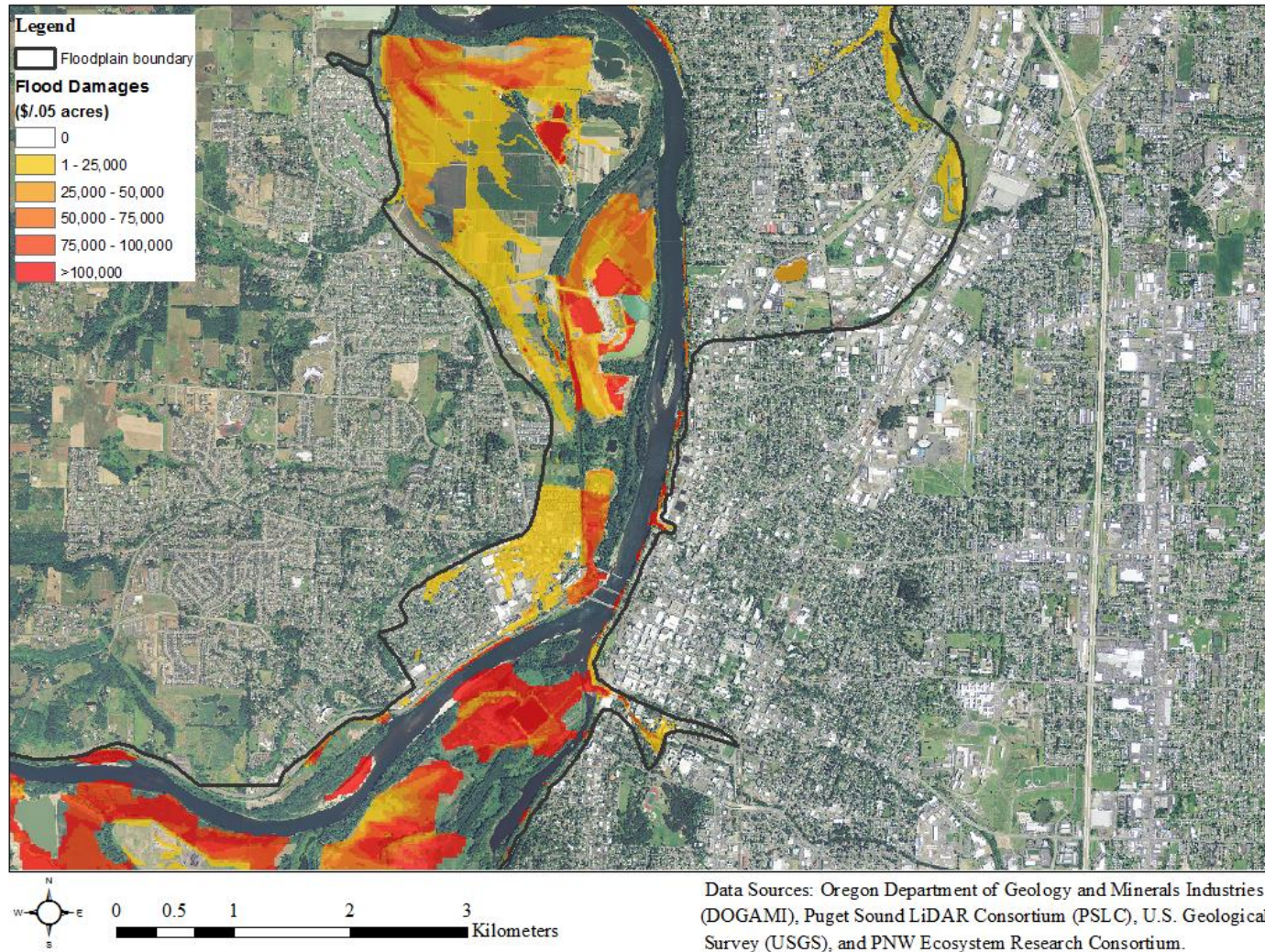


Figure 2.38. Flood damages in the Willamette's mainstem floodplain at Salem under the high population growth scenario in 2100. Orthoimagery as of 2012 from the National Map Viewer.

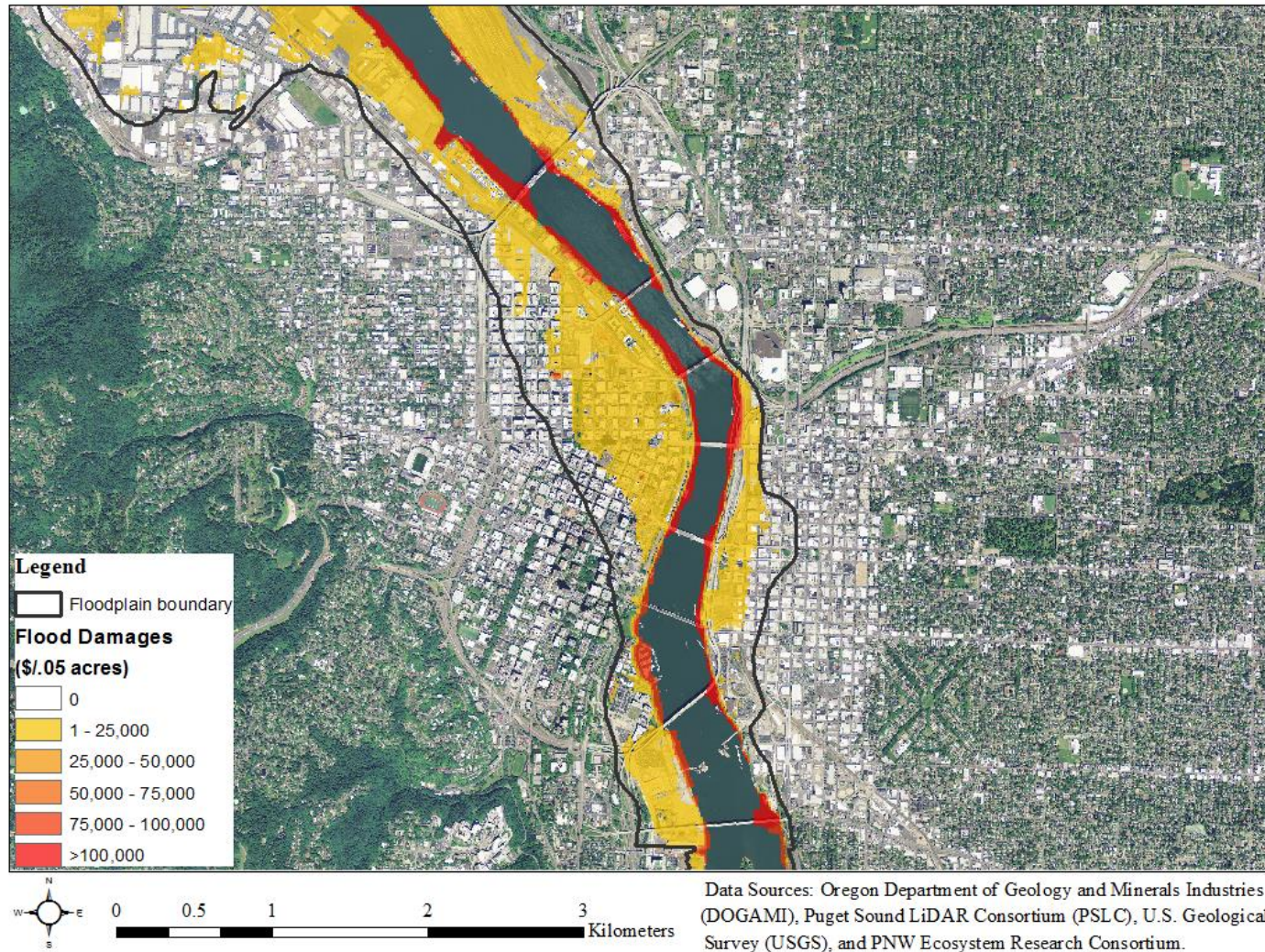


Figure 2.39. Flood damages in the Willamette's mainstem floodplain at Portland under the high population growth scenario in 2030. Orthoimagery as of 2012 from the National Map Viewer.

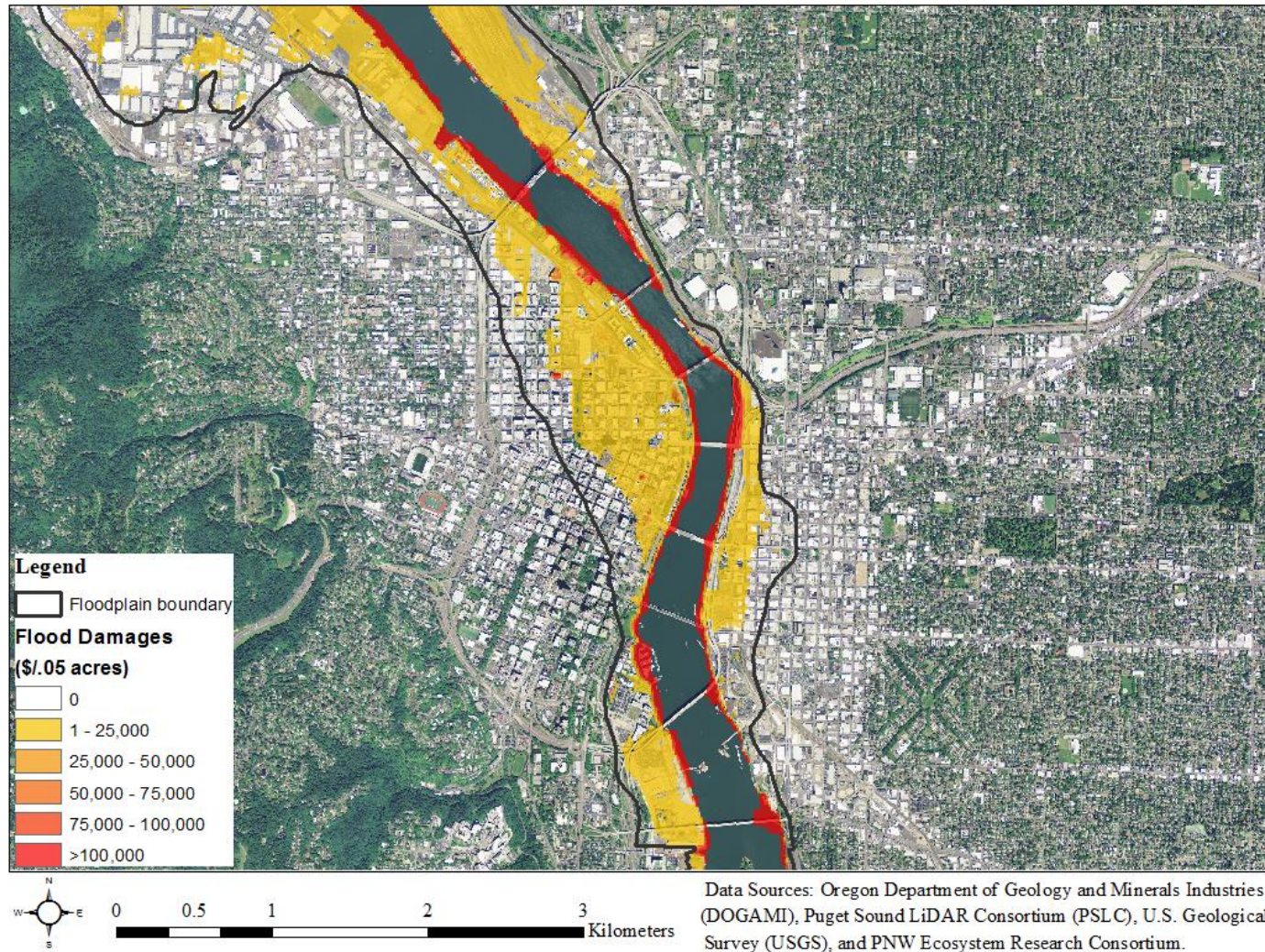


Figure 2.40. Flood damages in the Willamette's mainstem floodplain at Portland under the high population growth scenario in 2100. Orthoimagery as of 2012 from the National Map Viewer.

2.5.4 The value of reservoir management for flood damage reduction

For all the land use change scenarios investigated, the estimated marginal costs of flood damages increased as the level of flood inundation rose (Table 2.7), indicating that increasing amounts of structural value are susceptible to flooding as flood stage increases. The marginal costs rose especially rapidly from the major to the historical high flood stage categories. Across the land use scenarios, the marginal costs of flooding were lowest for the relaxed UGB scenario and highest for the high population growth scenario, with little difference in the estimated marginal costs between the reference case scenario and relaxed UGB scenarios across all flood stage categories. The amount and value of structural development in the floodplain, and the marginal costs of flood damages increased over time in all the scenarios. Under the reference case scenario in 2030, the estimated marginal costs of flooding ranged from \$1,654 per acre-foot at the flood stage category to \$3,288 per acre-foot for the historical high flood. On average these values increased by 75% in 2070 and by 145% in 2100, relative to 2030. Under the high population growth scenario, the marginal costs of flooding increased on average for all the flood stage categories by 182% in 2070 and by 303% in 2100 relative to the reference case scenario in 2030.

Given the assessed probability distributions of flooding, the expected flood damages that could be averted using reservoir capacity to store flood waters were highest in the week of January 15th, reaching a value of \$304 million under the reference case scenario in 2030 assuming that all reservoir storage capacity was available (Table 2.8, Figure 2.41). This value increased to \$539 million under the reference case scenario in 2070 and \$1,284 million under the high population growth scenario in 2100 (Table 2.8). As the reservoir fill level was increased and the storage capacity declined, the value of expected flood damages that could be averted

decreased (Figure 2.41). At full storage (1700 KAF) no damages could be averted since no further flood waters could be retained.

The expected value of averted flood damages tended to decrease between January and mid-May, and values were clustered in four periods corresponding to the probability of flooding (Table 2.8, Figure 2.41). From January 1st through the week of January 15th the maximum expected value of averted flood damages ranged from \$249-304 million under the reference case scenario in 2030, increasing to \$445-539 million under the reference case scenario in 2070, and \$1,079-1,284 million under the high population growth scenario in 2100. These values declined by approximately 50% for the period from mid-January through the end of February, followed by a decline to about 15% of the early January values over the period from the beginning of March through the first week of April. Following that few to no flood damages are anticipated through the end of May.

The loss functions resulting from the parametric relationship used to model the loss in expected flood damage buffering as the reservoir fill level increases each week ($R^2 = 0.91$), predict that losses are greatest at the beginning of January, and decrease towards zero over time (Figure 2.42). The cost of having no reservoir capacity available for flood damage reduction during the first week in January was estimated at \$295 million under the reference case scenario in 2030, and this cost increased by 77% for the reference case scenario in 2070 and by 322% for the high population growth scenario in 2100, and declined by 25% for the historical estimate in 2000.

Table 2.7. Marginal costs associated with each flood stage category calculated as the instantaneous change in total flood damages with respect to the associated increase in the volume of floodplain inundation within the WRB mainstem floodplain, for the Reference Case, the High Population Growth, and the Relaxed UGB scenarios of the WW2100 land cover change model for 2030, 2070, and 2100.

<u>Scenario</u>	<u>Year</u>	<u>Marginal Cost of Flood Damages (\$/acre-foot)</u>			
		<u>Flood</u>	<u>Moderate Flood</u>	<u>Major Flood</u>	<u>Historical High</u>
Reference Case	2030	1,654	1,808	1,989	3,288
	2070	2,979	3,235	3,493	5,444
	2100	4,301	4,652	4,931	7,012
High Population Growth	2030	1,950	2,125	2,349	4,022
	2070	4,999	5,351	5,619	8,084
	2100	7,296	7,871	8,217	10,553
Relaxed UGB	2030	1,614	1,779	1,968	3,220
	2070	2,987	3,290	3,611	5,550
	2100	4,231	4,652	5,012	7,008

Table 2.8. The maximum expected value of flood damage reduction using reservoir capacity in the WRB for each week from January 1st – May 20th given land cover in the Reference Case model in 2030, and 2070, and the High Population Growth model in 2100.

<u>Week Starting</u>	<u>Maximum Expected Flood Damages Averted (\$ Millions)</u>		
	<u>Reference Case</u>	<u>Reference Case</u>	<u>High Population Growth</u>
	<u>2030</u>	<u>2070</u>	<u>2100</u>
1-Jan	278	495	1,194
8-Jan	249	445	1,079
15-Jan	304	539	1,284
22-Jan	147	261	627
29-Jan	120	214	518
5-Feb	164	291	691
12-Feb	113	202	490
19-Feb	135	241	583
26-Feb	100	178	431
5-Mar	13	23	566
12-Mar	28	50	121
19-Mar	29	52	128
26-Mar	52	93	222
2-Apr	43	76	185
9-Apr	-	-	-
16-Apr	2	4	11
23-Apr	-	-	-
30-Apr	-	-	-
7-May	-	-	-
14-May	-	-	-

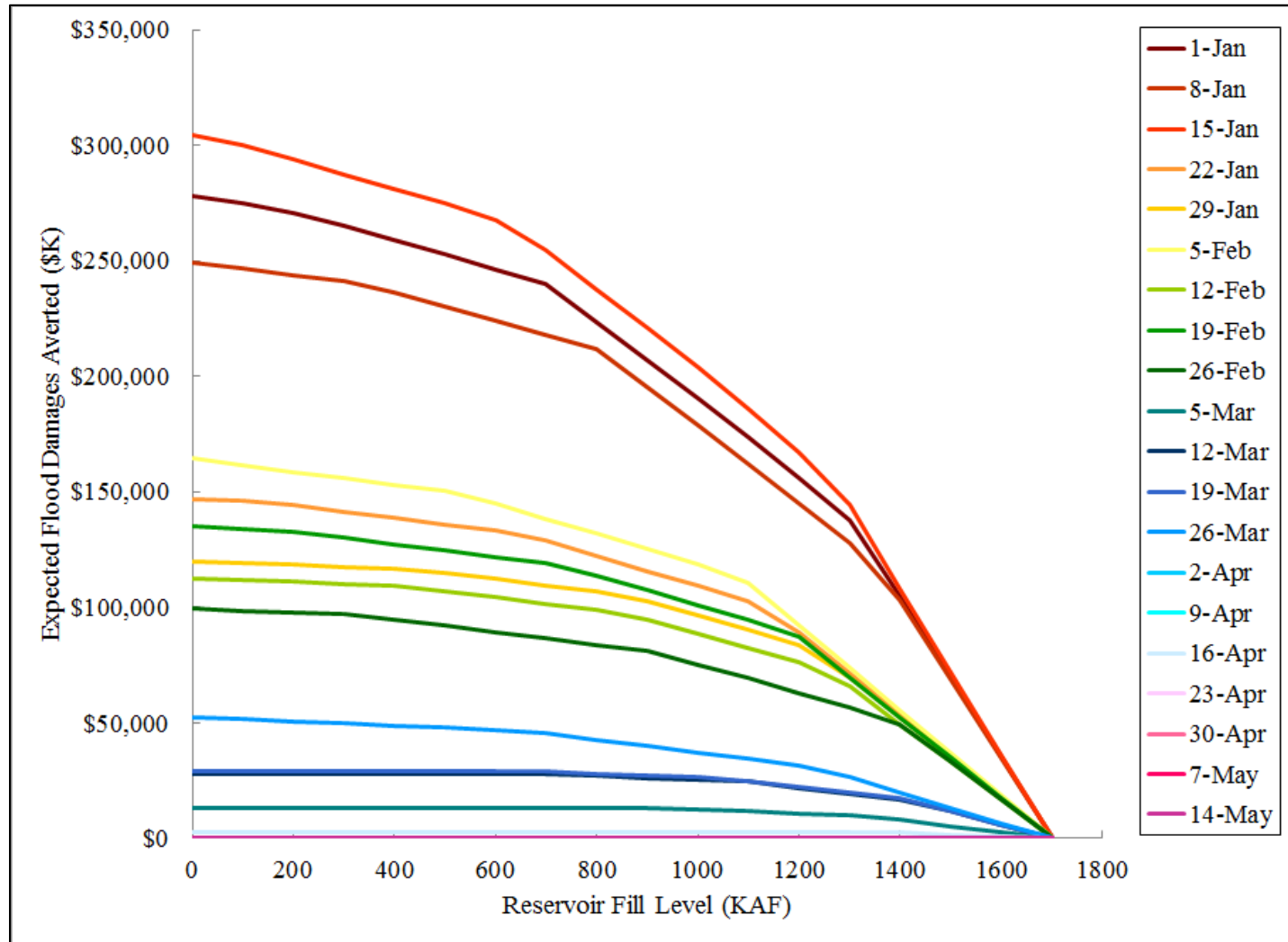


Figure 2.41. The expected value of flood damages that could be averted using reservoir capacity in the WRB by week from January 1st – May 20th estimated under the Reference Case scenario in 2030.

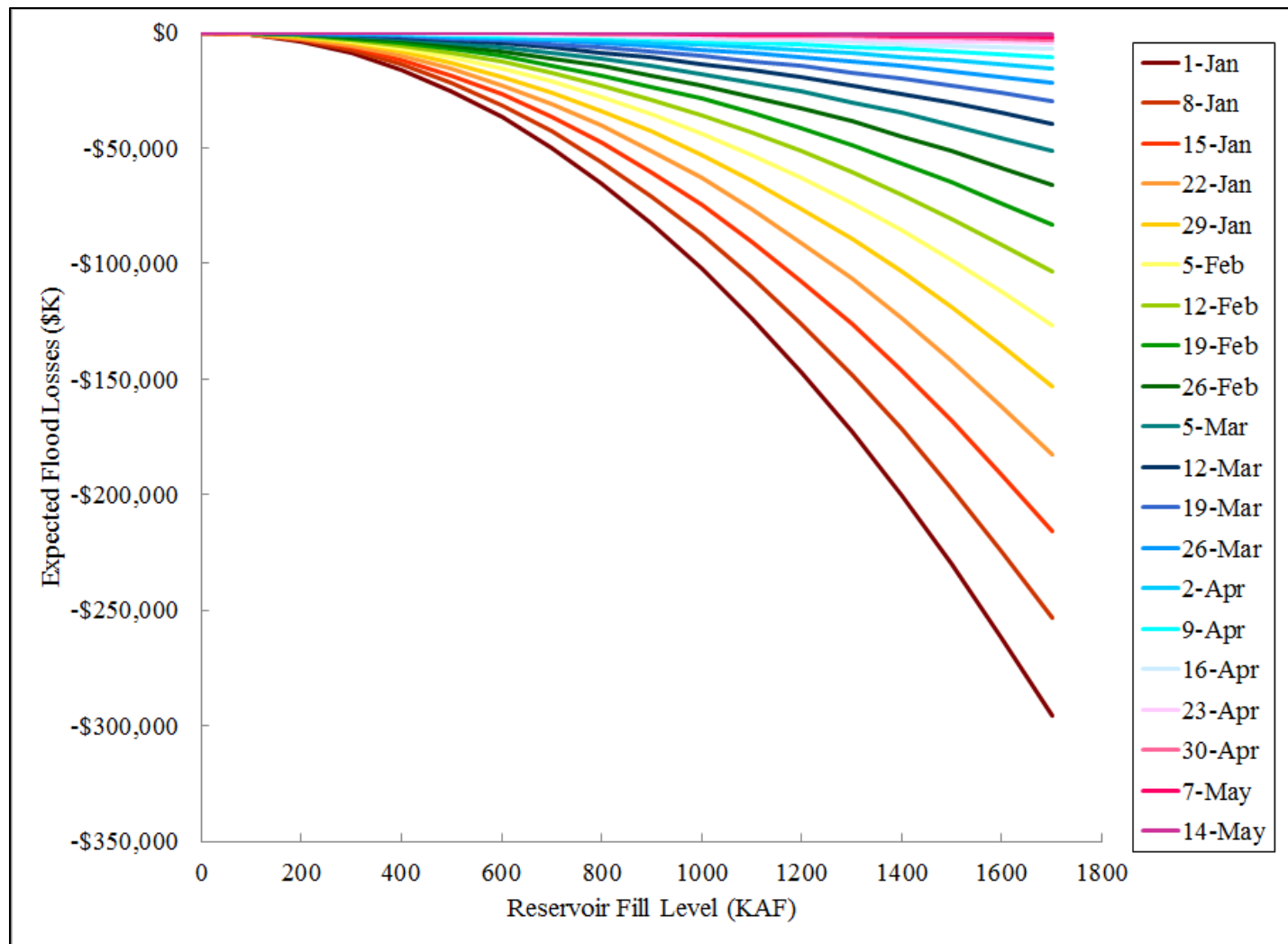


Figure 2.42. The modeled function for the expected loss of flood damage buffering due to reservoir fill in the WRB by week from January 1st – May 20th estimated under the Reference Case scenario in 2030.

2.6 Discussion

2.6.1 Accuracy of flood inundation mapping

Comparison of the inundation maps constructed for Corvallis, Salem, and Portland for the major flood category to the 1996 flood maps compiled by *Hulse et al.* [2002], indicates that the 'bathtub' methodology provides a reasonably accurate estimate of the depth and extent of flooding for a large flood event. The *River Design Group* [2012] found a similar result comparing a 'bathtub' method to an observed 2-year return interval flood in the WRB. These two findings suggest that the 'bathtub' method for flood inundation mapping works well for a range of flood sizes in the Willamette River floodplain, if the flood stage is known.

However, the flood stage and inundated area predicted in this analysis differed somewhat from the observed flood event of 1996. The 1996 flood stage observed at the gauging stations corresponded to a "moderate" flood at Corvallis, between a "major" and "historical high" flood at Salem, and a "major" flood at Portland (Figure 2.43). Given the assumptions of the inundation model, the predicted major flood category was reached at a stage that was 6 feet lower than the observed major flood stage at Corvallis; at a stage that was 3 feet higher than the observed major flood stage at Salem; and at a stage that within a foot of the observed major flood stage at Portland (Figure 2.43). Because stage of the predicted major flood category at Corvallis was 4 feet lower than the stage reached in the 1996 flood (Figure 2.43), the predicted area inundated by a major flood was smaller than the observed inundated area in the 1996 flood at Corvallis (Figure 2.26). At Salem the stage of the predicted major flood category was the same as the observed stage in the 1996 flood (Figure 2.43), and the predicted area of inundation, including those areas where the water table was predicted to be within 8 feet of the surface, closely resembled the observed area of inundation for the 1996 flood (Figure 2.27). At the Portland the stage of the

predicted major flood was the same as the stage of the observed 1996 flood (Figure 2.43), and the predicted extent of inundation closely resembled the observed extent of inundation in the 1996 flood (Figure 2.28).

There are several potential sources of error in the inundation model. The bankfull elevations along the Willamette River were estimated based on the average difference between the elevation given by the DEM and the known bankfull elevation at each gaging station. This resulted in an overestimation of bankfull in places where the DEM elevation was higher than the average difference below bankfull and an underestimation in the places where the DEM elevation was lower than the average difference. These errors might average out, and thus not affect the estimated area of inundation for each flood category across the entire floodplain. A second potential source of error stems from the 'bathtub' assumption that a similar return-period flood stage occurs throughout the Willamette floodplain, whereas in observed floods such as 1996, some parts of the basin receive more precipitation, producing spatial variation in flood stage in the basin. In addition, inundation estimates considered only the mainstem, whereas flooding and flood damages also occur along tributaries such as the Mary's River tributary at Corvallis, contributing to underestimation of flood inundation. Finally, the inundation model did not consider factors such as flood routing dynamics, channel connectivity, sediment deposition, and bank erosion. These factors could have contributed to over- or under-estimation of flood inundation in the model relative to observed floods. Despite these limitations, the model approximates inundation within the designated floodplain given the river stage in the associated reach, and it has the advantage of being conceptually simple and relatively easy to implement. Further work could investigate the tradeoff between the increased accuracy that might be gained

from a physically based model and the accompanying increased difficulty of implementation and uncertainty associated with model parameterization.

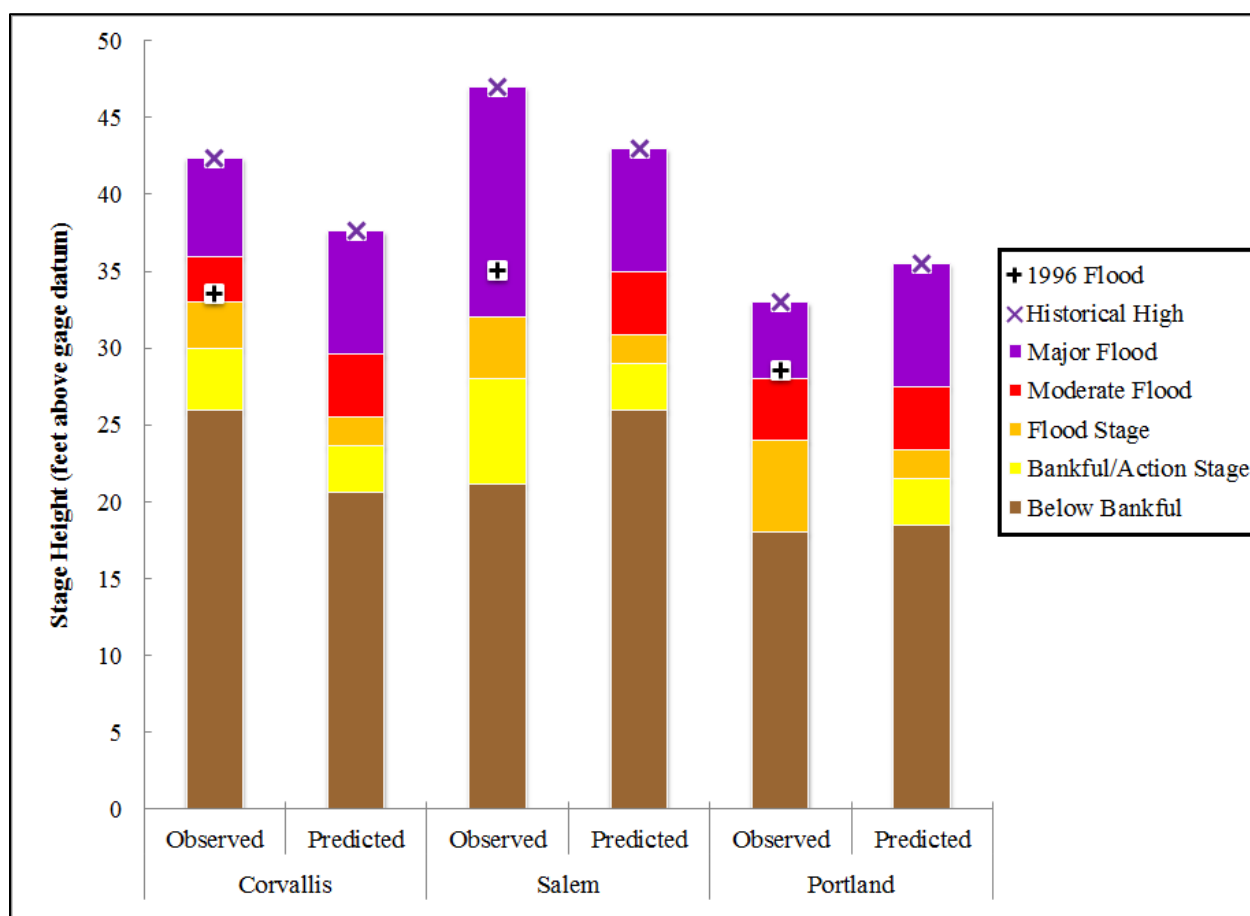


Figure 2.43. Flood category stages at the Corvallis, Salem, and Portland gauging stations as defined by NOAA (colored bars labeled "observed") compared to the flood category stages predicted by the inundation model at these locations. The maximum observed stage height reached during the 1996 flood as well as the historical high crest is also shown for each gauge.

2.6.2 Accuracy of flood damage estimation

The results demonstrate the value of having spatially explicit estimates of structural value in the floodplain at a resolution that matches the scale at which flood damages are likely to occur. LiDAR imagery provided high spatial precision of landforms. However, if land parcels and the associated value of structural development were mapped at relatively coarse spatial

resolution or were imprecisely defined, then flood damages may have been assigned to parts of land parcels that lacked structures, resulting in overestimation of flood damages. Land parcels from the WW2100 model at Corvallis, Salem, and Portland include land along the riverbanks, secondary channels and the main river channel, which are mapped as containing structures. These areas are likely to be inundated at bankfull stage and higher flows, but they do not have structures, resulting in an error of commission, i.e., an overestimation of flood damages. To mitigate this estimation error we adjusted the total damages estimated in each scenario by the damages estimated at bankfull stage.

The use of modeled land use data (e.g., the WW2100 model) to estimate flood damages also provides insights into the complex challenges of accurately modeling development in space and time. At Corvallis, the WW2100 model underestimated the extent of development in certain areas (Figure 2.29); this error of omission may have contributed to underestimation of potential flood damages. Use of modeled land cover data can also result in errors of commission. At Salem, under the high population growth scenario in 2100 (Figure 2.31), the WW2100 model predicted the development of areas including farmland and gravel bars within river channel. Such development is very unlikely given the location of these parcels within the inundation zone, and it may have contributed to an overestimation of flood damages.

Another potential source of error in using modeled land cover data arises from the estimation of structural value based on land cover classification and value in the WW2100 model (eq. 2.2). For example, at Corvallis and Salem (Figure 2.29, Figure 2.31) open areas such as golf courses and city parks were defined as developed by the WW2100 model, although these areas do not have structures, or the same kinds of structures, as private developed lands. When such parcels are within the area predicted to be inundated, the attribution of structural value based on

privately owned lands to these types of land parcels likely results in an overestimation of flood damages.

These findings highlight the importance of appropriate assumptions regarding classification and modeling of floodplain development. Predictions of future land use should consider the likelihood of flood inundation in addition to regulations or ownership that may preclude development within the floodplain [Muckleston, 1983]. The future scenarios of land use change investigated in this analysis represent a range from status quo to accelerated development, but future scenarios in the Willamette River basin may include significant conservation of floodplain areas [Baker *et al.*, 2004; Hulse and Gregory, 2004]. In such a scenario, structural development would be reduced in some parts of the floodplain and expectations for flood damages may subsequently be reduced.

Uncertainty in the estimated flood damages also stems from the use of depth-damage curves (Figure 2.5, Figure 2.6), which assess damages only as a function of flood inundation depth. However, flood damages may also depend on factors such as the transport of sediment and debris in flood waters and flood wave pulsing. The omission of these factors may result in an underestimation of flood damages.

2.6.3 Seasonal pattern of flood damages

Weekly flood damages were estimated as a continuous monotonically decreasing function of time from January to May (Figure 2.42). The flood frequency analysis indicated that flood damages may reach zero as early as mid-April, although the function that approximated these damages remained positive, leading to an overestimation of the value flood damage reduction in the remaining weeks. The fact that flood damages tended to decrease between January and mid-May (Table 2.8, Figure 2.41), has important implications for balancing the use

of reservoir capacity between flood damage reduction and stored water uses. As expected flood damages decline from winter to spring, the reservoir fill level can be increased to meet other objectives. To identify this timing, reservoir managers need information on expectations of streamflow and flood frequency at a time step appropriate for management decisions regarding the tradeoff between reservoir uses. Results of this study indicate that 3-week flood frequency information would be useful, and information on a weekly or even daily time step would more closely match the time scale of reservoir management decisions [USACE, 2012]. Moreover, whereas this study relied on flood frequency distributions based on historical data to estimate the values of flood damage reduction under scenarios of future land cover, reservoir managers would benefit from future climate model downscaling efforts [e.g., Salathé *et al.*, 2014] to provide region specific estimates of future flood series at this time step.

2.7 Summary and Conclusions

Flood damage reduction, which requires reservoirs to maintain unfilled storage capacity, is the primary authorized purpose of reservoirs in the Willamette River Basin, whereas storage of water for recreation, irrigation, municipal supply, hydropower, navigation, and requirements for downstream environmental flows, is a secondary objective. Because the storage capacity of the reservoirs cannot be used for both flood damage reduction and water storage at the same time, these two competing uses are traded off during the transition from the wet to the dry season, as the most important or dominant use of the reservoir shifts from reducing flood peaks to storing water. Both climate change and increased population are expected to increase dry season water scarcity, implying a need to critically evaluate the priority given to flood damage reduction in current reservoir operations. The recent availability of fine-scale topographic information (LiDAR), combined with historical flood frequency information, and spatially explicit estimates

of current and future value of structural development in the Willamette River floodplain provided the opportunity to quantify expected flood damages under various future scenarios of climate, population, and development. Estimated flood damages ranged from just over \$900 million for moderate floods given current population growth in 2030, to over \$16 billion for historical high floods given accelerated population growth in 2070. Estimated flood damages increased over the period 2030 to 2100 as the amount and value of developed land increased within the inundation zone of the floodplain. Higher rates of population growth further augmented estimated future flood damages. Historically expected flood damages have tended to decrease between January and mid-May. The rate of decline of flood damages influences the rate at which the reservoir fill level can be increased to store water to meet secondary objectives. It would be helpful for reservoir managers to have information on future expectations for streamflow and flood frequency on a daily basis. Ideally, with more accurate spatial modeling of structural values in the floodplain, and estimates of the probability distributions of future streamflows, the approach developed in this study could be used to provide daily information on the expected value of flood damage reduction, and enable efficient management decisions regarding the tradeoff between filling and spilling at a particular reservoir on any given day.

2.8 Acknowledgements

This project was supported by the National Science Foundation under Grant No. 1039192. Data for this research were obtained from the River Design Group, the Willamette Water 2100 Project, the US Geological Survey, and the US Army Corp of Engineers. We thank Daniel Bigelow for providing historical tax lot data for the estimation of structural values in the Willamette Basin. We are grateful for early input on this work from the River Design Group in Corvallis, Oregon.

2.9 References

- Baker, J. P., D. W. Hulse, S. V. Gregory, D. White, J. Van Sickle, P. A. Berger, D. Dole, and N. H. Schumaker (2004), Alternative futures for the willamette river basin, oregon, *Ecological Applications*, 14(2), 313–324, doi:10.1890/02-5011.
- Bales, R. C., N. P. Molotch, T. H. Painter, M. D. Dettinger, R. Rice, and J. Dozier (2006), Mountain hydrology of the western United States, *Water Resources Research*, 42(8), W08432, doi:10.1029/2005WR004387.
- Barnett, T. P. et al. (2008), Human-Induced Changes in the Hydrology of the Western United States, *Science*, 319(5866), 1080–1083, doi:10.1126/science.1152538.
- BPA, USBR, and USACE (2001), The Columbia River System Inside Story, Available from: http://www.bpa.gov/power/pg/columbia_river_inside_story.pdf (Accessed 15 April 2015)
- Chang, H., and I.-W. Jung (2010), Spatial and temporal changes in runoff caused by climate change in a complex large river basin in Oregon, *Journal of Hydrology*, 388(3-4), 186–207, doi:10.1016/j.jhydrol.2010.04.040.
- Chou, F. N.-F., and C.-W. Wu (2013), Expected shortage based pre-release strategy for reservoir flood control, *Journal of Hydrology*, 497, 1–14, doi:10.1016/j.jhydrol.2013.05.039.
- Department of Land Conservation and Development (2010), Oregon’s Statewide Planning Goals & Guidelines, Available from: http://www.oregon.gov/LCD/docs/goals/compilation_of_statewide_planning_goals.pdf (Accessed 30 March 2015)
- Elsner, M. M., L. Cuo, N. Voisin, J. S. Deems, A. F. Hamlet, J. A. Vano, K. E. B. Mickelson, S.-Y. Lee, and D. P. Lettenmaier (2010), Implications of 21st century climate change for the hydrology of Washington State, *Climatic Change*, 102(1-2), 225–260, doi:10.1007/s10584-010-9855-0.
- Graf, W. L. (1999), Dam nation: A geographic census of American dams and their large-scale hydrologic impacts, *Water Resources Research*, 35(4), 1305–1311, doi:10.1029/1999WR900016.
- Hamlet, A. F., and D. P. Lettenmaier (2007), Effects of 20th century warming and climate variability on flood risk in the western U.S., *Water Resources Research*, 43(6), W06427, doi:10.1029/2006WR005099.
- Hulse, D., S. Gregory, and J. P. Baker (2002), *Willamette River Basin Planning Atlas: Trajectories of Environmental and Ecological Change*, Oregon State University Press.
- Hulse, D., and S. Gregory (2004), Integrating resilience into floodplain restoration, *Urban Ecosystems*, 7(3), 295–314, doi:10.1023/B:UECO.0000044041.94705.52.
- Jaeger, W., A. Plantinga, R. Haggerty, and C. Langpap (2014), Anticipating Water Scarcity with Climate Change in the US Pacific Northwest: Using a Landscape Model of a Coupled

- Natural-Human System, in *World Conference of Environmental and Resource Economists*, p. 52, Istanbul, Turkey.
- Jefferson, A., A. Nolin, S. Lewis, and C. Tague (2008), Hydrogeologic controls on streamflow sensitivity to climate variation, *Hydrological Processes*, 22(22), 4371–4385, doi:10.1002/hyp.7041.
- Jung, I. W., and H. Chang (2012), Climate change impacts on spatial patterns in drought risk in the Willamette River Basin, Oregon, USA, *Theoretical and Applied Climatology*, 108(3-4), 355–371, doi:10.1007/s00704-011-0531-8.
- Knowles, N., M. D. Dettinger, and D. R. Cayan (2006), Trends in Snowfall versus Rainfall in the Western United States, *J. Climate*, 19(18), 4545–4559, doi:10.1175/JCLI3850.1.
- Mote, P. W. (2003), Trends in temperature and precipitation in the Pacific Northwest during the twentieth century, *Northwest Science*, 77(4), 271–282.
- Mote, P. W., and E. P. Salathé (2010), Future climate in the Pacific Northwest, *Climatic Change*, 102(1-2), 29–50, doi:10.1007/s10584-010-9848-z.
- Mote, P. W., A. F. Hamlet, M. P. Clark, and D. P. Lettenmaier (2005), Declining Mountain Snowpack in Western North America, *Bulletin of the American Meteorological Society*, 86(1), 39–49, doi:10.1175/BAMS-86-1-39.
- Muckleston, K. W. (1983), The Impact of Floodplain Regulations on Residential Land Values in Oregon1, *JAWRA Journal of the American Water Resources Association*, 19(1), 1–7, doi:10.1111/j.1752-1688.1983.tb04549.x.
- Nolin, A. W., and C. Daly (2006), Mapping “at risk” snow in the Pacific Northwest, *Journal of Hydrometeorology*, 7(5), 1164–1171.
- Poff, N. L., J. D. Allan, M. B. Bain, J. R. Karr, K. L. Prestegard, B. D. Richter, R. E. Sparks, and J. C. Stromberg (1997), The Natural Flow Regime, *BioScience*, 47(11), 769–784, doi:10.2307/1313099.
- Population Research Center (2012), Available from: <http://www.pdx.edu/prc/home> (Accessed 1 March 2015)
- Richard M. Cooper (2005), *Estimation of Peak Discharges for Rural, Unregulated Streams in Western Oregon*, Scientific Investigations Report / U.S. Geological Survey.
- River Design Group (2012), *Willamette River Floodplain Inundation Mapping*, Corvallis, OR.
- Salathé, E. P., A. F. Hamlet, C. F. Mass, S.-Y. Lee, M. Stumbaugh, and R. Steed (2014), Estimates of Twenty-First-Century Flood Risk in the Pacific Northwest Based on Regional Climate Model Simulations, *Journal of Hydrometeorology*, 15(5), 1881–1899, doi:10.1175/JHM-D-13-0137.1.
- Serreze, M. C., M. P. Clark, R. L. Armstrong, D. A. McGinnis, and R. S. Pulwarty (1999), Characteristics of the western United States snowpack from snowpack telemetry

- (SNOTEL) data, *Water Resources Research*, 35(7), 2145–2160, doi:10.1029/1999WR900090.
- Stewart, I. T., D. R. Cayan, and M. D. Dettinger (2005), Changes toward earlier streamflow timing across western North America, *Journal of climate*, 18(8), 1136–1155.
- USACE (2000), Economic Guidance Memorandum (EGM) 01-03, Generic Depth-Damage Relationships., Available from:
<http://planning.usace.army.mil/toolbox/guidance.cfm?Option=Type&BL=None&Type=EGM&Sort=Default> (Accessed 15 April 2015)
- USACE (2003), Economic Guidance Memorandum (EGM) 04-01, Generic Depth-Damage Relationships for Residential Structures with Basements., Available from:
<http://planning.usace.army.mil/toolbox/guidance.cfm?Option=Type&BL=None&Type=EGM&Sort=Default> (Accessed 15 April 2015)
- USACE (2011), Willamette Valley - Operating the reservoirs, introducing the rule curve, Available from:
http://www.nwp.usace.army.mil/Portals/24/docs/pubs/WV_water_mgmt_FS_2011a.pdf (Accessed 26 February 2015)
- USACE (2012), *Willamette Basin Guide Standard Operating Procedures (SOP) for Reservoir Control Center*, United States Army Corp of Engineers, Portland, OR.
- U.S. Army Engineer Institute for Water Resources (2013), *Flood Risk Management*, U.S. Army Engineer Institute for Water Resources.
- USFWS (2008), *Biological Opinion on the Continued Operation and Maintenance of the Willamette River Basin Project and Effects to Oregon Chub, Bull Trout, and Bull Trout Critical Habitat Designated Under the Endangered Species Act.*, U.S. Fish and Wildlife Service.
- U.S. Interagency Advisory Committee on Water Data (1982), *Guidelines for Determining Flood Flow Frequency Bulletin 17-B of the Hydrology Subcommittee*, U.S. Geological Survey, Office of Water Data Coordination.
- Vonk, E., Y. P. Xu, M. J. Booij, X. Zhang, and D. C. M. Augustijn (2014), Adapting Multireservoir Operation to Shifting Patterns of Water Supply and Demand, *Water Resources Management*, 28(3), 625–643, doi:10.1007/s11269-013-0499-5.
- Yu, P.-S., T.-C. Yang, C.-M. Kuo, J.-C. Chou, and H.-W. Tseng (2014), Climate change impacts on reservoir inflows and subsequent hydroelectric power generation for cascaded hydropower plants, *Hydrological Sciences Journal*, 59(6), 1196–1212, doi:10.1080/02626667.2014.912035.

Chapter 3: The Value of Stored Water for Summertime Reservoir Recreation in the Willamette River Basin, Oregon

3.1 Abstract

Reservoir recreation, which requires the maintenance of relatively high water levels, has become an important use of reservoirs in the western US. Lowered water levels can impact recreation through compromised amenities and aesthetics such as ‘bathtub rings’, increased mud flats and loss of ramp access. The demand for high water levels potentially puts recreation in competition with other reservoir uses. Because climate change is expected to exacerbate water scarcity in the western US, the expected value of stored water for reservoir recreation should be considered as an important component of future water resources decision-making. The availability of eleven years of monthly visitor count data on reservoir use for nine reservoirs in the Willamette River Basin provided the opportunity to quantify how visitor days was related to variation in water levels. The estimated relationship was then used to estimate the implied value of stored water for reservoir recreation. Visitor days were found to decline by as much as 2% per foot drop in water level below full pool. Reservoirs with shallower water depths or shorter boat ramps were associated with a greater reduction in visitor days with falling water levels, while greater proximity to population centers increased the number of visitor days at a reservoir. Based on this evidence of visitor response, we estimated a marginal value of stored water for recreation ranging from \$0.10 to \$78 per acre-foot per month, depending on the reservoir. These values are comparable to prior estimates in other parts of the western US. Since the estimated value of water to irrigated agriculture in the Willamette River Basin falls within this range, these results suggest that it would be beneficial to society to release stored water from some reservoirs for downstream needs in the basin, while maintaining full reservoir capacity for recreation in others.

3.2 Introduction

Public reservoirs constructed for flood control or irrigation objectives often serve as sources of recreation in large river basins in the western US. Management of those reservoirs involves tradeoffs between competing uses when decisions favoring one objective compete with other objectives. Managing reservoirs for recreation requires maintenance of high water levels; lowered water levels can impact recreation through compromised amenities and aesthetics such as ‘bathtub rings’, increased mud flats and loss of ramp access. Because climate change is expected to exacerbate water scarcity in the western US [Stewart *et al.*, 2005; Barnett *et al.*, 2008; Chang and Jung, 2010; Elsner *et al.*, 2010], understanding the value of water for competing uses will increase in importance.

The value of stored water to reservoir recreation is an important component of water resources decision-making. However, the value of water for reservoir recreational use is largely a “non-market value” where market prices and quantities are not observable as a way to measure the social value of water made available for this particular use. In contrast information on farm costs, revenues, and profits make estimation of the value of water for irrigation in agriculture relatively easy to estimate.

The objective of this chapter is to estimate the value of stored water for summertime reservoir recreation in the Willamette River Basin, Oregon. The United States Army Corps of Engineers (USACE) operates a system of 13 reservoirs, including 11 storage reservoirs, in the Willamette River Basin (WRB) known as the Willamette Project (Figure 3.1). Outdoor recreation has become a major use of the WRB reservoirs with an estimated 4.3 million annual recreational visits [USFWS, 2008]. The increased importance of recreation has put pressure on the USACE to provide reservoir fill levels that are at or close to full pool over the recreational

season (June through August) [USFWS, 2008]. To the extent that reservoir managers aim to maximize the value of reservoirs to society, an estimate of the value of stored water for reservoir recreation may contribute to better decision making [Loomis, 2000].

The method used for this analysis relies on eleven years of observed recreational visits at nine of the Willamette Project reservoirs. The availability of this data provided an opportunity to quantify how recreational visits respond to changes in reservoir water levels, and to use that information to estimate the value of stored water for reservoir recreation. We addressed four questions:

- 1) How do recreational visits respond to changes in reservoir water levels?
- 2) What is the implied marginal value of stored water for reservoir recreation?
- 3) How do (1) and (2) vary among the Willamette Project reservoirs?
- 4) What geographic characteristics of Willamette Project reservoirs might contribute to this variation?

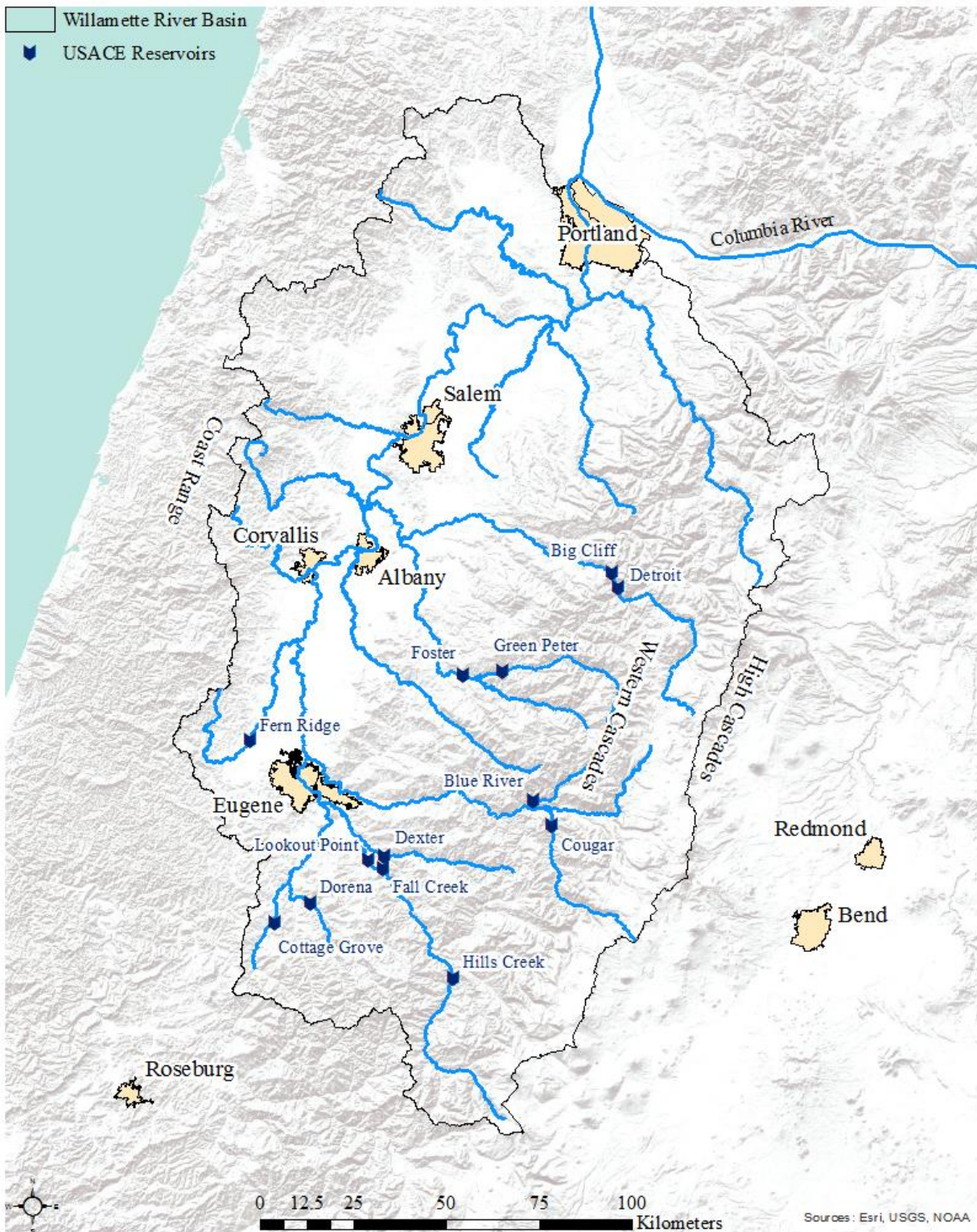


Figure 3.1. Locations of the Willamette Project reservoirs and nearby population centers.

3.3 Study Site

The WRB encompasses an area of approximately 30,000 km², which is bounded by the Oregon Coast Range to the west and the Cascade Mountains to the east (Figure 3.1). Elevation in the basin ranges from close to sea level to over 3000 m. Climate is classified as Mediterranean with cool, dry summers and mild, wet winters. Annual precipitation ranges from 1000 mm in the Willamette Valley to 4000 mm at the crest of the Cascades, and approximately 80% of annual precipitation falls between October and May [*Chang and Jung*, 2010]. The topographic effects of the Coast Range and the Cascades result in a slight rain shadow in the western part of the basin and steep orographically controlled precipitation gradients in the Cascades. Up to half of the annual precipitation falls as snow in the high elevations of the Cascades [*Serreze et al.*, 1999] while a negligible proportion of snow occurs in the Coast Range and the Willamette Valley. Catchments draining the High Cascades exhibit a snow-dominated pattern of annual streamflows, whereas the lower elevation catchments in the Western Cascades are transitional (mixed rain-snow) in nature and the tributaries draining the Coast Range are rain-dominated. Streamflow timing in the Willamette River matches precipitation timing. More than half the annual flow at the mainstem Salem gauge (USGS station number 14166000) occurs between November and February and approximately 87% of flow for the water year (Oct-Sep) occurs by the end of May.

The Willamette Project reservoirs are located primarily in the southern portion of the basin, predominantly on tributaries draining the Cascade Range (Figure 3.1). During the winter flood season from December to February, the volume of water in the WRB reservoirs is kept at a minimum to provide storage capacity to buffer storm events. Starting February 1st the USACE begins adding water to storage with the goal of having the reservoirs at full by May 20th, ahead

of the Memorial Day holiday. The reservoirs are kept as full as possible for recreation through the summer, with prioritized releases for downstream flow requirements and competing uses of stored water such as irrigated agriculture [*USACE and OWRD, 2000; USFWS, 2008*].

Normal reservoir storage capacity ranges from 30 KAF at Cottage Grove and Foster to 337 KAF at Lookout Point (Table 3.1). The combined full pool storage capacity is just over 1.7 million acre-feet (2.1 cubic km). Different landform settings for the reservoirs result in varying rates of decline in the volume of stored water as the water level falls below full pool. Reservoir volume decreases rapidly as reservoir level declines at Fern Ridge, Lookout Point, Detroit, Green Peter, and Hills Creek (Figure 3.2). The surface area of the reservoirs at full pool ranges from 241 acres at Cottage Grove to 8,593 acres at Fern Ridge (Table 3.1). Surface area also declines relatively rapidly as reservoir level decreases at Fern Ridge, Lookout Point, Detroit, and Hills Creek (Figure 3.3).

Access points to public ramps for recreational boating activities at the Willamette Project reservoirs range from two (at Green Peter, Cougar, Dorena, and Cottage Grove) to nine (at Detroit) per reservoir. These boat ramps access various depths below the full pool water level (Table 3.1). As reservoir water level drops, Fall Creek reservoir loses boat ramp access first, because one of its boat ramps extends to only 5 feet below full pool. Foster, Fern Ridge, Dorena, Lookout Point, Detroit, and Cottage Grove all lose some boat ramp access when reservoir level drops between 6 to 11 feet below full pool. Blue River, Hills Creek, and Green Peter lose some boat ramp access at reservoir levels 20 to 30 feet below full pool. Cougar reservoir loses all boat ramp access at a reservoir level 55 feet below full pool. Complete loss of ramp access at each reservoir ranges from 10 feet below full pool at Fern Ridge to over 100 feet below full pool at Fall Creek, Detroit, Hills Creek, and Lookout Point.

Table 3.1. Characteristics of the Willamette Project storage reservoirs. Source: USACE.

<u>Reservoir</u>	<u>Storage Volume*</u> (KAF)	<u>Surface Area†</u> (Acres)	<u>Boat Ramps</u> (#)	<u>Ramp Elevation Range</u> (Feet below full pool)	<u>Depth to Full Pool‡</u> (Feet)
Lookout Point	337	4,340	4	6 - 105	241
Detroit	301	3,560	9	8 - 114	369
Green Peter	268	309	2	30 - 91	315
Hills Creek	200	2,800	3	21 - 100	299
Cougar	148	1,300	2	55	399
Fall Creek	116	254	3	5 - 141	161
Fern Ridge	95	8,593	4	6 - 10	26
Blue River	86	1,025	2	20 - 55	253
Dorena	71	255	2	7 - 67	100
Cottage Grove	30	241	2	11 - 45	73
Foster	30	1,300	3	6 - 24	115

*The total capacity from minimum to full pool. Water storage below minimum pool is maintained for power production purposes and is not included in the total.

†The surface area at full pool storage.

‡The depth from empty to full pool.

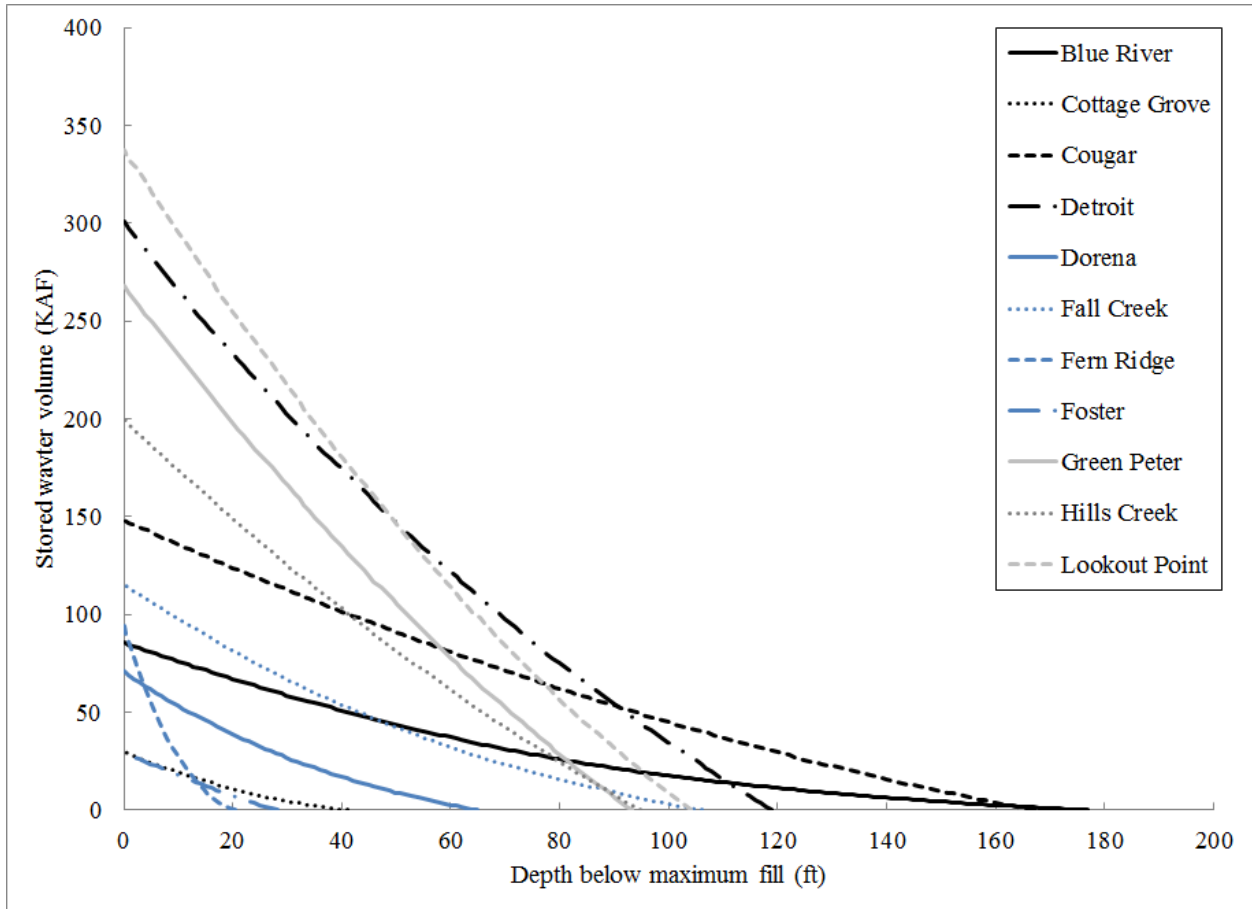


Figure 3.2. The change in volume of stored water as the water level falls below full pool at each of the Willamette Project storage reservoirs.

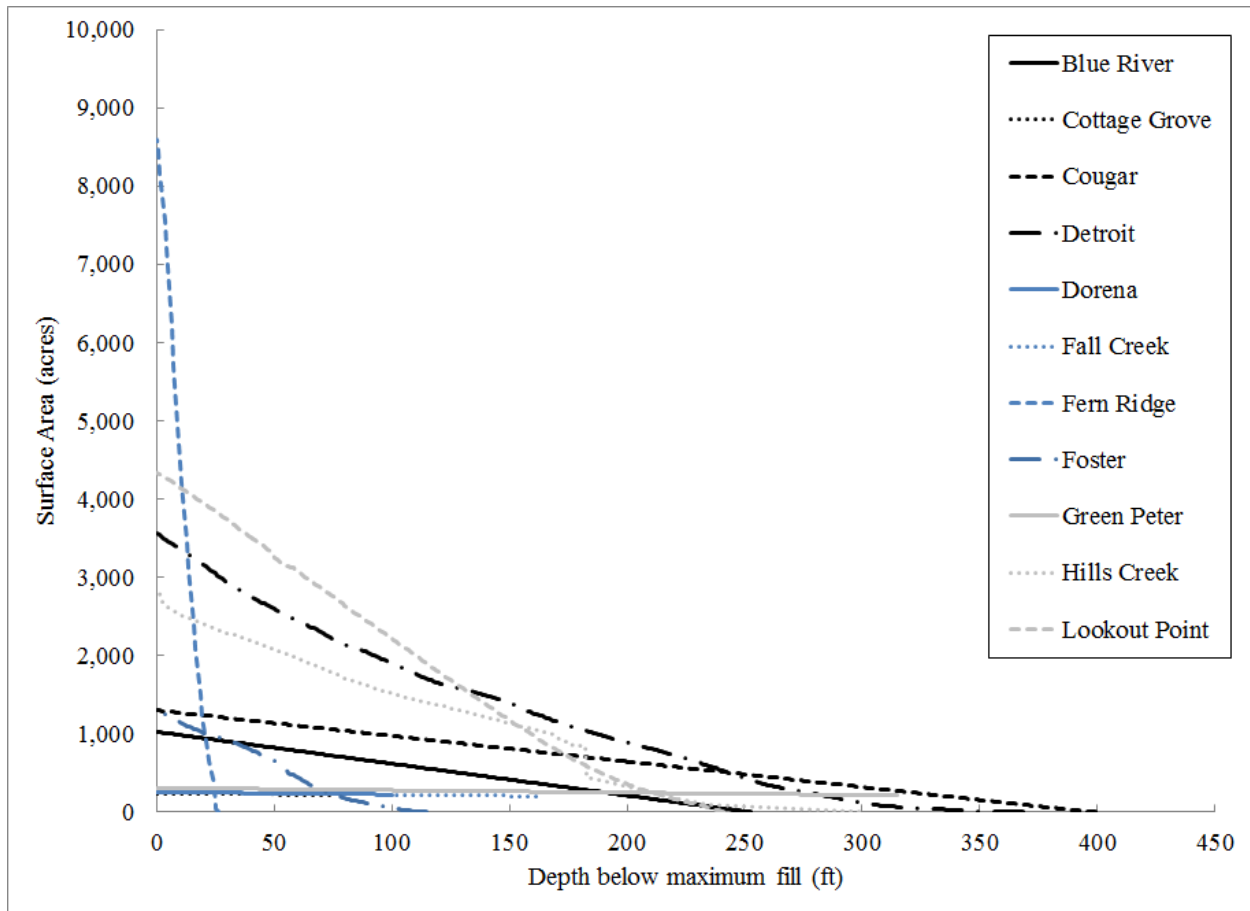


Figure 3.3. The decline in the water surface area at each of the Willamette Project storage reservoirs as the water level falls below full pool.

3.4 Theory and Methods

3.4.1 Theoretical model

The value of a reservoir for recreational purposes depends on many factors including amenities, aesthetics, geographic characteristics, accessibility to population centers, and the fill level. The recreational value, W , of a reservoir can be decomposed into components of the average value per visit (willingness-to-pay), WTP , and the number of visits R , where R is a function, $F(X', z)$, of a vector, X' , of factors including the amenities, aesthetics, and geographic characteristics of the reservoir. R is also a function of the reservoir fill level, z , which in turn

depends on the volume of water, φ , in the reservoir and the shape, g , of the reservoir. For the set of storage reservoirs (indexed by j) in the WRB we can write this as:

$$W_t = (WTP_{avg}) * \sum_{j=1}^{11} F(X'_j, z(\varphi_j, g_j)) \text{ for all periods } t. \quad (3.1)$$

The value of stored water for reservoir recreation is then given by:

$$\frac{dW}{d\varphi} = (WTP_{avg}) \frac{\partial F}{\partial z} \frac{\partial z}{\partial \varphi} \quad (3.2)$$

The third term of this expression ($\frac{\partial z}{\partial \varphi}$) is determined by the shape of each reservoir (surface area relationship to volume). In the following sections we describe the methods used to estimate the change in recreational visits as the reservoir fill level falls below full pool ($\frac{\partial F}{\partial z}$), and the average value per recreational visit (WTP_{avg}).

3.4.2 Estimating response in recreational visitor days to reservoir water level

In this section we describe the methods used to estimate the behavioral response of recreational visits to falling reservoir water levels. Monthly estimates of visits to recreation sites at the Willamette Project storage reservoirs were obtained from the USACE (Tamara Schroeder, personal communication) for the months of June, July, and August, corresponding to the summertime recreational period, which lasts from Memorial Day until Labor Day [*USACE and OWRD*, 2000]. Data from 2001-2006 and 2008-2011 were in units of visitor days and data from 2001-2007 were in units of visitor hours. Hourly data for 2007 were converted into visitor days using the ratio of hours to days in the corresponding month from the closest year with data. The

data were collected by the USACE with automated vehicle counters [USACE, 2013]. The USACE maintains the data in their Visitation Estimation and Reporting System (VERS), which is not publically accessible.

The number of recreational sites per reservoir monitored for visitors by the USACE ranged from zero at Detroit to 15 at Fern Ridge during the study period (Table 3.2). In general the number of sites monitored at the reservoirs has increased over time. The number of recreational visitor days varied both by month and across reservoir sites (Table 3.2). Visitation tended to be highest in July: visitor days/month averaged almost 40,000 at one of the recreation sites at Dorena, 35,000 at a site at Foster reservoir, and 34,000 at a site at Fall Creek. Visitor days/month exceeded 30,000 in August at one of the Cottage Grove sites, and almost reached 23,000 in June at a Dorena site. However, there were also sites with fewer than 1,000 visitor days per month in June, July, and August at Lookout Point, Fall Creek, Dorena, and Cottage Grove reservoirs. Visitor days varied by more than an order of magnitude among sites at Fall Creek, Fern Ridge, Dorena, Cottage Grove, and Foster reservoir.

Due to concern in reporting accuracy of visitor days based on vehicle counters [USACE, 2013], the analysis included only sites with five or more years of visitor day data, and reservoirs with at least two monitored sites. Detroit and Hills Creek reservoirs were therefore omitted from the analysis of visitor day response to reservoir water level. Data from the remaining reservoir sites were tested for normality, and found to have outliers. Five model structures were tested, each with some outliers removed. Outliers were defined as values of visitor days that were more than three standard deviations from the following values, calculated by excluding the potential outlier:

- 1) The monthly average.
- 2) The monthly average, where standard deviation was calculated for all summer months.
- 3) The average for all summer months.
- 4) The average for that month over the two adjacent years.
- 5) The average for that month over the two adjacent years where standard deviation was calculated for all summer months.

These definitions flagged 18-20% of the visitor day observations as outliers.

Reservoir water level data were obtained from the USACE hydrometeorological database (<http://www.nwd-wc.usace.army.mil/cgi-bin/dataquery.pl>). For each reservoir, multiple data sensors were combined to provide maximum coverage of the study period. The data were interpolated to a uniform time-step of 30-minute intervals, and average daily values were calculated for all days with at least one water level observation. Average monthly values were then calculated to match the resolution of the visitation data.

In June (of 2001 to 2011) the median depth of reservoir water level below full pool ranged from 0.2 feet at Fern Ridge and Foster to 12.3 feet at Lookout Point and 15.7 feet at

Cougar reservoir (Figure 3.4). The values at Cougar are influenced by the complete drawdown of the reservoir in 2002-2004 for the installation of a temperature control tower [USFWS, 2008].

Excluding these years, the median shortfall in fill level at Cougar during June was only 5.0 feet.

Apart from Cougar, the maximum shortfall in fill level during June ranged from 0.9 feet at Foster to 71.7 feet at Blue River. In July the median shortfall ranged from 0.3 feet at Foster to 22.1 feet at Green Peter, while the maximum shortfall ranged from 7.9 feet at Foster to 75.5 at Blue River.

In August the median values ranged from 0.3 feet at Foster to 36.9 feet at Lookout Point, and the maximum values ranged from 14.5 feet at Foster to 104 at Blue River.

The effect of reservoir water level on recreational visitor days was estimated using the following model specification:

$$\alpha_{it} = \beta_0 + \beta_1 z_{it} + \beta_2 (z_{it} * D) + \beta_3 y_{it} + \beta_x X'_{it} + \gamma_i + \epsilon_{it} \quad (3.3)$$

Where the index term t refers to time (year-month) and i denotes the recreation site. The model was specified by recreation site rather than at the reservoir level because of the lack of visitor day data for all reservoir recreation sites. The response variable α was normalized as the ratio of visitor days at a recreation site to the average number of visits at the site during the study period. This assumes that the responses are proportional to the expected number of recreational visits at each site. The coefficients on the explanatory variables are therefore interpreted as the percentage change in visitor days per unit change in the explanatory variable. The explanatory variable z gives the reservoir water level depth in feet below full pool. The interaction term, $z_{it} * D$, multiplies the water level by a dummy variable, D , for the reservoir associated with the recreation site. This term allows different responses in visitor days at each reservoir to changes in

water level. The variable y is binary, and is set to 1 if the reservoir water level is above the elevation of the lowest boat ramp, and is 0 otherwise. X' is a vector of other control variables included in the model including the month, weather (temperature and precipitation), and the proximity of each reservoir to population centers (Table 3.3). The term γ is a fixed effects term for each recreation site, which acts like a dummy variable, and captures site specific characteristics that are assumed to be constant over time [Englin and Cameron, 1996; Ashenfelter et al., 2002]. The inclusion of γ accounts for the possibility of unobservable heterogeneity. The statistical software Stata was used to estimate the model and compute heteroskedasticity robust standard errors.

Table 3.2. The range in visitor days at recreation sites at the Willamette Project reservoirs for the months of June-August, averaged over the period 2001-2011.

<u>Reservoir</u>	<u>Number of Recreation Sites Monitored*</u>	<u>Range in Average Visitor Days at Recreation Sites[†]</u>		
		<u>June</u>	<u>July</u>	<u>August</u>
Lookout Point	3 - 4	572 – 3,320	671 – 4,736	401- 3,821
Detroit	0 - 1	-	-	-
Green Peter	3 - 4	1,963 – 12,414	2,612 – 13,795	2,698 – 11,358
Hills Creek	1 - 3	-	-	-
Cougar	2	2,991 - 5,025	3,912 – 5,911	3,921 – 6,106
Fall Creek	4 - 5	571 – 11,765	627 – 34,192	571 – 20,256
Fern Ridge	9 - 15	1,606 – 13,774	1,700 – 20,921	1,369 – 25,807
Blue River	2	3,648 – 3,866	4,123 - 4,945	4,006 - 4,569
Dorena	5 - 6	846 – 22,688	875 – 39,749	838 – 29,076
Cottage Grove	5 - 6	974 – 20,914	1,083 – 22,720	1,138 – 30,636
Foster	6 - 8	1,848 – 21,628	2,987 – 35,354	1,288 – 29,601

*The number of recreation sites monitored for recreational visitors by the USACE during the study period 2001-2011.

[†]Estimated over the study period from 2001-2011 for sites included in this analysis, which were limited to those having a minimum of 5 years of data, and reservoirs with at least 2 monitored sites.

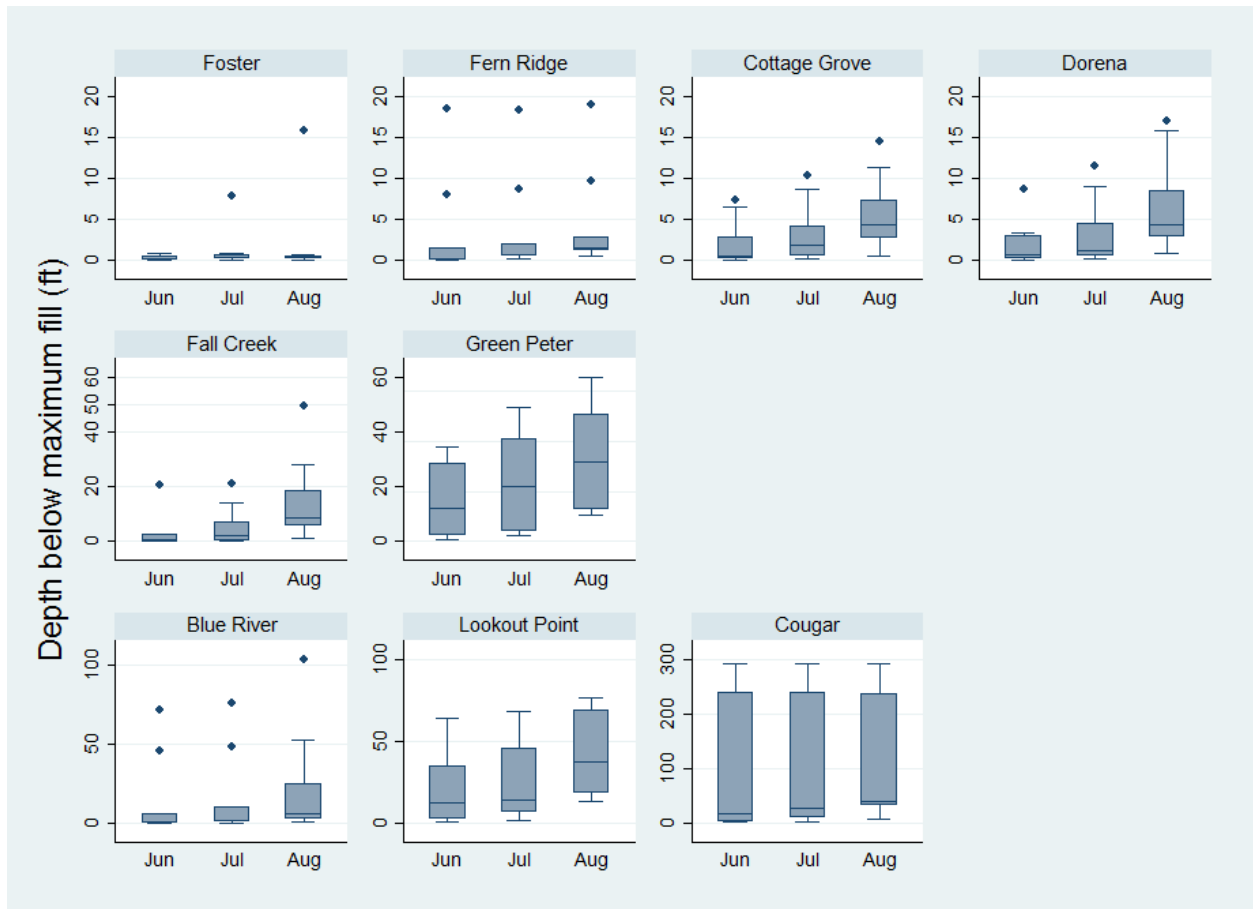


Figure 3.4. Summary statistics of summertime (June-August) water level variation by reservoir during the study period from 2001-2011. The horizontal line within each box gives the median, the box extents give the 25th and 75th percentiles, the box whiskers give the most extreme values within 1.5 times the interquartile range, and the dots give the values of observations that fall beyond this range.

Table 3.3. Control variables included in the vector X' in the empirical model estimating the effect of reservoir water level on recreational visitor days. Data Sources: U.S. Historical Climatology Network (station 351862), Population Research Center at Portland State University and Google maps.

<u>Control Variable</u>	<u>Description</u>
Month	Month dummy variables (June, July, August).
Extra weekend	Dummy variable – 1 if a month has 10 weekend days, 0 otherwise.
Temperature	Average monthly air temperature in the Willamette Valley from station data in Corvallis, Oregon ¹ (Figure 3.1).
Precipitation	Total monthly precipitation in the Willamette Valley from station data in Corvallis, Oregon ¹ (Figure 3.1).
Remoteness Index	A weighted index of population within the vicinity of each reservoir. Defined as the ratio of total population in the three cities closest to each reservoir ² (Figure 3.1), to the average travel time to the reservoir from the cities weighted by the respective populations ³ . Low values of the remoteness index indicated that few people live within the vicinity of a reservoir. Over the study period the average value of the index ranged from 170 thousand people within an hour travel of Detroit reservoir to 441 thousand people within an hour travel of Fern Ridge reservoir.

¹ U.S. Historical Climatology Network Station 351862.

² Defined as having at least 20,000 residents as of the 2010 census. Data Source: Population Research Center at Portland State University.

³ Travel time computed using Google maps.

3.4.3 Estimating total visitor days for all reservoirs

In this section we estimate the total number of visitor days – or average level of visitation – at each reservoir, drawing on the available sources of data. In order to estimate the change in the number of recreational visitor days as the reservoir fill level falls below full pool ($\frac{\partial F}{\partial z}$ in eq. 3.2), we need an estimate of the total number of expected visitor days at each reservoir along with the percentage change in visitor days due to falling water levels estimated in eq. 3.3. Measurement and estimation errors represented challenges for the current analysis, and estimates of visitor days were not available for all reservoir recreation sites. We explain here how we

utilized existing data to develop best estimates of total recreational visitor days at the reservoirs under study.

At each reservoir, the total number of visitor days across all recreational sites monitored by the USACE vehicle monitors and included in the analysis to examine the response of visitor days to reservoir water level, ranged from none at Detroit and Hills Creek reservoirs to an average of 114,602 visitor days per month (Jun-Aug) at Fern Ridge over the study period (Table 3.4). However, the USACE vehicle-counter data represents only a portion of the expected visitor days at the Willamette Project reservoirs [USACE, 2013], because not all recreation sites are monitored. Based on the USACE vehicle counters and the addition of some areas managed by the state of Oregon, the USACE and OWRD estimated total recreational visitor days across all the reservoirs at 4.3 million recreational visits annually [USACE and OWRD, 2011], with the majority of these visits expected to occur in the summer [USACE and OWRD, 2000]. A survey of registered boat owners by the Oregon State Marine Board (OSMB) in 2007 found that 73% of reservoir visits in Oregon occur between May and September [OMSB, 2008]. The OSMB survey also estimated the annual number of “activity days” by boat owners at waterbodies in Oregon, where an activity day was defined as “one individual participating in one recreation activity during any reasonable portion or all of one day” [OMSB, 2008]. The number of activity days at each reservoir by boat owners in 2007 estimated by the Oregon State Marine Board, ranged from 168 at Cougar to 81,335 at Detroit (Table 3.4).

Using 1) the total annual recreational visitor days across all the reservoirs estimated by the USACE and OWRD [*USACE and OWRD, 2011*], 2) the expected proportion of visitation during the summer [*OMSB, 2008*], and 3) the relative proportion of activity days (A) among the Willamette Project reservoirs [*OMSB, 2008*], we estimated the average number of recreational visitor days at each reservoir for the months of June-August as:

:

$$E(R)_j = \frac{4.3e06 * 73\%}{5} * \frac{A_j}{\sum_{j=1}^{11} A_j} \quad (3.4)$$

The resulting expected number of visitor days per month at each reservoir ranged from 497 at Cougar to 240,640 at Detroit (Table 3.4).

Table 3.4. Comparison of three estimates of recreational visitor days at Willamette Project reservoirs. Column 2 shows the total number of visitor days per month (Jun-Aug) observed by the USACE vehicle monitors used in this study. Column 3 provides the number of “Activity Days” by boat owners during 2007 based on a survey by the Oregon State Marine Board. Column 4 provides the expected number of visitor days at each reservoir per month (Jun-Aug) calculated in this study using eq. 3.4.

<u>Reservoir</u>	<u>USACE Monitored Visitation</u> <u>Average Monthly (Jun-Aug) Visit Days¹</u>	<u>OSMB Survey</u> <u>Annual “Activity Days”²</u>	<u>Expected</u> <u>Monthly (Jun-Aug) Visit Days³</u>
Detroit	-	81,335	240,640
Fern Ridge	114,602	50,337	148,928
Foster	89,588	32,277	95,496
Green Peter	28,236	16,012	47,374
Dorena	62,326	9,944	29,421
Fall Creek	38,671	5,252	15,539
Cottage Grove	70,078	6,332	18,734
Blue River	8,364	5,970	17,663
Hills Creek	-	3,137	9,281
Lookout Point	8,590	1,429	4,228
Cougar	9,328	168	497

¹Based on the USACE vehicle counter estimates at sites used in this study.

²OSMB, 2008.

³Calculated based on estimates from USACE&OWRD (2011) and OSMB (2008).

3.4.4 Estimating benefits per visit for reservoir recreation

The USACE data on recreational visits at the Willamette Project reservoirs did not include information on the locations from which visitors had travelled, precluding an estimate of willingness-to-pay per recreational visitor day using a travel cost method [e.g. *Ward et al.*, 1996]. Instead, a benefit transfer approach was used to infer the willingness-to-pay for a recreational visitor day from existing studies that included detailed surveys in other locations. In particular, drawing on a meta-analysis of studies on the value of recreation at sites across the U.S. [*Loomis, 2005*], we estimated an average willingness-to-pay per visitor day of \$55 based on the activities that we expect to occur at reservoir recreation sites (Table 3.5).

Table 3.5 The average willingness-to-pay (2014 dollars) per visitor day (\$/visitor/day) from the meta-analysis by Loomis (2005) for recreational activities that are expected to occur at reservoir sites.

<u>Activity</u>	<u>Number of Study Estimates</u>	<u>Average Willingness-to-Pay Per Activity Day (\$)</u>
Camping	48	47
Fishing	177	59
Motorboating	32	58
Picnicking	13	52
Swimming	26	53
Waterskiing	4	61
Average		55

3.5 Results

In this section we report on the analysis results related to each of the four questions stated at the outset, starting with the response in recreational visits to changes in reservoir water levels. Recreational visitor days decreased significantly with falling water levels at three of nine Willamette Project reservoirs: Fall Creek, Fern Ridge, and Foster ($p < 0.10$) (Table 3.6). On

average, for all nine reservoirs, the number of visitor days declined by 0.3% for every foot the reservoir water level fell below full pool. At Fall Creek the number of visitor days declined by 1% per foot of drop in reservoir water level below full pool ($p < 0.01$), irrespective of outlier removal. At Fern Ridge and Foster reservoirs the number of visitor days declined by 2% per foot of drop in reservoir water level below full pool ($p < 0.10$). Results were consistent for three (Fern Ridge) and two (Foster) of the five models.

The value per acre-foot of stored water at Fall Creek, Fern Ridge, and Foster reservoirs, was estimated using the indicated response in visitor days at each reservoir to falling water levels (Table 3.6), the total number of visitor days per month (Jun-Aug) at each reservoir observed by the USACE vehicle monitors (Table 3.4, column 2). The resulting marginal value of stored water for recreation in dollars per acre-foot per month was \$11 at Fall Creek, \$13 Fern Ridge, and \$78 at Foster (Table 3.7). If the value per acre-foot of stored water was instead estimated using the average response across the reservoirs of a 0.3% reduction in visitor days per foot the water levels drops (Table 3.6), along with the expected number of monthly visitors at each of the Willamette Project storage reservoirs (Table 3.4, column 4), the marginal value of stored water to recreation ranged from \$0.10 to \$12 per acre-foot per month across the reservoirs (Table 3.8, Figure 3.5).

Overall 15% of the variation in visitor days at the reservoir sites was explained by the variables included in the empirical model (Table 3.6). Recreational use of the reservoirs varied by month (Table 3.6): July had the highest number of visitor days, followed by August and then June. July had 33% more visitor days than June ($p\text{-value} < 0.01$), while August had 19% more than June ($p\text{-value} < 0.05$). The number of visitor days was not responsive to the number of weekends during these summer months (Table 3.6). Reservoir visitor days were significantly

negatively related to precipitation, but not related to air temperature (Table 3.6). Air temperature ranged from 14-21°C during the study period, and monthly precipitation ranged from zero to 76 mm. An increase of 1 inch (25 mm) of precipitation during a month caused an 8% decline in the number of reservoir visitor days (p -value <0.01) (Table 3.6). Visitor days were strongly positively related to boat ramp access (Table 3.6). Visitor days were estimated to be 27% higher when reservoir water levels were above the elevation of the lowest boat ramp than when ramp access was lost (p -value <0.05). Visitor days were positively related to the accessibility of the reservoir, measured by the remoteness index ($p < 0.05$) (Table 3.6). Visitor days increased by 0.7% for every additional 1,000 people living within an hour of the reservoir (Table 3.6).

Blue River and Green Peter reservoirs showed some unexpected evidence of a positive relationship between recreational visitor days and falling water levels (Table 3.6). At Green Peter this positive relationship occurred in only one of the models, and accounted for less than a 1% change in visitor days per foot of water depth. At Blue River the positive relationship was significant ($p < 0.05$) for all models, and it accounted for a 0.3% increase in visitor days per foot of water depth below full pool. Very low reservoir levels in 2001 (Figure 3.4) prevented ramp access over the entirety of the recreational season at Blue River. When the ramp access variable was excluded from the model, the coefficient at Blue River became statistically insignificant.

Table 3.6. Results of the empirical model estimation for the five model structures, each of which omitted outliers according to different rules.

Explanatory Variable	Model structure based on outlier definition									
	1		2		3		4		5	
	Coefficient	P-value	Coefficient	p-value	Coefficient	p-value	Coefficient	p-value	Coefficient	p-value
Constant	-1.4		-1.3		-1.3		-1.2		-1.4	
Water Level:										
Fern Ridge	-0.02		-0.02	<0.10	-0.02	<0.10	-0.02		-0.02	<0.10
Foster	-0.03	<0.10	-0.02		-0.02		-0.03	<0.10	-0.01	
Green Peter	0.003		0.005		0.007	<0.10	0.003		0.004	
Dorena	-0.00005		0.008		0.008		0.008		0.008	
Fall Creek	-0.01	<0.01	-0.01	<0.01	-0.009	<0.01	-0.01	<0.01	-0.01	<0.01
Cottage Grove	0.01		0.01		0.01		0.01		0.009	
Blue River	0.003	<0.01	0.003	<0.05	0.003	<0.05	0.003	<0.05	0.003	<0.05
Lookout Point	-0.004		-0.003		-0.002		-0.003		-0.003	
Cougar	0.0008		0.0006		0.0005		0.0007		0.0006	
Ramp Access	0.3	<0.05	0.3	<0.05	0.3	<0.05	0.2	<0.05	0.3	<0.05
Month:										
July	0.4	<0.01	0.3	<0.01	0.3	<0.01	0.4	<0.01	0.3	<0.01
August	0.2	<0.01	0.2	<0.05	0.2	<0.05	0.2	<0.01	0.2	<0.05
Extra Weekend	-0.02		-0.007		0.005		-0.03		-0.01	
Precipitation	-0.07	<0.01	-0.09	<0.01	-0.08	<0.01	-0.07	<0.01	-0.08	<0.01
Temperature	-0.008		-0.006		-0.005		-0.01		-0.007	
Remoteness Index	0.007	<0.05	0.007	<0.05	0.007	<0.05	0.007	<0.05	0.007	<0.05
Observations	1,334		1,366		1,365		1,342		1,366	
R ²	0.16		0.14		0.13		0.15		0.14	
F-statistic	12.54		12.09		11.61		72.73		11.75	

Table 3.7. The magnitude of the visitation response to declining reservoir water levels and the associated marginal value of stored water to recreation at Fern Ridge, Fall Creek, and Foster reservoirs.

Reservoir	Estimated Visitation Response to Reservoir Water Level (% Δ in visit days/foot below full pool)	Estimated Value of Stored Water for Reservoir Recreation (\$/acre-foot)
Fern Ridge	2%	\$13
Fall Creek	1%	\$11
Foster	2%	\$78

Table 3.8. The marginal value of stored water to recreation at the Willamette Project reservoirs based on 1) the expected number of visit days per month for Jun-Aug at each reservoir (Table 3.4), the average response across the reservoirs of a reduction of 0.3% in the number of visitor days for every foot the water levels drops below full pool, and 3) an estimated willingness-to-pay per visit of \$55 based on the *Loomis* (2005) meta-analysis (Table 3.5).

Reservoir	Estimated Visit Days per Month (Jun-Aug) ¹	Estimated Value of Stored Water for Reservoir Recreation (\$/acre-foot/month) ²
Detroit	240,640	\$11
Fern Ridge*	148,928	\$3
Foster*	95,496	\$12
Green Peter	47,374	\$2
Dorena	29,421	\$3
Fall Creek*	15,539	\$1
Cottage Grove	18,734	\$3
Blue River	17,663	\$3
Hills Creek	9,281	\$1
Lookout Point	4,228	\$0.2
Cougar	497	\$0.1
Average		\$4

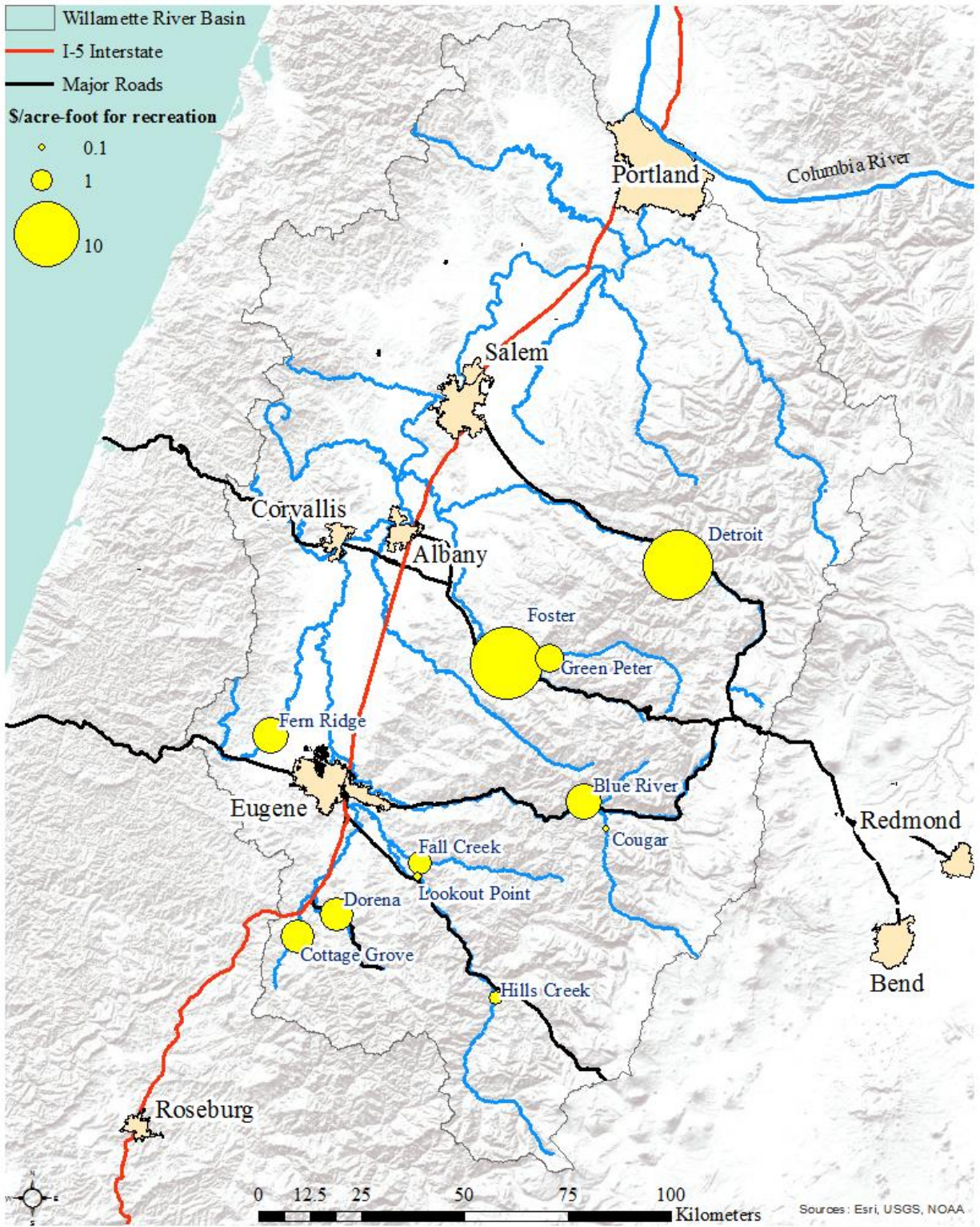


Figure 3.5. The Willamette Project storage reservoirs symbolized according to the estimated relative value (\$/acre-foot) of stored water to recreation (Table 3.8).

3.6 Discussion

Numerous studies have estimated the value of water to recreational activities, including the effect of reservoir water levels on demand for recreational reservoir use [*Creel and Loomis*, 1992; *Cordell and Bergstrom*, 1993; *Cameron et al.*, 1996; *Ward et al.*, 1996; *Fadali and Shaw*, 1998; *Huszar et al.*, 1999; *Eiswerth et al.*, 2000]. In general published studies have found that reservoir water level was positively associated with recreational use of reservoirs. Similarly, in this analysis recreational visitor days at reservoirs in the WRB responded to changes in reservoir water levels. Furthermore, there were reductions in the value of recreation when reservoir level fell below full pool in summer. The geographic characteristics of reservoirs may have contributed to variation in visitor days among reservoirs, as well as differences in visitor day responses to reduced fill levels.

The value of water to recreational users estimated in this study varied by nearly three orders of magnitude from \$0.10 to \$78 per acre-foot per month (averaged over the summer recreation period from June to August) among the USACE storage reservoirs in the WRB. Ward et al. [1996] estimated a value of \$9 to \$900 per acre-foot per year for recreational users of USACE reservoirs in the Sacramento, California, District. If these recreational benefits are assumed to be evenly divided across the year, the estimated values per month ranged from \$0.80 to \$75 and are comparable to those estimated in this study. However, confidence in the estimated values is tempered by uncertainty in the transferred willingness-to-pay benefit as well as the quality of the visitor day data collected by the USACE and the total number of expected visitor days at each reservoir.

3.6.1 Methodological uncertainty in estimating the value of stored water

This study used revealed preference data to estimate the value to recreational users of water stored in reservoirs because long-term data on observed reservoir use were available. Relatively few published studies have examined long-term data on observed recreational visitor day responses to variation in water levels (but see *Ward et al.*, (1996). When long-term observed data are lacking, stated preference surveys [e.g. Creel and Loomis, 1992; Cordell and Bergstrom, 1993] can be used to determine responses to hypothetical changes in water levels. These methods can assess responses to scenarios that lie beyond the range of historical observation [*Cameron et al.*, 1996], and can also directly elicit willingness-to-pay estimates (contingent valuation) or estimate willingness-to-pay based on hypothetical behavior (contingent behavior) from survey respondents. However, stated preference survey data are subject to response bias, which occurs when the responses of surveyed individuals deviate from reality [*Cameron et al.*, 1996; *Whitehead et al.*, 2008]. The use of revealed preference data in this study avoided response bias, but the inferences of the study are limited to the range of observed conditions in reservoir water levels.

Revealed preference data can also be used to estimate the willingness-to-pay per recreational visitor day using a travel cost method if the locations from which visitors travel are included in the data collection [*Ward et al.*, 1996]. Because this information was lacking in the USACE data used in this study, we drew on a meta-analysis of prior studies to infer the average willingness-to-pay for a recreational visitor day at the Willamette Project reservoirs. The accuracy of the inferred benefit is likely to depend on both the similarity of the regions and the recreational activities, as well as the accuracy of the initial estimates [*Loomis et al.*, 1995; *Loomis*, 2005]. The data used [*Loomis*, 2005] includes areas that are geographically different

than the Pacific Northwest setting of the Willamette Project reservoirs. Use of data for only the Pacific Northwest (from [Loomis, 2005]) reduced the average willingness-to-pay for reservoir recreation from \$55 to \$47 per visitor day. However, there were no previous estimates of the value of waterskiing in the Pacific Northwest, which had a high willingness-to-pay value relative to other recreational activities, averaging \$61 per visitor day at sites across the US [Loomis, 2005]. The willingness-to-pay estimate applied in this study of \$55 per visitor day is high relative to the willingness-to-pay values estimated by the USACE and OWRD for recreational visitor days at the Willamette Project reservoirs values using a survey and travel cost model in 1996, which ranged from \$2 per visitor day at Fern Ridge to \$5 at Detroit for day use, and from \$5 at Fall Creek to \$17 at Detroit for overnight use [USACE and OWRD, 2000]. However, Cameron et al. [1996], suggest that values for water-based recreation range from \$30 to \$90 per visitor day. Clearly, more work is needed to determine the willingness-to-pay for recreational use of reservoirs in the Pacific Northwest.

3.6.2 Sources of uncertainty in data and model structure

The expected number of visitor days at each reservoir estimated using eq. 3.4 was less than the number of visitor days estimated by the USACE vehicle counters for almost half the reservoirs (Table 3.4). This suggests either that the boat owners surveyed by the OSMB do not accurately represent all recreational users of the Willamette Project reservoirs or that the USACE vehicle counters overestimate the number of visitor days at the recreational sites monitored. It seems more likely that boat owners are only a subset of recreational users of the Willamette Project reservoirs, and that the number of visitor days observed by USACE vehicles counters represents a conservative estimate of the total recreational visitors days at the reservoirs. Further

monitoring efforts would be useful to clarify the accuracy of the expected number of recreational users used in this study.

Uncertainty in the estimated values per acre-foot of water also stems from the empirical model fit. The relatively low variability explained by the model (15%, Table 3.6) indicates that unobserved variables, which are not site-specific characteristics that remain constant over time, are responsible for most of observed variation in the number of visitor days at reservoir sites.

3.6.3 Differences among reservoirs in the value of stored water

The results of this analysis suggest that geographic characteristics of the reservoirs such as the proximity to population centers affect the number of visitor days at the reservoir. Higher numbers of recreational visitors at reservoirs such as Detroit, Fern Ridge, and Foster are associated with a higher value of stored water in these reservoirs, all other factors being equal.

Varied physical characteristics and landscape settings of the reservoirs also contributed to the observed differences in the response of visitors to water levels below full pool. Shallower reservoirs experience loss of amenity, such as exposed mud flats, as water levels fall, while reservoirs with short boat ramps may lose boat ramp access. Shallow water depths may explain the relatively large response of visitor days to declining water level at Fern Ridge and Foster. Short boat ramps may explain the visitor response to falling water levels at Fall Creek (where one boat ramp extends only 5 feet below full pool), Foster, and Fern Ridge reservoirs (which lose some boat ramp access at 6 feet below full pool). Some landscape settings may also attract recreators, such as campers or hikers, whose activities depend less on water levels than do recreators engaged in boating or fishing, leading to less sensitivity of visitor days to water level.

The different shapes of the reservoirs also result in varying rates of decline in the volume of stored water as the water level falls below full pool, which affects the estimated value of

stored water to recreation. For example, the value of stored water to recreation is lower per unit volume at Fern Ridge compared to Foster, because reservoir volume declines faster per unit drop in water level at Fern Ridge relative to Foster. While it might seem to make more sense to measure the value of stored water for reservoir recreation per unit depth, the value needs to be estimated per unit volume in order to allow comparison to the values associated with other reservoir uses.

Differences in the characteristics of the reservoirs probably also results in variation in the willingness-to-pay per recreational visitor day among the reservoirs [*USACE and OWRD, 2000*]. However, this study applied a uniform willingness-to-pay estimate across the reservoirs. A higher willingness-to-pay per visitor day at reservoirs such as Foster and Detroit, which already have the highest estimated values of water per acre-foot to recreation, would increase the estimated values per acre-foot of stored water at these reservoirs.

3.6.4 Implications for reservoir management

The estimated value of water per acre-foot per month to recreational users ranged from \$0.10 to \$78 across the USACE storage reservoirs in the WRB. The estimated average value of water to irrigated agriculture in the WRB is \$17/acre-foot [*Kalinin, A., 2013*]. This would suggest that it is most beneficial to society to release stored water from some reservoirs for agricultural needs in the WRB while maintaining full reservoir capacity for recreation in others. Current management of Willamette Project reservoirs is consistent with our findings: Lookout Creek, which had low value to recreational users in this study, is drawn down first, while Detroit, Fern Ridge, and Foster reservoirs, which had high value to recreational users, are the last to be drawn down [*USFWS, 2008*].

3.7 Conclusions

Reservoir recreation, which depends on full reservoirs, is a major use of the Willamette Project reservoirs, with an estimated at 4.3 million visitor days each year [USFWS, 2008].

Lowered water levels can impact recreational use in various ways including compromised aesthetics such as ‘bathtub rings’ and exposed stumps, loss of boat ramp access, increased mud flats, and reduced fishing opportunities. The demand for reservoir fill levels near full pool potentially puts recreation in competition with other authorized reservoir uses.

The expected effects of climate change on water scarcity and anticipated increases in recreational demand for reservoirs imply a need to critically assess the expected value of stored water for reservoir recreation relative to other objectives of reservoir management in the Willamette River Basin. The availability of time series data on recreational visits to Willamette Project reservoirs provided the opportunity to quantify the recreational response to variation in water levels, and to assess the implied value of stored water to reservoir recreation. Visitor days were found to decline by as much as 2% per foot of drop in water level below full pool. The average decline in visitor days across the reservoirs was 0.3% for every foot of drop of reservoir level below full pool. The implied value of water per acre-foot per month to recreational users ranged from \$0.10 to \$78 across the reservoirs. Differences in the physical characteristics and the landscape setting of the reservoirs may explain differences in the value of stored water for recreation. Reservoirs with shallower water depths or short boat ramps were associated with a greater reduction in visitor days with falling water levels, while greater proximity to population centers increased the number of visitor days at a reservoir. The differences among reservoirs in the value of stored water to recreation indicate that reservoirs with high recreational value could be prioritized to remain at full pool during the summer recreation period, while reservoirs with

low recreational value could be managed to meet downstream water uses and flow requirements, as currently prescribed.

Future decisions regarding the tradeoffs between reservoir uses and the prioritization of drawdowns would benefit from improved estimates of recreational visits at individual Willamette Project reservoirs, collection of demographic data needed to estimate reservoir specific willingness-to-pay for a recreational visit, and a contingent valuation survey to provide information on the expected response of recreation visitation to water levels that are beyond the range of historical variability.

3.8 Acknowledgements

This project was supported by the National Science Foundation under Grant No. 1039192. Data for this research were obtained from the US Army Corp of Engineers, the US Geological Survey, and the Willamette Water 2100 Project. We thank Tamara Schroeder, Joseph Ross, and Matthew Rea at the Portland District of the US Army Corp of Engineers for providing assistance in using their data on visitation at the Willamette Project reservoirs.

3.9 References

- Ashenfelter, O., P. B. Levine, and D. J. Zimmerman (2002), *Statistics and Econometrics: Methods and Applications*, John Wiley & Sons Australia, Limited.
- Barnett, T. P. et al. (2008), Human-Induced Changes in the Hydrology of the Western United States, *Science*, 319(5866), 1080–1083, doi:10.1126/science.1152538.
- Cameron, T. A., W. D. Shaw, S. E. Ragland, J. M. Callaway, and S. Keefe (1996), Using Actual and Contingent Behavior Data with Differing Levels of Time Aggregation to Model Recreation Demand., *Journal of Agricultural & Resource Economics*, 21(1), 130–149.
- Chang, H., and I.-W. Jung (2010), Spatial and temporal changes in runoff caused by climate change in a complex large river basin in Oregon, *Journal of Hydrology*, 388(3-4), 186–207, doi:10.1016/j.jhydrol.2010.04.040.

- Cordell, H. K., and J. C. Bergstrom (1993), Comparison of recreation use values among alternative reservoir water level management scenarios, *Water Resources Research*, 29(2), 247–258, doi:10.1029/92WR02023.
- Creel, M., and J. Loomis (1992), Recreation Value of Water to Wetlands in the San-Joaquin Valley - Linked Multinomial Logit and Count Data Trip Frequency Models, *Water Resources Research*, 28(10), 2597–2606, doi:10.1029/92WR01514.
- Eiswerth, M. E., J. Englin, E. Fadali, and W. D. Shaw (2000), The value of water levels in water-based recreation: A pooled revealed preference/contingent behavior model, *Water Resources Research*, 36(4), 1079–1086, doi:10.1029/1999WR900332.
- Elsner, M. M., L. Cuo, N. Voisin, J. S. Deems, A. F. Hamlet, J. A. Vano, K. E. B. Mickelson, S.-Y. Lee, and D. P. Lettenmaier (2010), Implications of 21st century climate change for the hydrology of Washington State, *Climatic Change*, 102(1-2), 225–260, doi:10.1007/s10584-010-9855-0.
- Englin, J., and T. A. Cameron (1996), Augmenting travel cost models with contingent behavior data, *Environmental and Resource Economics*, 7(2), 133–147, doi:10.1007/BF00699288.
- Fadali, E., and W. D. Shaw (1998), Can recreation values for a lake constitute a market for banked agricultural water?, *Contemporary Economic Policy*, 16(4), 433–441.
- Grossmann, M. (2011), Impacts of boating trip limitations on the recreational value of the Spreewald wetland: a pooled revealed/contingent behaviour application of the travel cost method, *Journal of Environmental Planning and Management*, 54(2), 211–226, doi:10.1080/09640568.2010.505827.
- Huszar, E., W. D. Shaw, J. Englin, and N. Netusil (1999), Recreational damages from reservoir storage level changes, *Water Resources Research*, 35(11), 3489–3494, doi:10.1029/1999WR900235.
- Kalinin, A. (2013), Right as Rain? The Value of Water in Willamette Valley Agriculture, M.S., Oregon State University, Department of Applied Economics.
- Loomis, J. (2000), Environmental Valuation Techniques in Water Resource Decision Making, *Journal of Water Resources Planning and Management*, 126(6), 339–344, doi:10.1061/(ASCE)0733-9496(2000)126:6(339).
- Loomis, J., B. Roach, F. Ward, and R. Ready (1995), Testing transferability of recreation demand models across regions: a study of corps of engineer reservoirs, *Water Resources Research*, 31(3), 721–730.
- Loomis, J. B. (2005), *Updated outdoor recreation use values on national forests and other public lands*, US Department of Agriculture, Forest Service, Pacific Northwest Research Station.
- Oregon Marine State Board (2008), Boating in Oregon, Available from: <http://www.oregon.gov/OSMB/library/docs/trisuv2008.pdf> (Accessed 25 March 2015)

- Serreze, M. C., M. P. Clark, R. L. Armstrong, D. A. McGinnis, and R. S. Pulwarty (1999), Characteristics of the western United States snowpack from snowpack telemetry (SNOTEL) data, *Water Resources Research*, 35(7), 2145–2160, doi:10.1029/1999WR900090.
- Stewart, I. T., D. R. Cayan, and M. D. Dettinger (2005), Changes toward earlier streamflow timing across western North America, *Journal of climate*, 18(8), 1136–1155.
- USACE (2013), *COP Reservoir Recreation Impact Report*, United States Army Corp of Engineers, Portland, OR.
- USACE and OWRD (2000), Willamette Basin Reservoir Study Interim Report, Available from: http://www.oregon.gov/owrd/docs/2000_01_Willamette_Interim_Report.pdf (Accessed 23 March 2015)
- USACE and OWRD (2011), Small-Scale Water Supply Allocation Process Willamette River Basin, Available from: http://www.oregon.gov/owrd/pages/mgmt_res_study.aspx (Accessed 15 April 2015)
- USFWS (2008), *Biological Opinion on the Continued Operation and Maintenance of the Willamette River Basin Project and Effects to Oregon Chub, Bull Trout, and Bull Trout Critical Habitat Designated Under the Endangered Species Act.*, U.S. Fish and Wildlife Service.
- Ward, F. A., B. A. Roach, and J. E. Henderson (1996), The economic value of water in recreation: Evidence from the California drought, *Water Resources Research*, 32(4), 1075–1081, doi:10.1029/96WR00076.
- Whitehead, J. C., S. K. Pattanayak, G. L. Van Houtven, and B. R. Gelso (2008), Combining Revealed and Stated Preference Data to Estimate the Nonmarket Value of Ecological Services: An Assessment of the State of the Science, *Journal of Economic Surveys*, 22(5), 872–908, doi:10.1111/j.1467-6419.2008.00552.x.

Chapter 4: Optimizing Reservoir Operations to Adapt to 21st Century Expectations of Climate and Social Change in the Willamette River Basin, Oregon

4.1 Abstract

Many reservoir systems in the western US are managed to serve two main competing purposes: to reduce flooding during the winter and spring, and to provide water supply for multiple uses during the summer. Because the storage capacity of a reservoir cannot be used for both flood damage reduction and water storage at the same time, these two uses are traded off as the reservoir fills during the transition from the wet to the dry season. Climate change, population growth, and development may exacerbate dry season water scarcity and increase winter flood risk, implying a need to critically evaluate reservoir operations. Focusing on the Willamette River Basin, Oregon, we used a dynamic programming approach to social welfare maximization, and estimated the optimal reservoir fill path for both historical conditions and future scenarios of climate and social change. Anticipated future increases in winter flood risk and reductions in spring streamflow led to an optimal fill path in which reservoir fill began earlier and proceeded more slowly, compared to the optimal fill path under historical conditions. Increased value of stored water associated with increased demand for reservoir recreation or irrigation water for agriculture also shifted the initiation of reservoir fill to an earlier date and increased the likelihood of achieving full pool by the end of May. Conversely, an increase in the value of flood damage reduction relative to the value of stored water, driven by land use change and development in the floodplain associated with increasing population led to an optimal fill path in which reservoir fill began later and the final optimal reservoir fill level was decreased, compared to the optimal fill path under historical conditions. These findings may contribute to policies for adapting reservoir management to future changes in water supply and demand.

4.2 Introduction

A central characteristic of many large river basins in the western US is the lack of spatial and temporal concurrence between the supply of and demand for water. Water sources typically are concentrated in forested mountain regions distant from municipal and agricultural water users, while precipitation is super-abundant in winter and deficient in summer. To cope with these disparities, systems of reservoirs were constructed throughout the western US, predominantly in the 1950s through 1970s [Graf, 1999]. The basins are coupled natural-human systems in which people and ecosystems have adapted to, and rely upon, environmental conditions as modified by the management of the reservoir system [Poff *et al.*, 1997; Graf, 2001]. The primary authorized purpose of many of these reservoir systems is flood damage reduction, but secondary uses include recreation, irrigation, municipal supply, hydropower, navigation, and requirements for downstream environmental flows.

The Columbia River Basin delivers the largest volume of streamflow from North America to the Pacific Ocean. The river flows 1,954 km from its headwaters in the Rocky Mountains of British Columbia to its mouth near Astoria, Oregon, draining 670,000 km² across the Pacific Northwest and producing an average annual runoff of about 198 million acre-feet (244 billion m³) [BPA, USBR, and USACE, 2001]. The Willamette River Basin (WRB) is the predominate sub-basin of the Columbia located west of the Cascade Mountain Range (Figure 4.1). Although the WRB represents only 4% of the drainage area in the Columbia River Basin, it contributes approximately 15% of the total annual runoff [Chang and Jung, 2010]. The United States Army Corp of Engineers (USACE) operates a system of 13 reservoirs, including 11 storage reservoirs, known as the Willamette Project in the WRB. Flood damage reduction is the primary authorized use for these storage reservoirs [USACE, 2012], but stored water uses

including the provision of downstream flow requirements for endangered species, municipal flows, and reservoir recreation have become increasingly important [USFWS, 2008].

Flood damage reduction is achieved by maintaining unfilled storage capacity in reservoirs, which is used to temporarily store and release floodwaters during the winter flood season, reducing downstream flooding. Because the storage capacity of a reservoir cannot be used for both flood damage reduction and water storage at the same time, these two competing uses are traded off during the transition from the wet to the dry season, as the highest priority use of the reservoir shifts from reducing flood peaks to storing water. This tradeoff is expressed in the reservoir fill path given by a rule curve for reservoir operations that specifies the target level to which the reservoir is filled throughout the year [USACE, 2011] (Figure 4.2). Ideally a rule curve accurately captures the societal values placed on the competing uses of the reservoir, taking account of the levels and variability of expected streamflows. While reservoir rule curves are usually established with limited information at the time the reservoir is built, climate change, population growth, and shifting social goals may alter the suitability of a rule curve over time [Chou and Wu, 2013; Vonk et al., 2014; Yu et al., 2014].

Climate change is expected to increase winter flood risk and reduce spring streamflow in the Pacific Northwest [Elsner et al., 2010; Salathé et al., 2014], coinciding with the transition period when reservoirs are filling according to a rule curve. Temperature in the region rose by 0.8°C during the twentieth century [Mote, 2003], and is expected to increase another 3°C by the 2080s [Mote and Salathé, 2010]. Higher winter and spring temperature has speeded snowmelt [Mote et al., 2005] and increased the proportion of precipitation falling as rain rather than snow [Knowles et al., 2006], altering streamflow [Hamlet and Lettenmaier, 2007]. As demonstrated in the 2014-15 water year, the snowpack in much of the Oregon Cascade Range is liable to

disappear as air and sea surface temperature increases [Nolin and Daly, 2006]. The loss of snowpack is expected to shift peak streamflow to earlier in the water year [Stewart et al., 2005; Jefferson et al., 2008; Chang and Jung, 2010; Elsner et al., 2010], increasing the intensity and variability of winter flooding [Salathé et al., 2014], and exacerbating summer water scarcity [Bales et al., 2006; Barnett et al., 2008; Jung and Chang, 2012].

Population growth and development will also affect the potential costs of future flood risk. Approximately 75% of Oregon's population lives in the WRB. The state's three largest cities – Portland, Eugene, and Salem – are situated along the mainstem of the Willamette River, and they are experiencing more rapid population growth than the state or the nation [Population Research Center, 2012]. As population increases, more land will be converted to developed use [Jaeger et al., 2014], and if additional development occurs in the floodplain, land use conversions may increase the potential for flood damages.

The expected effects of climate change, population growth, and development imply a need to critically evaluate reservoir operations in the WRB [Jaeger et al., 2014]. Drawing on chapters 2 and 3, which evaluated the value of reservoir operations for flood damage reduction and water storage in the WRB, and employing a dynamic programming approach within a normative economic framework of social welfare maximization, we investigated how reservoir management in the WRB can adapt to the anticipated changes in water supply and demand. Specifically we asked:

1. What is the optimal rule curve for the Willamette Project reservoirs?
2. How does the derived optimal rule compare to existing rule curves?
3. How does the derived optimal rule change under future scenarios of climate, population and development?

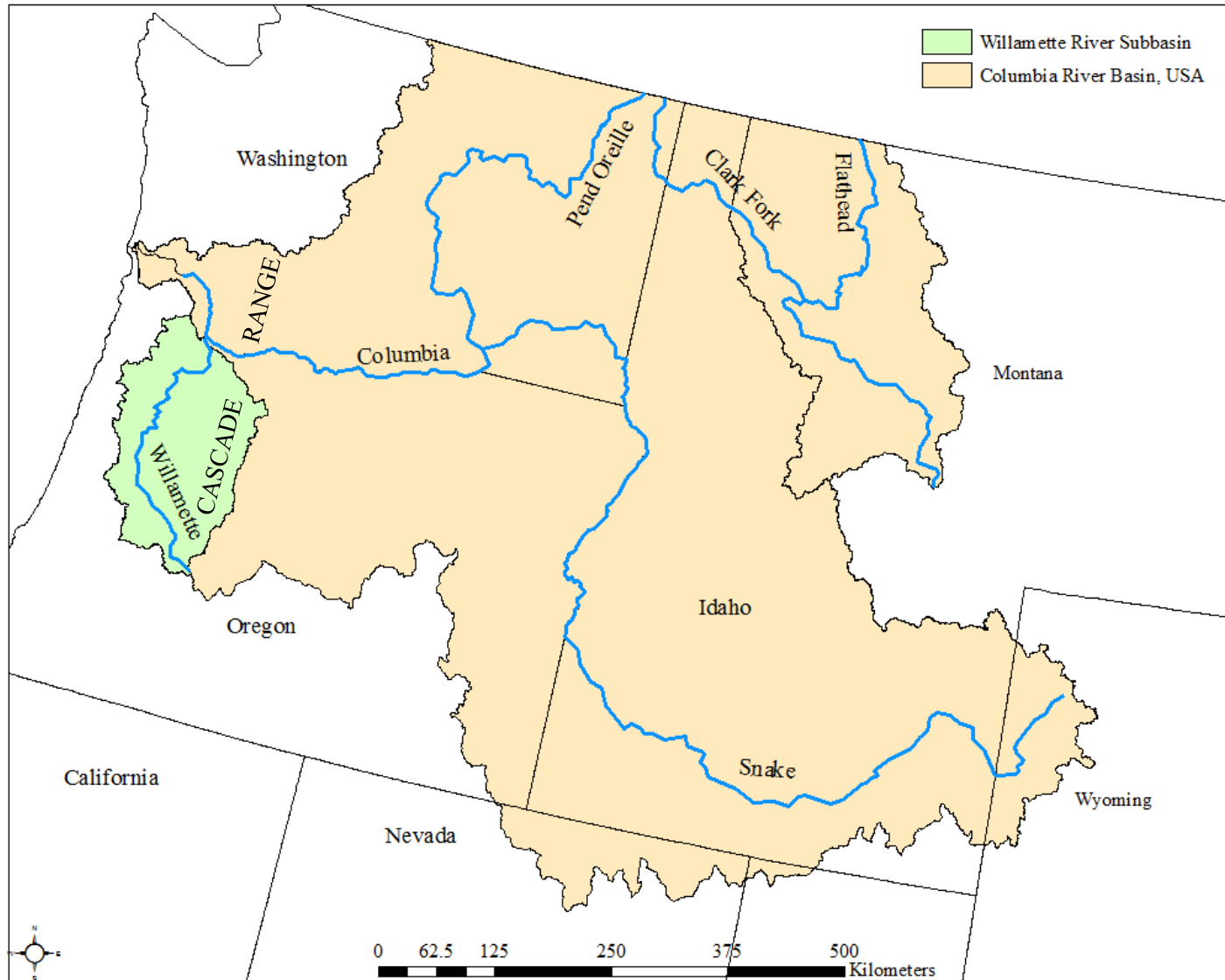


Figure 4.1. The location of the Willamette River Basin in the Pacific Northwest.

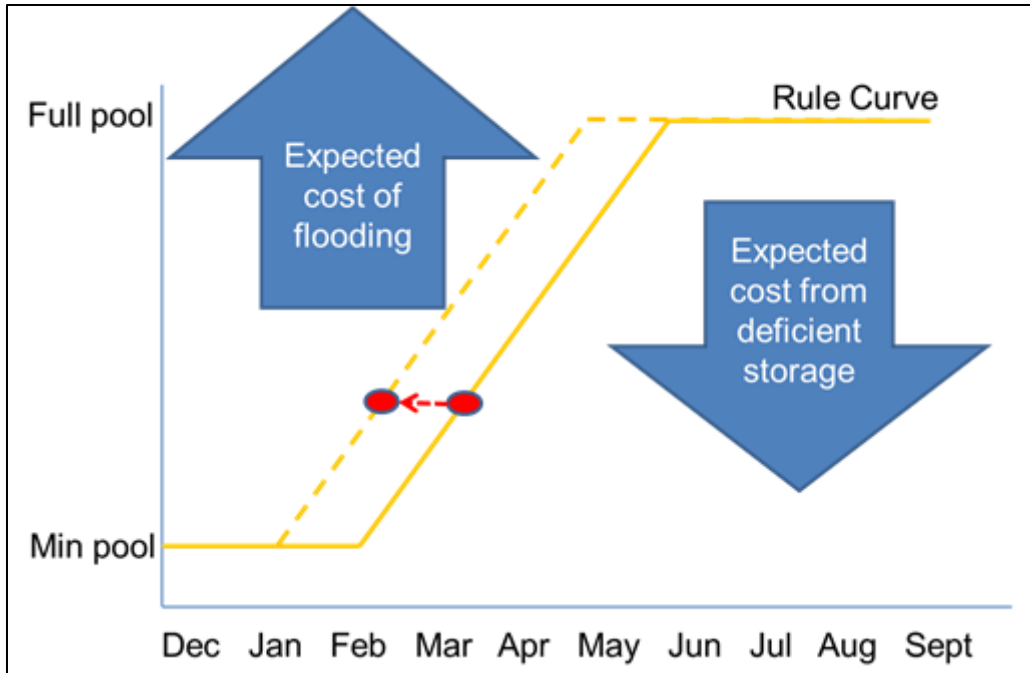


Figure 4.2. An operations rule curve gives the tradeoff between the flood damage reduction and the stored water benefits of a reservoir.

4.3 Study Site

The WRB encompasses an area of approximately 30,000 km², including parts of the Oregon Coast Range to the west and the Cascade Mountains to the east. Elevation in the basin ranges from close to sea level to over 3000 m. The climate is classified as Mediterranean with cool, dry summers and mild, wet winters. Annual precipitation ranges from 1000 mm in the Willamette Valley to 4000 mm at the crest of the Cascades, and approximately 80% of annual precipitation falls between October and May [*Chang and Jung*, 2010]. The topographic effects of the Coast Range and the Cascades result in a slight rain shadow in the western part of the basin and steep orographically controlled precipitation gradients in the Cascades. Up to half of the annual precipitation falls as snow in the high elevations of the Cascades [*Serreze et al.*, 1999] while a negligible proportion of snow occurs in the Coast Range and the Willamette Valley. Annual streamflow hydrographs are dominated by snowmelt in the High Cascades, by mixed rain and snow in the western Cascades, and by rain in the Coast Range. Streamflows in the Willamette River show the same seasonal pattern as precipitation: at the mainstem Salem gauge (USGS station number 14166000) more than half the annual flow occurs between November and February and approximately 87% of flow for the water year (Oct-Sep) occurs by the end of May.

The Willamette Project reservoirs are primarily located in the southern portion on the basin, predominately on tributaries draining the Western Cascades (Figure 4.3). The reservoirs have a combined full pool storage capacity of 1.7 million acre-feet (2097 million cubic meters) (Table 4.1). The current rule curves define the seasonal path for the target volume of water storage across the Willamette Project reservoirs (Figure 4.4). During the winter flood season from December to February, the volume of water in the WRB reservoirs is kept at a minimum to provide storage capacity to buffer storm events. Starting February 1st the USACE begins adding

water to storage with the goal of having the reservoirs full by May 20th, before the Memorial Day holiday. The reservoirs are kept as full as possible for recreation through the summer, with prioritized releases for downstream uses and flow requirements [USFWS, 2008; USACE, 2012]. Following Labor Day the reservoirs are gradually drawn back down to minimum conservation pool in preparation for the next winter flood season. The operation of the Willamette Project reservoirs has therefore altered the natural flow regime of the river [Poff *et al.*, 1997], lowering peak flows during the winter for flood damage reduction and increasing summer low flows [Hulse *et al.*, 2002].

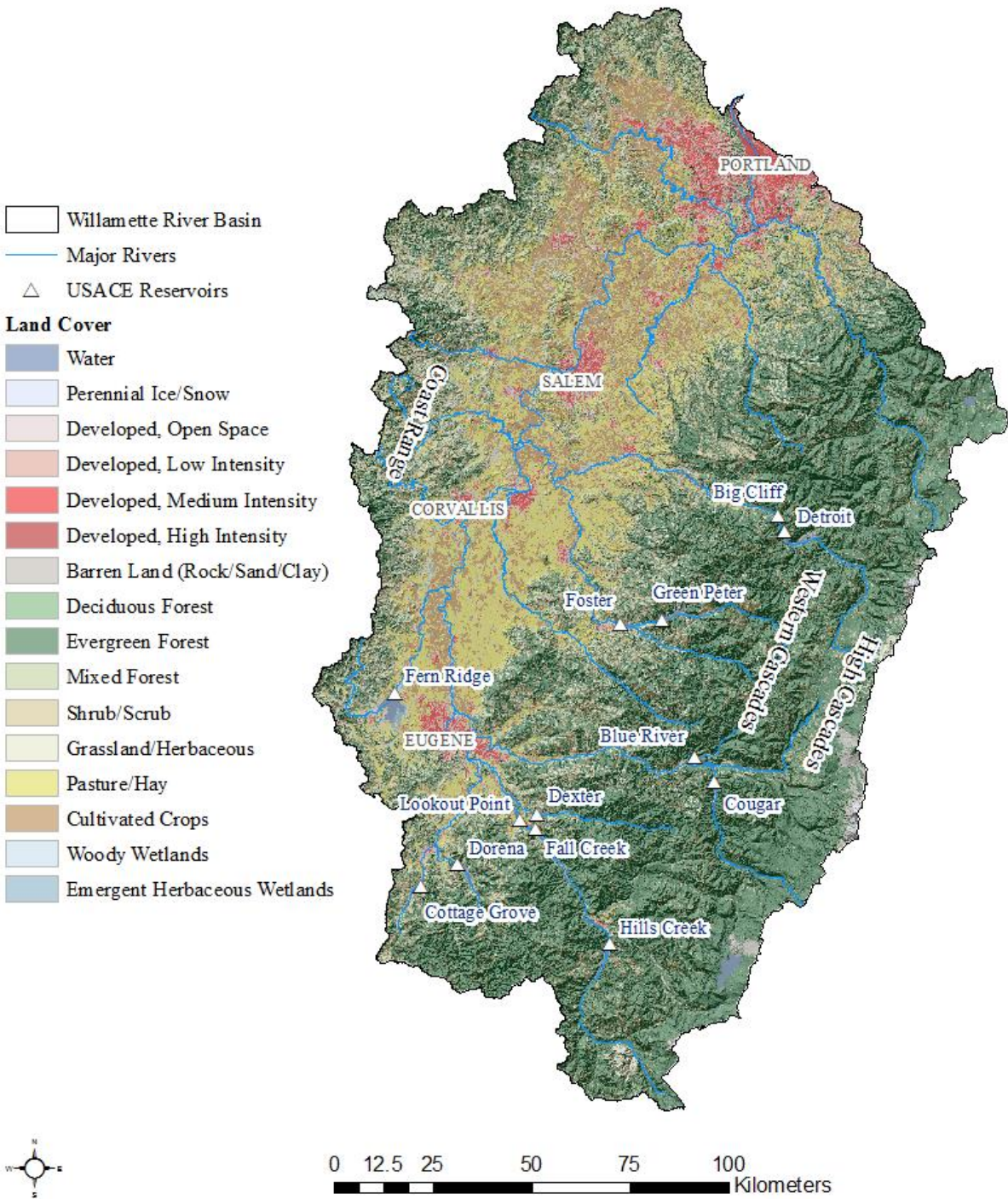


Figure 4.3. The Willamette River Basin, Oregon. The Willamette Project reservoirs are located in the southern portion on the basin, predominately on tributaries draining the Western Cascades

Table 4.1. Names and storage capacities of Willamette Project reservoirs. Source: USACE (2012).

Reservoir	Full Pool Storage (KAF)	Proportion of total storage (%)
Lookout Point	337	20
Detroit	301	18
Green Peter	268	16
Hills Creek	200	12
Cougar	155	9
Fall Creek	115	7
Fern Ridge	110	6
Blue River	86	5
Dorena	71	4
Cottage Grove	30	2
Foster	30	2
Big Cliff*	-	-
Dexter*	-	-
Total	1702	100%

*Re-regulating reservoir.

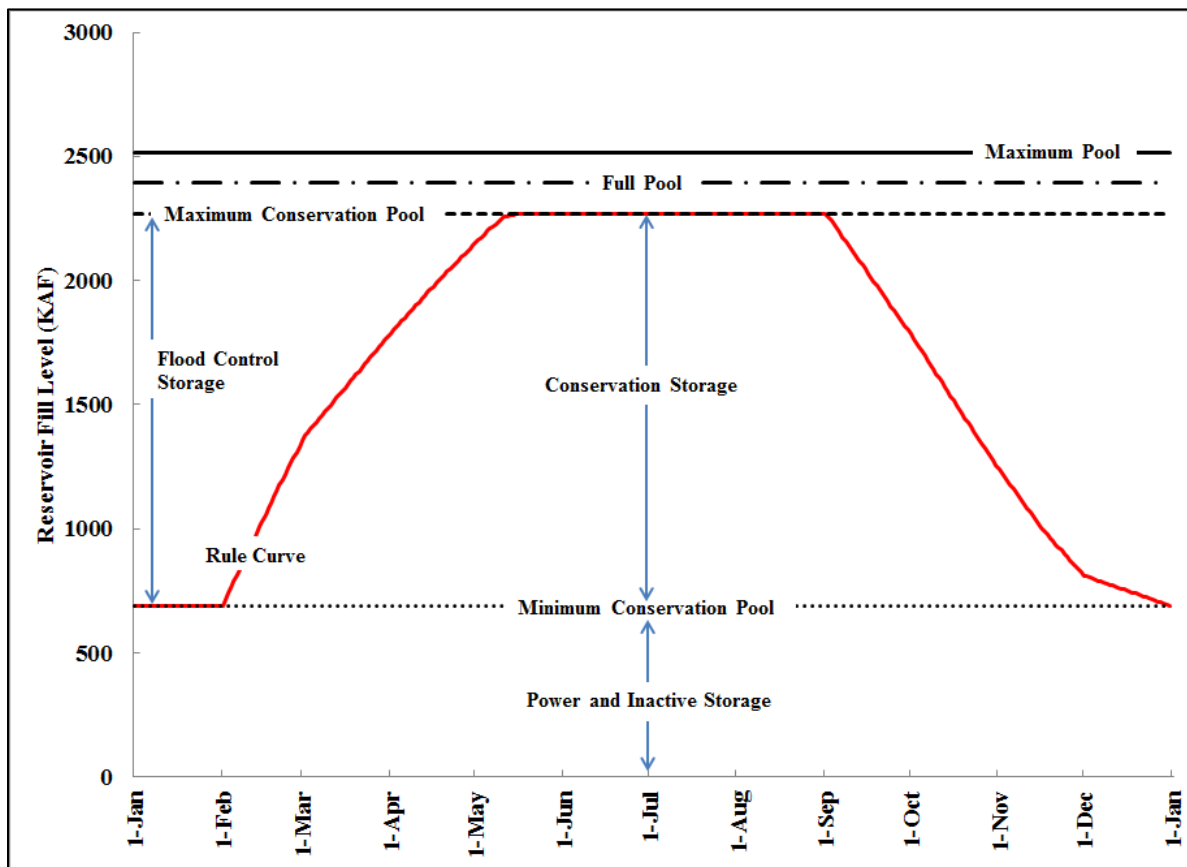


Figure 4.4. The target storage level across the Willamette Project reservoirs as specified by the current rule curves.

4.4 Methods

4.4.1 Theoretical framework

The specific allocation question being evaluated here is how to maximize the benefits from use of a reservoir inter-seasonally, to balance: a) the expected benefits associated with flood damage reduction during the winter and spring, and b) the expected benefits from stored water for reservoir recreation, environmental flows, and water supply to agricultural and urban consumers in the summer. A reservoir with a fill level below full pool has the potential to mitigate flood damage by using the available storage capacity to capture storm flows. During the transition from winter to summer this capacity for flood damage reduction is traded off against the benefit of storing water for summertime uses. As time remaining to fill the reservoir before summer dwindles, and expected inflows and flood risk decline, the priority use of the reservoir storage capacity shifts to the storage goals. To maximize social benefits, the choice of fill level on any given date should balance the expected benefits of these competing uses. When resources are allocated to achieve the maximum possible social benefits (including taking account of externalities), this outcome is described in economic terms as welfare maximizing or socially efficient.

Standard analytics demonstrate that resource allocation will be efficient when it equalizes the marginal value of the resource across competing uses. Stated formally, let

$U = f(w_{1t}, w_{2t}, \dots, w_{Nt})$ denote the social welfare function of water allocation, which maps individual preferences in the society to collective values for water allocation using reservoir capacity. The social welfare function may depend not only on the total amount of economic and environmental benefits derived, but also on distributional impacts and social justice considerations. The function f is assumed to capture the complex interactions between

components of the biophysical-human system. An allocation of water is optimal if it maximizes social welfare subject to expected water availability (q) and reservoir storage capacity (S):

$$\text{Max}_{(w_{1t}, w_{2t}, \dots, w_{Nt})} U = f(w_{1t}, w_{2t}, \dots, w_{Nt}) \quad (4.1)$$

Subject to:

$$w_{1t} + w_{2t} + \dots + w_{Nt} \leq q_t;$$

$$s_t \leq S$$

Where s_t is the volume of water in reservoir storage at time t .

4.4.2 Bellman's Principle of Optimality and Dynamic Programming

In the case of the optimal reservoir fill path, the objective is to maximize the present value of net benefits from flood damage reduction and water storage over the transition from winter to the beginning of summer. This problem can be represented as a discrete time Markov decision model with a finite horizon, where for every incremental period t , the reservoir fill level (s_t) is observed, and a decision (action) regarding the volume of inflows to be added to storage (x_t) is taken. The optimal reservoir fill path is generated by the sequence of actions over a time horizon T that will maximize the present value of expected net benefits from flood damage reduction and water storage.

The optimal sequence of actions (termed the optimal policy) can be solved for using Bellman's [Bellman, 1957] Principle of Optimality, which states: "An optimal policy has the property that, whatever the initial state and decision are, the remaining decisions must constitute an optimal policy with regard to the state resulting from the first decision." Bellman's principle motivates the use of dynamic programming, an approach which structures the optimization

problem into a sequence of simpler sub-problems, and implementing a recursive functional equation (the Bellman equation):

$$V_t(s) = \max_{x \in X_t(s, q_t)} \{f_t(s_t, x_t) + \delta E_t V_{t+1}(g_t(s_t, x_t, e_{t+1}))\}, s \in S \quad (4.2)$$

Subject to:

$$s_0,$$

$$V_{T+1} = h(s_{T+1})$$

$V_t(s)$ is the period t value function, which specifies the maximum attainable present value of current benefits (f_t) and expected future benefits ($E_t V_{t+1}(g_t)$) given a reservoir fill level of s in time t . The initial reservoir fill level is given by s_0 , δ is a discount factor, and V_{T+1} is the terminal condition, which specifies the value of stored water earned following the final action and determined by the resulting reservoir fill level. The reservoir fill level is subject to the reservoir storage capacity (S), while decision regarding the volume of inflows to add to storage is subject to both the reservoir fill level and the expected inflows available for storage each time period (q_t). The period value functions are unknown a priori since V_t can only be derived with knowledge of V_{t+1} . The function g_t gives the transition in the reservoir fill level between periods, which is dependent on the prior fill level, the action taken, and a serially independent exogenous random shock (e_{t+1}) to capture the stochastic nature of streamflows and is assumed to be unknown in period t :

$$s_{t+1} = g_t(s_t, x_t, e_{t+1}) \quad (4.3)$$

The first-order equilibrium conditions (Euler conditions) for a continuous state and action Markov decision model can be derived by applying the Karush-Kuhn-Tucker and Envelope Theorems to the Bellman equation [Miranda and Fackler, 2004]. If actions are assumed to be unconstrained, the Karush-Kuhn-Tucker conditions imply that the optimal action (x), given a reservoir fill level (s), must satisfy the equimarginality condition:

$$f_x(s_t, x_t) + \delta E_\epsilon [\lambda_{t+1}(g(s_t, x_t, \epsilon_{t+1}))g_x(s_t, x_t, \epsilon_{t+1})] = 0 \quad (4.4)$$

And the Envelope Theorem implies:

$$f_s(s_t, x_t) + \delta E_\epsilon [\lambda_{t+1}(g(s_t, x_t, \epsilon_{t+1}))g_s(s_t, x_t, \epsilon_{t+1})] = \lambda_t(s) \quad (4.5)$$

Subject to the terminal condition:

$$\lambda_{T+1}(s) = h_s \quad (4.6)$$

Where $\lambda(s) \equiv V'(s)$ and f_x , f_s , g_x , and g_s denote partial derivatives. λ is termed the shadow price function as it gives the marginal value attributed to the state variable (the reservoir fill level). If the stochastic shock is fixed at its mean, it follows that along the optimal fill path:

$$f_x(s_t^*, x_t^*) + \delta \lambda_{t+1}^* g_x(s_t^*, x_t^*) = 0 \quad (4.7)$$

$$f_s(s_t^*, x_t^*) + \delta \lambda_{t+1}^* g_s(s_t^*, x_t^*) = \lambda_t^* \quad (4.8)$$

Conceptually this means that the cost of adding a unit of water to the reservoir (i.e. the reduction in expected flood buffering) must equal the marginal gain in the value of water storage, and that the present valued shadow price of stored water is given by the sum of the marginal cost of reduced flood buffering capacity and the marginal value of stored water. The optimality conditions indicate that additions of stored water above s_0 will not increase the expected present value of net benefits so long as the reduction in expected flood buffering is greater than the increase in expected stored water value. Based on the climate and hydrology of the WRB, flood risk is expected to diminish monotonically over the transition period from winter to summer (see chapter 2 for details), implying that over this time it will become desirable to begin to raise the reservoir fill level.

4.4.3 Reference case model

We apply the Bellman equation to identify the optimal reservoir fill path for a generic reservoir representing the Willamette Project reservoir system, given an objective function representing benefits of flood damage reduction and water storage, subject to constraints on the availability and timing of water inflows to the reservoir. The time horizon for the dynamic program was the transition from winter to summer, defined over 20 one-week periods from Jan 1st to May 20th. The 11 storage reservoirs within the WRB were treated as a single unit representing the total reservoir capacity available for either flood damage reduction or water storage. The problem was solved numerically using the CompEcon Matlab Toolbox [*Miranda and Fackler, 2004*]. The numerical basis for the value functions comes from the prior analyses on expected flood damages (chapter 2) and the expected value of stored water (chapter 3). The expected inflows constraint and variability are based on historical conditions. The alternative scenarios of social and hydrologic change examined are described in the next section.

Current benefits, (f_t) in the Bellman equation, were specified as the loss in expected flood buffering associated with increasing the reservoir fill level in each time period. For the reference case model, this function was parameterized for the expected value of flood buffering estimated for the year 2000 (see chapter 2 for details):

$$f_t(s_t, x_t) = \alpha * (x + s)^2 * (1 - \beta)^t * (1 - \gamma)^{t^2} * (1 - \rho)^{t^3} \quad (4.9)$$

Where: $\alpha = -0.10, \beta = 0.14, \gamma = 0.0029, \text{ and } \rho = 0.00023$

$$t = 0, 1, \dots, 19$$

Losses in current flood buffering benefits increase as the reservoir fills ($\frac{\partial f}{\partial s} < 0$), since there is less capacity available to buffer storm events, but decrease over time ($\frac{\partial f}{\partial t} > 0$) as the magnitude of expected storm events decline.

The value of stored water is earned following the final decision period, and is given by terminal condition V_{T+1} in the Bellman equation, which was specified based on the average value of stored water to recreation estimated across the Willamette Project reservoirs (see chapter 3 for details):

$$V_{T+1} = \kappa * s_{T+1}^2 + \varphi * s_{T+1} \quad (4.10)$$

Where: $k = -0.03, \quad \varphi = 120$

This function implies a marginal value of stored water of \$3/acre-foot/month at full pool for the 3 month summer recreation period from June through August. The marginal value declines to zero at maximum pool to prevent additions of water to storage beyond this level.

To prevent discounting of benefits inter-seasonally, the discount factor in the Bellman equation was set to 1. For each period, the value function ($V_t(s)$) was approximated using a linear combination of 75 piecewise linear basis functions over the interval [0; 2000 KAF], which covers the storage capacity of the Willamette Project reservoir system.

The system constraints included 1) the initial reservoir fill level and 2) the available inflow in each time period. The initial reservoir fill level was normalized to zero to represent minimum conservation pool. Expected reservoir inflow was estimated by fitting an OLS regression equation for the 5th order polynomial to the historical streamflow record (Figure 4.5). The record used was the average (1975-2012) inflows to the eleven storage reservoirs less the outflows at the Green Peter and Hills Creek reservoirs (which are in series above other reservoirs). The resulting function ($R^2 = 0.95$, $F = 162.45$) was:

$$q(t) = a + bt + ct^2 + dt^3 + ut^4 + vt^5 \quad (4.11)$$

Where: $a = 274.63, b = -32.29, c = 4.50, d = -0.25, u = 0.0057, v = -4e - 05$

The variability of inflows was incorporated into the model by multiplying the action variable (x_t) with a stochastic shock (e_{t+1}) in each period. The transition in the reservoir fill level between periods was therefore given by:

$$s_{t+1} = s_t + x_t + (x_t * e_{t+1}) \quad (4.12)$$

Where: $x_t \in [0, q(t)]$

This allows the volume of inflows added to storage each period to deviate from the desired addition by a relative amount. The stochastic shock was modelled as:

$$e \sim i. i. d. N(0, \sigma^2) \quad (4.13)$$

Where:

$$\sigma^2 = 0.06$$

Because the shock represents the probability that inflows may fall short of the desired level, the value of the variance was based on the likelihood of low flows in the historical record (Figure 4.6). This parameterization has the effect of limiting the desired gain by approximately 75% at the 99th percentile of the shock. A 5 node Gaussian quadrature scheme was used to discretize the distribution of the shock for numerical modelling.

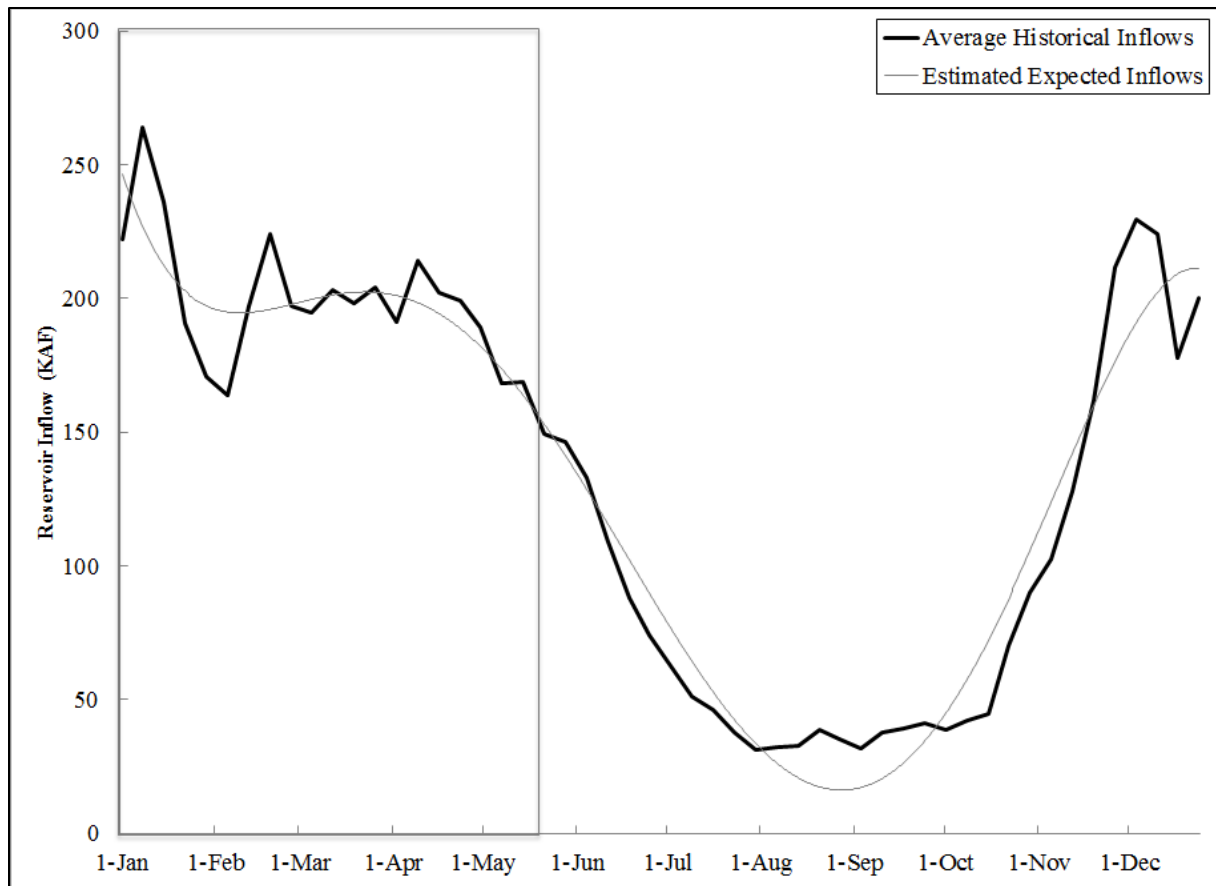


Figure 4.5. Expected reservoir inflow for the reference case model specification was estimated by fitting an OLS regression equation for the 5th order polynomial to the historical streamflow record. The grey box indicates the period modelled for reservoir refill.

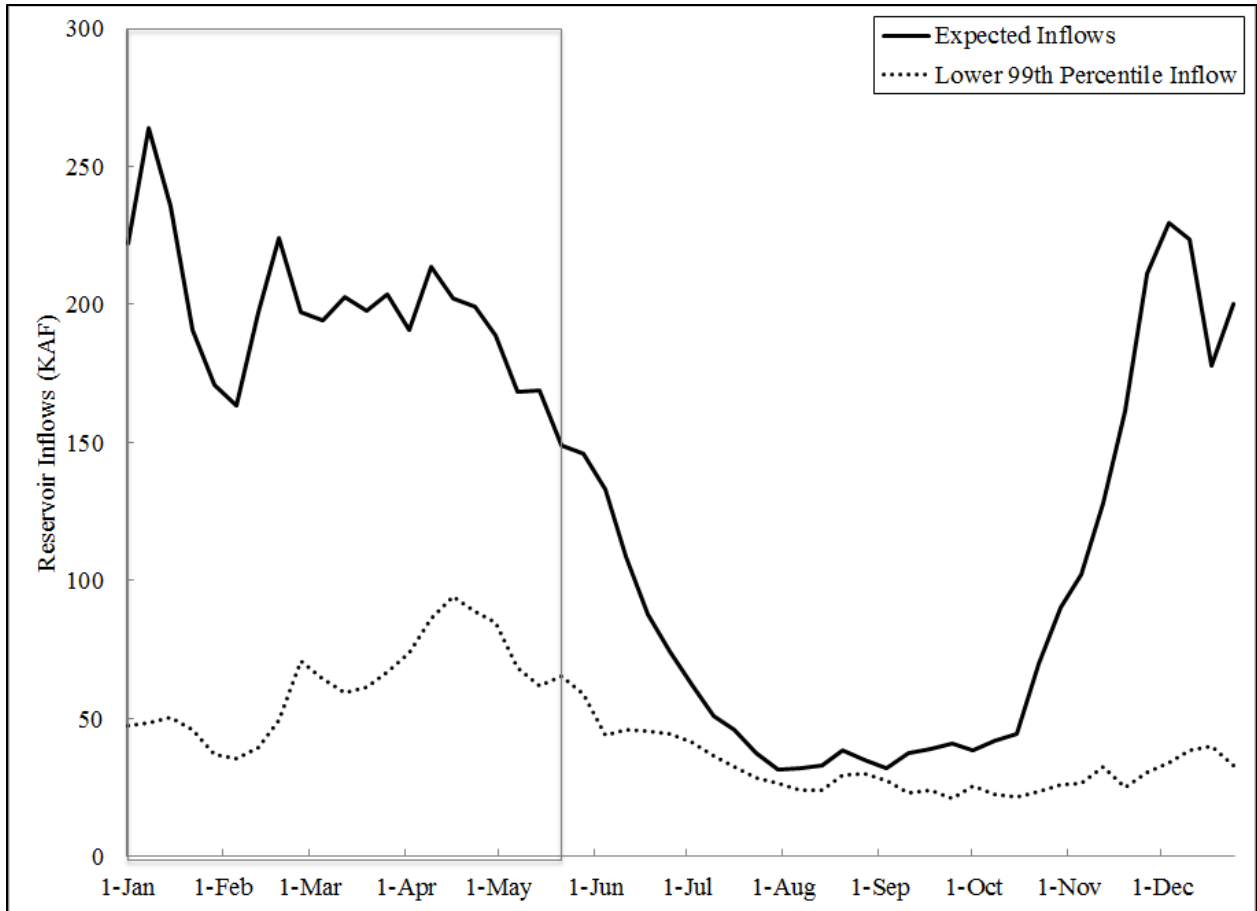


Figure 4.6. The expected reservoir inflows and the lower 99th percentile inflows based on the historical record. The grey box indicates the period modelled for reservoir refill.

4.4.4 Alternative model specifications

Several alternative specifications of the optimization problem were formulated to test the sensitivity of the optimal reservoir fill path to requirements for downstream flows, and changes in hydrology, expected flood costs and the value of stored water (Table 4.2). If the derived optimal reservoir fill path resulted in a final storage level below full pool, the specified model was also iteratively solved to determine the value of stored water that would be required to achieve full pool storage.

In the first alternative specification (hereafter Alternative 1 etc.), the expected inflows available for storage were reduced to account for downstream flow requirements based on the 2008 Biological Opinion (BiOP) [*USFWS*, 2008; *USACE*, 2012]. As a conservative estimate of required releases, the minimum flow targets downstream each series of dams were summed together by week and subtracted from the expected inflow constraint to yield a modified discretionary inflow (Figure 4.7).

In Alternative 2, the price of stored water at full pool was increased to \$17/acre-foot, the estimated value of water to irrigated agriculture in the WRB [*Kalinin, A.*, 2013]. Alternative 3 doubled this estimate to \$34/acre-foot. These alternatives provided conservative estimates for the value of stored water to account for a) the possibility that agricultural demands may increase in the future, and b) the likelihood that the value of reservoir recreation will increase if population rises.

Alternatives 4 and 5 tested the sensitivity of the optimal path to alternative formulations of the flood loss function. The flood loss function was modified to reflect an estimated 33% increase in flood losses for the year 2030 (Alternative 4), and an estimated 136% increase in

flood losses for the year 2070 (Alternative 5), relative to the reference case model (see Chapter 2 for details).

Alternatives 6 and 7 examined the impact of expected or possible effects of climate change on streamflow (Figure 4.8). In Alternative 6 future reservoir inflows were assumed to resemble historical streamflow in the rain-dominated zone of the Cascade Range, as exemplified by WS9 (1968-2012) in the H.J. Andrews Experimental Forest in the McKenzie River catchment of the WRB. WS9 has high winter streamflow associated with rain events and little to no snowmelt to bolster flows in the spring. In Alternative 7 future reservoir inflows were assumed to resemble historical streamflow (1963-1981, 2001-2013) in Coyote Creek WS 4 in the South Umpqua Experimental Forest (south of the WRB and east of Roseburg, OR). This scenario made the assumption that climate in the WRB changed to resemble current climate in southern Oregon, representing both a future loss of snowpack, as well as increases in evapotranspiration.

In Alternative 8, the stochastic shock was doubled to test the sensitivity of the optimal fill path to the potential for increased variability in streamflow. This has the effect of reducing available inflows to almost zero at the 99th percentile of the distribution.

In Alternative 9, the coefficients in the time dependent terms of flood loss function (hereafter "flood loss multiplier") were altered to increase expected flood costs in the winter and decline faster during the spring. This scenario tested the effects of an expected change to rain-dominant streamflow, which may shift the timing of flooding earlier, and increase flood intensity (Figure 4.9).

Table 4.2. Model specifications. The first row provides the specification for the reference case. The rows following provide the changes for each alternative specification relative to the reference case model.

<u>Model</u>	<u>Flood Cost Function</u>	<u>Storage Value Function</u>	<u>Inflows Function</u>	<u>Stochastic Shock</u>
Reference case	$f_t(s_t, x_t) = \alpha * (x + s)^2 * (1 - \beta)^t * (1 - \gamma)^{t^2} * (1 - \rho)^{t^3}$	$V_{T+1} = \kappa * s_{T+1}^2 + \varphi * s_{T+1}$	$f(t) = a + bt + ct^2 + dt^3 + ut^4 + vt^5 + wt^6$	$e \sim i. i. d. N(0, \sigma^2)$
	With $\alpha = -0.077, \beta = 0.14, \gamma = 0.0029, \rho = 0.00023$	With $\kappa = -0.03, \varphi = 120$	With: $a = 274.63, b = 32.29, c = 4.50, d = -0.25, u = 0.0057, v = -4e - 05, w = 0$	With $\sigma^2 = 0.06$
Alternative 1			$a = 191.35, b = -17.29, c = 1.75, d = -0.059, u = -0.00083, v = 5.92e - 05, w = -6.10e - 07$	
Alternative 2		$\kappa = -0.07, \varphi = 260$		
Alternative 3		$\kappa = -0.14, \varphi = 520$		
Alternative 4	$\alpha = -0.10$			
Alternative 5	$\alpha = -0.18$			
Alternative 6			$a = 347.75, b = 26.54, c = -7.80, d = 0.57, u = -0.020, v = 0.00032, w = -2.00e - 06$	
Alternative 7			$a = 192.29, b = -2.96, c = -1.16, d = 0.088, u = -0.0029, v = 4.51e - 05, w = -2.60e - 07$	
Alternative 8				$\sigma^2 = 0.12$
Alternative 9	$\beta = 0.05, \gamma = 0.02, \rho = 0$			

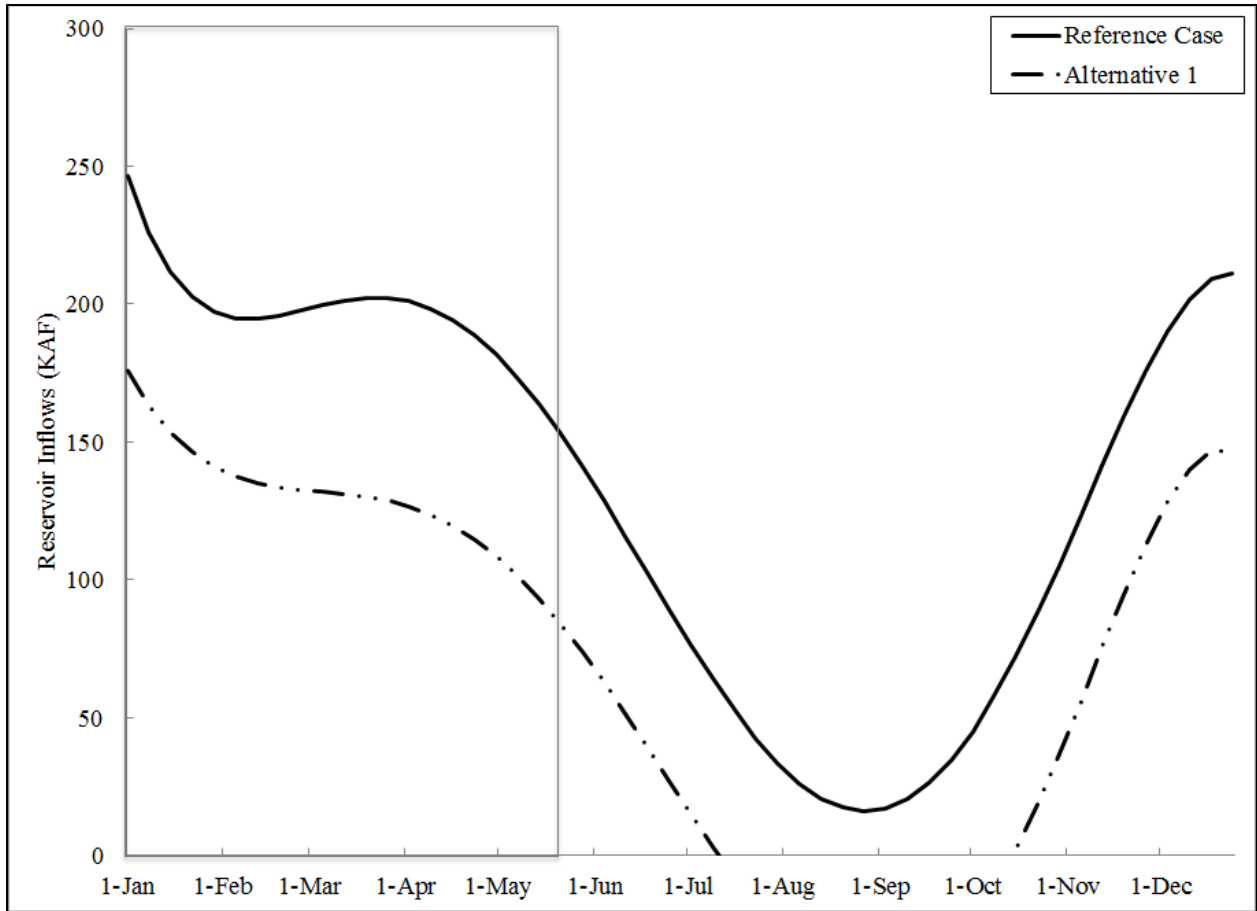


Figure 4.7. Reservoir inflows available for storage under the reference case specification and under Alternative 1 specification where available inflows were reduced to account for downstream flow requirements. The grey box indicates the period modelled for reservoir refill.

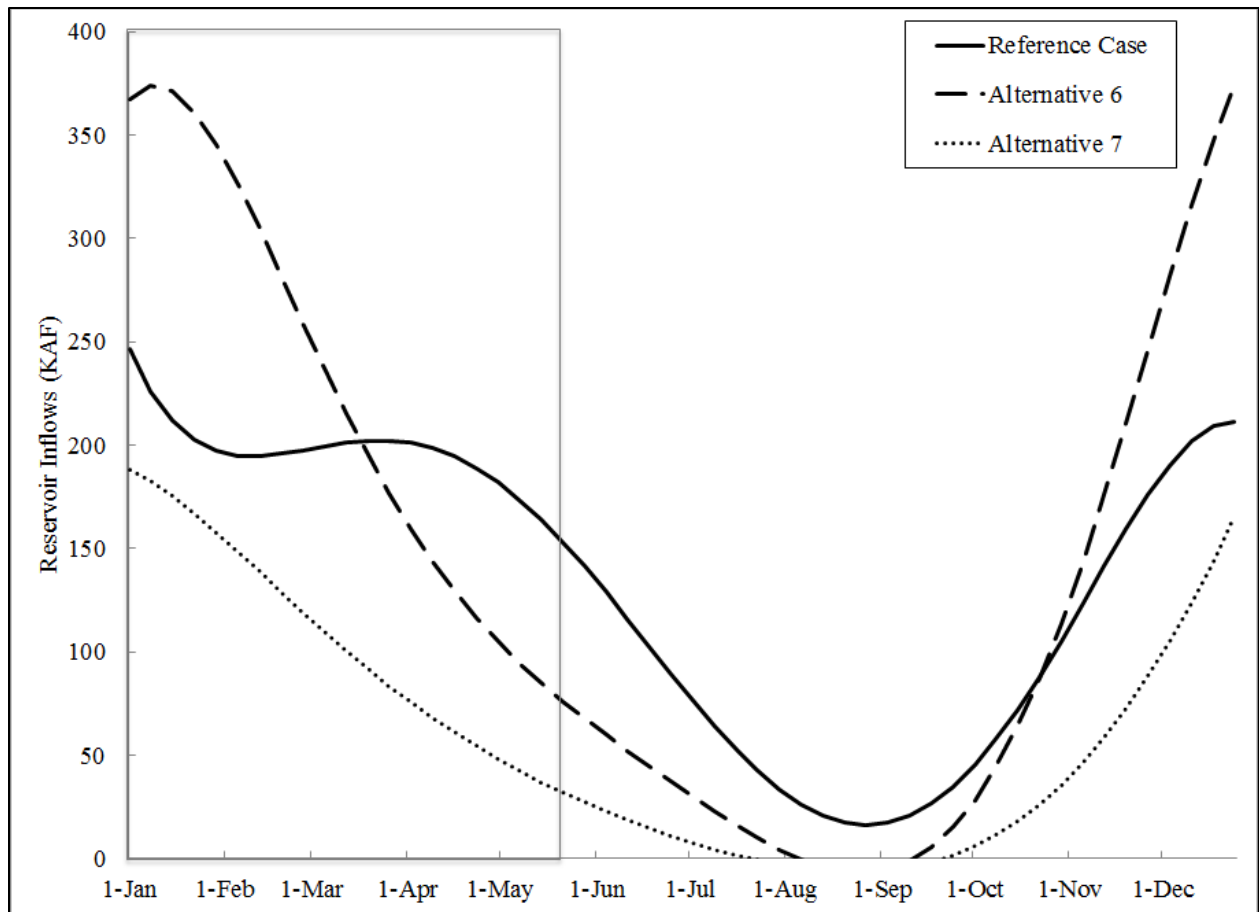


Figure 4.8. Reservoir inflows available for storage under the reference case specification, the Alternative 6 specification in which future reservoir inflows were assumed to resemble historical streamflow in the rain-dominated zone of the Cascade Range, and the Alternative 7 specification in which future reservoir inflows were assumed to resemble historical streamflow in southern Oregon representing both a future loss of snowpack, as well as increases in evapotranspiration relative to historical conditions. The grey box indicates the period modelled for reservoir refill.

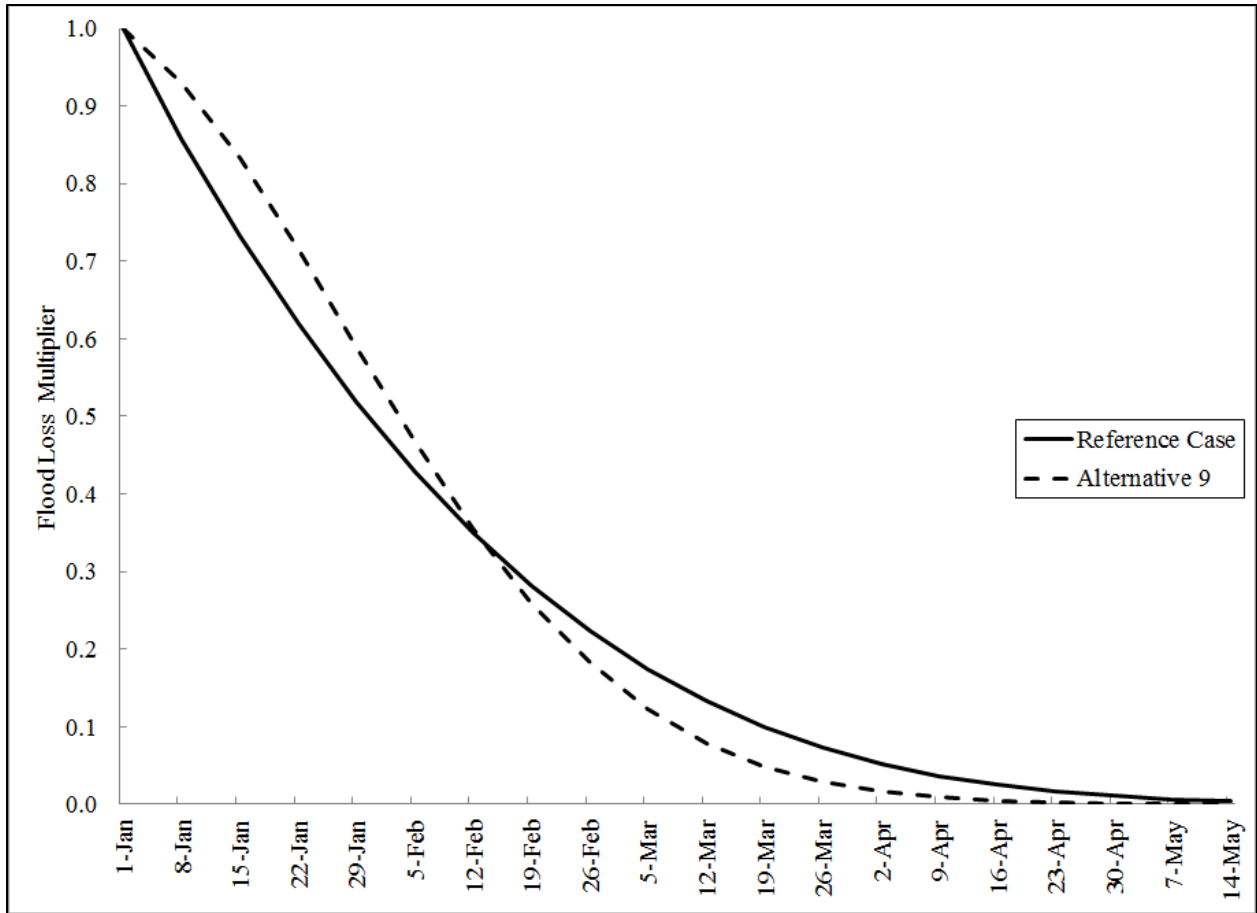


Figure 4.9. The product of the time dependent terms of flood loss function (the “flood loss multiplier”) under the reference case model specification, and under the Alternative 9 specification, which simulates increased flood costs in the winter and decreased flood costs in the spring.

4.5 Results

In this section the numerical results for the optimization model are presented starting with the reference case specification. The sensitivity of the optimal reservoir fill path to downstream flow requirements is presented next, followed by a comparison of the derived optimal fill path to the current filled used by the USACE for the Willamette Project reservoirs. Finally, the sensitivity of the optimal reservoir fill path to possible future changes in hydrology, and the expected values of stored water and flood damages are presented.

4.5.1 Reference case model

Under the reference case model specification, the derived optimal policy kept the reservoir fill level close to minimum pool from the beginning of January to the third week in March (Figure 4.10), indicating that expected flood damages dominate during this period. By the end of the third week in March the optimal storage level was increased to 110 KAF. Starting the following week, the reservoir was filled as rapidly as possible through May 21st given expected available inflows (Figure 4.11). The final volume of stored water reached was 1610 KAF, which falls short of full pool storage by just less than 100 KAF (Figure 4.10). Full pool storage was achieved if the marginal value of stored water at full pool was increased to \$15/acre-foot per the three month summer period, all else the same. The resulting optimal reservoir fill policy still kept the reservoir fill level close to minimum pool until the second week in March (Figure 4.12). However, beginning the second week in March, optimal additions to storage are increased relative to the reference case specification (Figure 4.13). By the end of March the reservoir fill level is about 100 KAF greater as a result of the increased value of stored water. All the gains in storage relative to the reference case specification have occurred by the beginning of April because expected inflows start to constrain additions to reservoir storage (Figure 4.13).

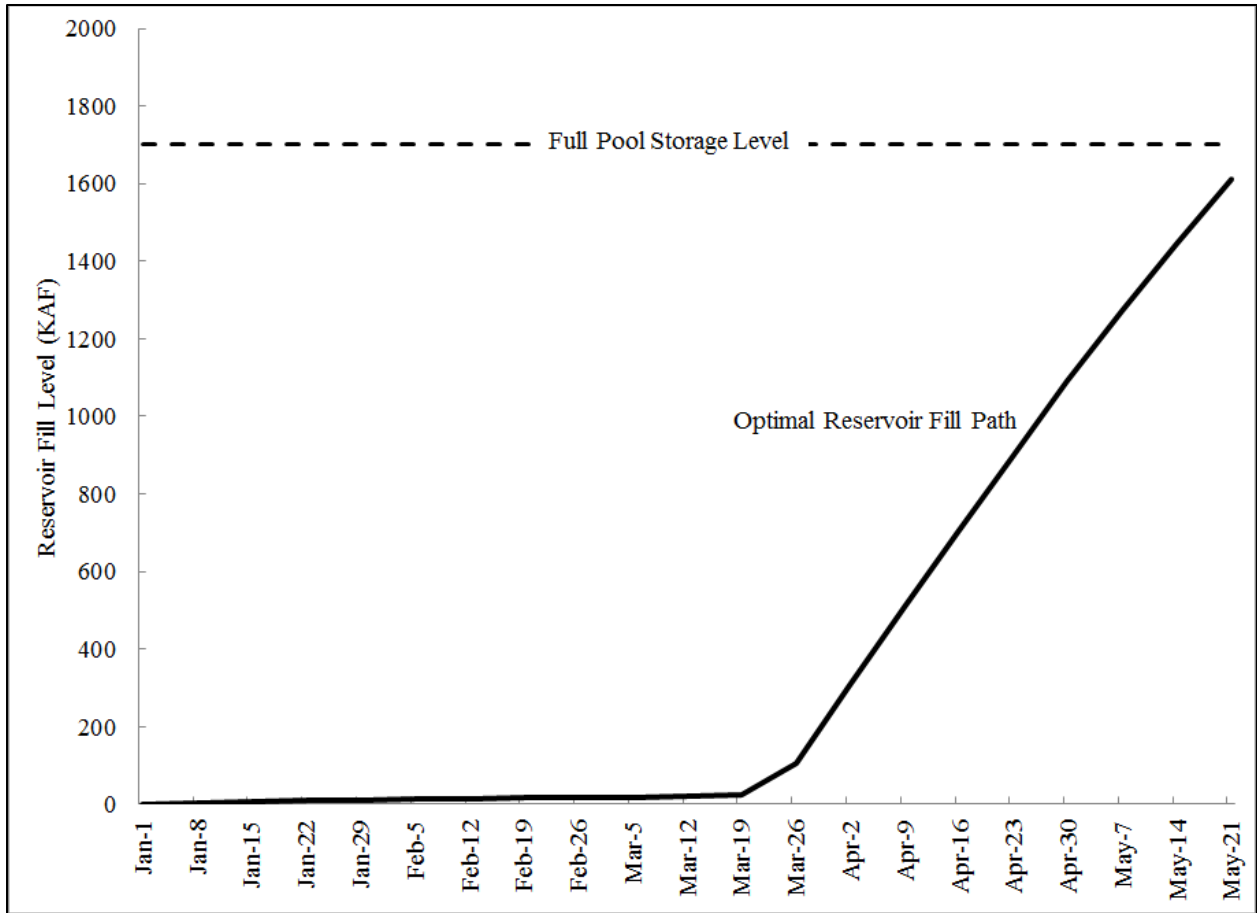


Figure 4.10. The optimal reservoir fill path derived under the reference case model specification.

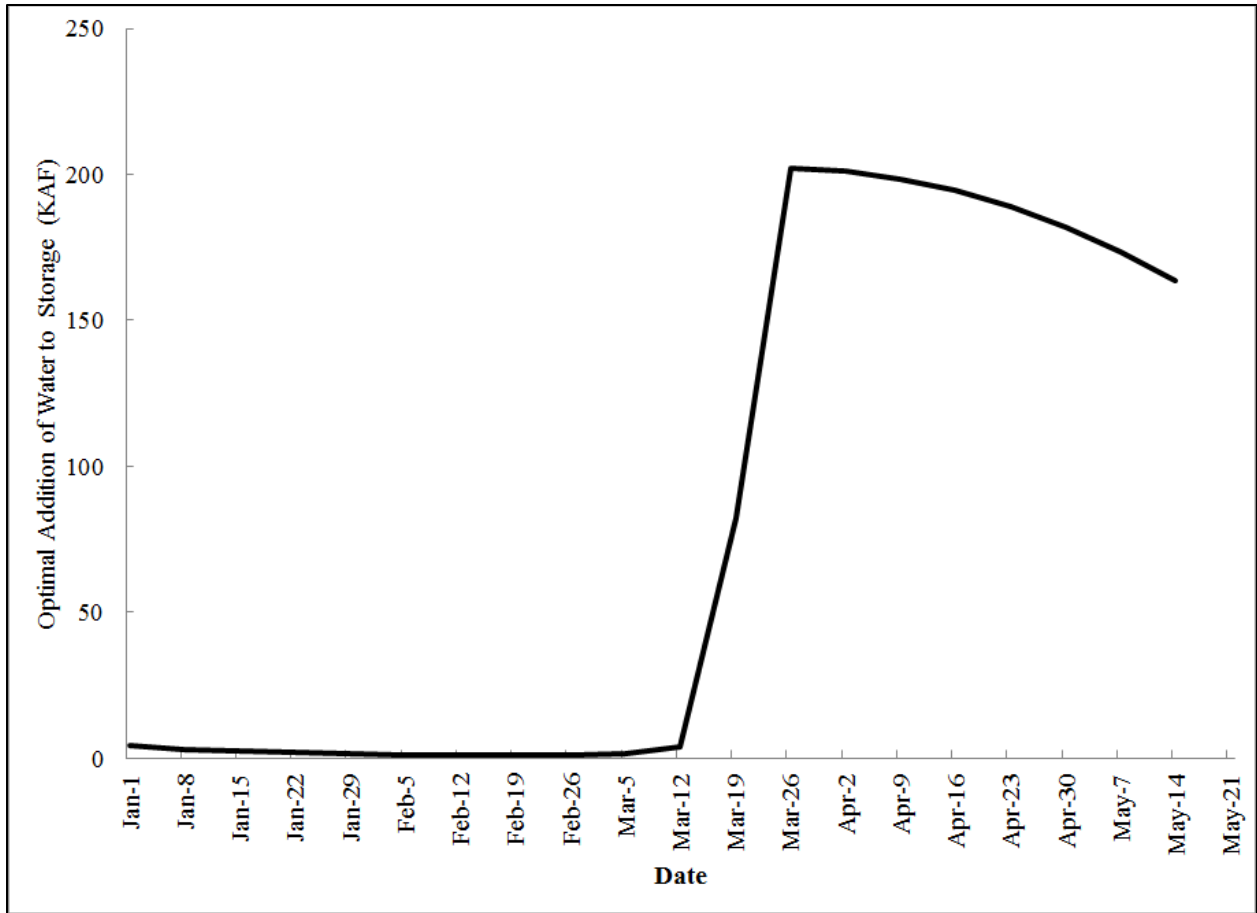


Figure 4.11. The optimal policy for additions of water to reservoir storage under the reference case model specification.

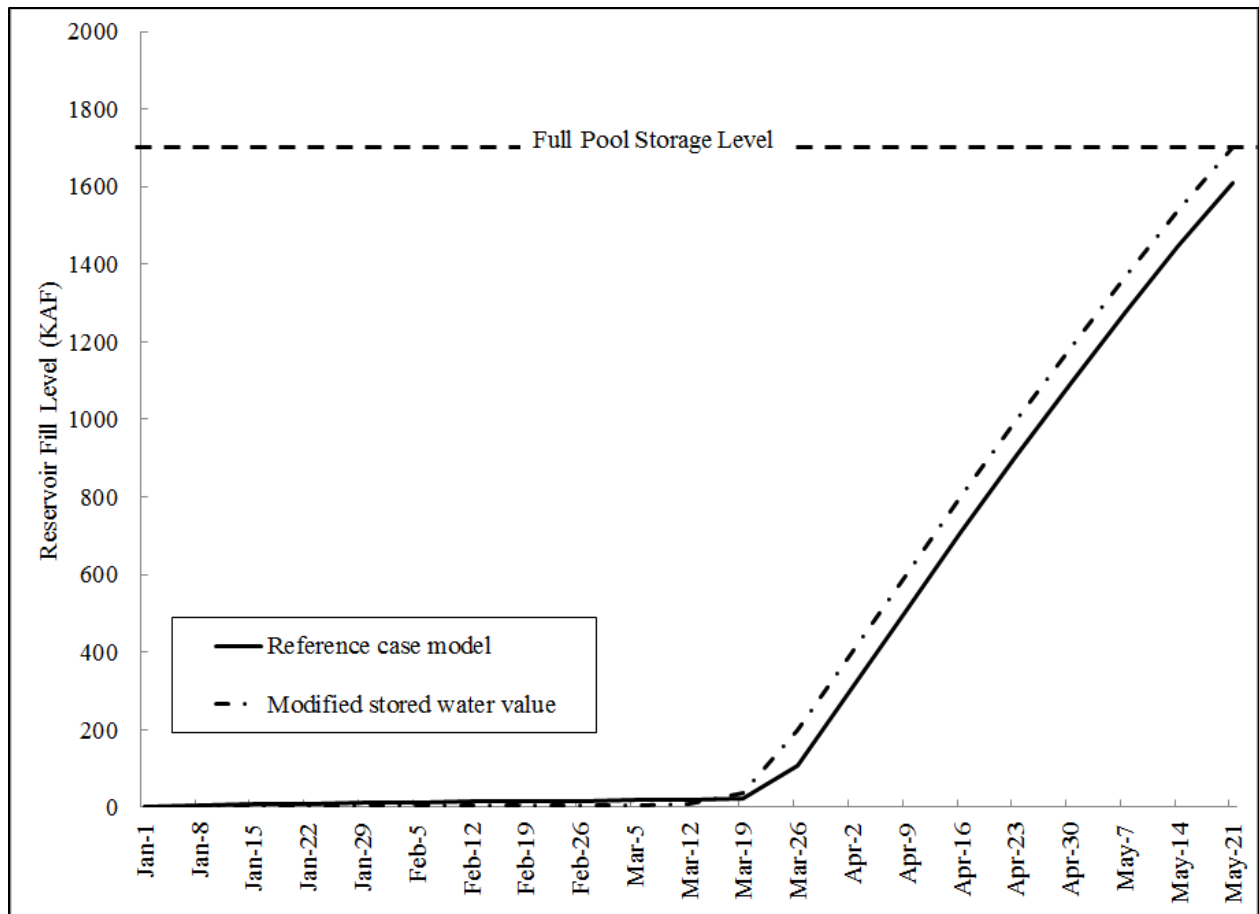


Figure 4.12. The optimal reservoir fill path under the reference case specification compared to the optimal reservoir fill path given an increase in the value of stored water at full pool to \$15/acre-foot/3 month summer period – the increase required to achieve full pool storage by May 21st, all else the same.

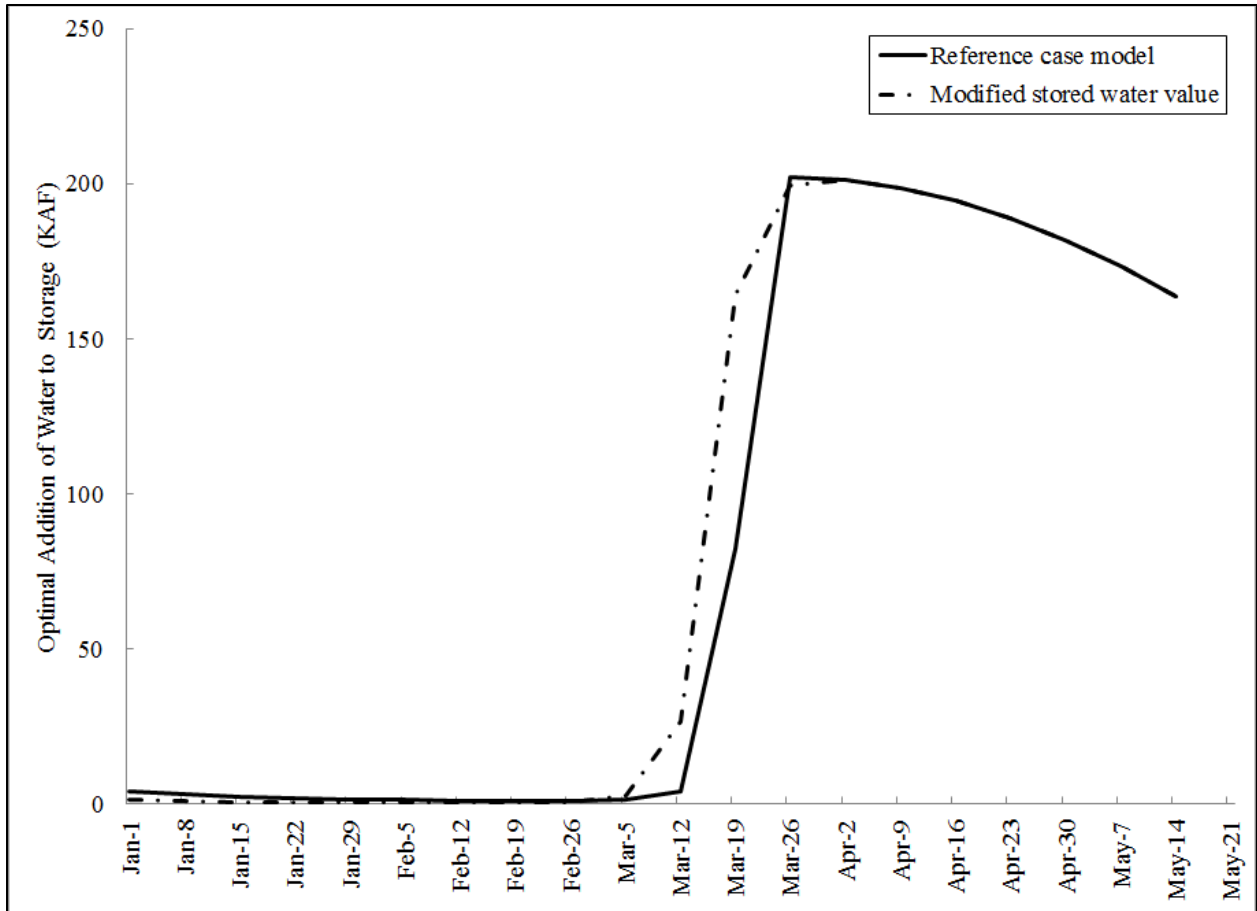


Figure 4.13. The optimal policy for additions of water to reservoir storage under the reference case specification compared to the optimal policy for additions of water to reservoir storage given an increase in the value of stored water at full pool to \$15/acre-foot/3 month summer period – the increase required to achieve full pool storage by May 21st, all else the same.

4.5.2 Sensitivity to downstream flow requirements

Incorporating downstream flow requirements in the estimation of expected available inflows shifted the optimal reservoir fill path to start filling three weeks earlier, and to fill at a slower rate relative to the reference case specification (Figure 4.14, Figure 4.15). By the third week in March the reservoir had filled more than 12 times the level reached under the reference case specification (Figure 4.15). However, due to the slower fill rate the final volume of stored water achieved by May 21st was 1347 KAF, which is 263 KAF less than under the base case specification and 355 KAF below full pool storage. In order for full pool storage to be achieved, the marginal value of stored water at full pool was required to increase \$64/acre-foot/3 month summer period, all else the same. Given this increase in the value of stored water, the optimal reservoir fill path shifts an additional 2-3 weeks earlier (Figure 4.16), with gains to storage of over 100 KAF by February 12th (Figure 4.17). These earlier additions to storage allow full pool storage to be achieved by May 21st despite the reduction in inflows available for storage (Figure 4.17).

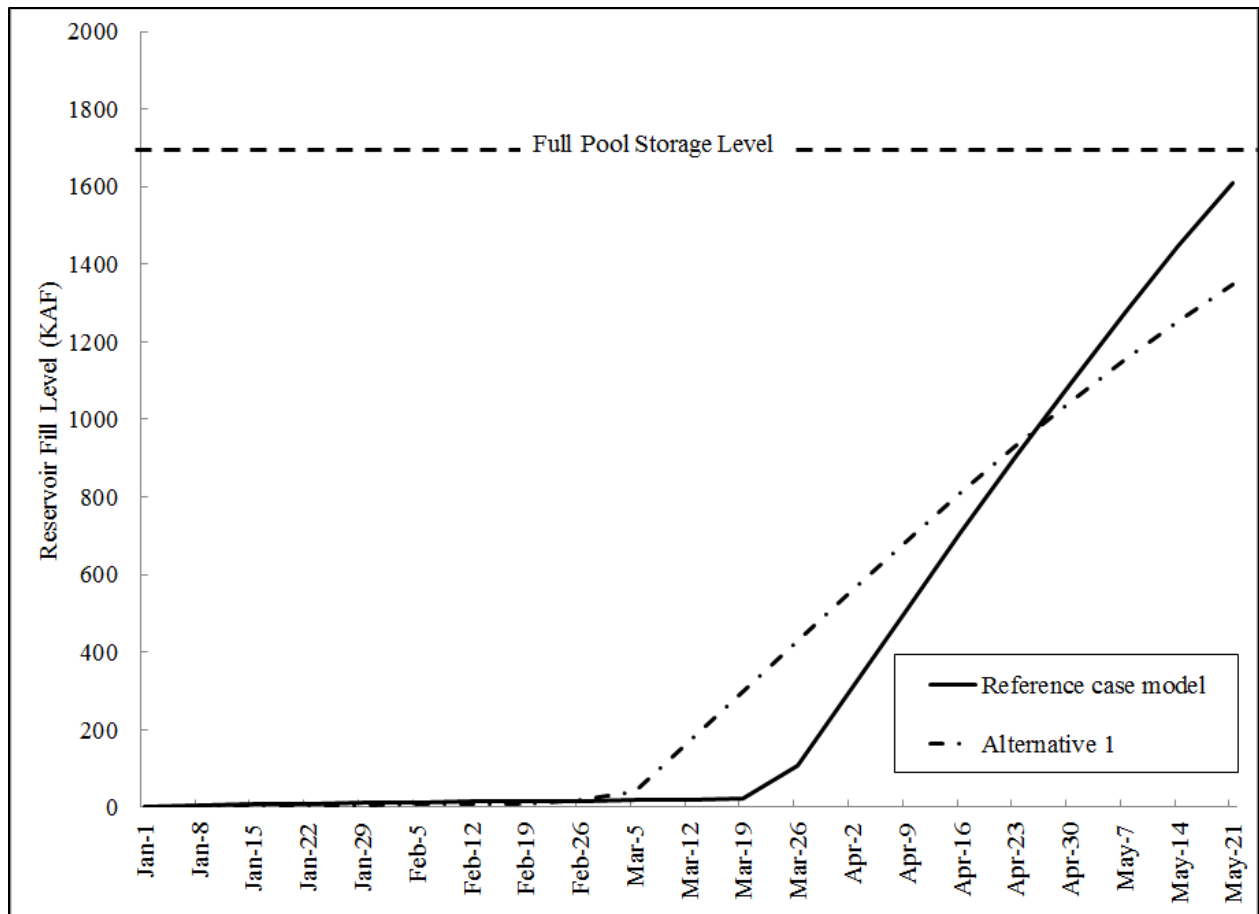


Figure 4.14. The optimal reservoir fill path under the reference case specification compared to the optimal reservoir fill path given modified discretionary inflows as specified in Alternative 1 to account for downstream flow requirements.

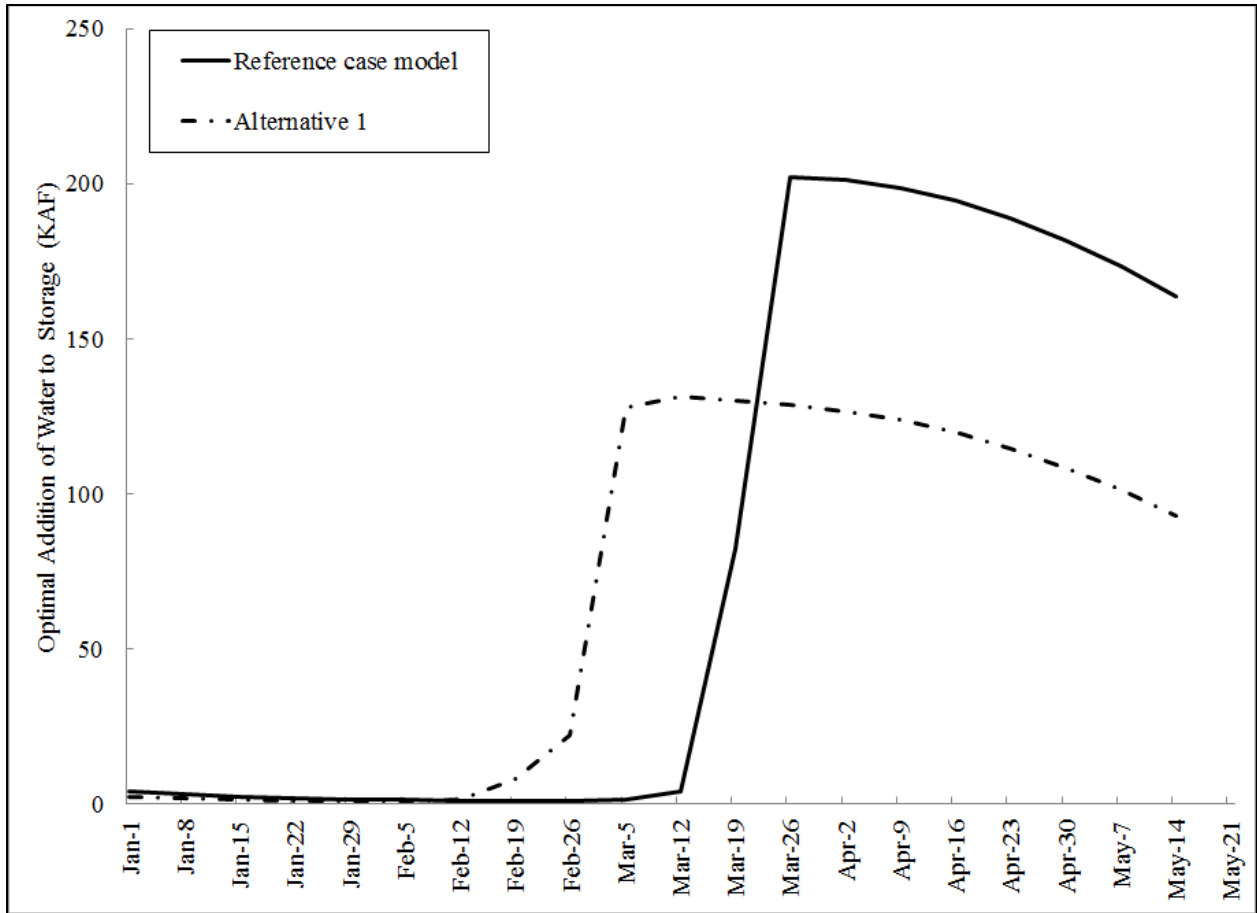


Figure 4.15. The optimal policy for additions of water to reservoir storage under the reference case specification compared to the optimal policy for additions of water to reservoir storage given modified discretionary inflows as specified in Alternative 1 to account for downstream flow requirements.

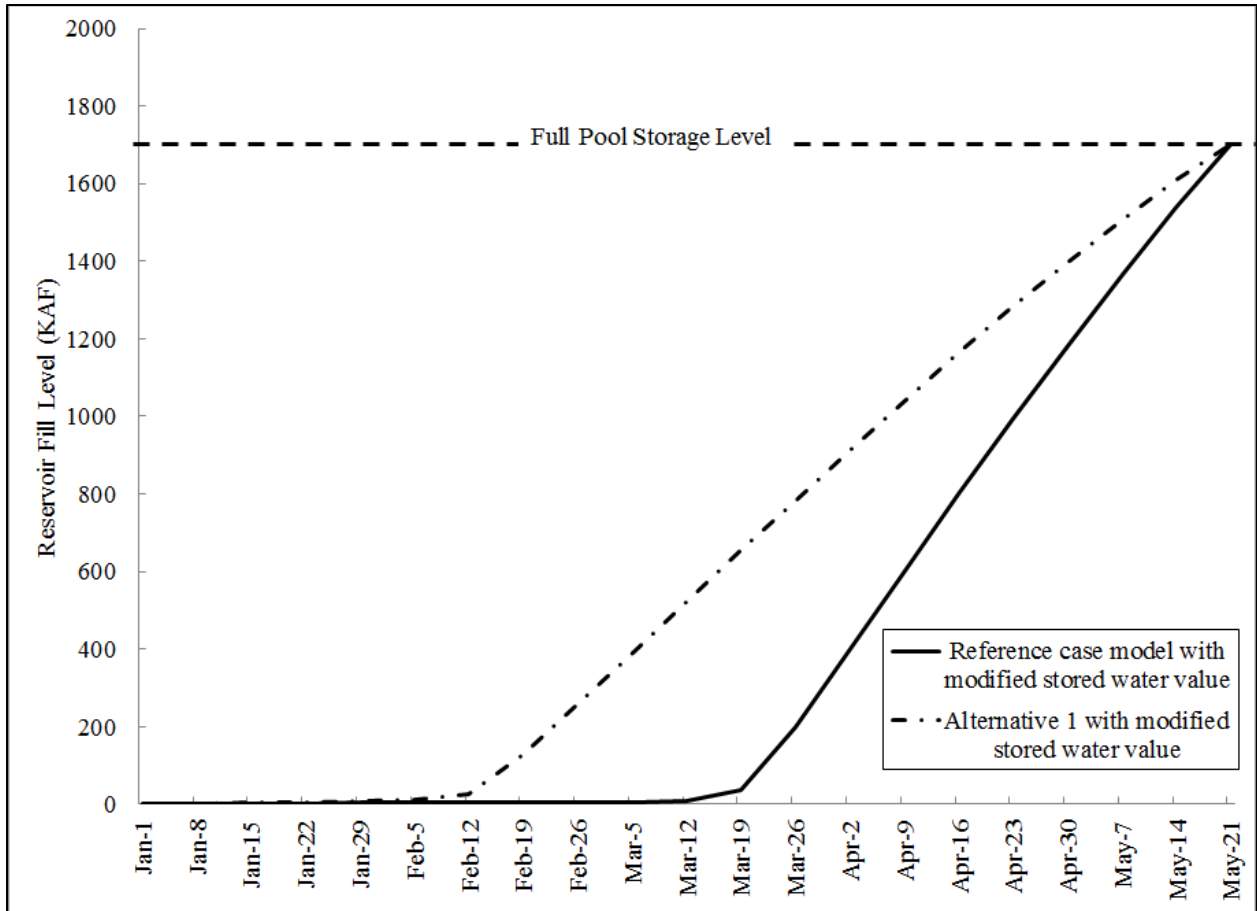


Figure 4.16. The optimal reservoir fill path compared for expected inflows under the reference case specification and modified discretionary inflows for downstream flow requirements, given the increase in the value of stored water at full pool required to achieve full pool storage by May 21st, all else the same.

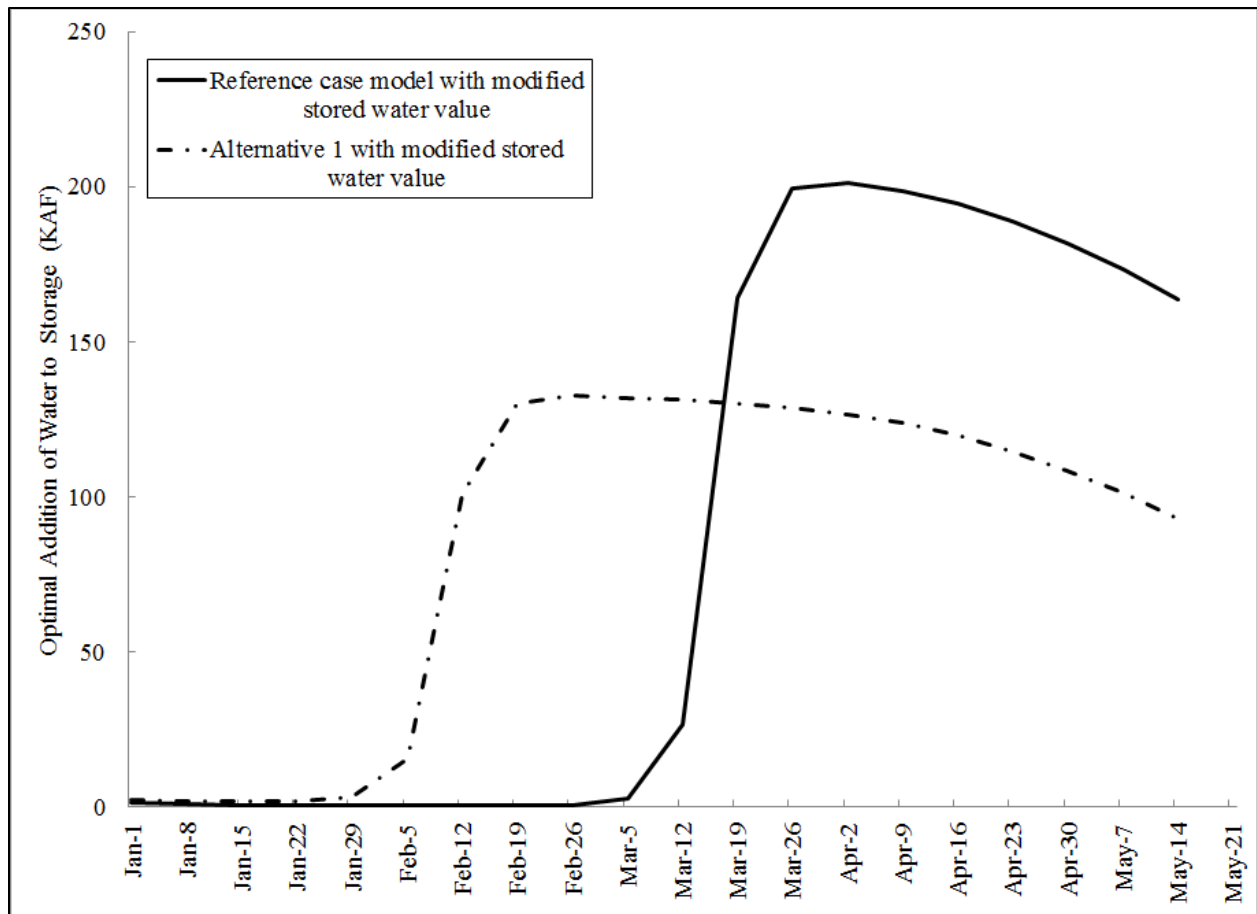


Figure 4.17. The optimal policy for additions of water to reservoir storage compared for expected inflows under the reference case specification and modified discretionary inflows for downstream flow requirements, given the increase in the value of stored water at full pool required to achieve full pool storage by May 21st, all else the same.

4.5.3 Comparison to the existing fill path

The current USACE rule curves for the Willamette Project reservoirs begin filling the reservoirs February 1st at an average rate of 145 KAF/week through the end of February (Figure 4.18). Starting in the first week of March, the rate at which the current rule curves add water to storage slows to an average of 89 KAF/week through April. This is followed by further slowdowns to 45 KAF the week of May 7th and 7 KAF the week of May 14th. On May 21st the

volume of water storage given by the current rule curves is 1580 KAF, which is about 120 KAF less than full pool storage.

The estimated optimal fill path accounting for downstream flow requirements differed from the current USACE target fill path (Figure 4.18). Additions of water to storage lagged four weeks behind the current USACE target path and the fill rate was faster than the current USACE target rate, averaging 115 KAF/week from the first week in March through May 21st (Figure 4.18). Furthermore, the final reservoir fill level in this specification was 233 KAF less than the final USACE target level. When the marginal value of stored water was increased such that full pool storage was achieved by May 21st, the delay in filling relative to the current USACE target path was reduced to approximately 2 weeks (Figure 4.18). However, the average fill rate remained higher than that of the current USACE path, at 120 KAF/week from the second week in February through May 21st as compared to the USACE current rate over the same period of 99 KAF/week (Figure 4.18).

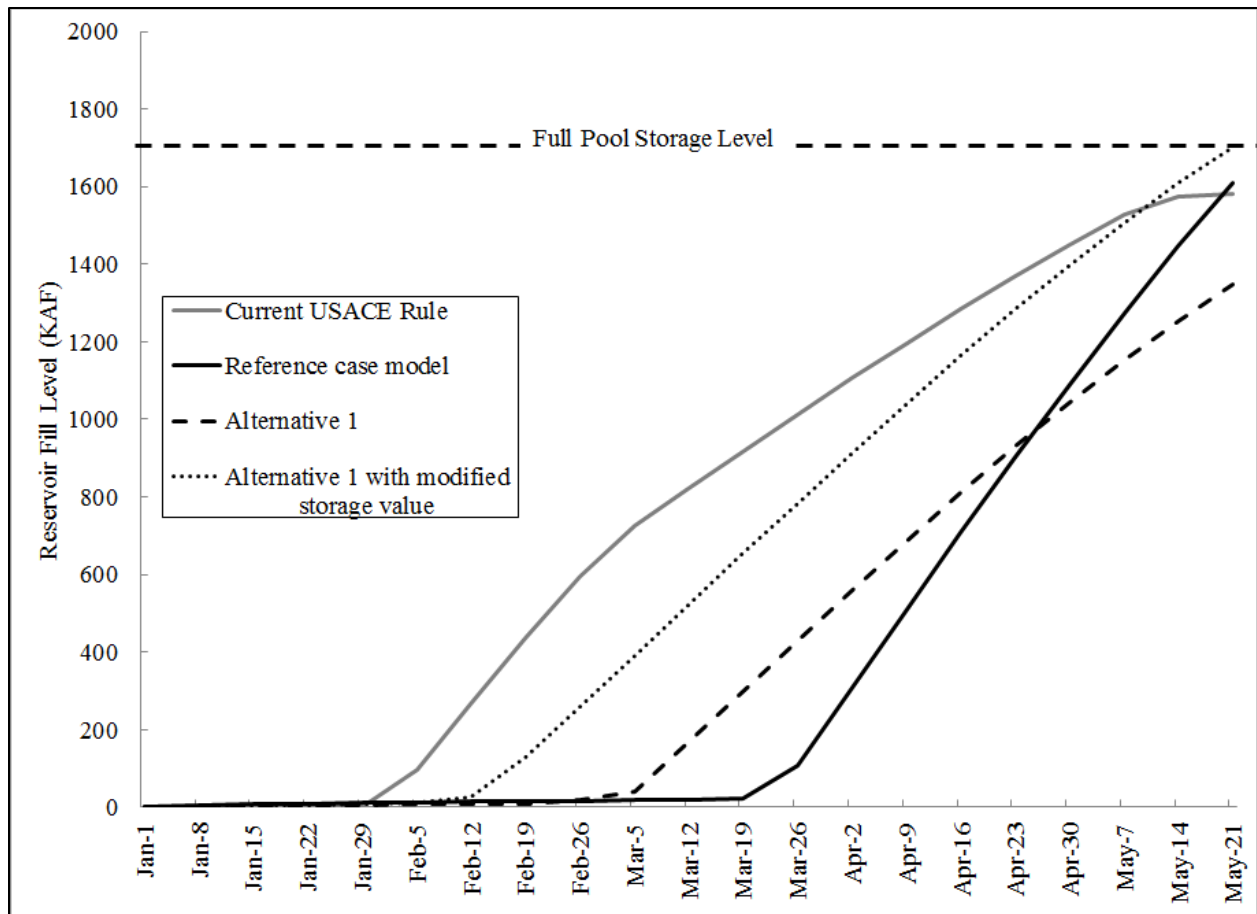


Figure 4.18. Comparison of the current USACE target fill path for the Willamette Project reservoirs to the estimated optimal reservoir fill paths under 1) the reference case specification, 2) reduced discretionary inflows to account for downstream flow requirements, and 3) reduced discretionary inflows to account for downstream flow requirements as well as the increase in the value of stored water at full pool required to achieve full pool storage by May 21st, all else the same.

4.5.4 Sensitivity to changes in use values

When the value of stored water at full pool was increased to \$17/acre-foot for the three month summer period to match the value of water to irrigated agriculture in the WRB, the derived optimal reservoir fill path continued to keep the reservoir at minimum pool through the first week in March (Figure 4.19). This remained the case when the value of stored water was increased further to \$34/acre-foot (Figure 4.19). However, during the second and third week in

March the estimated optimal policy increased additions of water to storage relative to the reference case model such that by the end of March the reservoir fill level was greater the reference case level by 120 KAF when the value of stored water was at \$17/acre-foot and by 204 KAF when the value of stored water was at \$34/acre-foot. Starting at the beginning of April, the additions of water to storage were identical to the reference case model for the remainder of the refill period due to the constraint of inflows (Figure 4.20). However, under both of the alternative values of stored water, the earlier additions of water to storage allowed full pool storage to be achieved by May 21st (Figure 4.19).

Increasing the costs associated with flooding, as modeled for 2030 and 2070, delayed additions of water to storage relative to the reference case (Figure 4.21 and Figure 4.22). Under the assumption of flood losses modelled for 2030, the reservoir filled at a slower rate through the beginning of April, gaining 50 KAF less than the reference case model. Since expected inflows constrained all following gains to storage, the fill level remained at this shortfall relative to the reference case level through the remainder of the refill season (Figure 4.21 and Figure 4.22). The final volume of water storage achieved on May 2st was 1560 KAF (Figure 4.21). When flood costs were increased further to the estimated 2070 level, the delay in reservoir fill is increased, with additions of water to storage of less than 30 KAF prior to the last week in March (Figure 4.21 and Figure 4.22). The resulting final fill level was reduced to 1446 KAF – a shortfall to full pool storage of 256 KAF (Figure 4.22).

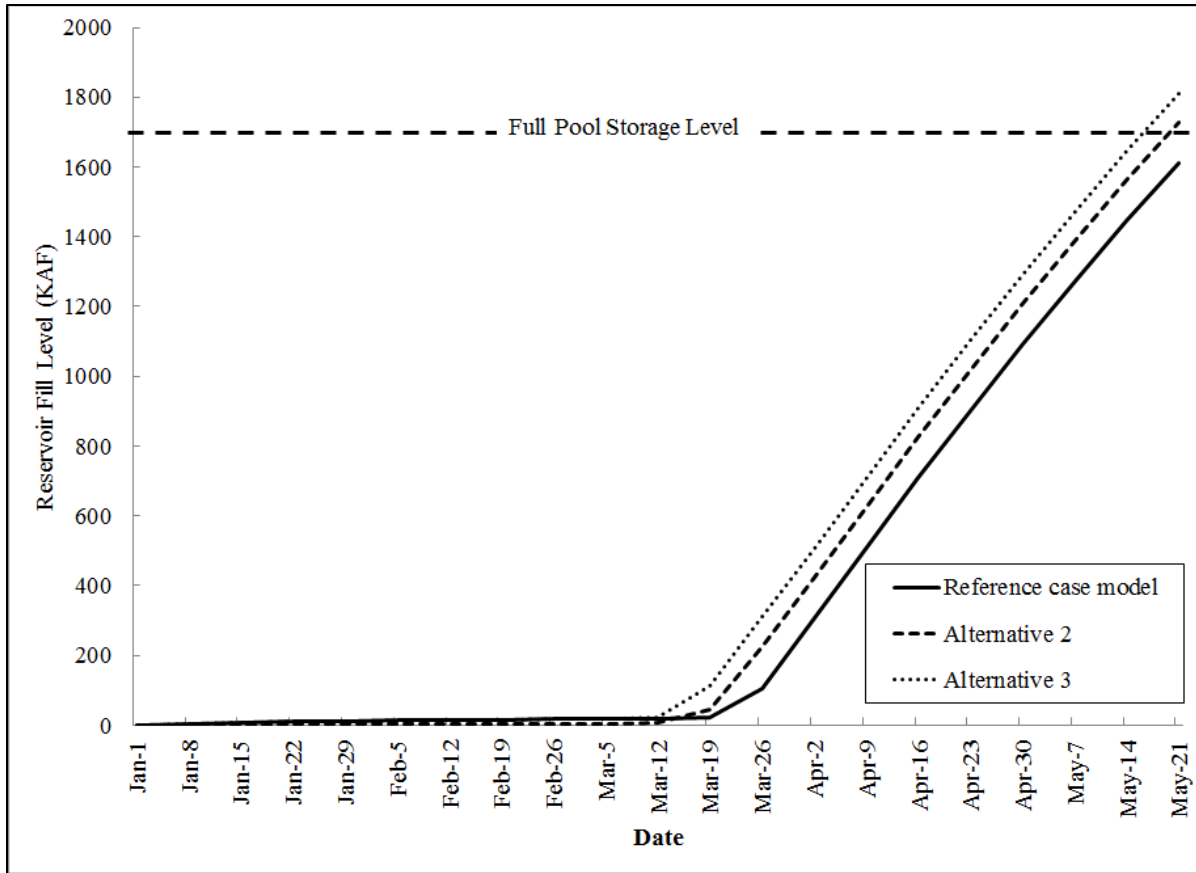


Figure 4.19. The optimal reservoir fill path compared for the reference case model specification, the Alternative 2 specification in which the price of stored water at full pool was increased to \$17/acre-foot – the estimated value of water to irrigated agriculture in the WRB, and the Alternative 3 specification in which the price of stored water at full pool was increased further to \$34/acre-foot.

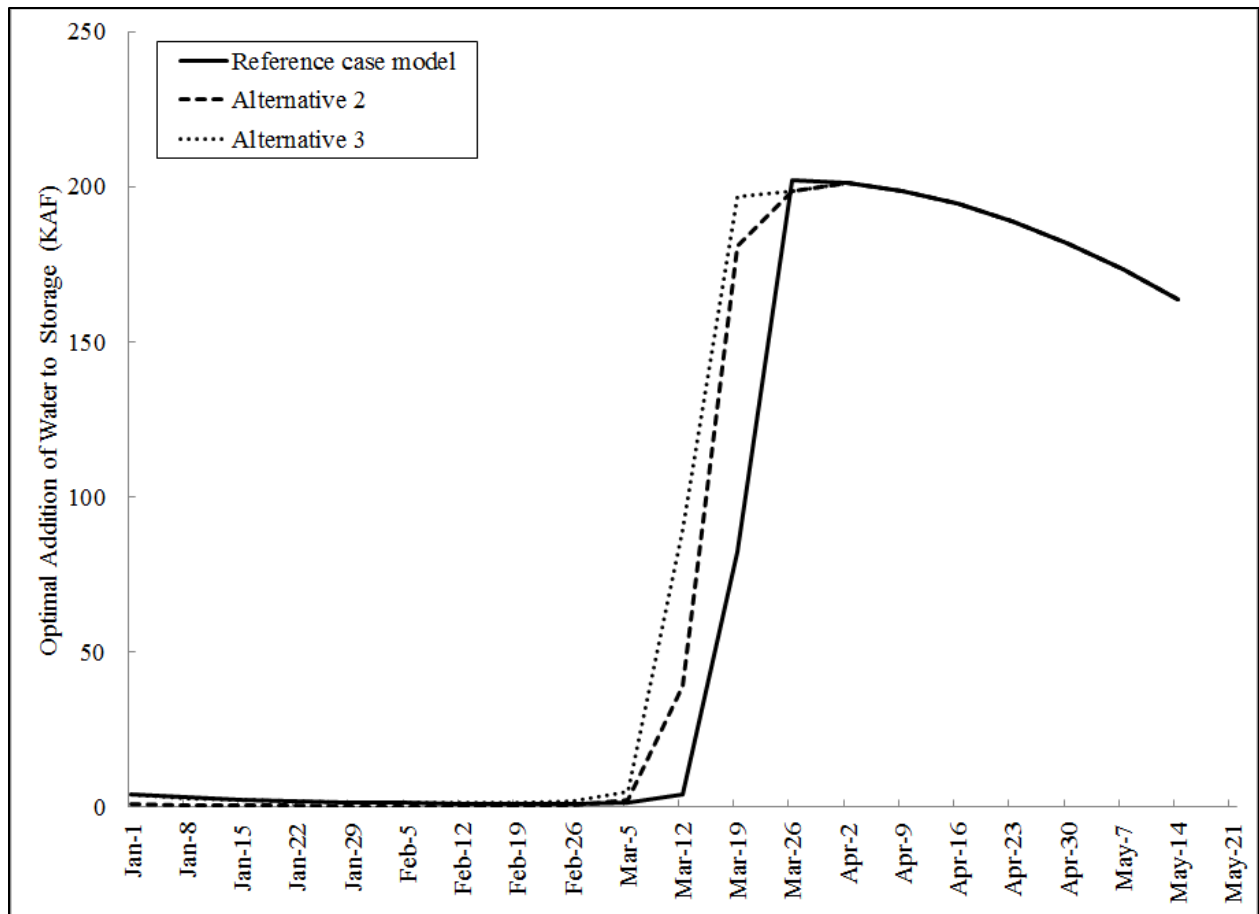


Figure 4.20. The optimal policy for additions of water to reservoir storage compared for the reference case model specification, the Alternative 2 specification in which the price of stored water at full pool was increased to \$17/acre-foot – the estimated value of water to irrigated agriculture in the WRB, and the Alternative 3 specification in which the price of stored water at full pool was increased further to \$34/acre-foot.

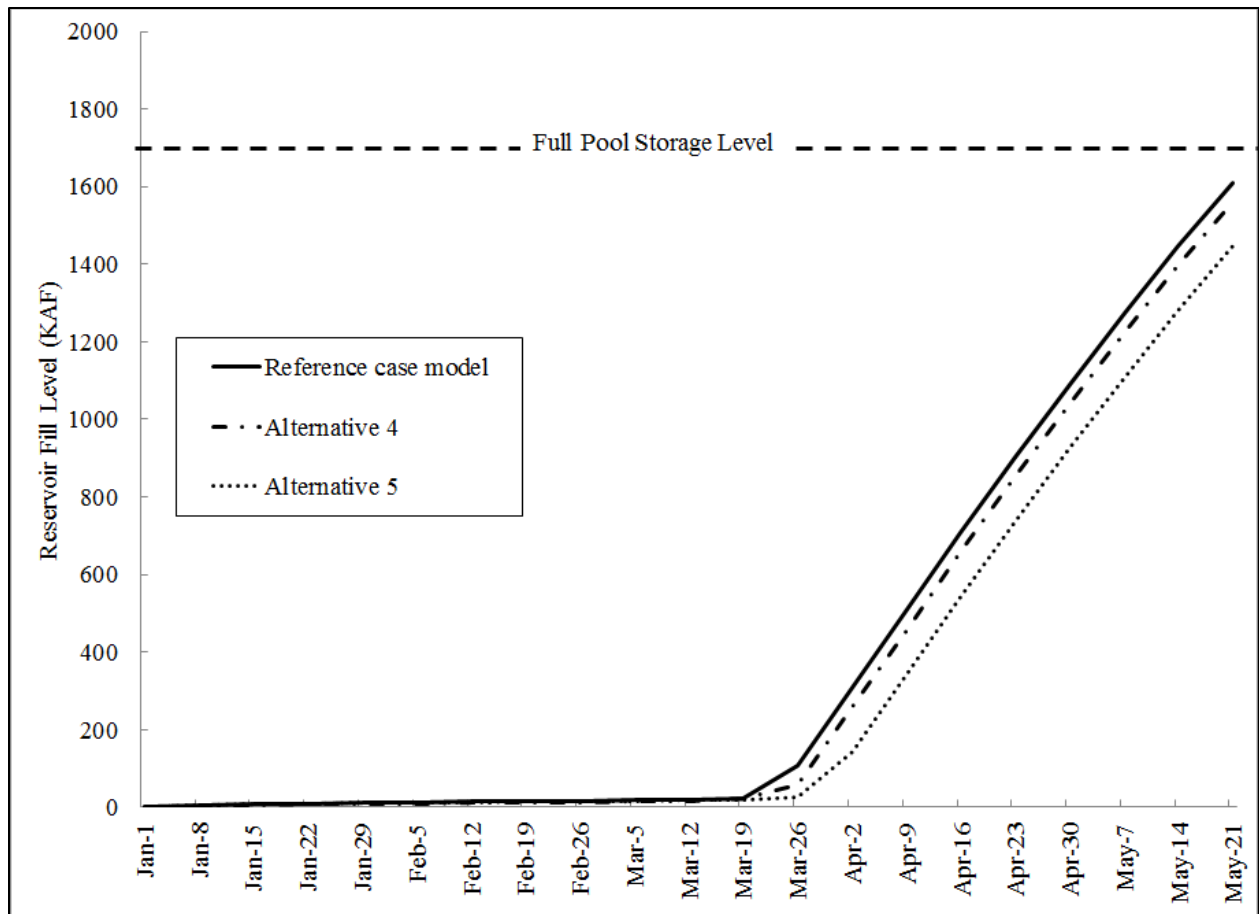


Figure 4.21. The optimal reservoir fill path compared for the reference case model specification, the Alternative 4 specification in which flood losses were increased by 33% relative to the reference case as estimated for the year 2030, and the Alternative 5 specification in which flood losses were increased by 136% relative to the reference case as estimated for the year 2070.

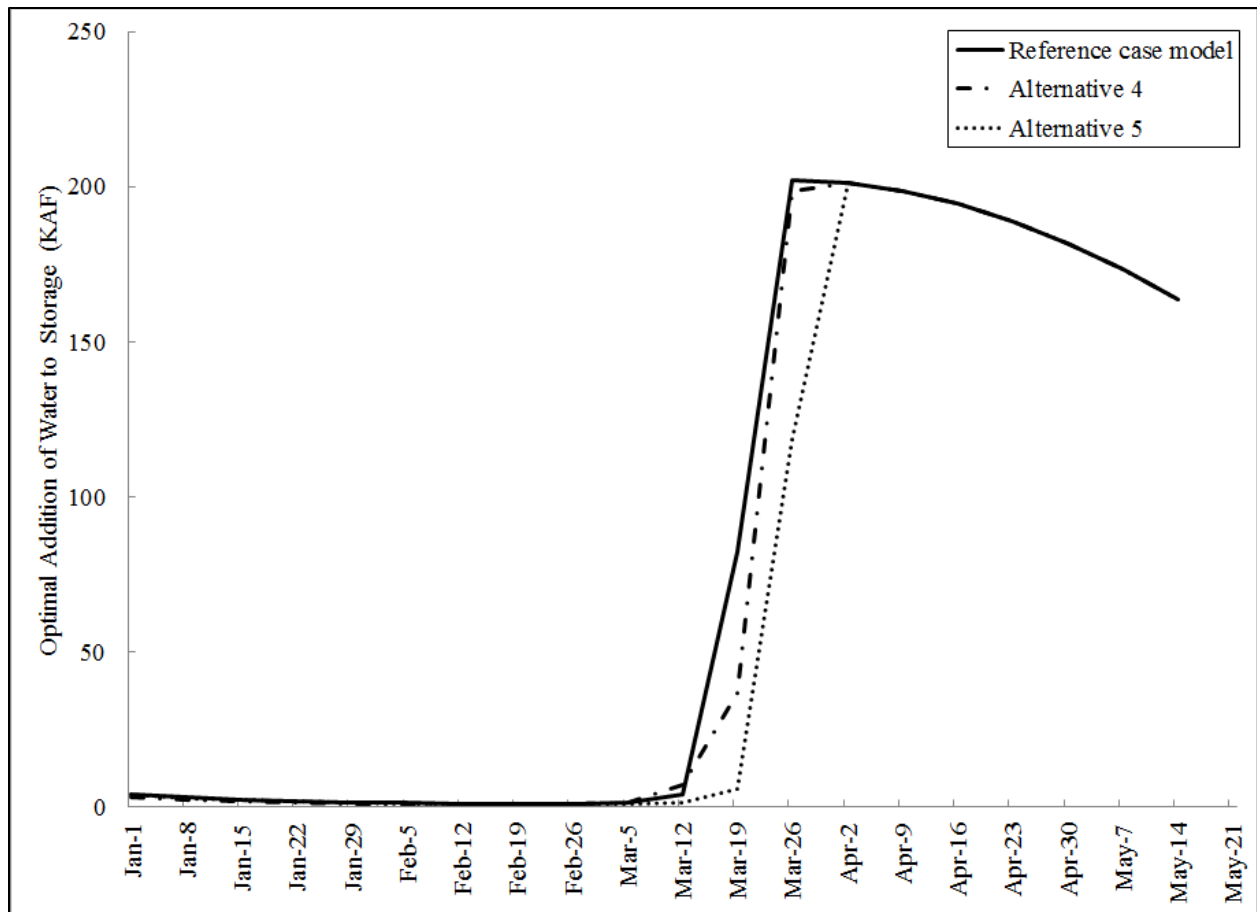


Figure 4.22. The optimal policy for additions of water to reservoir storage compared for the reference case model specification, the Alternative 4 specification in which flood losses were increased by 33% relative to the reference case as estimated for the year 2030, and the Alternative 5 specification in which flood losses were increased by 136% relative to the reference case as estimated for the year 2070.

4.5.5 Sensitivity to changes in hydrology

Altering the reservoir inflows constraint to reflect an expectation that future streamflows from the contributing catchments may look like the past streamflows in the rain zone of the Cascades shifted the optimal reservoir fill path to start filling about a week earlier than under the reference case model (Figure 4.23, Figure 4.24). By the third week in March the reservoir had filled more than twice the level reached by the last week in March under the reference case model (Figure 4.23). After the third week in March reduced spring inflows constrain additions of

water to storage (Figure 4.24). The final reservoir fill level on May 21st was 1426 KAF (Figure 4.23), which was lower than that achieved in the reference case model by 184 KAF, and short of full pool storage by 276 KAF. In order for full pool storage to be achieved, the marginal value of stored water at full pool was required to increase \$35/acre-foot, for all else the same. This shifted the optimal reservoir fill path an additional 1-2 weeks earlier resulting in a reservoir fill level by the end of March that was 7 times higher than under the reference case model (Figure 4.25, Figure 4.26).

Reducing expected reservoir inflows further to simulate both a loss of snowpack as well as increases in evapotranspiration relative to historical conditions, resulted in even earlier additions of water to storage (Figure 4.23, Figure 4.24). Under this model specification, the optimal reservoir fill path was shifted about four weeks earlier than under the reference case model, resulting in a higher reservoir fill level at the end of February than that reached a month later under the reference case model (Figure 4.23). Despite these earlier additions of water to storage the final reservoir fill level on May 21st fell short of full pool by 658 KAF due to constraint of reduced spring inflows (Figure 4.23, Figure 4.24). In order for full pool storage to be achieved, the marginal value of stored water at full pool was required to increase \$181/acre-foot, all else the same. This shifted the optimal reservoir fill path an additional 4-5 weeks earlier with additions of water to storage of over 80 KAF by mid-January (Figure 4.25, Figure 4.26). By the end of March, the resulting reservoir fill level was 12 times higher than under the reference case model, which allows full pool storage to be achieved by May 21st.

Changing the coefficients in the time dependent terms of flood loss function to simulate increased flood costs in the winter and decreased flood costs in the spring, shifted the optimal reservoir fill path to start filling about a week earlier than under the reference case (Figure 4.23,

Figure 4.24). Under this model specification, the reservoir fill level at the end of March was 3 times under the reference case model (Figure 4.23). These earlier additions of water to storage result in full pool storage being achieved by the end of the refill season on May 21st, given specified the inflows constraint (Figure 4.23).

Similar to the other potential hydrologic changes examined, increasing the variability of inflows shifted the optimal reservoir fill path to start adding water to storage earlier (Figure 4.23, Figure 4.24). However, relative to the other hydrologic changes modelled, the impact of doubling the stochastic shock on the optimal reservoir fill path was small. The effect was limited to a gain in the reservoir fill level of 20 KAF relative to the reference case model by the end of March (Figure 4.23), after which additions of water to storage are the same as those in the reference case specification due to the constraint of inflows (Figure 4.24).

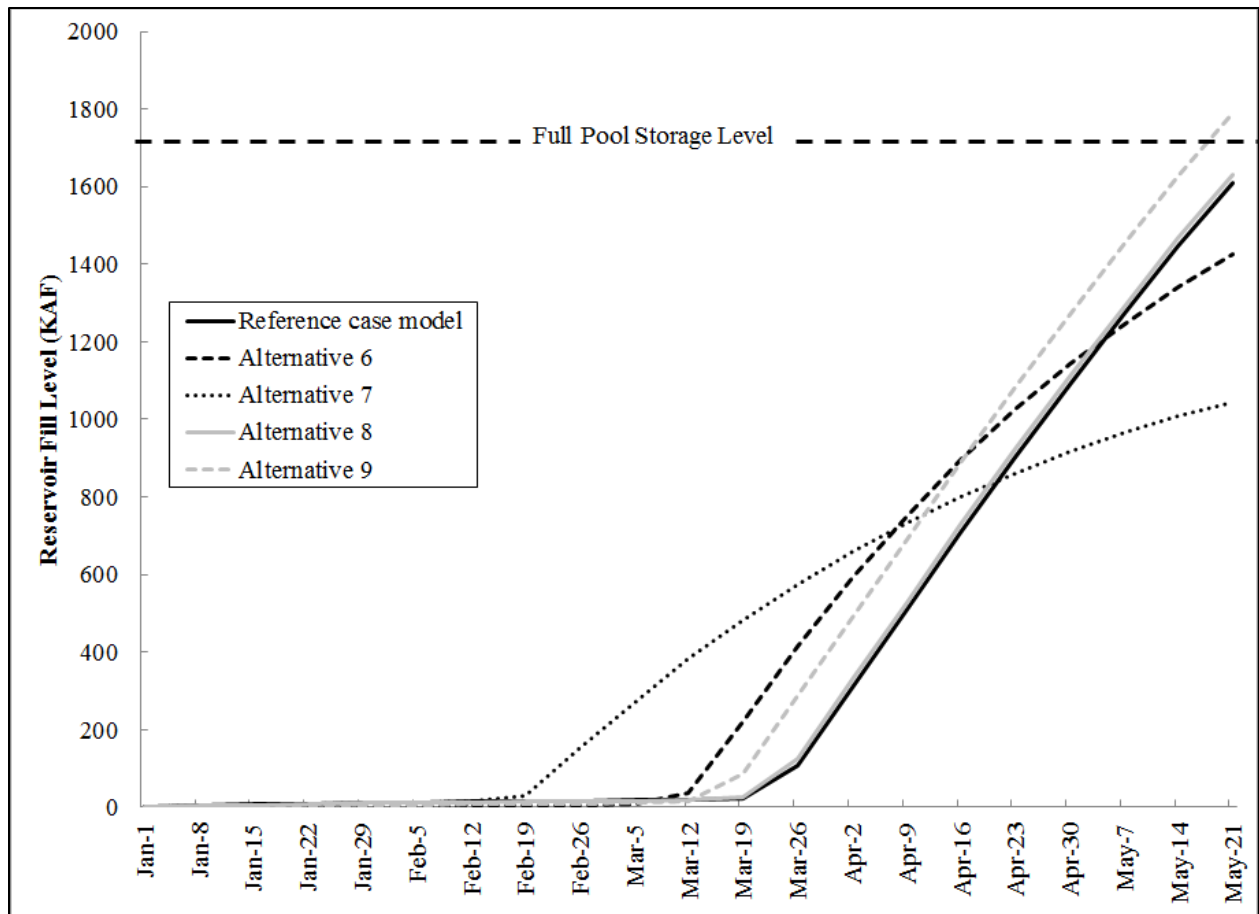


Figure 4.23. The optimal reservoir fill path compared for the reference case model specification, the Alternative 6 specification in which future reservoir inflows were assumed to resemble historical streamflow in the rain-dominated zone of the Cascade Range, the Alternative 7 specification in which future reservoir inflows were assumed to resemble historical streamflow in southern Oregon representing both a future loss of snowpack, as well as increases in evapotranspiration relative to historical conditions, the Alternative 8 specification in which the stochastic shock was doubled to simulate increased variability in streamflow, and the Alternative 9 specification the coefficients in the time dependent terms of flood loss function were altered to simulate increased flood costs in the winter and decreased flood costs in the spring.

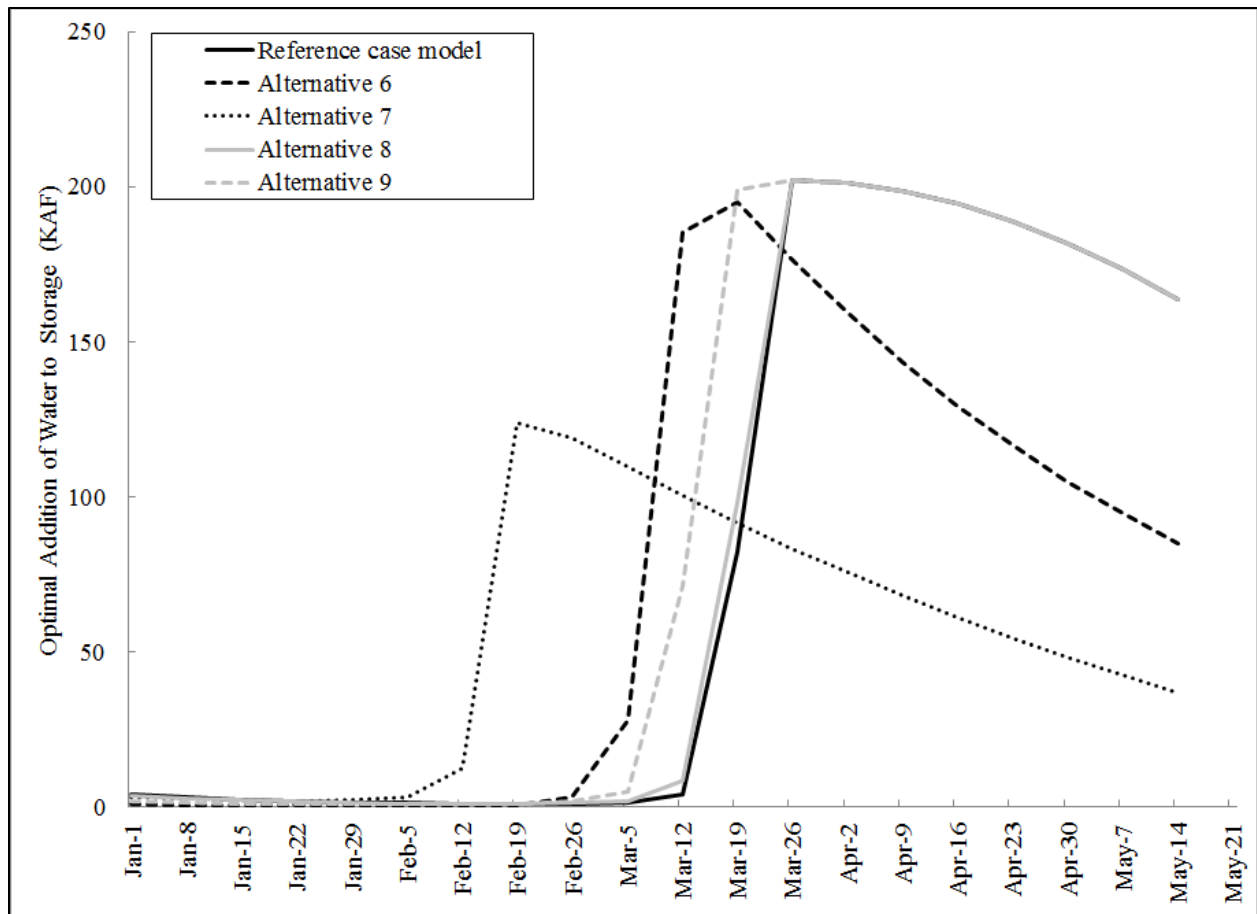


Figure 4.24. The optimal policy for additions of water to reservoir storage compared for the reference case model specification, the Alternative 6 specification in which future reservoir inflows were assumed to resemble historical streamflow in the rain-dominated zone of the Cascade Range, the Alternative 7 specification in which future reservoir inflows were assumed to resemble historical streamflow in southern Oregon representing both a future loss of snowpack, as well as increases in evapotranspiration relative to historical conditions, the Alternative 8 specification in which the stochastic shock was doubled to simulate increased variability in streamflow, and the Alternative 9 specification the coefficients in the time dependent terms of flood loss function were altered to simulate increased flood costs in the winter and decreased flood costs in the spring.

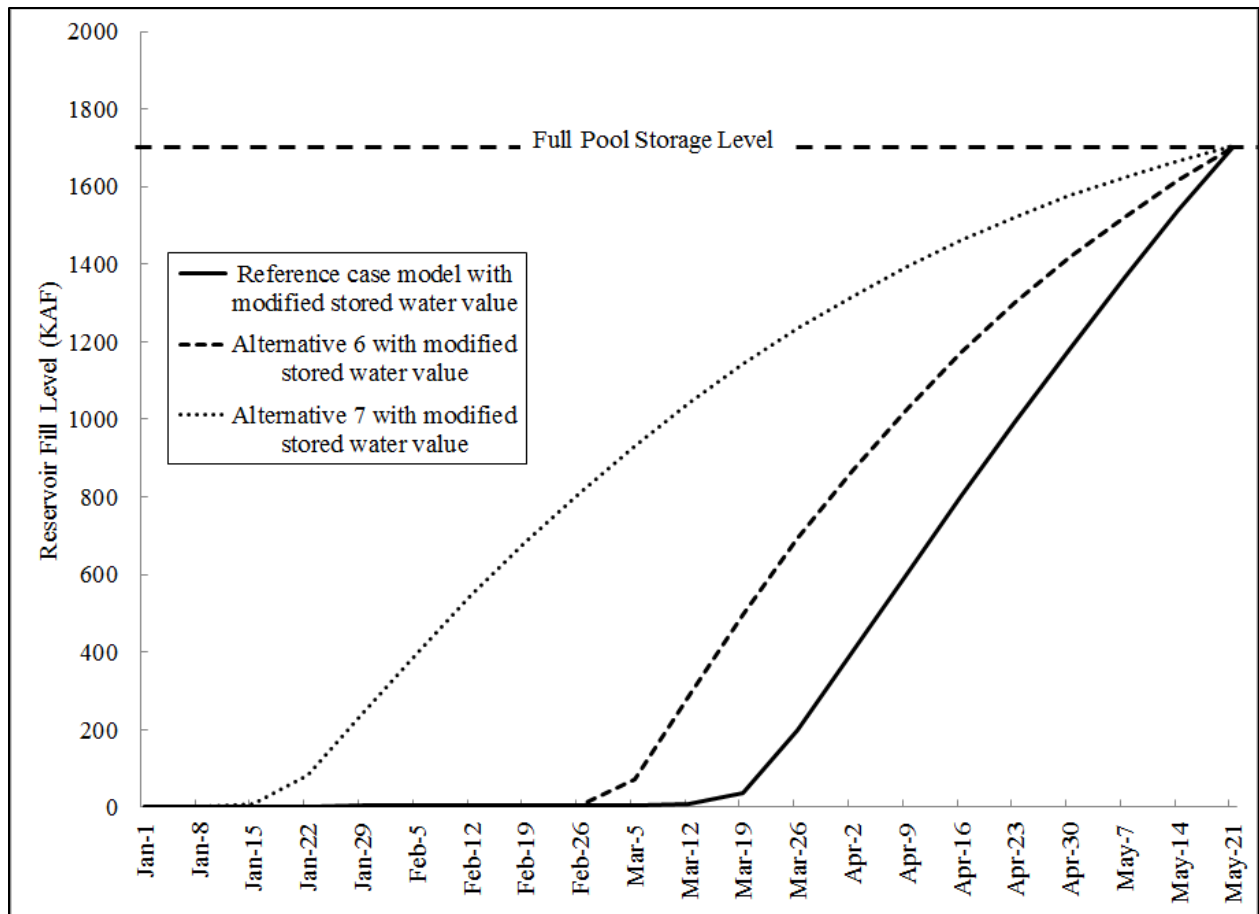


Figure 4.25. The optimal reservoir fill path compared for the reference case model specification, the Alternative 6 specification in which future reservoir inflows were assumed to resemble historical streamflow in the rain-dominated zone of the Cascade Range, and the Alternative 7 specification in which future reservoir inflows were assumed to resemble historical streamflow in southern Oregon representing both a future loss of snowpack, as well as increases in evapotranspiration relative to historical conditions, given the increase in the value of stored water at full pool required to achieve full pool storage by May 21st, all else the same.

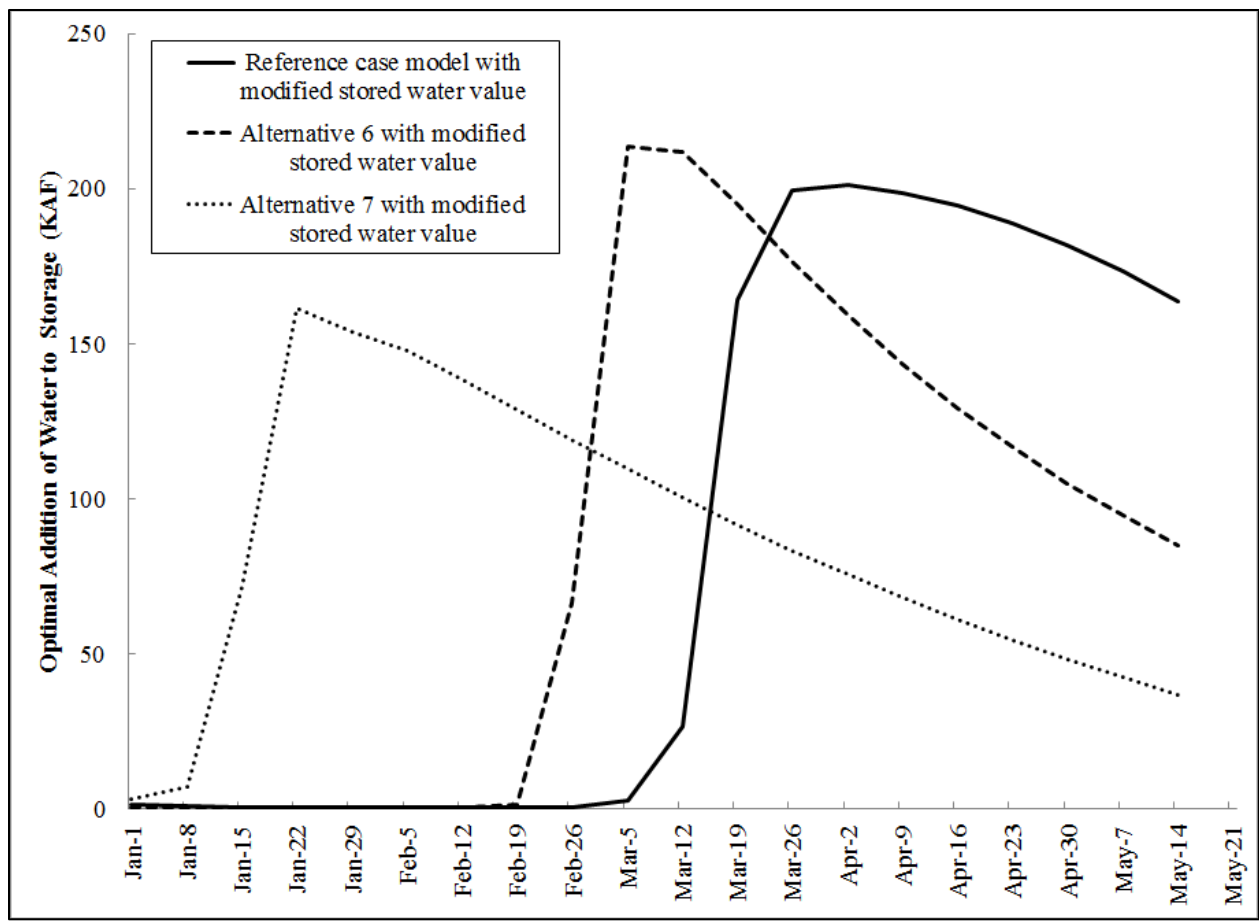


Figure 4.26. The optimal policy for additions of water to reservoir storage compared for the reference case model specification, the Alternative 6 specification in which future reservoir inflows were assumed to resemble historical streamflow in the rain-dominated zone of the Cascade Range, and the Alternative 7 specification in which future reservoir inflows were assumed to resemble historical streamflow in southern Oregon representing both a future loss of snowpack, as well as increases in evapotranspiration relative to historical conditions, given the increase in the value of stored water at full pool required to achieve full pool storage by May 21st, all else the same.

4.6 Discussion

The analysis presented here suggests that the optimal fill path for the Willamette Project reservoirs differs from the fill path given by the current USACE operating rules, and the results might imply that the USACE operating rules be improved.

According to the current USACE fill path or rule curve, reservoir filling initiates four weeks earlier than specified by the derived optimal fill path for Alternative 1, which best represents current expectations for hydrology, downstream flow requirements and the tradeoff between flood damage reduction and stored water benefits (Figure 4.18). The earlier initiation of reservoir refill under the current USACE operating rules results in a higher reservoir fill level than that given by the derived optimal path over the refill period of February 15 to May 21, even though the current USACE fill path has a slower rate of refill in the spring (Figure 4.18).

This disparity between the "optimal" and current fill path could indicate that the current USACE operating rules place a relatively higher value on completely filling the reservoirs as compared to the balance of benefits given by the estimated values of flood damage reduction and stored water in this analysis. The derived optimal fill path achieved full pool by May 21 when the marginal value of stored water at full pool was increased to almost 8 times its current estimated value, but the derived optimal fill path still lagged the current USACE fill path by approximately 2 weeks in initiating reservoir refill, and the reservoir fill level remained at a lower level than the current USACE target level until the end of the first week in May (Figure 4.18).

An additional explanation for the difference between the estimated optimal fill path and the USACE rule curve could be that the current USACE operating rules are based on lower expected inflows during the spring than shown by the historical record (1975-2012). Controlling

for all other factors, the derived optimal reservoir fill path was shifted earlier when expected future spring inflows were reduced (Figure 4.23). The current USACE fill path is bracketed by the derived optimal fill paths of modified Alternatives 1 and 7, when the value of stored water was increased to \$64/acre-foot (modified Alternative 1) and \$181/acre-foot (modified Alternative 7) so that full pool storage was achieved by May 21 (Figure 4.27). Alternative 1 represents inflows and downstream requirements based on historical conditions, and Alternative 7 represents a future with less snowpack and increased evapotranspiration relative to historical conditions. Under modified Alternatives 1 and 7, reservoir fill begins approximately 2 weeks later (Alternative 1) and two weeks earlier (Alternative 7) with faster (Alternative 1) and slower (Alternative 7) rates of fill compared to the current USACE fill path (Figure 4.27). This indicates that the current USACE rule curves may already mitigate anticipated future increased winter flood risk and reduced spring streamflow associated with climate change in the Pacific Northwest. Nevertheless, even an earlier initiation of reservoir refilling to compensate for reduced future spring inflows may be insufficient to attain full pool by May 21 based on the expected timing and relative values of flood damage reduction benefits and water storage estimated in this study (Figure 4.23).

The shape of the optimal reservoir fill path depends on the relative benefits of flood damage reduction and stored water, which are unknown, and were estimated for this study. As argued above, current USACE operating rules appear to implicitly value completely filling the reservoirs more than given by the balance of benefits estimated in this analysis for flood damage reduction and stored water. If the benefits estimated in this study accurately represent the current tradeoff between flood damage reduction and water storage, the USACE fill path initiates reservoir filling earlier than is optimal, and the USACE stated goal of achieving full pool storage

by May 21 may be suboptimal. If the value of stored water relative to flood damage reduction increases in the future due to increased demands for agriculture and/or reservoir recreation, the optimal reservoir fill path will shift earlier, similar to the current USACE fill path. Conversely, if the value of flood damage reduction is increased relative to stored water in the future due to increased development in the floodplain as population increases, the optimal reservoir fill path will shift later and the final optimal reservoir fill level may be decreased.

In addition to uncertainty regarding the estimated values of flood damage reduction and stored water (discussed in chapters 2 and 3), limitations of dynamic programming also affect interpretation of these results. Limitations of the dynamic programming approach used here include the requirement for continuous input functions (described above) and the treatment of the reservoirs as a single unit rather than separate or coordinated analyses of each of the 13 reservoirs in the WRB. Although the derived optimal fill paths may represent the system as a whole, the ability to allocate storage decisions across the reservoirs could provide substantial additional flexibility of reservoir operation in practice. Despite these limitations, this research provides a basis for welfare maximizing decisions regarding how reservoir management in the Willamette River Basin can adapt to the anticipated changes in water supply and demand.

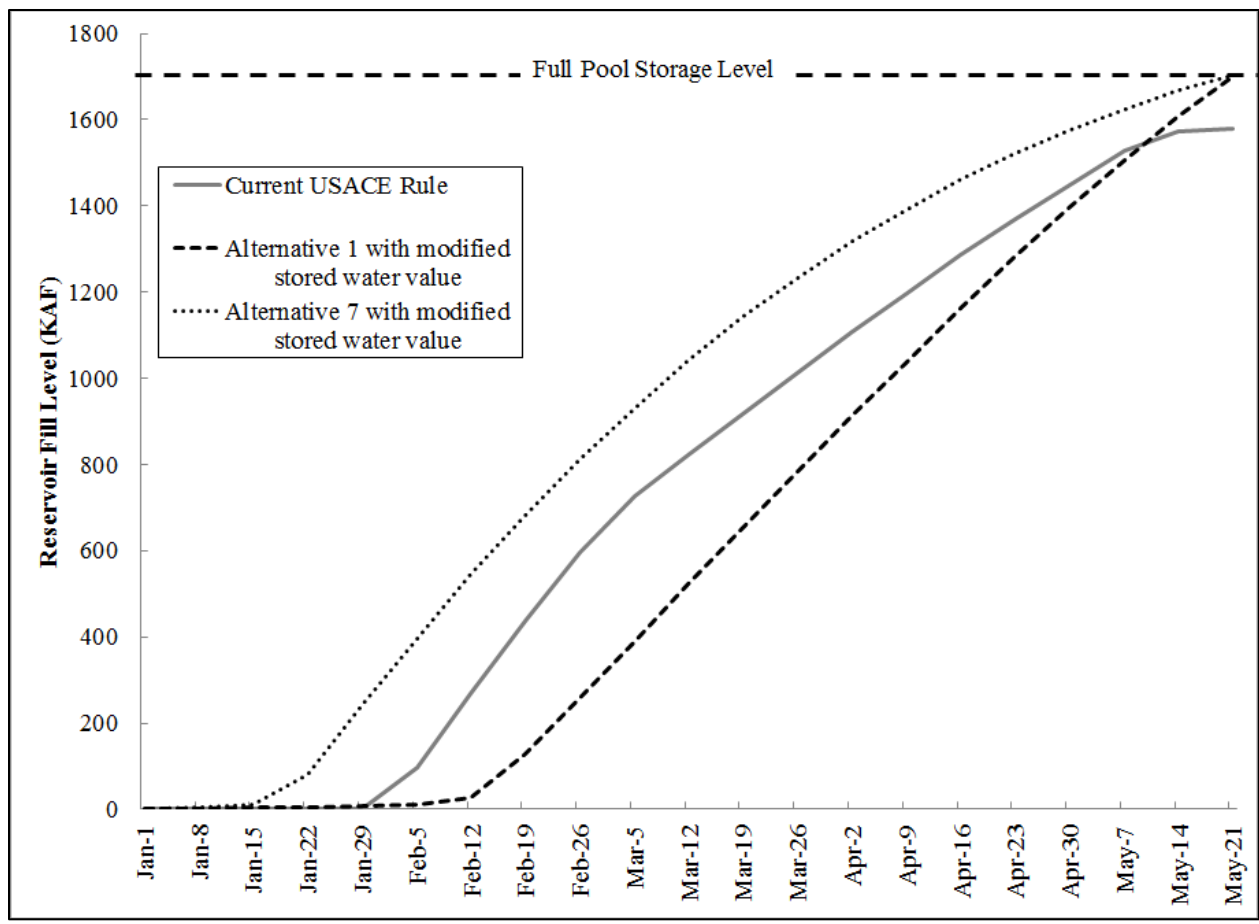


Figure 4.27. The current USACE fill path for the Willamette Project reservoirs compared to the derived optimal reservoir fill paths for the Alternative 1 specification, which best represents current expectations for hydrology and downstream flow requirements, with the value of stored water at full pool increased to \$64/acre-foot, for all else the same, and the Alternative 7 specification in which future reservoir inflows available for storage were assumed to resemble historical streamflow in southern Oregon representing both a future loss of snowpack, as well as increases in evapotranspiration relative to historical conditions, with the value of stored water at full pool increased to \$181/acre-foot, all else the same.

4.7 Conclusions

Reservoir systems play a key role in mitigating the intra-annual variability of water supply in the western United States, where precipitation is super-abundant in winter and sparse in summer. Flood damage reduction is the primary authorized purpose of many of these reservoir systems, but recreation, irrigation, municipal supply, hydropower, navigation, and requirements for downstream environmental flows are important secondary uses. Flood damage reduction is achieved by maintaining unfilled storage capacity in reservoirs, whereas secondary uses depend on full or nearly full reservoirs. As a result, these two competing uses are traded-off during the transition from the wet to the dry season, as the most important or dominant use of the reservoir shifts from reducing flood peaks to storing water. This tradeoff is expressed in the reservoir fill path given by a rule curve for reservoir operations that specifies the target level to which the reservoir is filled for each day of the year. Reservoir rule curves are usually established at the time the reservoir is built. However, the expected effects of climate change, population growth, and development in the western US imply a need to critically evaluate existing reservoir operations.

We employed a dynamic programming approach to social welfare maximization to investigate how reservoir management could adapt to anticipated changes in water supply and demand. Focusing on the Willamette River Basin, Oregon, we derived the optimal reservoir fill path under historical conditions as well as future scenarios of climate and social change. Expected flood damages declined relative to the value of stored water during the transition from winter to summer, defining the timing and rate of reservoir filling. The optimal initiation and rate of reservoir refill depended on expected timing and magnitude of water inflows as well as the expected benefits from flood damage reduction and stored water.

According to the optimal fill path derived for historical stream inflows, current population, and estimated current values of flood damage reduction and water storage, reservoir refilling began four weeks later and filled faster than the current USACE rule curve. The earlier initiation of reservoir refill under the current USACE operating rules results in a higher reservoir fill level than that achieved by the derived optimal path over the entirety of the refill period, despite the fact that the current USACE fill path has a slower rate of refill in the spring. These findings could indicate that 1) the current USACE operating rules place a relatively higher value on stored water compared to the balance of benefits given by the estimated values of flood damage reduction and stored water in this analysis, and/or 2) the current USACE operating rules are based on lower expected spring inflows than shown by the historical record.

Given anticipated increased winter flood risk and reduced spring streamflow in the future, the optimal reservoir fill path is expected to shift earlier in the water year. The optimal final reservoir fill level also may be lower than full pool in the future, depending on the relative magnitude of benefits of flood damage reduction and stored water in the future. If the value of stored water increases relative to flood damage reduction due to increased demands for agriculture and/or reservoir recreation, the optimal reservoir fill path will be shifted earlier, and full pool storage will be more likely to be achieved. Conversely, if increased population and associated development in the floodplain raises the value of flood damage reduction relative to the value of stored water, the optimal reservoir fill path will be shifted later and the final optimal reservoir fill level may be decreased. These findings insights that could help improve decisions regarding how reservoir management in the Willamette River Basin can adapt to the anticipated changes in water supply and demand.

4.8 Acknowledgments

This project was supported by the National Science Foundation (NSF 1039192). Data for this research were obtained from the Willamette Water 2100 Project, the US Geological Survey network of stream gauges, the US Army Corp of Engineers, and the HJ Andrews Experimental Forest research program, which is funded by the National Science Foundation's Long-Term Ecological Research Program (DEB 1440409), US Forest Service Pacific Northwest Research Station, and Oregon State University. Streamflow measurements at the HJ Andrews and South Umpqua Experimental Forests were collected by the US Forest Service. We are grateful for guidance from Andrew Plantinga, Yong Chen, and Robert M. Miller.

4.9 References

- Bales, R. C., N. P. Molotch, T. H. Painter, M. D. Dettinger, R. Rice, and J. Dozier (2006), Mountain hydrology of the western United States, *Water Resources Research*, 42(8), W08432, doi:10.1029/2005WR004387.
- Barnett, T. P. et al. (2008), Human-Induced Changes in the Hydrology of the Western United States, *Science*, 319(5866), 1080–1083, doi:10.1126/science.1152538.
- Bellman, R. (1957), *Dynamic Programming*, Princeton University Press.
- BPA, USBR, and USACE (2001), The Columbia River System Inside Story, Available from: http://www.bpa.gov/power/pg/columbia_river_inside_story.pdf (Accessed 15 April 2015)
- Chang, H., and I.-W. Jung (2010), Spatial and temporal changes in runoff caused by climate change in a complex large river basin in Oregon, *Journal of Hydrology*, 388(3-4), 186–207, doi:10.1016/j.jhydrol.2010.04.040.
- Chou, F. N.-F., and C.-W. Wu (2013), Expected shortage based pre-release strategy for reservoir flood control, *Journal of Hydrology*, 497, 1–14, doi:10.1016/j.jhydrol.2013.05.039.
- Elsner, M. M., L. Cuo, N. Voisin, J. S. Deems, A. F. Hamlet, J. A. Vano, K. E. B. Mickelson, S.-Y. Lee, and D. P. Lettenmaier (2010), Implications of 21st century climate change for the hydrology of Washington State, *Climatic Change*, 102(1-2), 225–260, doi:10.1007/s10584-010-9855-0.
- Graf, W. L. (1999), Dam nation: A geographic census of American dams and their large-scale hydrologic impacts, *Water Resources Research*, 35(4), 1305–1311, doi:10.1029/1999WR900016.

- Graf, W. L. (2001), Damage control: restoring the physical integrity of America's rivers, *Annals of the Association of American Geographers*, 91(1), 1–27.
- Hamlet, A. F., and D. P. Lettenmaier (2007), Effects of 20th century warming and climate variability on flood risk in the western U.S., *Water Resources Research*, 43(6), W06427, doi:10.1029/2006WR005099.
- Hulse, D., S. Gregory, and J. P. Baker (2002), *Willamette River Basin Planning Atlas: Trajectories of Environmental and Ecological Change*, Oregon State University Press.
- Jaeger, W., A. Plantinga, R. Haggerty, and C. Langpap (2014), Anticipating Water Scarcity with Climate Change in the US Pacific Northwest: Using a Landscape Model of a Coupled Natural-Human System, in *World Conference of Environmental and Resource Economists*, p. 52, Istanbul, Turkey.
- Jefferson, A., A. Nolin, S. Lewis, and C. Tague (2008), Hydrogeologic controls on streamflow sensitivity to climate variation, *Hydrological Processes*, 22(22), 4371–4385, doi:10.1002/hyp.7041.
- Jung, I. W., and H. Chang (2012), Climate change impacts on spatial patterns in drought risk in the Willamette River Basin, Oregon, USA, *Theoretical and Applied Climatology*, 108(3-4), 355–371, doi:10.1007/s00704-011-0531-8.
- Kalinin, A. (2013), Right as Rain? The Value of Water in Willamette Valley Agriculture, M.S., Oregon State University, Department of Applied Economics.
- Knowles, N., M. D. Dettinger, and D. R. Cayan (2006), Trends in Snowfall versus Rainfall in the Western United States, *Journal of Climate*, 19(18), 4545–4559, doi:10.1175/JCLI3850.1.
- Miranda, M. J., and P. L. Fackler (2004), *Applied Computational Economics and Finance*, MIT Press.
- Mote, P. W. (2003), Trends in temperature and precipitation in the Pacific Northwest during the twentieth century, *Northwest Science*, 77(4), 271–282.
- Mote, P. W., and E. P. Salathé (2010), Future climate in the Pacific Northwest, *Climatic Change*, 102(1-2), 29–50, doi:10.1007/s10584-010-9848-z.
- Mote, P. W., A. F. Hamlet, M. P. Clark, and D. P. Lettenmaier (2005), Declining Mountain Snowpack in Western North America, *Bulletin of the American Meteorological Society*, 86(1), 39–49, doi:10.1175/BAMS-86-1-39.
- Nolin, A. W., and C. Daly (2006), Mapping “at risk” snow in the Pacific Northwest, *Journal of Hydrometeorology*, 7(5), 1164–1171.
- Poff, N. L., J. D. Allan, M. B. Bain, J. R. Karr, K. L. Prestegard, B. D. Richter, R. E. Sparks, and J. C. Stromberg (1997), The Natural Flow Regime, *BioScience*, 47(11), 769–784, doi:10.2307/1313099.

- Population Research Center (2012), Available from: <http://www.pdx.edu/prc/home> (Accessed 1 March 2015)
- Salathé, E. P., A. F. Hamlet, C. F. Mass, S.-Y. Lee, M. Stumbaugh, and R. Steed (2014), Estimates of Twenty-First-Century Flood Risk in the Pacific Northwest Based on Regional Climate Model Simulations, *Journal of Hydrometeorology*, 15(5), 1881–1899, doi:10.1175/JHM-D-13-0137.1.
- Serreze, M. C., M. P. Clark, R. L. Armstrong, D. A. McGinnis, and R. S. Pulwarty (1999), Characteristics of the western United States snowpack from snowpack telemetry (SNOTEL) data, *Water Resources Research*, 35(7), 2145–2160, doi:10.1029/1999WR900090.
- Stewart, I. T., D. R. Cayan, and M. D. Dettinger (2005), Changes toward earlier streamflow timing across western North America, *Journal of climate*, 18(8), 1136–1155.
- USACE (2011), Willamette Valley - Operating the reservoirs, introducing the rule curve, Available from: http://www.nwp.usace.army.mil/Portals/24/docs/pubs/WV_water_mgmt_FS_2011a.pdf (Accessed 26 February 2015)
- USACE (2012), *Willamette Basin Guide Standard Operating Procedures (SOP) for Reservoir Control Center*, United States Army Corp of Engineers, Portland, OR.
- USFWS (2008), *Biological Opinion on the Continued Operation and Maintenance of the Willamette River Basin Project and Effects to Oregon Chub, Bull Trout, and Bull Trout Critical Habitat Designated Under the Endangered Species Act.*, U.S. Fish and Wildlife Service.
- Vonk, E., Y. P. Xu, M. J. Booij, X. Zhang, and D. C. M. Augustijn (2014), Adapting Multireservoir Operation to Shifting Patterns of Water Supply and Demand, *Water Resources Management*, 28(3), 625–643, doi:10.1007/s11269-013-0499-5.
- Yu, P.-S., T.-C. Yang, C.-M. Kuo, J.-C. Chou, and H.-W. Tseng (2014), Climate change impacts on reservoir inflows and subsequent hydroelectric power generation for cascaded hydropower plants, *Hydrological Sciences Journal*, 59(6), 1196–1212, doi:10.1080/02626667.2014.912035.

Chapter 5: Conclusions

Water sources in the western US are typically concentrated in forested mountain regions far from municipal and agricultural water users, while precipitation is super-abundant in winter and sparse in summer. Reservoir systems can play a key role in mitigating these disparities between water supply and demand. Although the primary authorized purpose of many reservoir systems in the western US is flood damage reduction, secondary uses include recreation, irrigation, municipal water supply, hydropower, navigation, and requirements for downstream environmental flows. Because the storage capacity of a reservoir cannot be used for both flood damage reduction and water storage at the same time, these two competing uses are traded off during the transition from the wet to the dry season, as the most important or dominant use of the reservoir shifts from reducing flood peaks to storing water for recreation and other uses. This tradeoff is expressed in the reservoir fill path, which is given by a rule curve for reservoir operations that specifies the target level to which the reservoir is filled throughout the year. Reservoir rule curves are usually established at the time the reservoir is built without detailed historical data with which to evaluate tradeoffs between uses. Because climate change and population growth are expected to increase winter flood risk and exacerbate water scarcity in the western US, current reservoir operations should be critically evaluated.

The objective of this analysis was to estimate the optimal rule curve for the system of reservoirs operated by the United States Army Corp of Engineers in the Willamette River Basin, Oregon under future scenarios of climate change and population growth. In chapter 2 we quantified the expected value of flood damage reduction for three scenarios of future land use simulated by the Willamette Water 2100 land transition model using mid-range projections of future climate (MIROC5) and assumptions regarding population growth. The findings indicated

that flood damages are expected to increase in the future as both the amount and value of developed land within the inundation zone of the floodplain increases. These changes are exacerbated with higher rates of population growth. At the weekly time scale, the estimated value of flood damage reduction ranged from a high in mid-January of \$304 million to \$1,284 million (depending on the rate of population growth), to near zero at the end of May.

In chapter 3 we estimated the value of stored water for summertime reservoir recreation, relying on eleven years of observed visitor day counts at the Willamette Basin reservoirs and, in particular, observed variation in visitor days with changes in reservoir fill levels. Visitor days were found to decline by as much as 2% per foot of drop in water level below full pool. The implied value of water per acre-foot per month to recreational users was estimated to range from \$0.10 to \$78 across the reservoirs. Since the estimated value of water to irrigated agriculture in the Willamette River Basin falls within this range, these results suggest that it is efficient to release stored water from some reservoirs for downstream needs in the basin, while maintaining full pool for recreation in others, as is the current practice.

In chapter 4 we used a dynamic programming approach to social welfare maximization, and estimated the optimal rule curve for the Willamette Project reservoirs based on expectations for streamflow and the values of flood damage reduction and stored water estimated in chapters 2 and 3. The findings indicated that as expected flood damages decline from mid-January to May, it is optimal to increase the fill level in the reservoirs for stored water uses. The estimated optimal fill path for historical conditions initiates reservoir refill four weeks later than the current operating rules. The earlier initiation of reservoir refill under the current operating rules results in a higher fill level over the entirety of the refill period compared to the estimated optimal path, despite the fact that the current fill path has a slower rate of refill in the spring. These findings

could indicate that 1) the current operating rules place a relatively higher value on stored water compared to the balance of flood damage reduction and stored water benefits estimated in this analysis, and/or 2) the current operating rules are based on an assumption of lower inflows available for storage during the spring than is indicated by the historical record.

Given possible future increases in winter flood risk and reductions spring streamflow, the findings indicate that the optimal reservoir fill path would shift earlier in the water year. It is also possible that the optimal final reservoir fill level may be less than full pool, depending on how the benefits of flood damage reduction and stored water change in the future. If, due to increased demands for agriculture or reservoir recreation, the value of stored water increases relative to flood damage reduction, the optimal reservoir fill path will be shifted earlier so that full pool storage is more likely to be achieved. Conversely, if the value of flood damage reduction increases relative to the value of stored water due to continued land use change and development in the floodplain, the optimal reservoir fill path would shift later and the final optimal reservoir fill level may be decreased.

Despite uncertainties in the estimated values of expected flood damage reduction and stored water for recreation, as well as the limitations of the dynamic program in modelling the coordinated management of multiple reservoirs, the approach and findings of this analysis contribute to our understanding of how reservoir management may need to adapt to future changes in water supply and demand. Future research efforts could focus on providing improved estimates of recreational visits at the Willamette Project reservoirs, collecting demographic data needed to estimate reservoir specific willingness-to-pay for a recreational visit, and a contingent valuation survey to provide information on the expected response of recreational visitation to water levels that are beyond the range of historical variability. Future decisions regarding

tradeoffs between reservoir uses would also benefit from an understanding of the marginal value of stored water not only near full pool, but also over the full range of reservoir storage to ensure appropriate accounting for other uses of stored water. Finally, reservoir managers need information on future expectations of streamflow and flood frequency at a time step appropriate for management decisions.